Modelling of the radiological impact of radioactive waste dumping in the Arctic Seas

Report of the Modelling and Assessment Working Group of the International Arctic Seas Assessment Project (IASAP)

INTERNATIONAL ATOMIC ENERGY AGENCY IAEA

January 2003

MODELLING OF THE RADIOLOGICAL IMPACT OF
RADIOACTIVE WASTE DUMPING IN THE ARCTIC SEAS
IAEA, VIENNA, 2003
IAEA-TECDOC-1330
ISBN 92–0–100203–3
ISSN 1011–4289

FOREWORD

In 1993 in response to the disclosure that the former Soviet Union had dumped radioactive wastes in the Arctic Seas for more than thirty years, the IAEA set up the International Arctic Seas Assessment Project (IASAP) in order to assess the radiological consequences to human beings and to the environment associated with the radioactive wastes dumped, and to recommend possible remedial actions.

According to the White Book of the President of Russia, published in 1993, the total amount of radioactive waste dumped in Arctic Seas was estimated to be approximately 90 PBq at the time of dumping. The dumped items included six nuclear submarine reactors containing spent fuel; a shielding assembly from an icebreaker reactor containing spent fuel; ten nuclear reactors without fuel; and solid and liquid low level waste. The nuclear reactors were dumped in the shallow fjords of Novaya Zemlya and in the Kara Sea.

Within the framework of IASAP, the Modelling and Assessment Working Group was established with the objectives of modelling the environmental dispersal and transport of nuclides to be potentially released from the dumped objects and of assessing the associated radiological impact on man and biota. The work of the group was organised by means of an IAEA Co-ordinated Research Programme.

The present report summarises the work carried out by the Modelling and Assessment Working Group in 1994–1996. The working group, which met six times, was chaired by M. Scott of the University of Glasgow who was also the main author of this report. The names of the working group members are listed at the end of the report. In developing the transfer models and assessing the potential environmental and health impacts posed by the dumped wastes the working group relied largely on information gathered from international cruises to the area, notably those organised by the Joint Norwegian Russian Expert Group, and information obtained through Technical and Research Contracts between the IAEA and Russian scientists: V. Pavlov of Arctic and Antarctic Research Institute, V. Ivanov of All-Russian Research Institute for Geology and Mineral Resources of the World Oceans and T. Sazykina of SPA "Typhoon". The information on potential radionuclide release rates from the dumped objects was obtained from the IASAP Source Term Working Group.

Other reports issued under the IASAP study are:

Radiological Conditions of the Western Kara Sea, Assessment of the Radiological Impact of the Dumping of Radioactive Waste in the Arctic Seas — Report of the International Arctic Seas Assessment Project (IASAP), Radiological Assessment Reports Series, IAEA (1998).

Predicted Radionuclide Release from Marine Reactors Dumped in the Kara Sea: Report of the Source Term Working Group of the International Arctic Seas Assessment Project (IASAP), IAEA-TECDOC-938 (1997).

Radioactivity in the Arctic Seas: Report for the International Arctic Seas Assessment Project (IASAP), IAEA-TECDOC-1075 (1999).

The IAEA wishes to express its gratitude to all those who participated in the work of the IASAP Modelling and Assessment Working Group and preparation of this report. The IAEA officer initially responsible for this work was K.-L. Sjoeblom and subsequently T. Cabianca of the Division of Radiation and Waste Safety.

EDITORIAL NOTE

CONTENTS

1. INTRODUCTION

1.1. BACKGROUND

In 1992, it was reported that the former Soviet Union had, for over three decades, dumped radioactive waste in the shallow waters of the Arctic Seas.

The International Arctic Seas Assessment Project (IASAP) was launched in 1993 by the IAEA in response to widespread concern with the following objectives:

(1) To assess the risks to human health and to the environment associated with the radioactive waste dumped in the Kara and Barents Seas; and

(2) To examine possible remedial actions related to the dumped waste and to advise on whether they are necessary and justified.

In the spring of 1993 the Russian Federation, at the request of the Consultative Meeting of Contracting Parties to the London Convention supplied data on the dumping activities of the former Soviet Union and the Russian Federation. The so-called 'White Book of the President of Russia' (provided to the London Convention as LC16/INF.2) indicates that high and low level radioactive waste was dumped in the Arctic Seas and the North-West Pacific during the period 1959–1992 and gave rough estimates of their activity content [1]. The items dumped included six nuclear submarine reactors and a shielding assembly from an icebreaker reactor containing spent fuel, totalling, as estimated, 85 PBq; ten reactors (without fuel) containing 3.7 PBq; liquid low level waste containing 0.9 PBq; and solid intermediate and low level waste containing 0.6 PBq. The packaged and unpackaged solid waste and the nuclear reactors were dumped in the Kara Sea – in the shallow fjords of Novaya Zemlya, where the depths of the dumping sites range from 12 m to 135 m and in the Novaya Zemlya Trough, at a depth of 380 m. The dump sites in the Kara Sea are shown in Figure 1 and the initial description of the dumped objects given in Tables I and II.

According to the 'White Book', more than 6000 containers of solid low level radioactive waste have been disposed of in the Kara and Barents Seas. They were dumped either individually or on barges. The packaged waste comprised mainly film coverings, tools, personal protective devices, filters and other contaminated objects produced during maintenance work. In addition, the 'White Book' reports the dumping of more than 150 large objects such as steam generators and reactor lids. The activity of these solid intermediate and low level wastes was estimated in the 'White Book' to be about 0.6 PBq at the time of dumping.

Low level liquid radioactive waste was also dumped in the Barents and Kara Seas during the period 1960–1993 [1]. Waste with a total activity of 0.45 PBq was dumped in the Barents Sea in five designated areas a and further 0.43 PBq outside the designated areas, including 0.32 PBq in the Kara Sea in 1973, 0.07 PBq in 1982 in Andreeva Fjord and 0.07 PBq in 1989 at the coast of Kola Peninsula in Ara Fjord. However, the total amount of liquid radioactive waste dumped in these Russian Arctic seas (0.88 PBq) is considerably smaller than the total activity of solid waste dumped in the area.
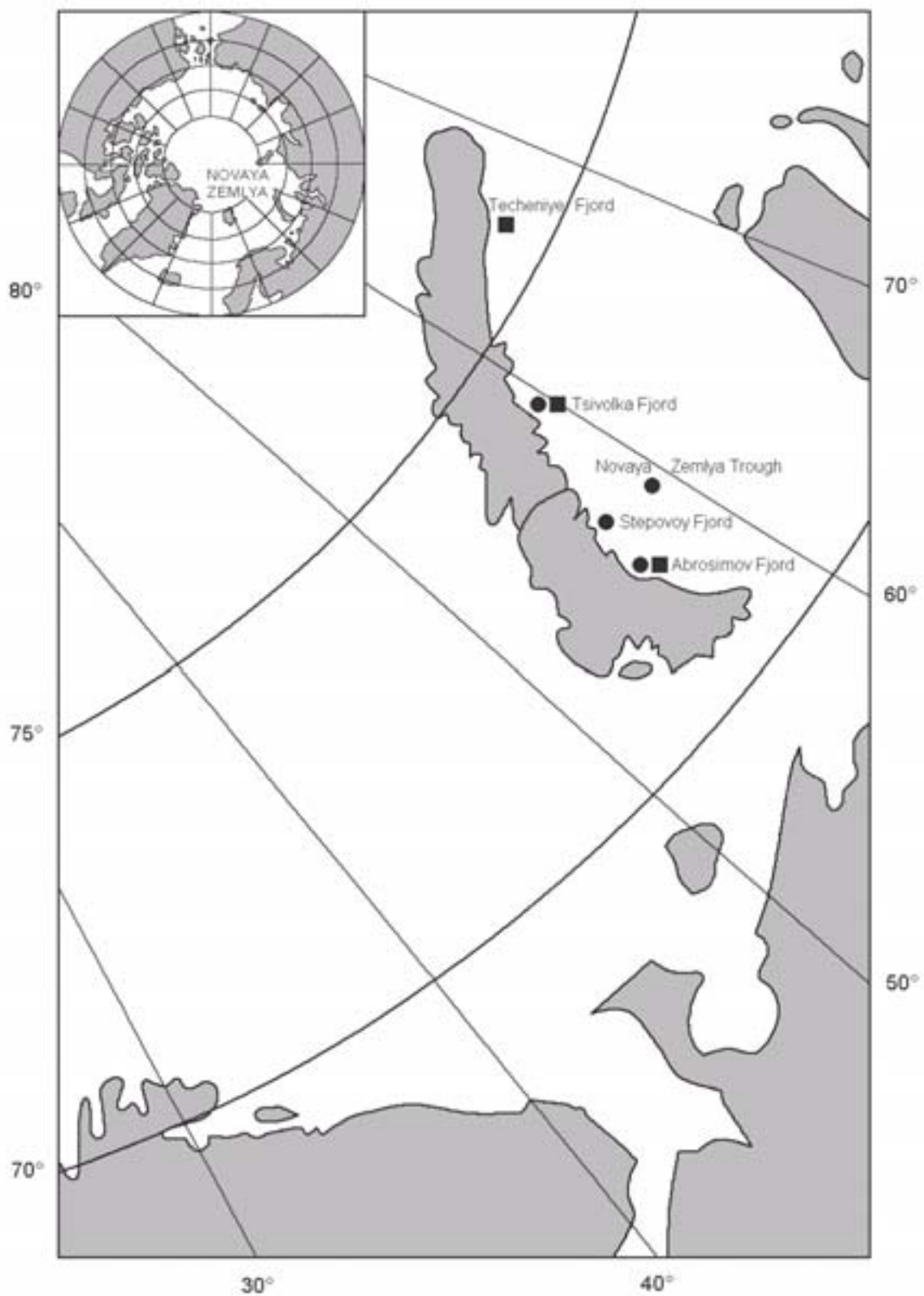
● – Reactors containing fuel; ■ – Reactors without fuel.

FIG. 1. Dumping sites for radioactive waste in the Arctic Seas.

TABLE I. OBJECTS WITH SPENT NUCLEAR FUEL DUMPED IN THE ARCTIC SEAS [1]

Object	Coordinates/ Year	Depth, Meters	Total Activity (max.) kCi (PBq)*	Radionuclide Content	Description of Protective Barriers
Compartment of NS Number 285 with 2 reactors, one containing SNF	71°56'2" N, 55°18'5" E, Abrosimov Fjord, 1965	20	800 (29.6)	Fission products	Reactor compartment and interior structures filled with Furfurol mixture
Compartment of NS Number 901 with 2 reactors containing SNF	71°56'2" N, 55°18'9" E, Abrosimov Fjord, 1965	20	400 (14.8)	Fission products	Reactor compartment and interior structures filled with Furfurol mixture
Shielding assembly of reactor from nuclear icebreaker *Lenin* with residual SNF (60% of original UO_2 fuel charge)	74°22'1" N, 58°42'2" E, Tsivolka Fjord, 1967	49	100 (3.7)	^{137}Cs (~50 kCi), ^{90}Sr (~50 kCi), ^{238}Pu, ^{241}Am, ^{244}Cm (~2 kCi)	SNF residue bound by Furfurol mixture, shielding assembly placed in reinforced concrete container and metal shell
Reactor of NS Number 421 containing SNF	72°40' N, 58°10' E, Novaya Zemlya Trough, 1972	300	800 (29.6)	Fission products	Metal container with lead shell dumped along with barge
NS Number 601 with 2 reactors containing SNF	72°31'15" N, 55°30'15" E, Stepovoy Fjord, 1981	50	200 (7.4)	Fission products	Reactor compartment and interior structures filled with Furfurol mixture
Total: 5 objects with 7 reactors containing SNF	1965–1981		2300 (85.1)		

*   Expert estimates were made at the time of dumping, based on power generated by NS reactors (12.5 GW·day).
NS   Nuclear Submarine.
SNF   Spent Nuclear Fuel.

1.2. RATIONALE FOR ESTABLISHING IASAP

When information on dumping practices in the Arctic Seas was revealed, most of the technical and environmental data needed for the proper evaluation of hazards to human health and the environment resulting from the dumped waste was not generally available. The first joint Norwegian–Russian exploratory cruise in summer 1992 was not able to take samples in the immediate vicinity of the dumped wastes. However, samples taken in the Kara Sea showed that present levels of radioactive contamination in that area were lower than or similar to those in other sea areas. This resulted in the preliminary conclusion that the impact of the dumped wastes on the overall level of radioactive contamination in the Kara Sea was insignificant [2].

However, it was understood that gradual deterioration of the waste packages and containments could lead to impacts in the future. These could result in contamination of the marine food chain, possibly with additional radiation exposure of humans through the consumption of fish and other marine foodstuffs as a consequence.

TABLE II. OBJECTS WITHOUT SPENT FUEL DUMPED IN THE ARCTIC SEAS [1]

Object	Coordinates Year	Depth, Meters	Total Activity kCi (PBq)	Radionuclide Content	Description of Protective Barriers
Reactor compartment of NS Number 285 with 2 reactors, one without SNF	71°56'2" N, 55°18'5" E, Abrosimov Fjord, 1965	20	Requires special analysis	Unclear	Reactor compartment structures
Reactor compartment of NS Number 254 (with 2 reactors)	71°55'13" N, 55°32'32" E, Abrosimov Fjord, 1965	20	Requires special analysis	Unclear	Reactor compartment structures
Reactor compartment of NS Number 260 (with 2 reactors)	72°56'2" N, 55°18'5" E, Abrosimov Fjord, 1966	20	Requires special analysis	Unclear	Reactor compartment structures
Steam generating installation of icebreaker *Lenin*, comprising 3 reactors with primary loop pipelines and water tight stock equipment	74°26'4" N, 58°37'3" E, Tsivolka Fjord, 1967	50	~50 kCi (~1.9 PBq)*	Mainly ^{60}Co	Biological shielding unit (B-300 steel + concrete)
2 reactors from NS Number 538	73°59' N**, 66°18' E, Techeniye Fjord, 1972	35–40	Requires special analysis	Unclear	Metal container with lead shell
Total: 5 objects with 10 reactors without SNF	1965–1988		Requires special analysis (possibly up to 100 kCi (3.7 PBq) at time of dumping)		

*   Expert estimates were made at the time of sinking, based on power generated by NS reactors (12.5 GW·day).
**   There is a printing error in the "White Book". The actual co-ordinate is 75°59' N.
NS   Nuclear Submarine.
SNF Spent Nuclear Fuel.

Because the wastes are lying in shallow waters, the possibility of radiation exposure through other routes, such as the movement and transport of the waste packages by natural events (ice or storm action), or by accidental or deliberate human intrusion, cannot be ruled out. In order to provide more information on these issues it was deemed necessary to evaluate the condition of the waste objects, existing and potential radionuclide releases, the transport and fate of released radionuclides and associated radiological exposures. The International Arctic Seas Assessment Project (IASAP) was established as mentioned earlier to answer these and other related questions. The multidisciplinary team of scientists adopted the following approach:

— They examined the current radiological situation in Arctic waters to assess evidence for releases from the dumped waste.

— They predicted potential future releases from the dumped wastes concentrating on the solid high level waste objects containing the major part of the radionuclide inventory of the wastes.

— They modelled environmental transport of released nuclides and assessed the associated radiological impact on humans and the biota.

— They examined the feasibility, costs and benefits of possible remedial measures applied to a selected high level waste object.

1.3. ROLE AND OBJECTIVES OF THE MODELLING AND DOSE ASSESSMENT GROUP

This working group was created specifically to model the dispersal and transfer of radionuclides released from the radioactive waste dumped in the bays of Novaya Zemlya and open Kara Sea.

Models were developed to model the dispersal of the pollutants and for the assessment of the radiological consequences of the releases from the dumped wastes in the Arctic. A number of complementary models were developed which reflect different modelling perspectives and accommodate the requirements within IASAP of providing predictions at very diverse space and time scales; the stated IASAP objectives require assessment of impact at local (near field), regional (intermediate field) on relatively short timescales and global (far field) over much longer timescales of thousands of years.

Within such a collaborative programme, where the main modelling need is for predictive capabilities, it is common practice to include a model inter-comparison and an evaluation of the different types of models on both theoretical and practical grounds. This would also include an evaluation of the data and modelling uncertainties and their subsequent effects on the predictions. The complementary nature of the models used in IASAP provides a mechanism of incorporating model uncertainties within the overall uncertainty analysis for ensuring the robustness of the predictions.

As a result of these considerations, an extensive model comparison exercise was devised and implemented. Results from this intercomparison are presented and discussed in Section 4.

The modelling working group consists of representatives both from the IAEA and from seven member countries. A list of the participants is given in the Contributors to Drafting and Review section at the end of this report. Within the general programme of the assessment of the present and future radiological impact of the dumped waste in the Kara Sea, the modelling group identified two specific objectives to contribute to the overall project.

The objectives which were identified are:

(1) development of predictive models for the dispersal of radioactive contaminants both within and from the Arctic Ocean and an assessment of their reliability; and

(2) evaluation of the contributions of dominating transfer mechanisms to the contaminant dispersal, and hence, ultimately the risks to human health and the environment.

In the first phase of the work, predictive models were prepared either by extending existing models or by developing new models. It was also identified that different models would be particularly suited to assessment at different scales (specifically at local and regional spatial and short time scales and global spatial and long time scales). This important point will be returned to in the discussion of the models and the comparison of their predictions.

To facilitate this work, and as part of the model intercomparison exercise which would follow, existing and available information on the Arctic region was collated and synthesized.

In the final stage, it was envisaged that the results from the model intercomparison exercise would be used as a basis on which to evaluate the estimates of concentration fields when detailed source term scenarios were used. Additionally, they would also be used to assess the uncertainties in ensuing dose calculations.

The work of the group has relied heavily on the information gathered from cruises to the area and the descriptions and modelling work done by the group tasked with describing the sources. It has also been staged, with three main phases: description of the area, collection of relevant and necessary information; extension to and development of predictive models including an extensive model inter-comparison and finally prediction of radiological impact, used in the evaluation of the need and options for remediation.

This report summarizes the work undertaken by a Working Group tasked to model the environmental transport of released radionuclides and to assess the potential doses.

2. GENERAL DESCRIPTION OF AREA

2.1. GENERAL OCEANOGRAPHIC AND GEOPHYSICAL DESCRIPTION

An oceanographic description of the region was prepared (see Figure 2), with certain features highlighted which might be important to consider in the design of an appropriate model. A simplified oceanographic description of the Kara and Barents Seas – two of the marginal seas of Arctic Ocean – was prepared as well as a general description of the Arctic Ocean. More detailed information was also given on Abrasimov Bay on Novaya Zemlya (one of the sites of dumping) which was considered as a generic bay.

The main sources of data were a number of publications, including reports of Pavlov [3, 4] and Ivanov [5] and the cruise reports of the joint Russian–Norwegian expeditions in 1993 and 1994 [6, 7].

2.1.1. A Novaya Zemlya Bay

Lacking detailed information on all the bays involved, a description of Abrosimov Fjord on the eastern coast of Novaya Zemlya was given to the modellers. Figure 3 shows the topography of the area as well as the location of a number of dumped objects (the source to be modelled is sited at station 5). The bay is everywhere very shallow and Table III gives the depths at each of the stations. The salinity is generally high and there is a thin layer (1 m) of low salinity water at the surface. Figure 4 shows typical salinity and temperature profiles for the bay. Bottom sediments are mixed, predominantly silt and mud, but in several location (notably the entrance) the sea floor is covered in stones. The top layers of the sediment are brown in colour, while deeper layers are black. The sedimentation rates and suspended load are also given in Table IV. The sediments were presumed bioturbated to a depth of 30 cm by worms and molluscs. There are two sources of freshwater from the shore side (no figures concerning river runoff were available). The turnover time of the bay was taken to be 6 months. This information was considered suffcent to allow the development of a generic bay model.

2.1.2. Kara Sea

2.1.2.1. Oceanographic description

The area of the Kara Sea is 883 000 km^2 with a volume of 98 000 km^3. The sea everywhere is rather shallow with an average depth of 120 m. There are however a number of deeper troughs, namely Novaya Zemlya Trough (300–400 m) to the east of Novaya Zemlya, and Svyataya Anna Trough to the North of Novaya Zemlya (600 m) and Voronin Trough (up to 450 m).

The western boundary of the Kara Sea is defined to be a line joining Kol'zat Cape with Zhelaniya Cape on Novaya Zemlya, and continuing southward along the eastern shore of Novaya Zemlya, Vaigach Island, and finally crossing the Matochki Shar, Kara Gate and Yugorsky Shar straits.

To the east it is separated from the Laptev Sea by the islands of the Severnaya Zemlya Archipelago.

To the north, the boundary is defined as the line from Kol'zat Cape to Arktochesky Cape on the Severnaya Zemlya.
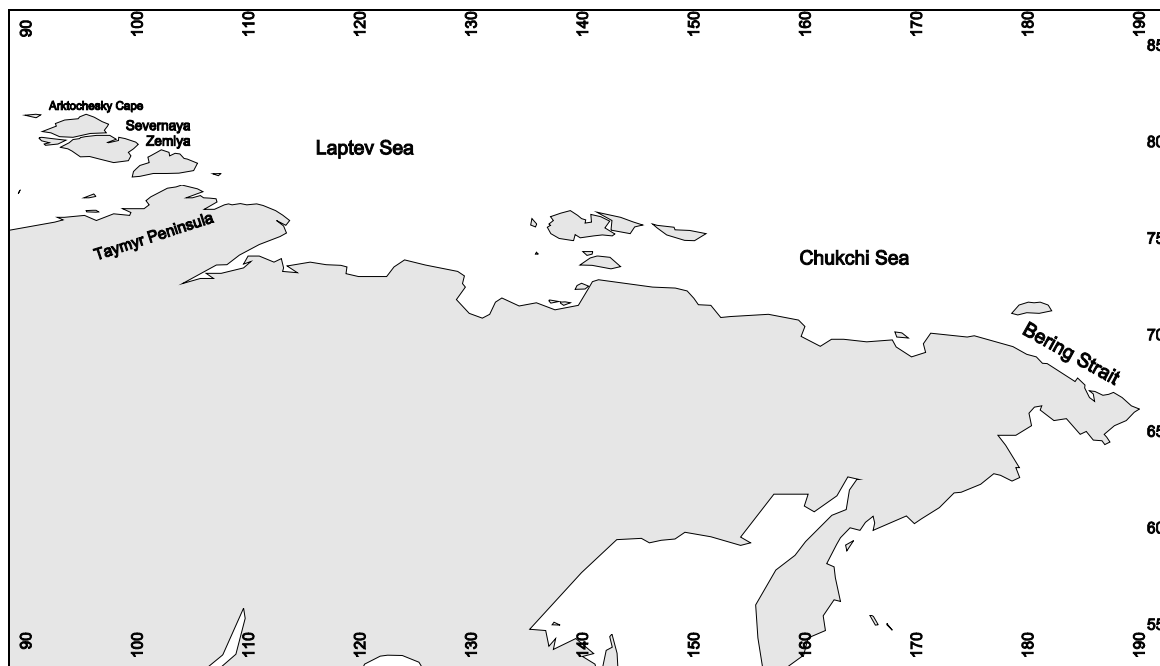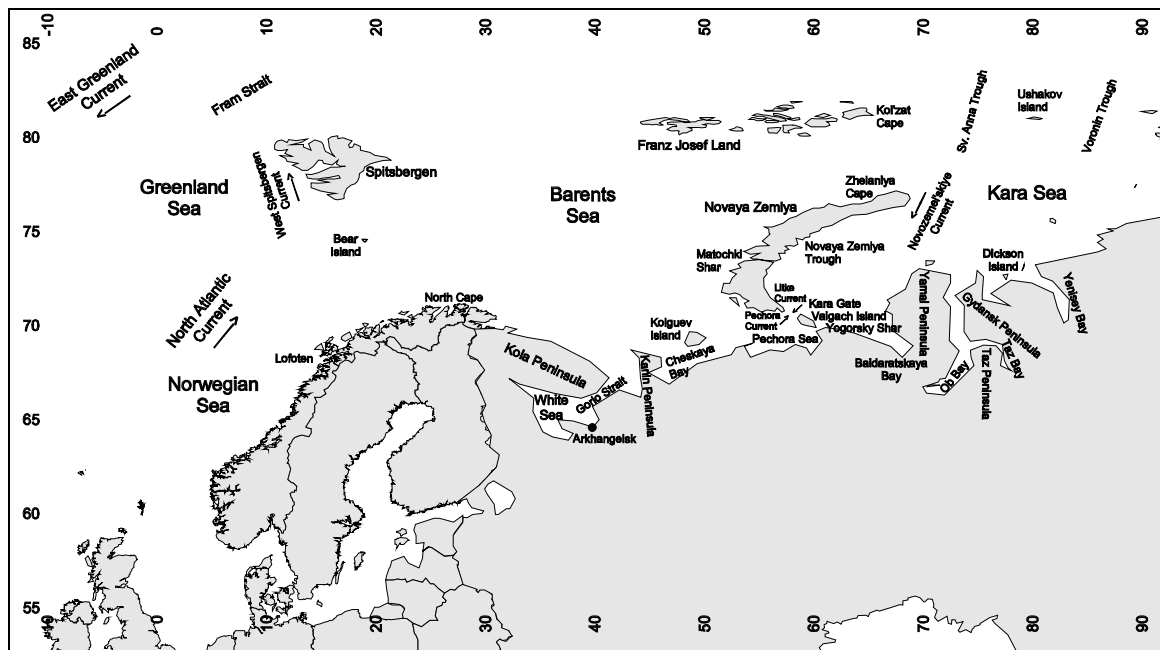
FIG. 2. Region of the Arctic Ocean included in the dispersal model of the IASAP Modelling and Dose Assessment Working Group.

Water, bottom sediments and
soil samling points location

N

2 1
+ +

1 mile

1 2 R. comp 3
3 4 5 Ship 1
R. comp 1,2 6 7 8 9 10 Ship 2
Ship 3 11 13 14 15
IA I
16 17 18 19 20 21
10 m 22 23 24 25 26 27 28 29
Sh. zone 33 34 35 36 II
20 m

4 +3

42 43
40 41
30 31
38

III

IV

44

10 m 20 m

+ 5

BOTTOM SEDIMENTS:

• stations for the bottom sediments
  radioactive contaminantion general
  mapping
▲ stations near located dumped objects

WATER:

◉ sea water samling together with bottom
  sediments sampling
O river water sampling
+ soil sampling

DUMPED OBJECTS LOCATED DURING
THE JOINT EXPEDITION

■ R.comp 1,2 - 2 nuclear submarine reactor compartments.
                both with spent fuel
■ R.comp 3   - Nuclear submarine reactor compartment,
                without spent fuel
▲ Ship 3   - Barge with 2 large cylindrical containers on
                deck
▲ Ship 1   - Barge
▲ Ship 2   - Barge
  IA   - Radioactive waste in steel containers

FIG. 3. Topography of the Abrosimov Fjord and locations of dumped objects [7].
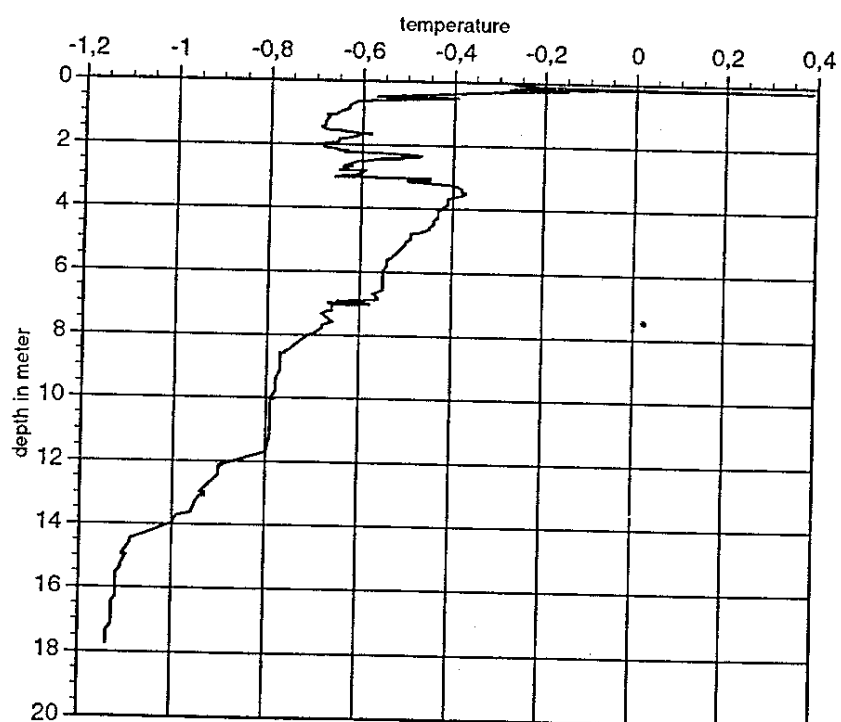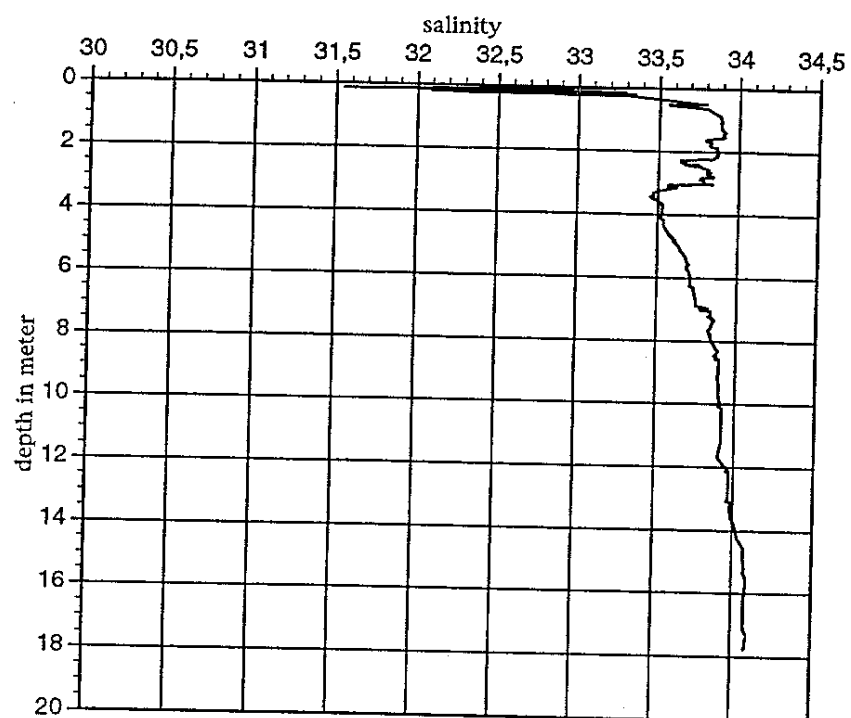
FIG. 4. Typical salinity and temperature profiles of the Abrosimov Fjord from the daily measurements with mini CRD during 30 August to 8 September 1994 [7].

TABLE III. CO-ORDINATES AND DEPTHS OF SAMPLING STATIONS IN FIGURE 3
(ABROSIMOV FJORD) [7]

Station Number	Positions from GPS				Depth m	Date 1994
1	71°	56,57' N	55°	17,89' E	10	30.08
2	71°	56,57' N	55°	18,55' E	10	30.08
3	71°	56,37' N	55°	17,89' E	10	30.08
4	71°	56,37' N	55°	18,55' E	15	30.08
5	71°	56,37' N	55°	19,20' E	10	30.08
6	71°	56,16' N	55°	19,20' E	20	30.08
7	71°	56,16' N	55°	19,85' E	16	30.08
8	71°	56,16' N	55°	20,50' E	17	01.09
9	71°	56,16' N	55°	21,13' E	17	01.09
10	71°	56,16' N	55°	21,78' E	15	01.09
11	71°	55,97' N	55°	20,50' E	15	01.09
I	71°	56,10' N	55°	21,10' E	15	31.08
13	71°	55,97' N	55°	21,78' E	15	01.09
14	71°	55,97' N	55°	22,20' E	18	01.09
15	71°	55,97' N	55°	23,06' E	20	01.09
16	71°	55,75' N	55°	21,13' E	12	01.09
17	71°	55,75' N	55°	21,78' E	14	01.09
18	71°	55,75' N	55°	22,40' E	17	01.09
19	71°	55,75' N	55°	23,06' E	17	01.09
20	71°	55,75' N	55°	23,70' E	19	01.09
21	71°	55,75' N	55°	24,32' E	20	01.09
22	71°	55,55' N	55°	21,78' E	13	08.09
23	71°	55,55' N	55°	22,40' E	15	08.09
24	71°	55,55' N	55°	23,06' E	17	08.09
25	71°	55,55' N	55°	23,70' E	16	08.09
26	71°	55,55' N	55°	24,32' E	19	08.09
27	71°	55,55' N	55°	24,98' E	21	08.09
28	71°	55,55' N	55°	25,46' E	22	08.09
29	71°	55,55' N	55°	26,30' E	22	08.09
30	71°	55,55' N	55°	26,94' E	22	01.09
31	71°	55,55' N	55°	27,60' E	25	01.09
33	71°	55,35' N	55°	23,70' E	20	08.09
34	71°	55,35' N	55°	24,32' E	20	08.09
35	71°	55,35' N	55°	24,99' E	15	08.09
36	71°	55,35' N	55°	25,64' E	23	08.09
II	71°	55,34' N	55°	26,63' E	26	04.09
38	71°	55,35' N	55°	26,94' E	24	01.09
40	71°	55,75' N	55°	26,94' E	26	01.09
41	71°	55,75' N	55°	27,60' E	27	01.09
42	71°	55,97' N	55°	26,94' E	24	01.09
43	71°	55,97' N	55°	27,60' E	29	01.09
I A	71°	56,00' N	55°	21,10' E	15	31.08
III	71°	56,94' N	55°	27,93' E	38	08.09
IV	71°	54,48' N	55°	27,93' E	26	08.09
SHIP 1	71°	56,10' N	55°	20,91' E	14	02.09
SHIP 2	71°	56,13' N	55°	21,54' E	19	02.09
SHIP 3	71°	56,25' N	55°	19,40' E	14	02.09
SH,ZONE					0.5	07.09
RComp 1,2	71°	56,44' N	55°	18,81' E	16	05.09
RComp 3	71°	56,50' N	55°	18,71' E		05.09

TABLE IV. GENERIC BAY DESCRIPTION

Volume		0.5 km^3
Average depth		20 m
Sediment type		silt/mud
Sedimentation rate		2 mm/y
Suspended load		24 mg/l
Turnover time		0.5 year
Bioturbation	biodiffusion depth	0.3 m
	biodiffusion rate	10^{-12} m^2/s

One of the most significant features of the Kara Sea is the continental runoff. Approximately 1200 km^3 of fresh river water enters the area annually (mainly from the rivers Ob and Yenisey). These fresh waters set up a northward current, diverging to the northeast along the mainland coast and westward to the shores of Novaya Zemlya. The inflow of river water shows a distinct maximum in the summer; there is a much reduced flow in the winter. Figure 5 shows the annual cycle of discharges for the main rivers.

A number of large scale flows in the structure of the quasi-constant water circulation were identified:

(1)   the Novozemel'skiye current along the eastern shore of Novaya Zemlya from north-east to south-west, transporting warm Barents Sea waters;

(2)   the Litke current, a continuation of the Novozemel'skiye current which passes through Kara Gate to the Barents Sea;

(3)   the Pechora current, from the Barents to Kara Sea through Kara Gate;

(4)   the Yamal current, flowing northward from Baidaratskaya Bay along the Yamal peninsula coast;

(5)   the current caused by river runoff, predominantly moving north and north-east, seasonal in nature;

(6)   the western Taimyr current eastward to the Laptev Sea;

(7)   a current flowing out to the Arctic basin between Ushakov Island and the Sevenaya Zemlya archipelago;

(8)   a current flowing in from the Arctic basin to the west of Ushakov Island.

Table V summarizes the main flows of the Kara Sea. Some of the figures were known only imprecisely, and ranges of values were given. They are functions of quasi-constant, tidal and wind-driven currents. An estimate of the general ventilation period for the Kara Sea was 3.5 years.
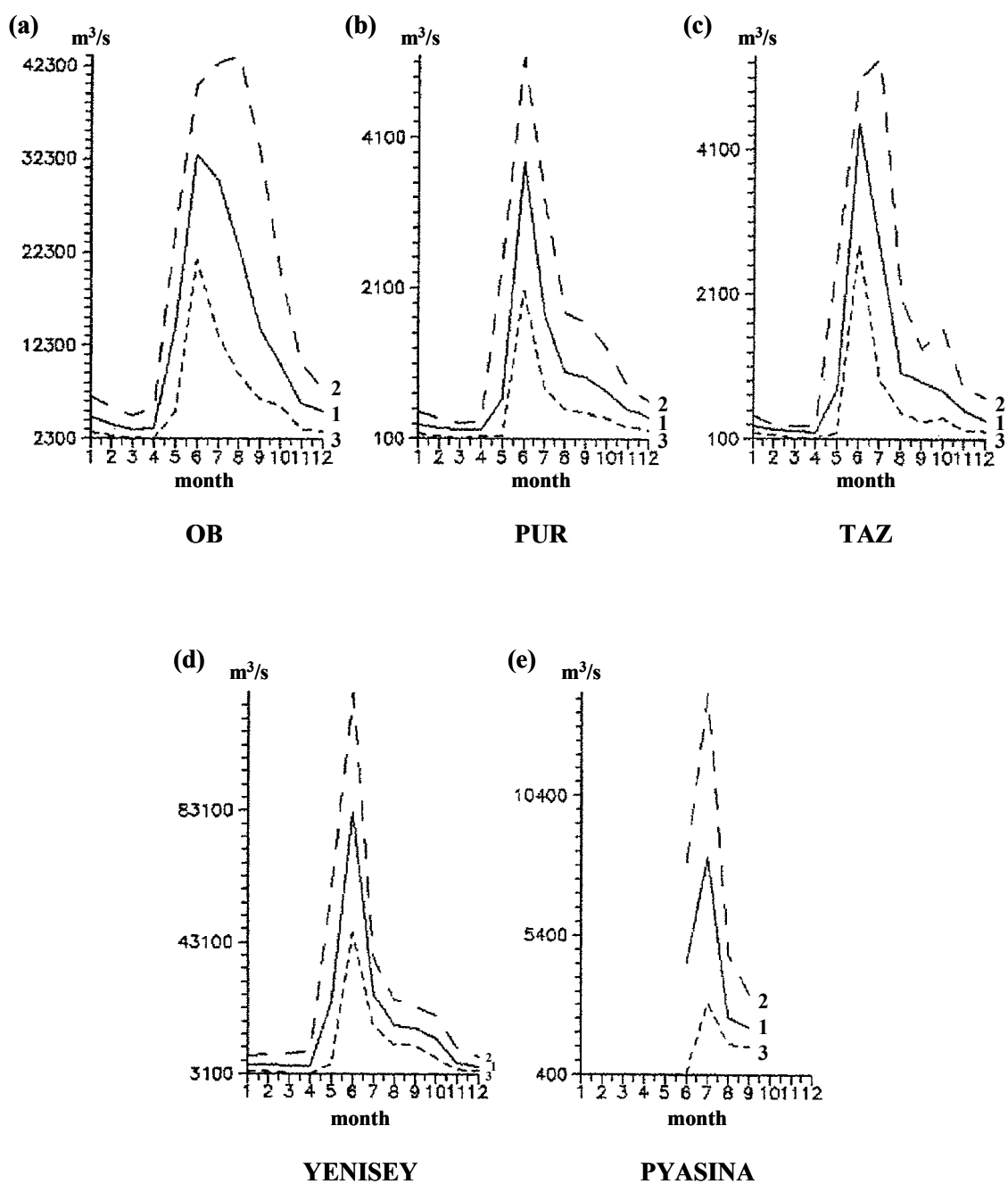
FIG. 5. Average annual cycle of river discharges to the Kara Sea (1 average, 2 maximum, 3 minimum) [4].

TABLE V. INFLOWS AND OUTFLOWS OF KARA SEA (SVERDRUP)[a]

	In	Out	Reference
Through Kara Gate	0.04 – 0.6[b]		[4]
Around northern top of Novaya Zemlya	0.15 – 0.54[b]		[4]
River runoff	0.03		[4]
To Laptev Sea		0.16 – 0.3	[4]
Between Franz Josef Land and Severnaya Zemlya (to Arctic)		0.6 – 0.7[b,c]	[4]

[a]   Sverdrup = $10^6 \cdot m^3 \cdot s^{-1}$
[b]   Only approximate estimates.
[c]   Latter based on volume balance.

The water structure of the Kara Sea is governed by the water inflow from the Arctic basin and the Barents Sea as well as river run-off. There are five main masses:

(1)   the surface waters of the Arctic basin, located in the upper layers;

(2)   the surface waters of the Kara Sea, located in the surface sea layer;

(3)   water from the Ob and Yenisey rivers with low salinity and, in the summer, with a relatively high temperature (7–10°C);

(4)   Barents Sea waters of Atlantic origin with higher temperature and salinity from the north, northwest between Franz Josef Land and Novaya Zemlya and from the southwest through Kara Gate;

(5)   Atlantic waters entering from the Arctic basin by the Svyataya Anna and Voronin Troughs.

The sea is well stratified in summer (to 20 m) in northern and southwestern region but violent autumn storms may mix the entire water column. Salinities are around 32‰ offshore, and 10‰ around the Ob and Yenisey outfalls. Table VI shows the main characteristics of the water masses.

2.1.2.2. Sediment description

The Kara Sea is characterized by relatively low sedimentation rates, with coastal abrasion being the main source of the material. The sediments are predominantly terrigenous, and composed of silt.

Table VII characterizes three regions in the Kara Sea and gives typical values for suspended load and sedimentation rate. In the northern Kara Sea, no data was available, thus it was was assumed that the sedimentation rate was 0.1 mm/year and that the suspended load was 2.8 mg/l. Coastal K_d values were assumed appropriate and the default values as given by IAEA [8] were recommended for use.

In addition, the main rivers (Ob and Yenisey) discharge about 30 million tons of suspended matter annually, although most of this material does not reach the marine sedimentary basin.

The sediments were presumed bioturbated to a depth of 10 cm and a biodiffusion rate of 10^{-12} m^2/sec was assumed.

TABLE VI. MAIN CHARACTERISTICS OF THE WATER MASSES OF THE KARA SEA

Water masses		Surface water of the Arctic Basin	Surface water of the Kara Sea	Modified summer surface water	River water	Barents Sea water	Atlantic water
Winter	Temperature ^{o}C	-1.8	-1.4	–	0	-1.9	2.2
	Salinity ‰	32.0	25.0	–	1.0	35.6	35.0
Summer	Temperature ^{o}C	-1.8	-1.4	7.0	11.7	6.0	2.2
	Salinity ‰	32.0	22.0	24.5	1.0	35.3	35.0

TABLE VII. SEDIMENT PARAMETERS ASSUMED FOR THE KARA SEA

Kara Sea	Suspended load (mg/l)	Sedimentation rate (mm/a)
Novaya Zemlya Trough	5 – 7	0.3 – 0.4
Southeastern zone of Kara Sea	≈ 3.5	0.1 to 2–3
Northern Kara Sea	Insufficient data	Insufficient data

2.1.3. Barents Sea

2.1.3.1. Oceanographic description

The area of the Barents Sea is 1 424 000 km^2 with a volume of 3×10^5 km^3 and is largely open to the Norwegian Sea in the west and the central Arctic basin to the north. The average depth is 230 m, with a maximum depth of 500 m near Bear Island. The position of the Barents Sea between the Atlantic and Arctic Oceans gives it a key role to play in transport of pollutants.

The western boundary is defined by a line from South Cape (on Spitsbergen) to Bear Island to North Cape. The eastern boundary with the Kara Sea has already been defined in the Kara Sea section. The northern boundary is defined by the northern margin of the Franz Josef Land Archipelago, to the Spitsbergen Archipelago.

A number of rivers discharge into the Barents Sea, but the volume is considerably less than that for the Kara Sea. River runoff only significantly affects the southeastern part of the sea.

In the southern part of the Barents Sea, the direction of the currents is predominantly eastward, while in the north the direction is westward or south-westward [9].

A major warm current (the North-Atlantic Current) flows in from the west to the north of North Cape. It divides into two main branches – one which flows eastward (the coastal current system), and one which flows north into the central region. Cold Arctic water enters from the north between Spitsbergen and Franz Josef Land and between Franz Josef Land and Novaya Zemlya. The water circulation in the Barents Sea is generally anti-clockwise. The sea is stratified in spring, becoming well mixed in winter. Salinities are in the range 32–35‰. Table VIII details the main flows between the Barents Sea and adjacent basins.

TABLE VIII. INFLOWS AND OUTFLOWS OF THE BARENTS SEA (SVERDRUP)[a]

	In flow	Out Flow	Reference
Between Bear Island – Norwegian Coast	3.1		[10, 9]
White Sea	0.015		[4]
Pechora (river runoff)	0.003		[4]
Between Spitsbergen – Franz Josef Land	0.5		[4]
Between Bear Island – Norwegian Coast		1.2 (of which bottom 0.8)	[10, 9]
Through Kara Gate		0.04 – 0.6[b]	[4]
Around northern top of Novaya Zemlya		0.15 – 0.54[b,c]	[4]
Franz Josef Land		1.2[b,c]	[9]

[a]   Sverdrup = $10^6 \cdot m^3 \cdot s^{-1}$
[b]   These values are only approximate.
[c]   (Loeng [9] gives average of 1.6 Sv for flow in strait between Franz Josef Land and Northern top of Novaya Zemlya).

The water structure of the Barents Sea can be considered as having four main masses:

(1)   Arctic waters entering as surface currents from the North;

(2)   Atlantic water masses entering from the west as surface currents and from the north and northeast at depth from the Arctic basin;

(3)   coastal waters (forming from continental runoff);

(4)   Barents Sea waters which form within the sea as a result of mixing.

The main characteristics of these water masses are shown in Table IX. The Barents Sea water was estimated to have a renewal period of approximately 5 years. The Barents Sea is an area of high biological productivity, a point which is returned to in Section 2.2.

2.1.3.2. Sediment description

The Barents Sea is also characterized by a low sedimentation rate. The Barents Sea differs from the Kara Sea due to the penetration of warm Atlantic waters resulting in:

(i)   an extensive ice free area all year round where violent storms rework the coastal sediment; and

(ii)   generation of a system of bottom currents which result in dispersion of suspended matter.

Again, the main source of material results from coastal destruction in the Kanin Peninsula, Kolguev Island and Novaya Zemlya. Table X gives values for sedimentation rate and suspended load in four general regions of the Barents Sea. The prevailing types of sediments are silts (sandy and pelitic) [5]. Coastal K_d values were again recommended as default values. The sediments were assumed bioturbated to a depth of 5 cm. The biodiffusion rate was taken to be 10^{-12} m^2/sec.

TABLE IX. MAIN CHARACTERISTICS OF THE WATER MASSES OF THE BARENTS SEA

Water masses		Surface water of the Arctic Basin	Coastal waters	Barents Sea water	Atlantic waters	
					Main	Transformed
Winter	Temperature ^{o}C	1	0 – 4	1	3 – 5	1 – 3
	Salinity ‰	33.0 – 34. 0	33 – 34.5	34. 5 – 34.8	34.5 – 35	34.5 – 35
Summer	Temperature ^{o}C	1	5 – 9	7 – 8	8 – 10	3 – 5
	Salinity ‰	33.0 – 34.0	28 – 34.5	34.3 – 34.7	34.5 – 35	34.5 – 35

TABLE X. SEDIMENT PARAMETERS ASSUMED FOR THE BARENTS SEA

Barents Sea	Suspended load (mg/l)		Sedimentation rate (mm/a)
	range	mean	
Southern coastal zone	1.6 – 21.1	8.0	0.5 – 2.5
Central zone	2.8 – 8.2	5.2	0.1 – 1.2
West of Novaya Zemlya	≤ 5.0		0.1 – 1.2
Bays in Western Novaya Zemlya	1.0 – 300	23	up to 4 – 5

2.1.4. The Arctic Ocean

2.1.4.1. Oceanographic description

The Arctic Ocean has an area of 9.5×10^6 km^2 with a volume of 1.7×10^7 km^3 and is nearly land-locked. It is divided by three submarine ridges into a number of basins, with depths up to 4000 m in places. Large areas are permanently covered by sea-ice. The continental shelf on the European side is broad and divided into five shallow marginal seas.

There are considered to be three main water masses:

(i) Arctic surface water: stretching from the surface to 200 m depth, this water mass has varying temperature and salinity characteristics depending on the ice cover;

(ii) Atlantic water: lying immediately below the surface layer from 200 to 900 m, the temperature of this water mass is above 0°. Typical salinities are around 35‰;

(iii) Bottom water: below the Atlantic water and extending to the ocean floor.

The water budget of the Arctic Ocean is balanced by inflow through the Bering Strait and Norwegian Sea, by precipitation and river runoff and outflow to the Barents and Greenland Sea and through the Canadian archipelago. The estimated inflows and outflows are summarized in Table XI.

TABLE XI. INFLOWS AND OUTFLOWS ASSUMED FOR THE ARCTIC OCEAN (SVERDRUP)[a]

	In flow	Out flow	Reference
Bering Strait	(1.5)		[11]
	0.8 – 0.9		[4]
West Spitzbergen Current	4		[12]
W. of Severnaya Zemlya	0.6		[4]
Sv. Anna Trough	1.2		[11]
Canada Archipelago		2.1	[11]
E. Greenland Current		5	[11]

[a]   Sverdrup = $10^6 \cdot m^3 \cdot s^{-1}$

2.1.5. Ice cover and ice transport

2.1.5.1. Kara Sea

Sea ice begins to form in September, melting in June. In the centre of the sea, even in midwinter, the ice is not solid or continuous. Icebergs can be seen around the northern end of Novaya Zemlya. The ice drift is generally northward to the Arctic basin. In the spring, the ice drift is predominantly westward and southward. There is an extensive ice exchange between the Kara and Barents Sea through Kara Gate.

2.1.5.2. Barents Sea

The southern part of the sea does not freeze. The ice/sea boundary lies at 400–500 km from the mainland shore (at 75° N). Ice inflows occur between Spitsbergen and Franz Josef Land (from the Arctic), from the Kara Sea (around Novaya Zemlya tip in north) and through Kara Gate, and from the White Sea.

The Siberian shelf is thus an important area for ice formation, which is then transported west by the transpolar drift. The transit time from shelf region to the Fram Strait is of the order of 2–3 years. The Kara and Barents Sea export ice in the winter and import in the summer. Approximate values transported are given in Table XII [4]. These values are annual averages.

TABLE XII. ICE TRANSPORT (km^3/a)

Barents Sea to Central Arctic Ocean	32 – 33
Kara Sea to Barents Sea (Kara Gate)	4.6
Kara Sea to Barents Sea (around northern top of Novaya Zemlya)	140 – 198
Barents Sea to Kara Sea	20
Kara Sea to Laptev Sea	50
Kara Sea to Central Arctic Ocean	170
Central Arctic Ocean to Barents Sea	43.5 – 58
Barents Sea to White Sea	50
White Sea to Barents Sea	13.6
Central Arctic Ocean to Greenland Sea by the E. Greenland Current via Fram Strait	2600

2.1.6. Other features

There are a number of processes which are relevant to the area under consideration:

(a)   Deep water formation: The process of deep water formation is known to occur particularly in the Barents Sea, but also in the Kara Sea: – near Novaya Zemlya Island and Franz Josef Land. This may provide an important bypass of the usual vertical transport mechanisms;

(b)   River runoff: Some of the major Arctic rivers including the Ob, Yenisey and Pechora discharge into the Kara and Barents Seas. Estimates of river runoff to the Kara Sea are 1200 km^3/a, 700 km^3/a to the Laptev Sea, and 340 km^3/a to the Barents Sea [13].

2.2. BARENTS AND KARA SEAS ECOSYSTEMS

A schematic and simplified description of the ecology of the Barents and Kara Seas is given in the following section. Only species of commercial importance or species which form the basis of the food chain for fish and sea mammals were considered [14]. Some site specific information was incorporated, however information on the local population was limited. In the absence of the necessary site specific information, a number of simplifying assumptions were made.

2.2.1. Novaya Zemlya Fjord

A simple food chain model was used for the Novaya Zemlaya Fjordi and is shown in Figure 6. In the absence of site and species specific values, concentration factors from IAEA-TRS-247 [8] were recommended to be taken as default values for the foodchain model. For seals, it was suggested that the concentration factor for fish be used.
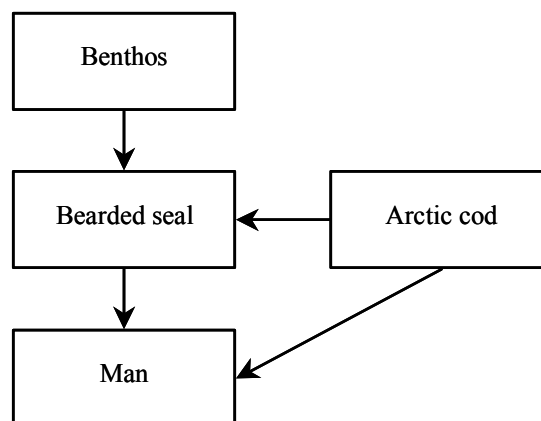
FIG. 6. Food chain model adopted in the study for the Novaya Zemlaya Fjord.

2.2.2. Ecological characteristics of the Kara Sea

The Kara Sea is a typical arctic shelf sea. The environmental conditions of the Kara Sea are influenced greatly by cold advection from the Arctic basin and vigorous flows of the large Siberian rivers (the Ob, the Yenisey, etc.). The mountainous barrier of the Novaya Zemlya archipelago reduces the influence of warm Atlantic waters and atmospheric cyclones on the Kara Sea climatic conditions. The Kara Sea climate is essentially polar and more severe than the Barents Sea climate. The extent of the Kara Sea from southwest to northeast results in significant climatic variations over different areas of the sea.

The vegetation season for the Kara Sea is about four months (July–October). There are no reliable estimates of the Kara Sea productivity since no year-round biological observations have been made over large areas of the sea. Tentatively, the Kara Sea productivity is 3–5 times lower as compared with the Barents Sea. The most productive zone of the sea is its southwestern sector which is influenced by the Barents waters entering through the Kara Strait and Yugorsky Char Strait and the freshened (brackish) sea waters which are influenced by the Ob and the Yenisey flows [15, 16].

The spring bloom of phytoplankton begins in July in the Kara Sea southern and southwestern sectors; then it shifts to the north and north-east areas of the sea. The spring complex of phytoplankton is formed by arctoboreal diatomic algae (the mass species: *Thalassiosira gravida, Th. nordenskioldii, Fragilaria oceanica*). In the second half of August the spring complex is replaced by the summer phytoplankton complex with predominance of peridinium algae.

The Kara Sea zooplankton biomass amounts, on the average to 50 mg/m^3; in the most productive sectors of the sea it may be as high as 500 mg/m^3. In the Kara Sea western regions the average benthos biomass is about 50 g/m^2; for the shoals it amounts to 100-300 g/m^2 and more. In the central regions this quantity is about 1–3 g/m^2; in the shoals the benthos consists mainly of mollusks Bivalvia.

The Kara Sea is far lower in ichthyofauna as compared with the Barents Sea. The severe climatic conditions prevent Barents Sea fish from moving here. The Atlantic boreal and arcto-boreal fish species have a limited occupational area in the Kara Sea being found mainly in the southwestern sectors.

Polar cod is the most numerous and widespread species in the Kara Sea [17]. Spawning of the Kara polar cod occurs in winter in the Barents southeastern region. It is possible also that spawning occurs under ice in the Kara Sea, typically in the most productive zones (along the coastal regions).

Navaga inhabits the coastal areas of the Baidaratskaya Bay. Spawning of navaga occurs in the freshened waters and river mouths (e.g. Ob) [16].

Polar plaice is found usually in the Kara freshened waters in the Yenisey and Ob Bays.

In the Kara Sea open waters, the fish population is small; made up mainly of species with no commercial value (*Licodes spp., Liparis spp.*).

The freshened seawaters of the Ob-Yenisey sector are of relatively high productivity; industrial fisheries have developed here [18]. In the Ob-Yenisey sector of the Kara Sea migratory and semi-migratory fish are of commercial importance (smelt, whitefish, nelma, golets, etc.); among sea fish, navaga and polar cod are of commercial value.

Sea mammals of commercial significance in the Kara Sea are ringed seal, bearded seal and white whale.

A general scheme of trophic relations in the ecosystem of the Kara Sea is given in Figure 7. The list of important fish species in the Kara Sea is presented in Table XIII.

2.2.2.1. Basic food chain

The basic food chains in the Kara Sea are shown in Figure 7. The arctic cod and to some extent, navaga, play the same roles in the ecosystem of the Kara Sea as capelin in the ecosystem of the Barents Sea. Sea mammals, such as greenland and ringed seals and white whales eat fish and so they, along with man, are top predators.

2.2.2.2. Fishing in the Kara Sea

There is no commercial catch of fish in the open part of the Kara Sea. Data on fisheries in the Kara Strait and the adjacent southwestern region of the Kara Sea are included in the statistical data for the Barents Sea. No separate fishery statistics for the Kara Sea are reported. According to many authors, fish from the Barents Sea reach the Kara Sea only occasionally, so there is no large exchange of fish populations from the Barents Sea to the Kara Sea. Statistical fishery data are reported for the largest gulfs of the Kara Sea: Yenisey and Ob Bays [19]. The data on the catch of fish in these gulfs are given in Tables XIV and XV. Owing to a considerable water exchange between the gulfs and the Kara Sea, all species of fish in the gulfs are in contact with seawater desalinated by the river flow. Of the most importance for radioecological assessment are data on the catch in the gulfs of those species that spend part of their life cycle in the sea. Among such species are sea fish (navaga and polar cod) moving to the gulfs for feeding, as well as migratory fish (smelt, whitefish, etc.). The migratory species of fish spend most of their life cycle in the Kara Sea (predominantly, its southwestern and southern parts, as well as gulfs) and go to the rivers only for spawning. Commercial fishing of the migratory species is usually carried out during spawning in the mouths of the Ob and Yenisey Rivers.

2.2.2.3. Commercial catch of sea mammals in the Barents and Kara Seas

Of commercial importance for the Barents and Kara Seas are the following species of sea mammals: Greenland seal, bearded seal, ringed seal and white whale.

An important area of sea mammal catch is the White Sea (actually, it is a great gulf of the Barents Sea). The main catch of Greenland seal occurs in the White Sea and amounts to 30 500 young animals (under 1 year) per year. The annual catch of ringed seal amounts to 1300 animals in the White Sea, 1600 animals in the remaining part of the Barents Sea and 5200 animals in the Kara Sea. The catch limits of bearded seal and white whale are 700 heads per year for each species in the entire area.
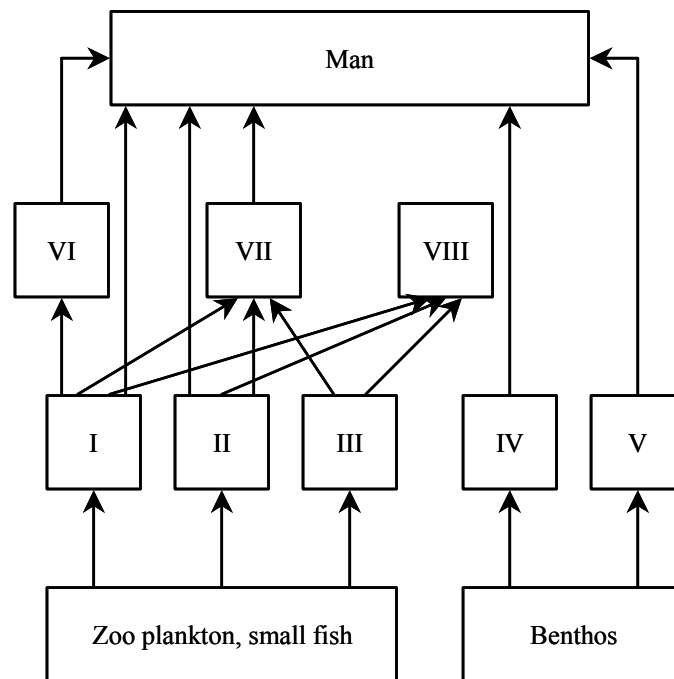
I – Arctic cod; II – Navaga; III – Liparis; IV – Polar flounder; V – Bearded seal;
VI – Greenland seal; VII – Ringed seal; VIII – Sea birds.

FIG. 7. Thropic relationshipships in the ecosystem of the Kara Sea [14].

TABLE XIII. FISH SPECIES ABUNDANT IN THE KARA SEA

Fish of commercial importance:	
Polar cod	*(Boreogadus saida)*
Navaga	*(Eleginius navaga)*
Smelt	*(Osmerus eperlanus dentex Stein.)*
Whitefish	*(Coregonus sardinella Val.)*
Arctic cisco	*(C. autumnalis)*
Muksun	*(C. muksun Pal.)*
Siberian whitefish	*(C. lavaterus pidschian)*
Nelma	*(Stenodus leucichtys nelma Pal.)*
Siberian sturgeon	*(Acipencer baeri)*
Golets	*(Salvenius alpinus)*
Non-commercial fish:	
Liparis spp.	(Fam. *Liparididae*)
Triclops spp.	(Fam. *Cottidae*)
Icelus spp.	(Fam. *Cottidae*)
Lycoes spp.	(Fam. *Zoarcidae*)
Gymnelis spp.	(Fam. *Zoarcidae*)
Lumpenus spp.	(Fam. *Lumpenidae*)

TABLE XIV. CATCH OF FISH TAKEN BY USSR IN THE OB BAY OF THE KARA SEA IN 1985–1990 (TONNES/YEAR) [14]

Fish	1985	1986	1987	1988	1989	1990
Total	2406	2215	2672	2120	2478	2362
Freshwater fish:	836	791	929	888	691	836
Sea fish, migratory and semi-migratory fish:						
Smelt	31	378	379	211	516	280
Whitefish	1356	981	1265	968	1209	1217
Siberian whitefish	6	29	7	3	9	11
Whitefish, muksun	17	11	77	14	17	18
Nelma	–	–	4	5	–	–
Navaga	2	–	–	–	–	–
Fish unsorted, unidentified	158	25	11	31	36	–

TABLE XV. CATCH OF MIGRATORY AND SEMI-MIGRATORY FISH IN THE YENISEI BASIN IN 1985–1990 (TONNES/YEAR) [14]

Fish species	1985	1986	1987	1988	1989	1990
Siberian sturgeon	23.4	4.1	12.6	8.1	11.7	12
Nelma	68.8	2.0	1.5	0.2	1.7	1
Whitefish	259.3	86.5	74.0	61.2	66.0	39
Arctic cisco *(Coregonus autumnalis)*	170.2	45.5	20.5	0.2	19.8	36
Cisco *(C. lavaterus)*	340.9	190.1	173.9	156.8	157.0	137
Whitefish, muksun	311.9	2.0	1.0	–	1.1	1
Smelt	107.2	2.7	0.5	–	0.1	–
Golets	–	8.7	7.0	4.3	3.9	0
Total	1281.7	341.6	291.0	230.8	261.3	226.0

2.2.3. Ecological characteristics of the Barents Sea

The Barents Sea is a high-latitude shelf sea. Its climate is a polar marine one with short cold summers and long winters. A unique feature of climatic conditions of the Barents Sea is the penetration of large water masses of the warm North-Atlantic current into the polar water body [20]. Together with an active light regime of the polar summer, the natural conditions of the Barents Sea are favourable for the development of highly productive marine ecosystems.

This section presents a brief ecological characteristic of the Barents Sea and a description of the main species of commercial importance.

2.2.3.1. The general structure of the Barents Sea ecosystem

Plankton is the basis for food chains of the Barents Sea ecosystems. The primary production of phytoplankton in the Barents Sea is estimated at 50–180 g of carbon under 1 m^2 per year [21]. Compared with southern seas, the phytoplankton is characterized by a small number of species and relatively short-term development. Species composition of phytoplankton was not considered important for this assessment and so is not presented here.

Marine zooplanktonic organisms of the Barents Sea are the main source of food for many commercial species of fish. Fry of predatory fish also feed on zooplankton. A small number of zooplankton species is typical of the polar seas. In particular, 80–90% of the biomass of mesozooplankton is accounted for by Calanus finmarchicus (length ~ 0.4 cm, mass ~ 1-2 mg). Large zooplankton are dominated by euphausiids (length ~ 3 cm, mass ~ 250 mg): Thysanoessa inermis and Th. raschii. Large-sized zooplankton, consisting mainly of "red" calanus and euphausiids with lengths of 0.5–5 cm are the main sources of food for the majority of young fish in the Barents Sea. The annual production of zooplankton is estimated at 0.6-0.9 g/m^2 per year [21].

The total natural reserves of fish in the Barents Sea are estimated at 30–40 million tonnes. Among the 150 species of fish of the Barents Sea, 20–25 species are of commercial importance. The most abundant of pelagic plankton-eating fish are capelin, polar cod and herring; of mixed feed and predatory fish are cod, redfish and Greenland halibut; of benthophages are haddock, catfish and European plaice. These are listed in Table XVI.

Among the invertebrates, only the northern pink shrimp *(Pandalus borealis)* and the red calanus *(Calanus finmarchicus)* are of commercial importance [22, 23].

Several species of sea mammals inhabit the Barents Sea. Of commercial importance are greenland seal, bearded seal, ringed seal and white whale (Table XVI).

Sea birds are numerous on the coastal zone and islands of the Barents Sea. The common feeding object of sea birds is fish. Eggs of sea birds can be used for food by natives.

A general scheme of trophic relations in the ecosystem of the Barents Sea is given in Figure 8.

TABLE XVI. COMMERCIALLY IMPORTANT SPECIES OF MARINE BIOTA IN THE BARENTS SEA

Fish:	
Arcto- Norwegian cod	*(Gadus morphua)*
Polar (artic) cod	*(Boreogadus saida)*
Atlantic herring	*(Clupea harengus)*
Capelin	*(Mallotus villosus)*
Haddock	*(Melanogrammus aeglefinus)*
Redfishes	*(Sebastes marinus, S. mentella)*
Saithe	*(Pollachius virens)*
Greeland halibut	*(Reinhardtius hippoglossoides)*
European plaice	*(Pleuronectes platessa)*
Sea mammals:	
Greenland seal	*(Pagophilus groenlandicus)*
Ringed seal	*(Pusa hispida)*
Bearded seal	*(Erignatus barbatus)*
White whale	*(Delphinapterus leucas)*
Invertebrates:	
Pandalid shrimps	*(Pandalus borealis)*
Red calanus	*(Calanus finmarchicus)*
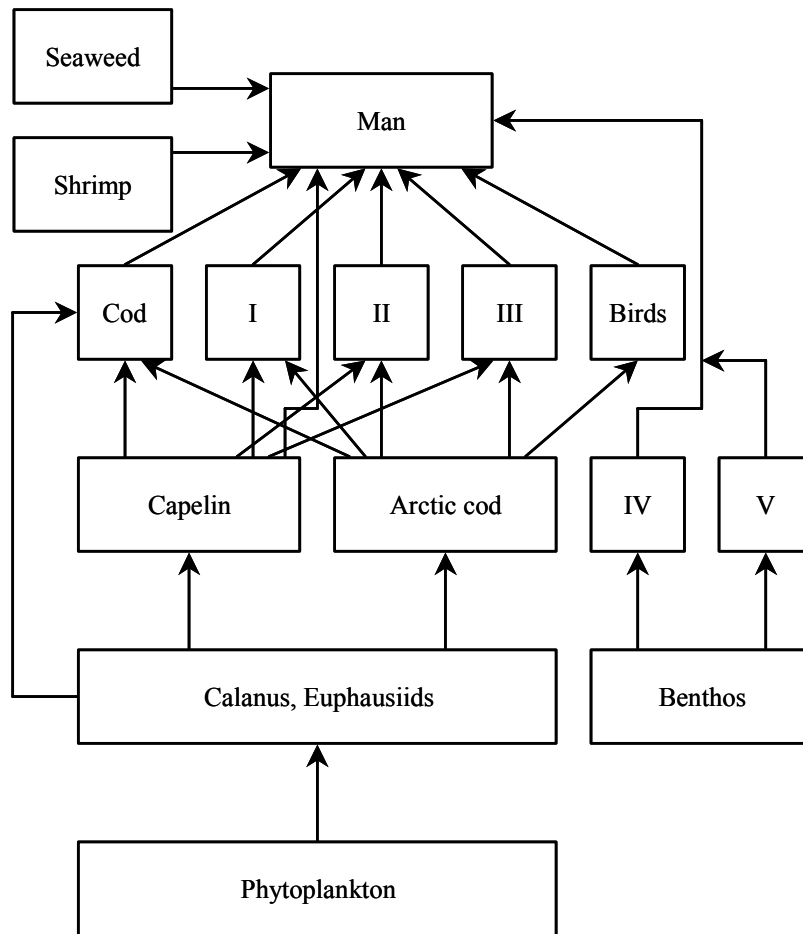
I – Haddock; II – Norway haddock; III – White whale, Ringed seal, Greenland seal; IV – Flounder; V – Bearded seals.

FIG. 8. Trophic relationships in the ecosystem of the Barents Sea [14].
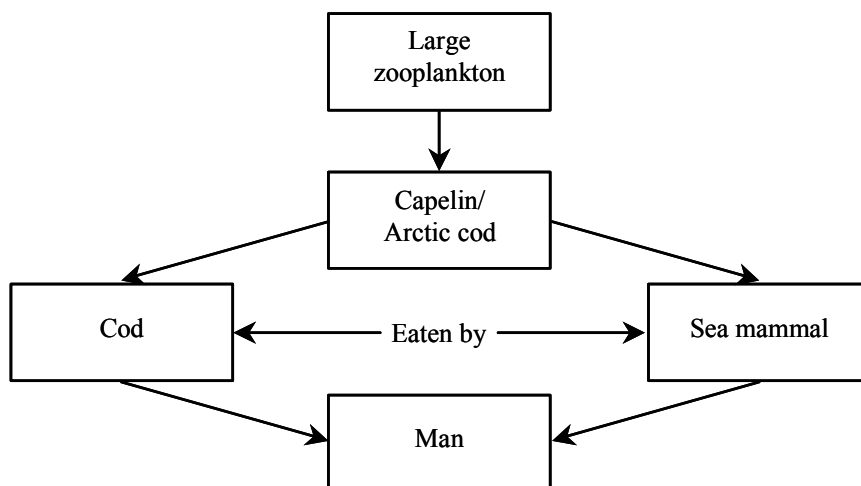
FIG. 9. Basic food chain model for the Barents Sea adopted in the study.

2.2.3.2. Basic food chains in the Barents Sea

The scheme of basic food chains in the Barents Sea is shown in Figure 8. The basic food for fish of relatively small size (length < 30 cm) is zooplankton (calanus, euphausiids). Zooplankton is used as a common food by capelin, herring, arctic cod and the young of predatory fish (cod, pollack, haddock). Predatory fish with length greater than 30 cm eat capelin, arctic cod and young fish of other species. The common food for sea mammals such as Greenland ringed seals and white whale is fish.

For the preliminary assessment a simplified 'typical' food chain for the Barents Sea is shown in Figure 9.

A typical benthic food chain was also defined, consisting of benthic organisms which are consumed by flounder and bearded seal, and then, in their turn, are caught by man. The benthic food chain may be important for any local scale assessment.

2.2.3.3. Fish migration, species location

Many commercial fish of the Barents Sea spawn in the Norwegian Sea (cod, herring, pollock, haddock and Norway haddock). Later small young fish come into the Barents Sea with warm currents and live there until reaching maturity (3–5 years). Adult fish return again to the Norwegian Sea to spawn. Thus, some of the fish which are caught near Norway have spent several years in the Barents Sea. Figures 10–13 show migratory paths of the commercially important species.

Many species of fish form local populations and spend all their time in the Barents Sea. Capelin, cod and flounder lay eggs at shallow spots near the Kola peninsula in the southwestern part of the Barents Sea. The preferred dwelling places for cod, Norway haddock, capelin, flounder are the southern and southwestern parts of the Barents Sea. During the summer months, there are seasonal migrations from the southwestern to the southeastern parts of the Barents Sea. These would extend to the western shores of Novaya Zemlya islands in warm years. Arctic cod abound near Kolguev Island and near the southwestern shores of Novaya Zemlya islands.

2.2.3.4. Commercial fishing in the Barents Sea

For a detailed assessment it is important to have precise information on the annual catch of fish from the Barents Sea by different countries. Statistical information on catches were collected based on ICES statistical data. Three ICES statistical areas were taken into considerations: Barents Sea (ICES subarea I), Norwegian Seas (ICES subarea IIa) Spitsbergen and Bear Island area (ICES subarea IIb). These statistical zones cover the whole area of Barents fish seasonal migrations. Detailed statistical data were published in ICES Bulletins for the period up to 1990. More recent information is available from Internet web site http://www.ices.dk. Tables XVII and XVIII show the catch figures for various fish species (1990) and other sea products (1988). Tables XIX(a) and XIX(b) give the total catch in three ICES fishing areas [22]. These figures were rather refined at the final scenario description for the calculation of collective dose.
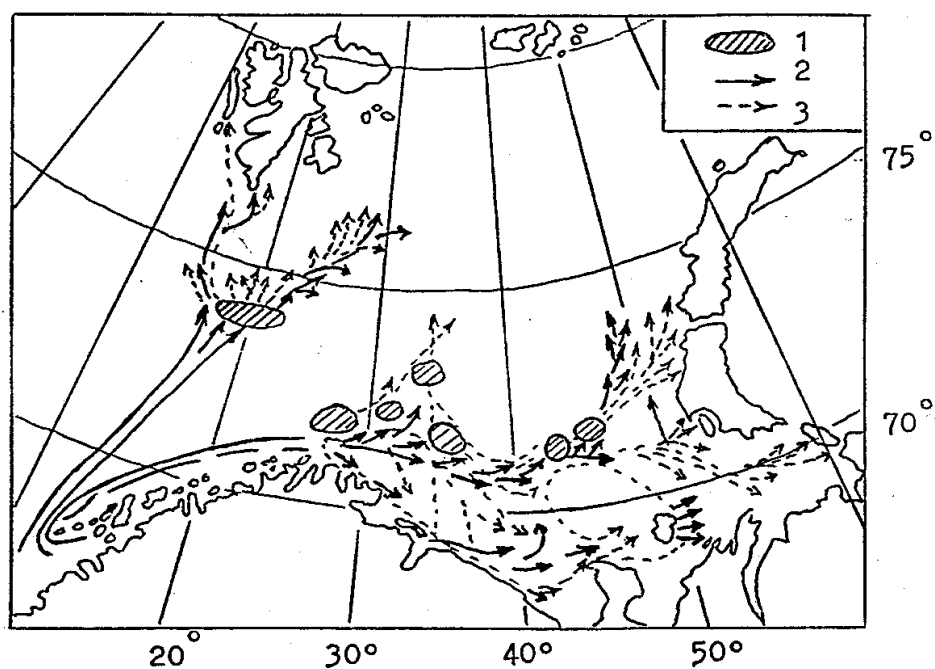
FIG. 10. Routes of the eastward migration of the Lofoten-Barents Sea cod [24].
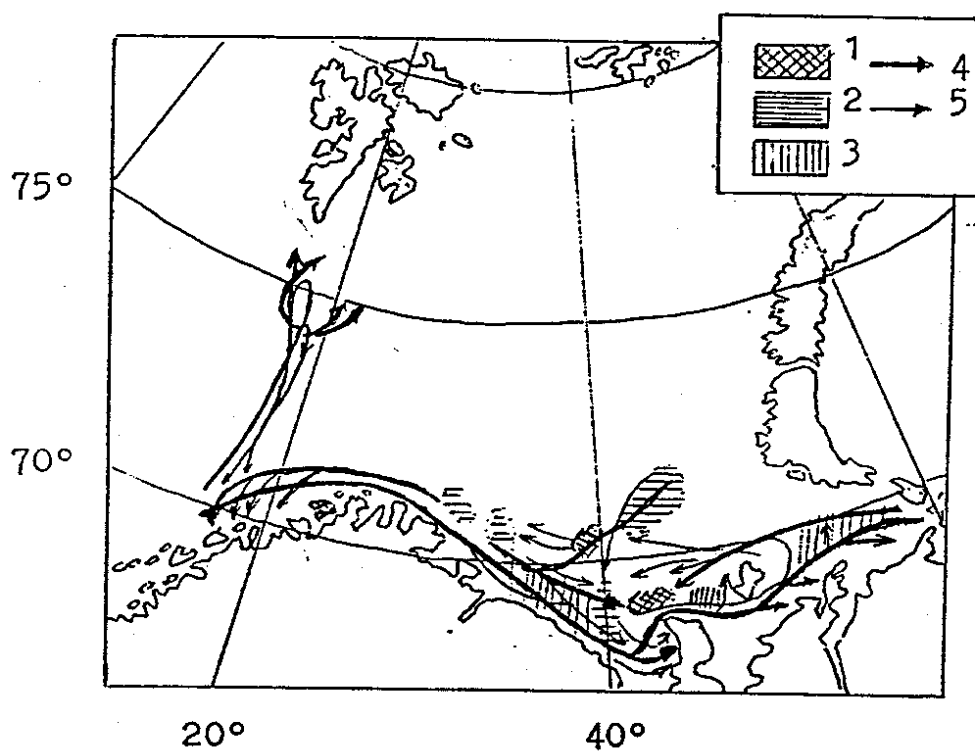
1 = pre-spawning concentrations of haddock; 2 = wintering areas; 3 = areas of summer and autumn concentrations; 4 = migrations of mature haddock; 5 = migrations of immature haddock.

FIG. 11. Migrations of haddock in the Barents Sea [24].

27

a)

1983

78°

74°

70°

10°   20°   30°   40°   50°   60°

0.1-1 ind/m²

1.1-10 ind/m²

10.1-100 ind/m²

over 100 ind/m²

ice edge

b)

1984

78°

74°

70°

10°   20°   30°   40°   50°   60°
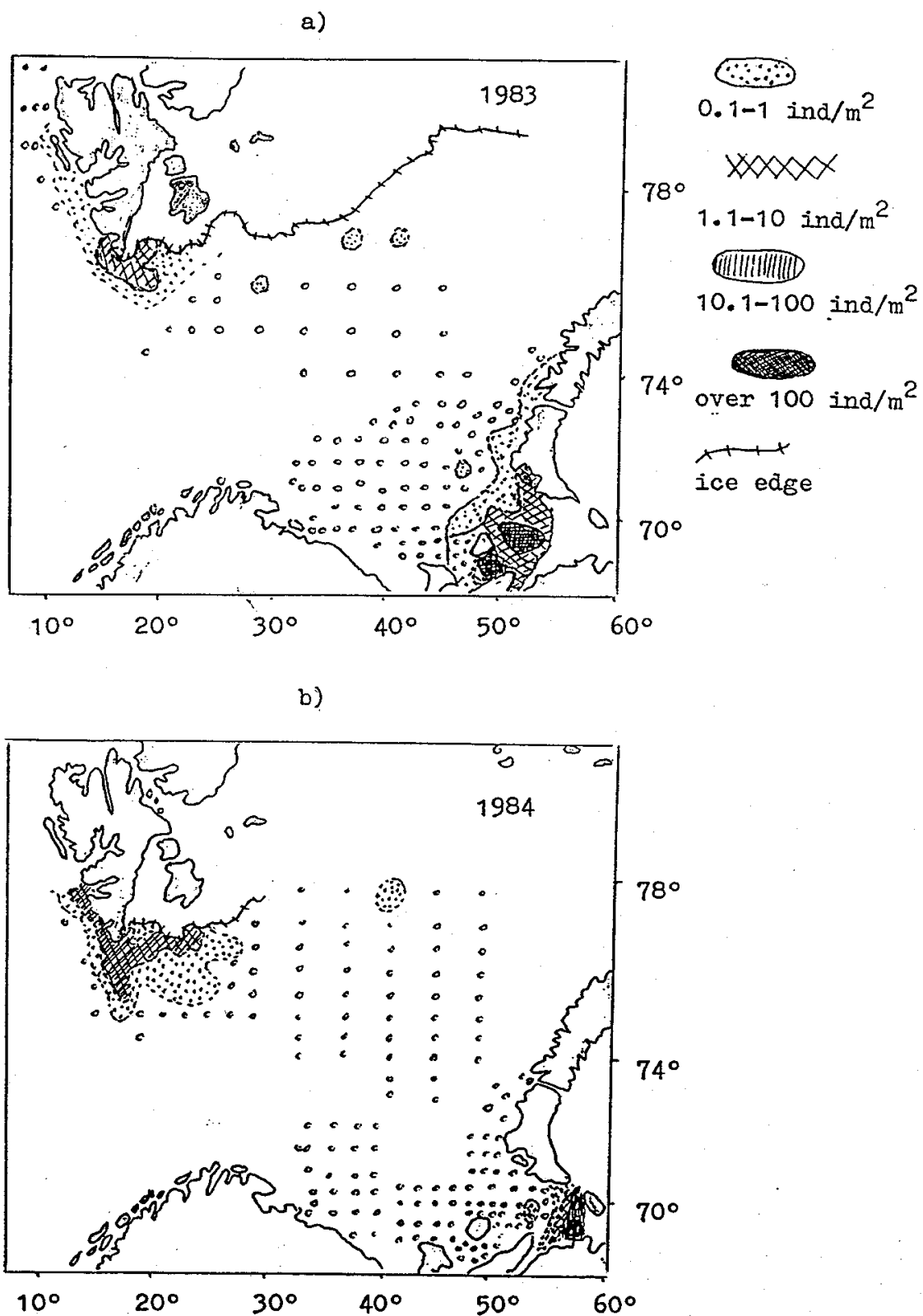
FIG. 12. Distribution of polar cod larvae in the Barents Sea in 1983 (a) and 1984 (b) [17].

28
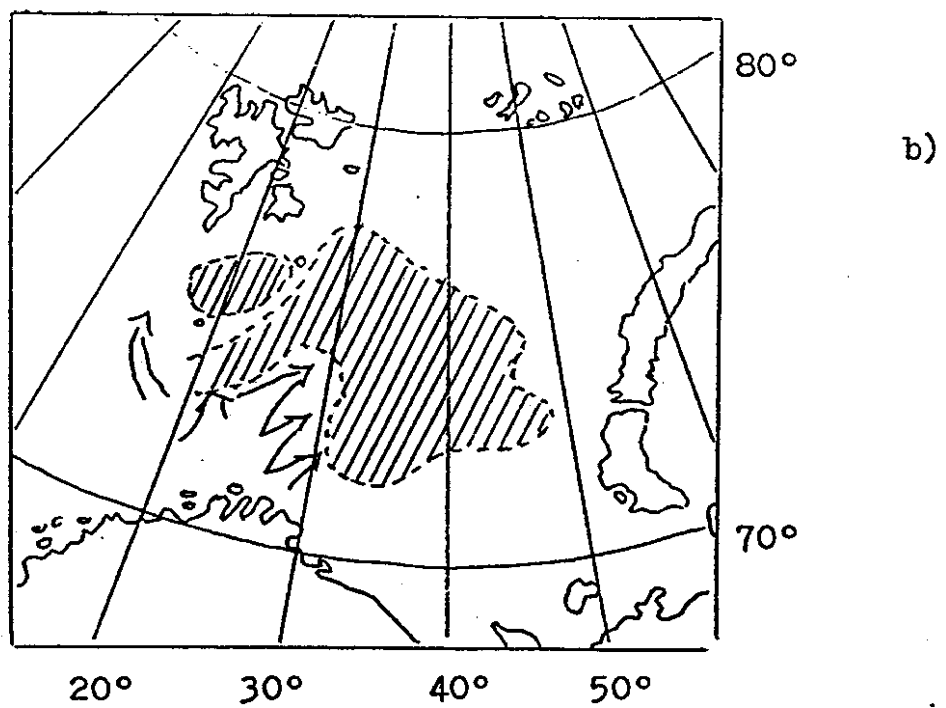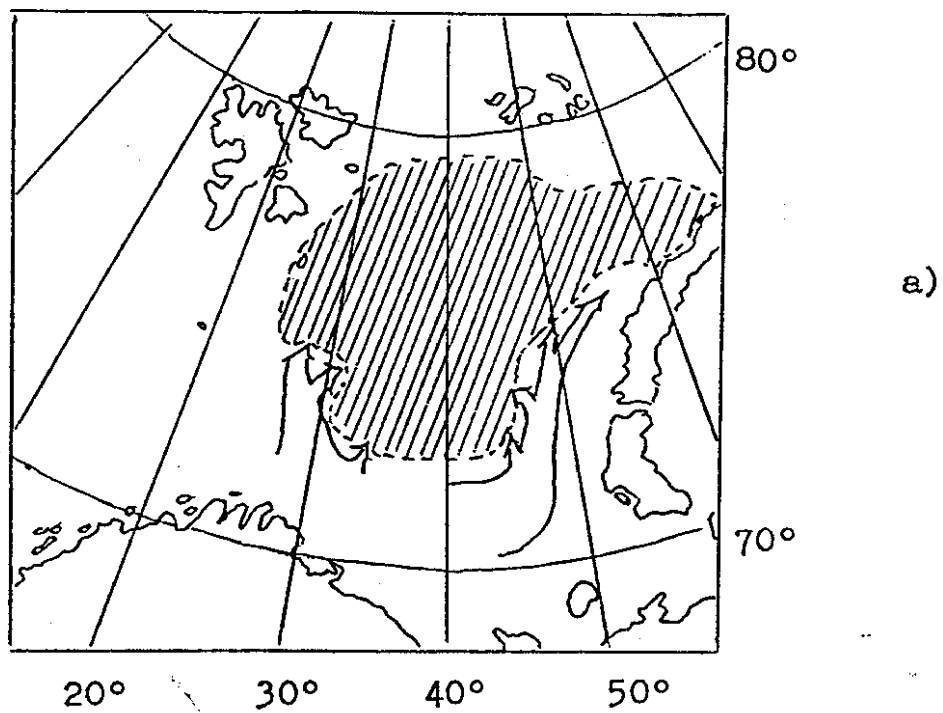
FIG. 13. Routes of the feeding migration of capelin in July–August and feeding areas in September (shaded) for warmer (a) and colder (b) [25].
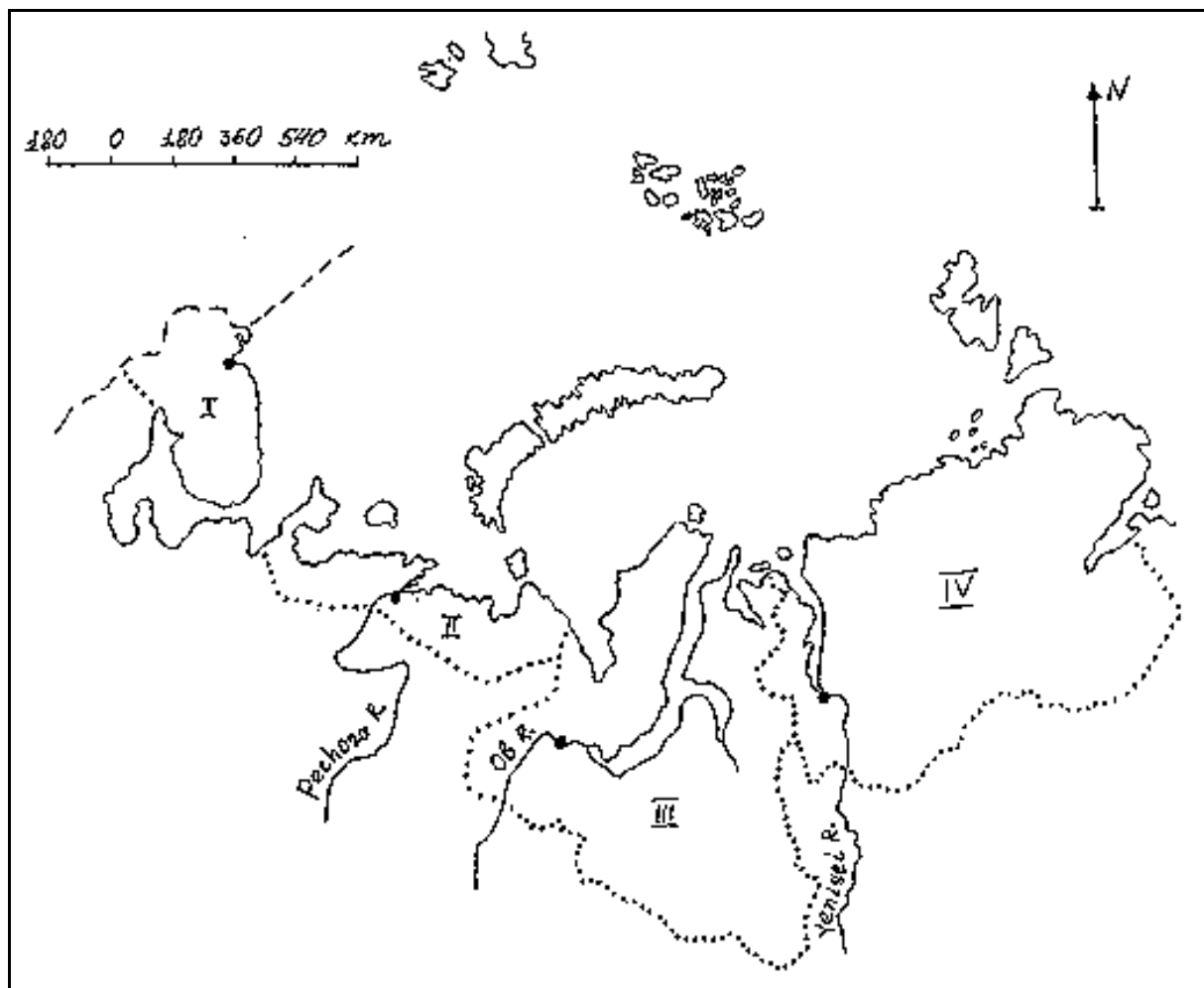
I = Murmansk Region (Murmansk); II = Nenets Autonomous District (Nariyan Mar);
III = Yamalo-Nenets Autonomous District (Salekhard); IV = Taymyr Autonomous District
(Dudinka).

FIG. 14. Administrative regions and centers of the Russian Federation adjacent to the study area.

TABLE XVII. NOMINAL CATCH (TONNES) OF THE VARIOUS SPECIES OF FISH TAKEN BY MEMBER COUNTRIES IN THE SUB-AREAS I (BARENTS SEA), IIa (NORWEGIAN SEA) AND IIb (SPITSBERGEN AND BEAR ISLAND) OF THE ICES STATISTICAL AREA IN 1990 [22]

Species/Country		1990		
		Barents Sea I	Norwegian Sea IIa	Spitsbergen Bear Island IIb
Cod	Soviet Union	40 826	25 728	7 837
	Norway	18 500	96 800	2000
Total (including other countries)		65 400	29 000	11 300
Capelin	Soviet Union	–	–	–
	Norway	–	3200	–
Total (including other countries)		–	8100	–
Haddock	Soviet Union	3375	1449	183
	Norway	9800	10 900	200
Total (including other countries)		13 500	13 000	500
Herring	Soviet Union	1758	11 818	–
	Norway	–	66 166	–
Total (including other countries)		1758	77 984	–
Saithe	Soviet Union	18	34	–
	Norway	7825	84 120	155
Total (including other countries)		7964	86 062	156
Redfishes	Soviet Union	114	6884	11 920
	Norway	8400	26 900	100
Total (including other countries)		8500	36 000	16 800
Greenland halibut	Soviet Union	292	1204	2840
	Norway	4300	9700	3300
Total (including other countries)		4600	11 000	7000
Polar cod	Soviet Union	63	–	–
	Norway	–	–	–
Total (including other countries)		63	–	–
Poutassou	Russia	–	1540	–
	Norway	–	600	–
Total (including other countries)		–	2100	–
Plaice (European)	Soviet Union	200	–	–
	Norway	–	–	–
Total (including other countries)		200	–	–

TABLE XVIII. NOMINAL CATCH (TONNES) OF INVERTEBRATES AND SEAWEEDS TAKEN BY MEMBER COUNTRIES IN THE SUB-AREAS I (BARENTS SEA), IIa (NORWEGIAN SEA) AND IIb (SPITSBERGEN AND BEAR ISLAND) OF THE ICES STATISTICAL AREA IN 1988 [22]

Species/Country		Barents Sea I	Norwegian Sea IIa	Spitsbergen Bear Island IIb
		1988		
Pandalid shrimps	Soviet Union	8118	–	4202
	Norway	14 272	3154	14 595
Total (including other countries)		22 459	3158	23 073
Various molluscs	Soviet Union	20	–	–
	Norway	593	640	19 035
Total (including other countries)		2400	640	23 900
Brown seaweeds[a]	Soviet Union	2563	–	520
	Norway	–	–	–
Total (including other countries)		2563	–	520
Red seaweeds[a]	Soviet Union	215	–	–
	Norway	–	–	–
Total (including other countries)		215	–	–

[a]   Dry weight.

TABLE XIX(a). TOTAL NOMINAL CATCH (TONNES) OF FISH TAKEN BY MEMBER COUNTRIES IN THE ICES STATISTICAL AREA IN 1988, BY FISHING AREAS [22]

Country	Barents Sea I	Norwegian Sea IIa	Spitsbergen Bear Island IIb	Total catch (Subareas I, IIa, IIb)	
		1988 Breakdown by ICES fishing area			
Denmark	–	367	–	367	(<1%)
Faroe Islands	7796	10 775	908	19 479	(1.5%)
France	–	6779	–	6779	(<1%)
German Dem. Rep.	244	1868	1035	3147	(<1%)
Germany, Fed. Rep.	607	8635	1060	10 302	(<1%)
Iceland	–	91 608	–	91 608	(7.4%)
Netherlands	134	–	–	134	(<1%)
Norway	96 766	608 527	21 393	726 686	(58.9%)
Poland	–	15	–	15	(<1%)
Portugal	–	615	2254	2869	(<1%)
Spain	–	11 073	–	11 073	(<1%)
UK (England & Wales)	1619	4285	3592	9496	(<1%)
UK (Scotland)	–	165	65	230	(<1%)
USSR	145 709	169 701	36 592	352 002	(28.5%)
Total	252 875	914 413	66 899	1 234 187	(100%)

TABLE XIX(b). TOTAL NOMINAL CATCH (TONNES) OF INVERTEBRATES TAKEN BY MEMBER COUNTRIES IN THE ICES STATISTICAL AREA IN 1988, BY FISHING AREAS [22]

Country	1988				
	Breakdown by ICES fishing area				
	Barents Sea I	Norwegian Sea IIa	Spitsbergen Bear Island IIb	Total catch (Subareas I, IIa, IIb)	
Faroe Islands	1856	4	9140	11 000	(14%)
Norway	14 868	5807	33 630	54 305	(70%)
USSR	8138	–	4202	12 340	(16%)
Total	24 862	5811	46 972	77 645	(100%)

2.3. HUMAN POPULATIONS

2.3.1. A demographic description of the Russian territories adjacent to the Barents and Kara Seas

2.3.1.1. Territories adjacent to the Barents Sea

The coastal areas of the Barents Sea administratively belong to the Murmansk Region and the Nenets Autonomous District, which is part of Arkhangelsk Region (see Figure 14).

Murmansk Region occupies the Kola Peninsula and extends to the southwestern coast of the Barents Sea.

Nenets Autonomous District is situated along the length of the southern coast of the Barents Sea from the Kanin Peninsula to Baidaratskaya Bay. Kolguev Island and the Novaya Zemlya archipelago also belong to the Nenets Autonomous District.

2.3.1.2. Territories adjacent to the Kara Sea

The southern coast of the Kara Sea administratively belong to the Yamalo-Nenets Autonomous District, which is part of Tyumen' Region, and the Taymyr Autonomous District, which is part of Krasnoyarsk Region (see Figure 14).

The Yamalo-Nenets Autonomous District occupies the Yamal peninsula, part of the Gydansk peninsula and the lower reaches of the Ob and Taz Rivers, including Ob and Taz Bays.

The Taymyr Autonomous District occupies the Taymyr peninsula; the lower reaches of the Yenisey River, including Yenisey Bay, the islands of Franz Josef Land and Severnaya Zemlya.

2.3.2. Population distribution and density

The area and population of administrative regions on the coast of the Barents and Kara Seas are given in Table XX [26].

The average population density in the Nenets, Yamalo-Nenets and Taymyr Autonomous Districts is less than 1 person per 1 km^2. In the coastal areas of the Kola Peninsula (Murmansk Region) the population density is less than 10 persons per 1 km^2. A more dense population is characteristic of the estuaries in the Barents and Kara Seas, as well as of the bays. The population density distribution is presented in Table XX.

2.3.3. Nationalities of the population in the regions adjacent to the Barents and Kara Seas

Russians constitute a major part of the population on the coast of the Barents and Kara Seas. The indigenous population is represented by "nationalities of the North" that are small in numbers, namely, nenets, dolgans, nganasans and selkoops.

Table XXI presents the numbers of the indigenous people living in the territory of the above listed administrative regions [27].

TABLE XX. THE AREA AND POPULATION OF ADMINISTRATIVE REGIONS ON THE COAST OF THE BARENTS AND KARA SEAS [26]

Administrative region	Area km$^2 \times 10^3$	Population	Urban %	Rural %	Population density per km^2
Murmansk Region	144.9	1 155 000	92	8	8.0
Nenets Autonomous District	176.7	55 000	62	38	0.3
Yamalo-Nenets Autonomous District	750.3	495 000	78	22	0.7
Taymyr Autonomous District	862.1	55 000	67	33	0.1

TABLE XXI. NATIONALITIES OF THE NORTH, LIVING IN THE REGIONS ADJACENT TO THE BARENTS AND KARA SEAS [27]

Administrative region	Indigenous population	Comments
Nenets Autonomous District	6000	Nenets
Yamalo-Nenets Autonomous District	19 000	Nenets (17 400), selkoops (1600)
Taymyr Autonomous District	8200	Nenets (2300), dolgans (5900)

2.3.4. Economic activities of the natives in the western part of the Russian Arctic

In the European part of the Russian Arctic, the Nenets population lives in the area between the eastern coast of the White Sea and the Ural Mountains. In the Asian part of the Russian Arctic, the Nenets people inhabit the lower reaches of the Ob' and Yenisey rivers, and the Yamal, Tazovsk and Gydansk peninsulas. Nenets settlements are also found on Kolguev and Vaigach islands.

The main occupation of the Nenets populations is reindeer breeding. They also hunt wild reindeers and fur-bearing animals, such as polar fox, polar wolf and Arctic hare.

An important economic activity is fishing. There is a network of fish factories in Arkhangelsk and Tyumen' Regions. Fish, such as whitefish, omul, pelad, Arctic char and white salmon (nelma), in rivers and tundra lakes occupies an important place in the life of the Nenets.

An important occupation of the population on coasts of the Arctic seas is hunting sea mammals. Hunting artels (co-operative associations) in the Ob', Gydansk and Taz Bays, as well as in the Yenisey Bay, are engaged in hunting ringed seals. Hunting bearded seals is typical of the western shores of the Yamal peninsula and Dikson island. White whales dwelling near the coast of Yamalo-Gydansk Region come to the Ob, Taz and Gydansk Bays, and to the Yenisey Bay, where hunting artels hunt these sea mammals. For the winter, white whales migrate to the Barents Sea by the Novaya Zemlya straits or round the Novaya Zemlya archipelago. In the Barents Sea, hunting ringed seals takes place in the Cheskaya Bay, Pechora Sea and on the Nenets shore (see Figure 14).

In the White Sea region, fish and sea mammals are caught by the Russian coast-dwellers and the Komi population. Fishing plays an important part in the life of the native-born (Komi and Russian) inhabitants of the White Sea coasts, Cheskaya Bay and Pechora Sea. Many artels are engaged in fishing. Most of the valuable fish species caught are offered for sale. The fish to be stored is predominantly slated, but also dry-cured or dried.

2.3.5. Peculiarities of the diet of the natives in the western part of the Russian Arctic

A.A. Perova, et al, investigated the diets of nationalities of the north, including Nenets and Lapps [28]. A specific character of the diet in the Extreme North is determined by the natural conditions. The consumption of meat or fish amounted to 0.5–1.0 kg/day and on holidays up to 1.5 kg/day. According to Perova's information the average daily assortment of food products consumed by Nenets (g/day) in 1930–1935 used to be:

Venison	832
Fish	150
Dried fish	114
Fish oil	17
Sea-animal fat	22
Reindeer blood	32
Bread	285
Flour products	61

According to the data obtained by D.I. Gusev [29], the fish consumption by the inhabitants of the Extreme North amounted to 500–1000 g/day, and the content of fish (g/day) in the diet of servicemen was as follows:

Soldier's ration	100
Naval Officer's ration	153
Officers (in remote areas)	206
Population (in coastal regions of the North)	150

The diet of reindeer breeders of the Extreme North was investigated by Troitskaya et al. in 1980 [30]. The venison consumption by male herdsman – reindeer breeders can be as great as 1 kg/day. However, this amount is likely to be a limiting value and refers to the winter period. In summer, fish makes a greater contribution to the diet. The fish consumption can be as great

as 1.0–1.5 kg/day. Fresh-water fish from tundra lakes and rivers constitutes a major portion of fish consumed by the reindeer breeders. The average fish consumption is estimated at 500 g/day.

By the character of diet, the population of the Russian Arctic can be classified into 3 groups:

(1)   Group 1 includes the indigenous population engaged in reindeer breeding. This group is represented mainly by the nationalities of the Extreme North and amounts to about 100,000 people. Reindeer breeders migrate seasonally: in summer to the north towards the coast of the Arctic seas and in winter to the south. Local food products occupy a significant place in their diet. In villages on the coast of the Arctic seas, the natives are engaged in sea animal hunting and fishing. No more than 10–15% of the natives of the North live directly on the coast.

(2)   Group 2 is represented by a rural population of non-native nationalities and by inhabitants of small villages and towns. The diet of this group has a mixed character, with a large portion of imported food products. The numbers of this group in the Russian Arctic were estimated at 200 000 people. Among the population living in the European part of the Russian Arctic, 80% is made up of non-native nationalities, and 20% by the nationalities of the North.

(3)   Group 3 includes the population of large ports and industrial cities of the Russian Arctic, including Murmansk, Arkhangelsk and others. The total numbers of this group are estimated a 1 million people. Their diet includes much imported food products.

The average fish consumption for the areas adjacent to the Barents Sea is given in Table XXII [31].

TABLE XXII. THE AVERAGE FISH CONSUMPTION RATE IN NORTHERN REGIONS OF RUSSIA (kg/a) [31]

Area	Year				
	1985	1990	1991	1992	1993
Northern Regions of Russia	34	32	28	18	17
Murmansk Region	68	53	50	23	19
Arkhangelsk Region	32	39	34	21	19

3. MODEL DESCRIPTION

Having been tasked with the objective of development of reliable assessment models for the Arctic area, the modelling group defined a number of working priorities. The first such priority was the collection and synthesis of existing physical data on the region to allow any necessary extensions to existing radiological assessment models. This data was described in detail in Section 2 of this document. The second priority was an evaluation of the models by means of an extensive model inter-comparison. Given the quite radically different model structures, data requirements and modelling objectives for which they had originally been developed, it was felt necessary to explore the effects of the model differences on the predictions, which could also be used in the final stages to assess the reliability of the model predictions. To this end a model inter-comparison scenario was developed.

3.1. MODELS USED IN IASAP WORK

3.1.1. Model descriptions

The models used in this work simulate the dispersion of radionuclides due to advection and diffusion within the water column and some also include interaction with suspended material and sediment. There were two main modelling approaches represented within the modelling Working Group: namely, compartmental or box models, and hydrodynamic circulation models. In addition, there was also a hybrid approach which uses a compartmental structure but at a finely resolved spatial scale. There were significantly differing modelling approaches taken for dealing with sedimentary processes and for modelling biological uptake. The modelling can be considered in two stages: the dispersal (by diffusion and advection) in the dissolved phase; and the interaction with sediment and biota as the second stage. By not basing the IASAP work on a single model or model type, it was hoped that the overall results would prove robust and that estimates of uncertainties on the endpoints would reflect the uncertainties arising from lack of knowledge and paucity of data, and different modelling strategies.

For modelling the advective and diffusive dispersal, compartmental models provide long time, spatially averaged (far field) capabilities, while the hydrodynamic models provide locally resolved, short timescale results. These model structures are discussed here in a general way, before considering the specific models used within the project.

3.1.1.1. Compartmental models

Compartmental models are widely used in radiological assessment when there is a requirement for predictions in distant locations and at long timescales. Such models are based on assumptions of instantaneous, homogeneous mixing within identified regions (compartments), dispersion of the contaminants is parameterised by flows between the model compartments, usually assumed time-independent and proportional to the inventories of material within the boxes. The model typically has more boxes in areas of high concentration gradients. Boxes may be depth stratified and may also include sediment-water interactions.

3.1.1.2. Circulation models

The second approach of circulation models provides finely resolved spatial predictions based on calculated flow fields related to the driving forces in the system, such as wind, heating (temperature) and salinity. Due to the high computational effort, such models can, however, only be run for limited timescales (of the order of tens of years).

3.1.1.3. Advantages and disadvantages of the different modelling approaches

Compartmental models

The principal advantages of the compartmental models used here are:

(1) Model runs spanning long time-scales, up to thousands of years are possible.

(2) The model is computationally expedient and low cost.

(3) The modelling is not limited to conservative radionuclides, but can be extended to deal with particle-reactive nuclides (detailed submodels for dispersal in sediment and biota can be attached simply to the compartmental model).

The main disadvantages of the compartmental models used here are as follows:

(1) Owing to the high degree of spatial averaging implicit in the design of compartments, no concentration gradient can be created within a compartment. Concentration gradients can only be resolved in the model by increasing the number of boxes in the region of the expected gradient. If these boxes are not included, the gradients cannot be described.

(2) Considerable uncertainties remain in some key parameters.

Hydrodynamic models

The principal advantages of the hydrodynamic models used here are:

(1) The ability to calculate two- or three-dimensional (2- or 3-D) flow fields based on realistic topography of the area and realistic forcing functions of wind and density.

(2) High temporal and spatial resolution, thus allowing for significant horizontal and vertical variations within small areas.

The main disadvantages of the hydrodynamic models used here are:

(1) The large numerical and computational effort involved in running such models limits the simulated time for dispersion forecasts to the order of decades.

(2) Much uncertainty resides in some of the key parameters, such as eddy viscosity and diffusivity coefficients.

(3) The considerable forcing data required for hydrodynamic models applied to the Arctic Ocean and Kara Sea: there is a major shortage of quality forcing data.

(4) Difficulties in the incorporation of sedimentary processes.

3.1.2. Validation and verification processes

The process of model validation is clearly important. Validation was in the main possible for those parts of the models which describe well characterized areas (e.g. Irish Sea, North Sea) and made use of the extensive data available for radionuclides discharged from Sellafield. The models were verified primarily against estimated transit times between Sellafield and northern waters. In addition, a comparison was made between literature values of water fluxes in the Arctic Ocean and those used by the box models and agreement was generally found to be good.

Validation was made difficult for the hydrodynamic models due to the lack of detailed information on essential parameters (temperature and salinity fields and meteorological information) for the Kara Sea.

In general, the validation process for both compartmental and hydrodynamic models was limited by the lack of appropriate data, particularly within the arctic area.

3.2. DETAILED MODEL DESCRIPTIONS

3.2.1. Compartmental models

3.2.1.1. TYPHOON, Modeller: T. Sazykina, Scientific Production Association "Typhoon", Russian Federation

Important model characteristics

The model ARCTIC was created in 1994 for the purposes of IASAP. The aim of the model is to predict the long term radiological consequences of the radioactive waste dumped in the Arctic Seas. ARCTIC is a regional, compartmental, dynamic and deterministic model. In it, the Barents Sea is considered as a set of four inter-connected boxes, the Kara Sea as two inter-connected boxes. First order differential equations are used for simulation of the transfer of water. Radionuclide concentration in water and sediment are calculated for instantaneous and prolonged releases of radionuclides from the waste burial sites. The model allows predictions to be made of radioactive contamination of the Arctic Seas for time periods of 0.3 years up to 100 years. A dynamic submodel has been developed to calculate the radionuclide concentration in commercial species of fish taking into consideration specific long distance seasonal migration of fish. A special submodel is designed to calculate doses to humans due to consumption of fish and other marine foodstuff from the Arctic Seas. The model also allows doses to fish and other marine organisms to be calculated.

The ARCTIC model has been designed as a set of Fortran subprograms. The Runge-Kutta method is used for solution of the differential equations.

Intended accuracy of model predictions

The accuracy of model predictions is strongly dependent on the accuracy of estimation of water fluxes between the subareas of the Arctic Seas and adjacent marine areas. The intended accuracy of predictions is within a factor of 10.

Method used for deriving uncertainty estimates

The uncertainty estimates are derived using a sensitivity analysis of the parameters of the model.

Past experience in model use

The ARCTIC model has been developed within the framework of IASAP. A simplified version of the model was used for a radiological assessment of the cooling water discharge of the Leningrad NPP (into Kopor Bay in the Gulf of Finland).

3.2.1.2. KEMA, Modeller: R. Heling, KEMA, The Netherlands

The calculations have been performed by means of the model developed at KEMA called ARCRA. This model has been developed by R. Heling and is based on several model descriptions in the literature. It is a compartmental model in which all the processes are described on the basis of first order differential equations. The model tool to solve the equations is the graphical tool "I think" [32].

Intended purpose of the model

The model ARCRA has been developed on the basis of large oceanographic models such as MARIN, constructed in the frame of the CEC project, MARINA. It predicts the levels of radionuclides in water, sediments, and fishery products in the marine environment. Several exposure routes such as the consumption of fishery produce, inhalation of seaspray and sediment particles near the shore, and external irradiation due to residence on the beach have been implemented in the model.

The model contains a dose model to assess both the short and long term radiological consequences via the distinct aquatic exposure routes in accidental circumstances and regular situations. The purpose is an enhanced risk analysis in which as many pathways as possible are evaluated.

Intended accuracy of the model predictions

The aim of the model is to estimate the levels of radionuclides in fishery products for reasons of health protection. The initial contamination due to distinct sources can result in enhanced levels of radionuclides in fishery products for years. The transfer of radionuclides through the foodchain has a rate such that the levels of radionuclides in the top predators in the Arctic like cod and seal reach their maximum values when the maximum levels in the seawater have diminished significantly. The required accuracy may not exceed a factor of 10. Because of the application of the model for risk assessment purposes, it is not desirable to underestimate the radionuclide concentrations in seafood and conservative assumptions in terms of input parameters are accepted if no site specific information is available.

Past experiences in operating the model

The model was originally developed to model the behaviour and fate of radionuclides released in the Dutch part of the continental shelf, in order to assess the radiological consequences following discharges of waste water from the offshore oil and gas platforms. The sea dispersion model was constructed to predict the long term behaviour of radionuclides in the abiotic and biotic part of the marine ecosystems [33].

Model structure

The arctic area is subdivided into boxes in which complete mixing occurs and in which the activity concentrations after a release can be predicted by a model based on the first order linear equations. The system of linear differential equations obtained by mass balances on all subcompartments is solved numerically. In the sediment layer, two boxes, in which homogeneous concentrations are assumed, can be distinguished to describe the downward and upward transport of radionuclides. In the sediment layer, both transport of adsorbed and dissolved radionuclides is modelled. The processes which are taken into account are: particle scavenging/sedimentation, molecular diffusion, enhanced migration of radionuclides in solution due to physical and biological processes, burial, i.e. the downward transfer of radionuclides in the bottom sediment as a result of the sedimentation process. Transports are the inflow of water from and to adjacent boxes. In case of continuous discharges of radionuclides by nuclear or non-nuclear industries, the uptake of radionuclides by aquatic organisms can be modelled using the concentration factor approach. In this approach the concentration in the organism is simply calculated by multiplying the total water concentration with the concentration factor for the specific organism. Site specific data are necessary to estimate the levels in aquatic organisms. In the absence of these data, generic values from literature have to be used.

In accidental or instantaneous situations, however a more dynamic approach is necessary, as the concentration factor approach tends to overestimate the concentration in the first period after the initial contamination. To improve predictions, the concentration in an organism can be modelled by means of a combination of this concentration factor approach with the biological half-life of a radionuclide in a specific organism. In that way the delay caused by the time the radionuclide needs to migrate through several trophic levels is better modelled. Still the transfer of radionuclides from organism to organism due to the predator–prey relationship is not modelled. Therefore a more accurate approach would be to take the position of the species in the foodchain into account. For that purpose knowledge about the foodchain in a certain water body and specific parameters like consumption rates and food preference are necessary. If these data are available they can simply be used as direct input data.

3.2.1.3. RISØ, Modeller: S.P. Nielsen, Risø National Laboratory, Denmark

Scope of the model

The model MADRAS (Model for the Assessment of Doses to Man form Radioactivity in the Arctic Seas) was developed for the assessment of the radiological consequences of releases of radioactive material to the marine environment covering the Arctic Seas and the North Atlantic, including European coastal waters. The model simulates the dispersion of radioactivity in the water due to advective transport, including mixing from wind and tidal forces. Association of radionuclides to suspended sediment material is taken into consideration in addition to subsequent transfer to sediment through particle scavenging. Further transfer of radionuclides between the water column and the sediments include diffusion, bioturbation and resuspension. From specified inputs of radioactivity to the marine environment, the model calculates time-dependent concentrations in seawater and sediments. These data are used to calculate doses to man from a range of exposure pathways including inhalation of seaspray and resuspended beach sediments. Doses are calculated to individual

members of critical groups and populations. Collective doses are generally truncated to 1000 years for long-lived radionuclides (e.g. ^{239}Pu, ^{241}Am, ^{129}I).

Type of model

Compartment or box-model analysis is used to simulate the movement of radionuclides between parts of the marine environment. Box-model analysis assumes instantaneous uniform mixing within each box with rates of transfer across the boundaries of the box being proportional to the inventories of material in the source boxes. The box-model analysis uses first order differential equations to describe the transfer of contaminant radionuclides between the boxes.

Most coastal areas are represented with one layer water boxes and underlying sediment boxes, but some areas with stratification (e.g. the Baltic Sea) include surface and deep waters. Most deep sea areas of the Arctic Seas and the North Atlantic include two layers (surface and deep waters). The sediments are represented by two layers; a surface layer and a deeper layer. The model includes a total of 140 boxes (water and surface-sediment boxes).

The rates of transfer between the aquatic boxes, $k_{ij}(a^{-1})$ are related to the volume exchanges, $R_{ij}(km^3/a)$ according to:

$$R_{ij} = k_{ij} V_i \tag{1}$$

where

V_i is the volume of water represented by box i.

At any given time the activity in the water column is partitioned between the water phase and the suspended sediment material. The fraction of the total activity (F_w) in the water column that is in aqueous solution is given by:

$$F_w = \frac{1}{1 + K_d \, SSL} \tag{2}$$

where

K_d is the sediment distribution coefficient (m^3/1000 kg);
SSL   is the suspended sediment load (1000 kg/m^3).

Activity on suspended sediments is lost to the underlying boxes when particulates settle out. The fractional transfer from a water column (box i) to the sediments (box j) due to sedimentation is given by:

$$k_{ij} = \frac{K_d \, SR_i}{d_i (1 + K_d \, SSL)} \tag{3}$$

where

d_i is the mean water depth of the water column (m);
SR   is the sedimentation rate (1000 kg·m^{-2}·a^{-1}).

The model includes transfer of radioactivity between the surface sediment layer and the bottom boundary layer. This transfer is represented by diffusivity through the pore water and mixing due to bioturbation, modelled as a diffusive process. Suspended sediment particles in

the coastal waters are partly maintained by a local depth-dependent resuspension of surface sediment particles to the water column, due to mechanical transfer of energy from wind and tidal forces to the surface sediments. Removal of activity from the top surface sediment to lower sediment layers is taken into account by assuming that the burial rate is equal to the flux of particles settling from the overlying waters. Radioactive decay is accounted for in all boxes. The model is implemented in the TIME ZERO modelling environment on a personal computer [34].

Accuracy of predictions

Subsets of the model have been tested by comparing model predictions of annual average concentrations of ^{99}Tc, ^{125}Sb, ^{137}Cs and ^{90}Sr in water and sediments against observations. These tests were limited to European coastal waters and the Baltic Sea and covered several decades considering discharges to sea from European reprocessing facilities, fallout from weapons testing and from the Chernobyl accident. These tests indicated a predictive accuracy of the model at the 95% confidence level for these areas of a factor of three. The present model has not been tested directly for the Arctic waters and the North Atlantic, but the author trusts the quality of the data and estimates for the entire model a predictive accuracy at the 95% confidence level of a factor of five (based on validation testing and expert judgement).

Strengths of the model

The box model can provide estimates of doses to individuals and populations considering short-range and short-term as well as long-range and long-term dispersion of radionuclides in the marine environment. This is in contrast to more realistic 3-D models that provide results of high resolution in space and time, but with a predictive time limit of a few tens of years and difficulties of dealing with suspended particles which are of importance for the dispersion of high K_d elements (Pu, Co, Am). The predictive accuracy of box models concerning dose estimates is most often adequate for radiological assessment purposes. The quality of the results depends mainly on the basic input data and the experience of the modeller. The computational costs are low since box models may be run on personal computers.

Weaknesses of the model

The basic assumption of the box-model technique, namely that of instantaneous uniform mixing within each box, is evidently an approximation to reality and not physically correct. Furthermore, the box model uses average conditions (e.g. advection and mixing) and is not suitable for reproducing spatial (meteorological) conditions. The degree of detail in time and space of the dispersed radioactivity calculated within the box model is limited.

3.2.1.4. MAFF, Modeller: P. Gurbutt, MAFF, United Kingdom

The model is a box model with 18 regions plus the rest of the world. The box design has taken into account the expected mean flows and the bathymetry of the northern seas. The dimensions of the boxes were calculated using GEBCO chart data. The exchanges between boxes were based upon the data in the benchmark scenario. However, they differ in some areas in order to maintain a water mass balance. There is only one water box in the vertical. This is an obvious deficiency within the model as there are complex water structures in the northern seas. Each water box has a constant suspended load, with variations as described in the benchmark scenario. There is no net sedimentation anywhere but sediment can be

transported in suspension between the regions. There is an interface box between the water and seabed sediment of depth 5 m everywhere. This has a higher suspended load than the water box to take account of the benthic boundary layer. The seabed consists of one box of depth 5 cm. The sediment is assumed to be all mud.

Strengths of the model

The methods for handling sediment transfer between boxes in water and between water and sediment have been extensively tested in the Irish Sea.

Weaknesses

Neither the vertical structure in the water column, nor ice transport is included. The circulation is fixed so no seasonal variability is included.

Intended accuracy

Unknown accuracy as yet, but likely to improve with increased vertical resolution. Standard sensitivity analyses have been used to find the likely range of variation in concentration estimates.

The model validation is limited, published tritium and caesium data have been used where possible. Estimates of the flushing of the seas will improve the circulation of the model.

Past experience

The code for this model has been used for dose calculations in the Irish Sea for discharges from Sellafield [35]. As a result the code and the parameterisations of the processes, particularly sediment scavenging have been extensively tested and validated.

The Irish Sea model used techniques developed in a model of the world ocean using isopycnal surfaces to improve the representations of the vertical and horizontal mixing, especially in the polar regions. This model was used for assessing the continued suitability of the NEA dumpsite in the northeast Atlantic for low level radioactive waste [36].

3.2.1.5. IAEA-MEL, Modeller: I. Osvath, IAEA Marine Environment Laboratory (MEL), Monaco

Scope of the model

The ARCTIC-5 model was developed to simulate aquatic (marine) dispersion of radionuclides released from the nuclear waste dumpsites in the Kara and Barents Seas on a global scale, to assess transfer of radionuclides to sediment and biota and radiological doses delivered via marine exposure pathways to human populations. The model was designed to respond to the requirements of IASAP, including modelling the transfer to biota (seaweed, mollusks, fish, sea mammals, seabirds/eggs), dose calculation for ingestion, inhalation of seaspray and resuspended shore sediment, external exposure from shore sediments, assessment of maximum individual and collective doses to hypothetical critical groups and to regional and global human populations, dose rates and committed doses.

Model characteristics

ARCTIC-5 is a compartmental (box) model suitable for timescales of 1–1000 years and spatial scales ranging from regional to global. Its structure comprises 48 single-layered compartments of water and bottom sediment. Generally the compartment boundaries were defined following those of the major oceanographic and hydrographic structures (Figure 15). Compartment parameters, water flows between compartments and river inflow were estimated based on data in the published literature and, for the Kara Sea compartments, also from results of the Hamburg Shelf Ocean Model HamSOM (presented in 3.2.2.2). The space resolution of the model was defined so as to be higher in the regions where steeper concentration gradients are expected ("source" regions), such as the Kara Sea and the Irish Sea areas. The structural detail in the European waters is to allow validation with field-derived data on transport of radionuclides released from the Sellafield reprocessing plant and impact assessment for fishing grounds in the region. Five compartments were defined for the Kara Sea, including a generic Novaya Zemlya bay compartment and a Novaya Zemlya Trough compartment, where the release sources were placed. The generic bay compartment was defined so as to describe each particular Novaya Zemlya bay simulated, depending on the scenario. Two compartments were defined for the Barents Sea.

The time evolution of radionuclide inventories in the compartments of the model domain can be described through a system of linear differential equations. Time-dependent release functions (source terms), radioactive decay, exchange between water compartments, between water, suspended and bottom sediment (dissolved and particulate phases), transfer to biota and delivery of doses to humans (rates and fractions related to ingestion, inhalation and shore occupancy, dose conversion factors) are parametrised in the model. Parameter values were taken from the literature [8, 22, 37–43] or from IASAP recommendations. Site-specific values were used where available and appropriate, generic values elsewhere. Yearly values were taken for the time dependent parameters. The model was implemented on a PC under FORTRAN using a modified version of the FRANNY software package [42] for dispersion calculations. Software modules were developed to monitor the numerical routines (convergence, stability, balance checks, full traceability of results), to calculate doses and to process output data.

Parameters

Input: time-dependant radionuclide release rate, source location

Model: water exchange rates between compartments, compartment morphometric parameters, K_d, suspended sediment load, sedimentation rate, thickness of active bottom layer, porosity, bulk particle density, catch of edible marine biota species, consumed fraction, individual intake of seafood, delay catch-consumption, dose conversion factors.

Output: time sequence of radionuclide concentrations in water, sediment and edible biota, parameters characterising the space-time dynamics of contamination, global collective effective dose commitment, maximum individual dose-rate, regional dose distribution, fractional contribution of different exposure pathways.

Validation

The model was validated using source term and field measurement data on the Sellafield ^{137}Cs release and its dispersion through the northern seas and estimated residence and transit times for the Arctic Seas [9].
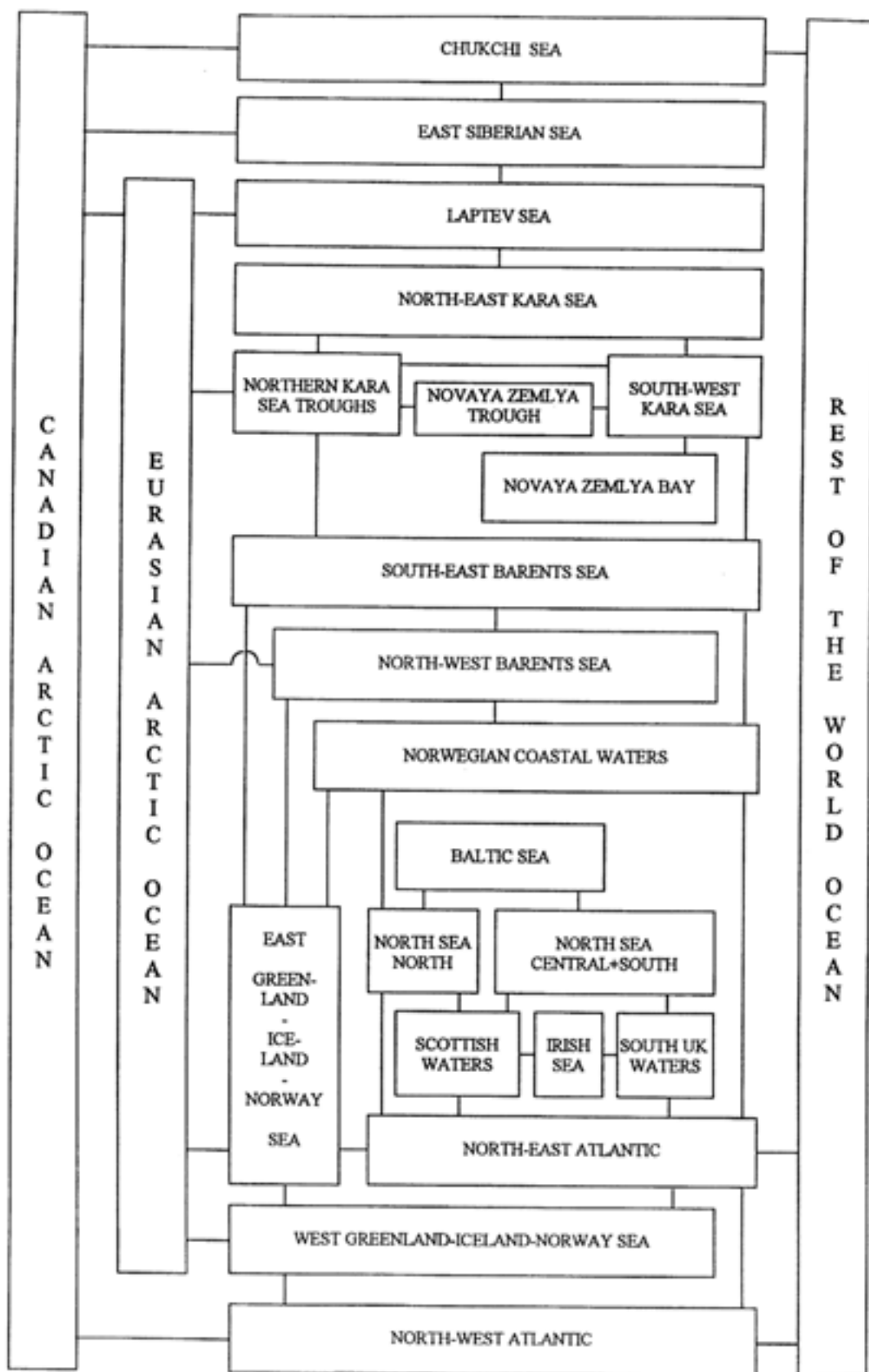
FIG. 15. ARCTIC-5 model.

Intended accuracy of model predictions

The intended accuracy of prediction is within a factor of 10 for radionuclide concentrations. The accuracy will depend on the quality of model parameters, in particular that of information on water circulation. An important uncertainty in predictions is obviously related to the flows in the Kara Sea region and in the Arctic in general, which are poorly documented. The accuracy for the global committed doses should however be better than a factor of 5.

Previous uses of the model

Earlier versions of the model had been used for preliminary first estimates of radiological doses for worst case scenarios of releases from the radioactive waste dumped in the Arctic Seas.

Strengths of model

The model is well suited to radiological assessment on the time-scales required by IASAP. The computer code is fast and can easily run on a higher performance PC. The software routines were developed so as to facilitate batch runs of sets of scenarios, which, together with the modest running time requirements, has allowed extensive sensitivity and uncertainty analyses. In general strengths and weaknesses are those described for compartmental models in 3.1.2.3.

Limitations of model

The time resolution is one year, therefore no seasonal variability can be accounted for. The parameters, e.g. the transfer coefficients, are constant in time, so no interannual variations are described by the model (but these had anyway not been included in any of the IASAP scenarios). Vertical stratification, which had been included in other versions of the model, has not been considered for this application. The K_d and CF models imply equilibrium situations and therefore do not cover short-term dynamic changes, but an adequate choice of the model time step can give reliable yearly averaged results.

3.2.2. Hydrodynamic models

3.2.2.1. USN, Modellers: R.H. Preller, Naval Research Laboratory, and A. Cheng, Sverdrup Technology, United States of America

The model

The three-dimensional, primitive equation multi-level, baroclinic ocean model described by Cox [44] was used for this study. This model has been designed so that multiple passive tracers, such as temperature and salinity could be calculated simultaneously. Such a capability is particularly useful since radionuclides may also be treated as a passive tracer. The tracer equation for the radionuclides can be written as follows [45]:

$$\frac{\partial T}{\partial t} + u.\Delta_H T + w\frac{\partial T}{\partial z} = A_{TH}\Delta_H^2 T + \frac{\partial}{\partial z}A_{tz}\frac{\partial T}{\partial z} - \lambda T + \beta T + (sources) \qquad (4)$$

where

T   is the radionuclide concentration (Bq/cm^3);
u   is the horizontal ocean current (cm/s);
∇_H is the horizontal gradient;

w	is the vertical ocean current (cm/s);
A_{TH}	is the coefficient of horizontal eddy diffusion (cm^2/s);
∇	is the horizontal Laplacian operator;
A_{tz}	is the coefficient of vertical eddy diffusion (cm^2/s);
λ	is the radioactive decay rate (s^{-1});
β	is the river outflow rate of radioactive pollutants (s^{-1}).

Sources are additional sources of radionuclides located in the model domain. Note that more passive tracers can be added into the model as long as either their beta or source value is known. The lambda values will vary depending upon the half-life of the tracer being used. The tracer equation for salinity is the same as Equation (1) minus the lambda T term and the sources terms. The beta value becomes a reduction rate for salinity, which is the ratio of river runoff and grid cell volumes outside the river mouth. The river runoff is assumed to contain totally fresh water (salinity = 0.0 ppt). The tracer equation for temperature is also the same as Equation (1) minus the lambda T term and the sources term.

The model domain

Chang and Preller [46] used the Cox model, coupled to a Hibler ice model [47, 48] to estimate monthly ice and ocean conditions in the northern hemisphere. They defined a new 'transformed' co-ordinate system to avoid a numerical singularity at the pole as well as possible instabilities at high latitudes. This study used the ocean model defined in the Cheng and Preller paper, but incorporated finer grid resolution, approximately 0.28 degrees (17-35 km). The model domain includes the entire Arctic basin and its marginal seas.

The model was defined by 360×360 grid points in the horizontal and 15 levels in the vertical. The first vertical level is 30 m deep and the subsequent level thickness increases towards the bottom. All boundaries in this model are solid wall boundaries.

The bottom topography, derived from the ETOPO5 bathymetry data is interpolated from the earth-oriented latitudes and longitudes to the new spherical coordinates using a two-dimensional cubic spline method over nine adjacent grid cells. Some minor smoothing is applied to the steepest topographic gradients to avoid numerical difficulties. After the cubic spline method is applied, the resulting topography is divided into 15 levels.

This numerical model requires approximately 32 Megawords of storage and takes approximately 15 hours of single processor time per model year on a Cray C-90 computer. Numerical simulations were run for 10 years.

Model initialization and forcing

Annual levitus climatology [49] for ocean temperature and salinity is used to initialize the model. The spatial resolution of the Levitus data (1 degree $\times$ 1 degree) is coarse when compared with that of the model (approximately 0.28 degrees). Such a difference could result in missing values near land boundaries once the data are interpolated to the model grid. To avoid this problem, the data are extrapolated to the coasts before using a three-dimensional cubic spline to interpolate to the model grid.

The 1986 and 1992 averaged winds from the Navy Operational Global Atmospheric Prediction System (NOGAPS) were used to test the model. Major features of the wind circulation in the north Pacific and Atlantic Oceans were similar during these years. In 1992, there is a strong component of the wind which blows from the Laptev Sea across the Arctic to

the Canadian coast and then along the northern coast of Greenland into the East Greenland Sea. In 1986, there is a strong component blowing from the Laptev and Kara Seas first toward the northeast and then turning toward the northwest and into the Canadian coast. Although the effects of the geotropic winds are felt below the surface of the ocean, they assert their strongest influences on the first level of the ocean models. The differences in this annual wind fields should be reflected in the patterns of radionuclide dispersion.

Arctic river runoff

Eight major Arctic rivers have been included in this model. Annual discharge values from Aagard and Carmack [50] are used for each of these rivers. For this study, the White Sea has been closed off from the Arctic as a result of the coarse resolution of the model. Therefore, the two rivers emptying into the White Sea, the Severnya Dvina and the smaller Onega are not included in this study. Note that in the Arctic, most of the river outflow occurs from late spring to early fall, with particularly large values in June [51]. This monthly variability in fresh water runoff should have a strong effect on the stability of the water column near the river mouth and on the growth and decay of sea ice in these regions. For simplicity in modelling only the ocean, we assumed each river had a constant runoff rate which summed over a year to those values cited by Carmack and Aagard.

3.2.2.2. IAEA-MEL/University of Hamburg, Modellers: I. Osvath, IAEA-MEL, I. Harms, University of Hamaburg, Germany

Hydrodynamic dispersion scenarios on local and regional scales were carried out using the Hamburg Shelf Ocean Model (HamSOM) which is a three-dimensional, baroclinic, circulation model.

The main components of HamSOM were developed in the early 1980s at the University of Hamburg for simulating North Sea dynamics [52]. Since then, the model has been applied to investigate the circulation of shelf seas (North Sea, Baltic Sea) and transport of pollutants [53, 54]. During these applications the model was continuously improved and extended.

In 1989, the model was applied to the Arctic Shelf Seas as part of an Arctic climate research project at the University of Hamburg. The model was coupled to a free drift thermodynamic ice model and was used to examine deep water formation in the Barents and Kara Seas [55]. First results on the barotrophic circulation and on the transport of pollutants in the Barents and Kara Seas were achieved in 1992 [56, 57].

The model is based on the non-linear primitive equations of motion invoking the Boussinesq approximation. Furthermore, the hydrostatic approximation and the equation of continuity are applied. The latter serves to predict the elevation of the free surface from the divergence of the depth mean transport. The numerical scheme of the circulation model is semi-implicit which allows for economic time steps. The equations are discretized as finite differences on an Arakawa C grid.

Spatial and time dependent variations of temperature and salinity (prognostic simulations) are calculated with transport equations that include a three-dimensional upstream advection scheme and the parameterisation of horizontal and vertical diffusion. The same algorithm is used for advection and diffusion of momentum. Vertical eddy diffusivity/viscosity coefficients are calculated depending on the shear production of the velocity field and the stability expressed by the buoyancy frequency. Horizontal eddy coefficients are constant in time and space.

Coupled ice ocean simulations include temperature variations in the upper layers depending on the surface heat fluxes. The salt flux (brine or freshwater release) at the surface is proportional to the thermodynamic ice production rate. The sea ice model consists of dynamic and thermodynamic components from which spatial and time dependent variations in ice thickness and ice compactness are calculated. The dynamic components include a free drift algorithm that accounts for the advection of ice thickness and compactness due to wind and water stress. Variations in thickness and compactness are calculated with an upstream advection scheme, which includes no ice rheology. The thermodynamic ice growth is determined using heat flux balance equations for the top and bottom of the ice cover. Heat fluxes are calculated with standard bulk formulae.

A detailed description of the circulation model with recent applications to the coastal waters of Canada (Vancouver) has been provided by Stronach, Backhaus and Murty [58].

Model configuration for the benchmark scenarios

The HamSOM code was applied to the Arctic shelves of the Barents and Kara Seas (regional scale) and with high spatial resolution to Abrosimov Fjord (local scale). The dispersion of radioactive tracers was determined with finite difference advection diffusion equations. As for temperature and salinity, the computation of horizontal diffusive processes was omitted due to the relatively high amount of numerical diffusion caused by this transport algorithm. Radionuclide concentrations in sediment were estimated by calculating the proportion of activity in sediment (0–5 cm) from the total activity in the water column. These estimates are based on stationary state dispersion patterns (continuous releases). K_d and suspended load parameters were taken from the benchmark scenario recommendations.

Regional scale modelling

The regional scale model covers the Barents and Kara Sea, including the continental slopes towards the Norwegian Sea and the Arctic Ocean. The model is implemented on a stereographic grid with an average size of 18 km. The vertical domain is resolved by 10 layers with a high resolution in the upper water column and a coarser spacing in the deep areas off the continental slopes. The timestep used is 15 minutes.

The forcing data used to drive the circulation model are wind stress, water density (dependent on temperature, salinity and pressure), semi-diurnal lunar tide and fresh water runoff from the four major rivers emptying into the Kara Sea.

The wind stress data were defined as monthly mean values from a global climatological surface wind data set [59]. The main tidal component in the Kara Sea [60] was included by forcing the open model boundaries with amplitudes and phases of the semi-diurnal lunar tide (M_2).

A major problem with the previous baroclinic simulations was the initialization with the temperature and salinity data. High resolution data sets from continuous observations are still not available from the Kara Sea. The benchmark scenarios were forced with two seasonal mean temperature and salinity fields (summer and winter) using linear interpolation between seasons. Both fields were previously developed with prognostic ice-ocean simulations that allow for temperature and salinity changes due to ocean currents (advection/diffusion) and surface heat and salt fluxes. The initial temperature and salinity distributions for these simulations were deduced from the Climatological Atlas of the World Oceans [49].

The resulting seasonal mean temperature and salinity fields for the Barents and Kara Sea are in good agreement with observations [61, 62]. Based on these fields, the baroclinic simulations reproduce the main features of circulation including the Norwegian Atlantic current, the Atlantic inflow into the Barents Sea between Bear Island and North Cape and the strong outflow between Franz Josef Land and Novaya Zemlya towards the Arctic Ocean. In particular, the simulated strong outflow via the Svyataya Anna Trough has been confirmed by recent current measurements [62].

Due to the high amount of computer time which is needed for hydrodynamic dispersion modelling, the results are a compromise between accuracy of prediction and simulated time period. The benchmark scenario simulations were usually truncated after 6–7 years of simulation. This time span turned out to be close to the average flushing time for the Kara Sea.The regional scale model requires approximately 20 hours CPU time on a DEC-3000 alpha workstation for the simulation of one year of dispersion.

Local scale modelling

The bays which include dumpsites for radioactive waste are not resolved by the coarse grid of the regional scale model. In order to follow the benchmark scenario recommendations, the HamSOM code was applied to the realistic topography of Abrosimov Fjord. The spatial resolution for the bay model was chosen to be 1/10 nautical miles (185.2 m), the time step is 32 minutes.

Wind was considered to be the most important driving force for the bay circulation. Two prevailing wind directions were applied, SE and WE-wind [4]. The benchmark results represent an average of these two wind directions. Due to missing information and lack of data on the bays, temporal and spatial variations of density as well as ice formation were not considered. Verification of the bay scale model was not possible.

The flushing times of the bays are in the range of 3–4 months using moderate wind speeds (5 m/s). the benchmark scenarios for the bays (instantaneous and continuous releases) were truncated after 3 years of simulation.

3.2.3. Modified compartment model

3.2.3.1. Nihon U, Modellers: A. Wada, Nihon University, T. Hozumi, ARK Information System Inc., Japan

The model has two parts which are described below:

Intended purpose of the model

To determine the flow of seawater in the area of interest.

Important model characteristics

(1)   The model provides the flow field making use of observational data (water temperature, salinity and concentration, meteorological data).

(2)   It is a diagnostic model to obtain a steady state.

Strengths

(1) The model can provide an appropriate flow field if good observational data are available.

(2) The flow field thus obtained satisfies, within bounds, the conservation of mass, salinity and heat energy based on observational values.

(3) Setting of boundary conditions is simplified compared with ordinary methods to solve partial differential equations.

Weaknesses

(1) The model cannot reach a non-steady flow state.

(2) As it is a diagnostic model based on observational data, the model is not suited for uses such as obtaining the predicted flow field in which existing conditions are modified.

(3) As the solution technique is based on non-linear programming, the model requires a great deal of calculation time and storage capacity.

(4) The model cannot cope with large numbers of boxes (mesh numbers).

(5) The quality of observational data used (accuracy, space and time resolution) has a direct effect on the quality of a solution.

Intended accuracy of the prediction

The model is suited to obtain the flow field for reproducing the existing condition, but it is not suited for the prediction of flow. However, as our objective is to predict the concentration of radionuclides in the existing flow field, this poses no problem at all and is suitable for our intended purposes.

Validation

Flow analyses were conducted in the Pacific Ocean and Tokyo Bay under the same input conditions using the three-dimensional mathematical model and this modified model, thus confirming that there is no major difference in the results obtained by both models.

Past experiences

(1) Flow analyses were conducted in the Pacific Ocean in order to assess the exposure due to radioactive waste discharged from reprocessing facilities.

(2) This model was applied to flow analyses (in Tokyo Bay, Osaka Bay, Ise Bay, etc.) for predicting the quality of water in the inner bay areas (using an ecosystem model).

Diffusion calculations

This part of the model is a modified version of the model which OECD/NEA used in assessing radioactive waste dumping sites in the North Atlantic Ocean. The intended purpose of the model is to calculate the concentration of radionuclides based on the seawater flow field obtained from the modified compartment model as well as the dumping conditions.

Important model characteristics

Changes in the concentration of radionuclides with the passage of time due to the following factors in the seawater and bottom materials are determined:

(a)   decay of the nuclides;

(b)   mixing due to advection and diffusion;

(c)   adsorption and sedimentation due to the interaction with suspended matter in the seawater;

(d)   burying and elution due to interaction with seabed deposits;

(e)   diffusion, burying and bioturbation movement in seabed deposits; and

(f)   removal due to burying into the seabed.

Strengths

Evaluation of scavenging effect. The model can make more precise analysis of the behaviour of seabed materials.

Weaknesses

In order to make more detailed calculations in the seabed, four seabed layers are added to the lower part of the seawater layer. However, as these four layers are so thin (1 mm in the thinnest layer), each calculation time Dt cannot be large, so that the calculation time is long.

Intended accuracy of the prediction

The model is not suited for short-term prediction because the annual mean flow field is used at present. For long term prediction, the accuracy will be higher.

3.2.4. Summary

An overall summary of the model properties is given in Table XXIII.

TABLE XXIII. SUMMARY OF MODEL PROPERTIES

Group (Country)	Model name	Model Description
Risø (Danish/Norwegian)	MADRAS	Global compartment model, with vertical stratification, linked to sediment sub-model, predictions beyond 1000 years.
MAFF (United Kingdom)	–	Global compartment model, with vertical stratification, linked to sediment sub-model, predictions beyond 1000 years.
Typhoon (Russian Federation)	ARCTIC	Regional compartment model of Kara and Barents Seas, linked to sediment sub-model and dynamic food chain model, predictions up to 100 years.
KEMA (The Netherlands)	ARCRA	Regional compartment model of Arctic region, linked to dynamic food chain model, predictions up to 1000 years.
Nihon U. (Japan)	–	Regional compartment model of Arctic region, with fine resolution grid, linked to detailed sediment model, predictions up to 1000 years.
IAEA-MEL[a]	ARTIC-5	Global compartment model, with vertical stratification, linked to sediment sub-model, predictions beyond 1000 years.
IAEA-MEL/University of Hamburg (Germany)[b]	HamSOM	Local 3-D baroclinic model for bay, predictions truncated after 3 years and regional 3-D baroclinic circulation model of Kara and Barents, including loss to sediment, linked to sea-ice model, predictions up to 10 years.
USN (United States of America)	–	Regional 3-D multi-level baroclinic model of Arctic Ocean, no sediment model, linked to sea-ice model, predictions up to 10 years.

[a] This model is indicated as "MEL box" in the remainder of the report.
[b] This model is indicated as "MEL regional" in the remainder of the report.

4. MODEL INTER-COMPARISON

Interpretation of the dose estimates and the observed variation can be aided by a comparison of the primary modelling results and the factors which influence them. One tool for this is a model inter-comparison. An extensive inter-comparison was conducted, and a summary of some of the key results are presented below.

The scope and philosophy of the hydrodynamic and compartmental models are generally very different. As already mentioned, the time span of the forecast and the spatial resolution of the model types differ considerably. The compartmental model gives a 'box' integrated value, which is assumed representative of a region covering several thousand square kilometers whereas the hydrodynamic model gives a 'point' value representing a much smaller area (a region of a few square kilometers). Furthermore, the hydrodynamic model is able to resolve seasonal or even tidal cycles of concentration. The comparison becomes more difficult for particle reactive nuclides; numerical diffusion effects will be important for such nuclides. The treatment of vertical migration of radionuclides in the water column is also different between the model types in IASAP. This may have quite large effects on predicted concentrations in the sediment and the overlying water column. The final dose calculations may then be affected, e.g., when considering ingestion pathways, for fish, the concentrations in the upper layers would be important, while for molluscs and crustacea, the bottom concentrations would be important. With regard to the importance of the sedimentary processes, a small sensitivity study of changes in sedimentary parameters was also undertaken and showed some differences between predicted sediment concentrations and that the degree of sensitivity to the parameters was model dependent. In addition to sediment, within the modelling group, two quite different approaches have also been taken to radioecological modelling. Several models have made use of the traditional approach, using concentration factors to give concentrations in biota, while others have developed dynamic models. A preliminary sensitivity analysis showed that the dynamic model resulted in doses approximately 15% higher than the traditional concentration factor approach. This discussion draws attention to some of the factors that must be considered when evaluating the final dose results.

This section presents and discusses the primary results from the model intercomparison or benchmarking (Tables I-I to I-XXIV in Appendix I), and some analysis of these results intended to describe and summarise the observed scatter in predictions.

The benchmark scenario had four major components:

(1)   the source terms and release patterns;

(2)   a general oceanographic and geophysical description of the area of interest (described in Section 2);

(3)   a description of the Arctic marine ecosystem (also described in Section 2): and

(4)   selected endpoints for prediction.

4.1. SOURCE TERM AND RELEASE PATTERNS

Two sources (Table XXIV) were considered, corresponding to dumped solid waste in Abrosimov Fjord on the eastern coast of Novaya Zemlya and in the Novaya Zemlya trough of the Kara Sea.

TABLE XXIV. SELECTED SITES FOR THE SOURCES

Source/sea	Description of the site and source placement
Novaya Zemlya Bay Kara Sea	Abrosimov Fjord on eastern coast of northern Novaya Zemlya Coordinates 71° 56,4' N, 55° 19,2' E Source placed at a depth of 20 m on the bottom
Novaya Zemlya Trough/Kara Sea	Coordinates 72° 40' N, 58° 10' E Source placed on the bottom at 300 m depth

TABLE XXV. RELEASE PATTERNS AND RADIONUCLIDES CONSIDERED FOR VARIOUS ASSESSMENTS

Scale	Sources considered (re. Table XXIV)	Radionuclides considered	Release patterns
Local	Novaya Zemlya Bay	^{137}Cs, ^{239}Pu, ^{99}Tc, ^{60}Co	– instantaneous: 1 TBq – 1 TBq per year for 10 years
Regional	Novaya Zemlya Bay	^{137}Cs, ^{239}Pu, ^{99}Tc, ^{60}Co	– instantaneous: 1 TBq – 1 TBq per year for 10 years
	Novaya Zemlya Trough	^{137}Cs, ^{239}Pu, ^{99}Tc, ^{60}Co	– instantaneous: 1 TBq – 1 TBq per year for 10 years

Radionuclides were selected as appropriate for the assessment (taking into account geochemical properties and half-life). The nuclides selected were ^{137}Cs, ^{239}Pu, ^{99}Tc and ^{60}Co.

No detailed time dependent release pattern was specified other than instantaneous or continuous and constant rate over a fixed number of years (details in Table XXV).

Decay chains were not considered.

Separate assessments were obtained corresponding to each source.

4.2. PREDICTION ENDPOINTS

The modelling endpoints were radionuclide concentrations in filtered seawater (Bq/m^3) and surface (0–5 cm) sediments (Bq/kg dw and Bq/m^2). At this stage there was no requirement to estimate dose.

The specific endpoints of interest were required at three spatial levels – local (within the Kara Sea), regional (Barents Sea) and global (around the Arctic basin and at key points beyond) and are detailed in Tables XXVI and XXVII.

As well as the timepoints detailed in Tables XXVI and XXVII, participants were also asked to provide maximum concentration at each location specified and the time at which the maximum occurred.

Although the endpoints were not depth specific, participants whose models were stratified were asked to provide depth profiles at the locations given in the tables. Endpoint co-ordinates are summarized in Table XXVIII.

TABLE XXVI. END POINTS RELATED TO THE CRITICAL GROUP DOSE CALCULATIONS – LOCAL AND REGIONAL SCALE

Release	End points	End points given at locations and timepoints
Abrosimov Fjord (a) Single release (1 TBq) (b) 1 TBq per year for 10 years	Filtered seawater concentration (Bq/m^3) Surface sediment concentration (Bq/kg dw) as above	Monthly for years 1 and 2; Seasonal figures for years 3 to 10 Annual figures for years 11 to 100 after start of release, at the following locations: 72ºN 65ºE (Kara Sea) 78ºN 92ºE (Kara Sea) 76ºN 76ºE (Kara Sea) 72ºN 45ºE (Barents Sea) 79ºN 58ºE (Barents Sea) 76ºN 20ºE (Barents Sea)
Novaya Zemlya Trough (a) Single release (1 TBq) (b) 1 TBq per year for 10 years	Filtered seawater concentration (Bq/m^3) Surface sediment concentration (Bq/kg dw) as above	Same as above

TABLE XXVII. END POINTS RELATED TO GLOBAL SCALE

Release	End points	End points given at timepoints and locations
Abrosimov Fjord (a) Single release (1 TBq) (b) 1 TBq per year for 10 years	Filtered sea water concentration (Bq/m^3) Surface sediment concentration (Bq/kg dw) as above	Timepoints as above (Table XXVIII) but also annually from year 100 till 1000 years after release at the following locations: (1) 70.5ºN, 143º W (Beaufort Sea) (2) 86ºN, 80ºE (Central Arctic) (3) 60ºN, 55ºW (Davis Strait) (4) 67ºN 20ºW (Iceland Sea) (5) 70ºN, 175ºW (Chukchi Sea),
Novaya Zemlya Trough (a) Single release (1 TBq) (b) 1 TBq per year for 10 years	Filtered sea water concentration (Bq/m^3) Surface sediment concentration (Bq/kg dw) as above	Same as above

TABLE XXVIII. BENCHMARK ENDPOINTS

Location	Identifier	Co-ordinates
Kara Sea	1	72°N 65°E
Kara Sea	2	78°N 92°E
Kara Sea	3	76°N 76°E
Barents Sea	4	72°N 45°E
Barents Sea	5	79°N 58°E
Barents Sea	6	76°N 20°E
Beaufort Sea	7	70.5°N 143°W
Central Arctic Ocean	8	86°N 80°E
Davis Strait	9	60°N 55°W
Iceland Sea	10	67°N 20°W
Chukchi Sea	11	70°N 175°W

4.3. RESULTS AND ANALYSIS OF MODEL INTER-COMPARISONS

The results from the benchmarking (maximum concentration and time to maximum) have been compiled and summarised (full tables are given in Appendix I). Summary tables showing the minimum and maximum concentrations in seawater and sediment and time to maximum for all nuclides for all source locations and behaviours are shown in Tables XXIX to XLIV.

These tables also include two summary measures of the scatter in the predicted concentrations; the coefficient of variation (CV) expressed as $100 \times$ standard deviation/mean, sometimes known as the relative variation and the level of agreement expressed as $\log_{10}$ (maximum/minimum). This latter figure was selected since in environmental modelling, discussion of orders of magnitude agreement is relatively common. Both coefficients are simple summary measures, easy to calculate but are not robust because they are both strongly influenced by extreme or outlying predictions. For the purpose of this benchmarking exercise, it was decided to include all the model predictions in the intercomparison, even those which were several order of magnitude lower or higher than the others. Only activity concentrations lower than 1×10^{-11} Bq/m^3 or Bq/kg (dry weight) were ignored. The choice of cut-off value is of course arbitrary, but it was felt that at this level, results reflect numerical imprecision rather than physically meaningful concentrations. The results have also been summarized in Figures 16–31.

Figures 16 through 31 show the CV and level of agreement at each of the selected endpoints, relating to the maximum reported concentration from each of up to eight different models. This summary analysis thus uses all results from compartmental, hydrodynamic and hybrid models. However, it should be noted that in only a few simulation conditions were results available from the hydronamic models.

TABLE XXIX. SUMMARY OF MODEL INTER-COMPARISONS FOR ^{137}Cs, INSTANTANEOUS RELEASE (1 TBq) IN ABROSIMOV FJORD

Location	Position	Medium	Minimum	Maximum	Time to max. (a)	CV (%)	Level of agreement
Kara Sea	72°N 65°E	Water	7.3×10^{-3}	4.8×10^{-2}	1–2	73.1	0.82
		Sediment	1.7×10^{-4}	6.3×10^{-3}	1–12	121.6	1.57
	78°N 92°E	Water	3×10^{-4}	4.6×10^{-3}	2–5	73.2	1.18
		Sediment	1.4×10^{-6}	9.8×10^{-4}	3–16	108.5	2.84
	76°N 76°E	Water	5.2×10^{-4}	7.5×10^{-3}	2–4	76.8	1.16
		Sediment	7.1×10^{-6}	9.8×10^{-4}	2–16	105.6	2.14
Barents Sea	72°N 45°E	Water	1.4×10^{-5}	3.6×10^{-3}	2–6	134.7	2.41
		Sediment	1×10^{-6}	5.9×10^{-4}	2–17	196.4	2.77
	79°N 58°E	Water	1×10^{-4}	3.6×10^{-4}	3–10	56.1	0.55
		Sediment	1.6×10^{-6}	3.6×10^{-5}	5–21	75.1	0.80
	76°N 20°E	Water	1.6×10^{-5}	3.7×10^{-4}	5–10	94.7	1.36
		Sediment	8×10^{-7}	3.6×10^{-5}	10–30	101.0	1.65
Beaufort Sea	70.5°N 143°W	Water	4.4×10^{-7}	2.6×10^{-5}	10–40	87.0	1.77
		Sediment	5.9×10^{-10}	9×10^{-6}	40–60	195.6	4.18
Central Arctic Ocean	86°N 80°E	Water	3.5×10^{-5}	9.7×10^{-5}	2–20	47.6	0.44
		Sediment	3.3×10^{-11}	1.5×10^{-5}	30–60	194.3	5.65
Davis Strait	60°N 55°W	Water	1×10^{-6}	5×10^{-6}	20–45	57.5	0.69
		Sediment	1.6×10^{-8}	1.2×10^{-6}	20–80	155.8	1.87
Iceland Sea	67°N 20°W	Water	3.1×10^{-7}	3.2×10^{-5}	5–30	60.2	2.01
		Sediment	2.3×10^{-9}	2.4×10^{-5}	20–50	217.9	5.01
Chukchi Sea	70°N 175°W	Water	7×10^{-8}	1.8×10^{-3}	10–35	218.9	4.41
		Sediment	9.2×10^{-11}	6×10^{-4}	10–60	223.3	6.81

TABLE XXX. SUMMARY OF MODEL INTER-COMPARISONS FOR ^{137}Cs, CONTINUOUS RELEASE (1 TBq/YEAR FOR 10 YEARS) IN ABROSIMOV FJORD

Location	Position	Medium	Minimum	Maximum	Time to max. (a)	CV (%)	Level of agreement
Kara Sea	72°N 65°E	Water	1.5×10^{-3}	3.5×10^{-1}	6–10	92.2	2.37
		Sediment	1.5×10^{-4}	6.2×10^{-2}	6–15	141.6	2.61
	78°N 92°E	Water	5.9×10^{-4}	3.8×10^{-2}	6–11	61.9	1.81
		Sediment	9.6×10^{-6}	9.7×10^{-3}	6–20	131.2	3.00
	76°N 76°E	Water	5.9×10^{-4}	8.6×10^{-2}	6–11	81.1	2.16
		Sediment	4.4×10^{-5}	9.7×10^{-3}	6–19	110.7	2.34
Barents Sea	72°N 45°E	Water	1.1×10^{-4}	1.8×10^{-2}	6–13	148.5	2.21
		Sediment	9.8×10^{-5}	8.7×10^{-2}	6–24	224.4	3.93
	79°N 58°E	Water	4.2×10^{-5}	2.7×10^{-3}	6–12	85.2	1.81
		Sediment	7.4×10^{-6}	8.7×10^{-2}	6–30	262.4	4.07
	76°N 20°E	Water	1.3×10^{-4}	3.4×10^{-3}	6–20	87.3	1.41
		Sediment	7.9×10^{-6}	3.6×10^{-4}	6–33	102.2	1.66
Beaufort Sea	70.5°N 143°W	Water	4×10^{-6}	2.4×10^{-4}	10–50	109.9	1.78
		Sediment	5.9×10^{-9}	9×10^{-5}	50–60	192.8	4.18
Central Arctic Ocean	86°N 80°E	Water	1.1×10^{-4}	6×10^{-3}	10–20	165.2	1.73
		Sediment	3.2×10^{-10}	4.4×10^{-4}	40–70	198.0	6.13
Davis Strait	60°N 55°W	Water	1×10^{-5}	4.7×10^{-5}	20–50	59.4	0.67
		Sediment	1.6×10^{-7}	1.2×10^{-5}	30–90	148.8	1.87
Iceland Sea	67°N 20°W	Water	1.5×10^{-6}	3.1×10^{-4}	10–25	96.2	2.31
		Sediment	2.3×10^{-9}	2.4×10^{-4}	20–50	219.2	5.01
Chukchi Sea	70°N 175°W	Water	4×10^{-7}	1.4×10^{-2}	10–40	239.5	4.54
		Sediment	9.2×10^{-10}	5.9×10^{-3}	20–60	223.3	6.81

Note: Water (Bq/m^3)
Sediment (Bq/kg dw)

TABLE XXXI. SUMMARY OF MODEL INTER-COMPARISONS FOR ^{137}Cs, INSTANTANEOUS RELEASE (1 TBq) IN NOVAYA ZEMLYA TROUGH

Location	Position	Medium	Minimum	Maximum	Time to max. (a)	CV (%)	Level of agreement
Kara Sea	72°N 65°E	Water	3.5×10^{-3}	1.5×10^{-1}	1–10	170.5	1.63
		Sediment	9.6×10^{-5}	6.1×10^{-3}	2–20	150.6	1.80
	78°N 92°E	Water	2.2×10^{-4}	4.9×10^{-3}	1–10	89.6	1.35
		Sediment	1.1×10^{-6}	8.3×10^{-4}	2–20	107.2	2.88
	76°N 76°E	Water	3×10^{-4}	5×10^{-3}	1–10	82.7	1.22
		Sediment	5.6×10^{-6}	8.3×10^{-4}	2–20	104.6	2.17
Barents Sea	72°N 45°E	Water	1.1×10^{-5}	4×10^{-3}	2–10	155.5	2.56
		Sediment	1×10^{-6}	6×10^{-4}	2–20	207.8	2.77
	79°N 58°E	Water	5.6×10^{-5}	3.3×10^{-4}	2–10	69.8	0.77
		Sediment	1.2×10^{-6}	3.7×10^{-5}	2–30	78.6	1.49
	76°N 20°E	Water	1.3×10^{-5}	2.9×10^{-4}	4–10	89.8	1.35
		Sediment	7.7×10^{-7}	3.7×10^{-5}	10–30	102.3	1.68
Beaufort Sea	70.5°N 143°W	Water	4.4×10^{-7}	2.2×10^{-5}	10–40	74.6	1.70
		Sediment	4.2×10^{-10}	9×10^{-6}	50–60	192.3	4.33
Central Arctic Ocean	86°N 80°E	Water	3.5×10^{-5}	7.7×10^{-4}	1–10	162.4	1.34
		Sediment	2.5×10^{-11}	4.4×10^{-5}	30–60	197.6	6.24
Davis Strait	60°N 55°W	Water	1.1×10^{-6}	4.7×10^{-6}	20–40	49.0	0.63
		Sediment	2×10^{-8}	1.2×10^{-6}	20–80	126.3	1.77
Iceland Sea	67°N 20°W	Water	2.1×10^{-7}	3.3×10^{-5}	4–30	63.7	2.19
		Sediment	1.6×10^{-10}	2.5×10^{-5}	20–50	217.7	5.19
Chukchi Sea	70°N 175°W	Water	5.1×10^{-8}	1.8×10^{-3}	10–40	220.3	4.55
		Sediment	6.7×10^{-11}	6.2×10^{-4}	10–60	223.3	6.97

TABLE XXXII. SUMMARY OF MODEL INTER-COMPARISONS FOR ^{137}Cs, CONTINUOUS RELEASE (1 TBq/YEAR FOR 10 YEARS) IN NOVAYA ZEMLYA TROUGH

Location	Position	Medium	Minimum	Maximum	Time to max. (a)	CV (%)	Level of agreement
Kara Sea	72°N 65°E	Water	1.5×10^{-3}	1.6×10^{-1}	6–10	115.4	2.03
		Sediment	1.4×10^{-4}	5.8×10^{-2}	6–20	184.2	2.61
	78°N 92°E	Water	6×10^{-4}	2.4×10^{-2}	6–11	120.7	1.60
		Sediment	7.8×10^{-6}	8.3×10^{-3}	6–30	153.8	3.03
	76°N 76°E	Water	6×10^{-4}	2.4×10^{-2}	6–11	114.1	1.74
		Sediment	1.6×10^{-5}	8.3×10^{-3}	6–30	141.4	2.71
Barents Sea	72°N 45°E	Water	8.8×10^{-5}	1.7×10^{-2}	6–14	143.8	2.28
		Sediment	1×10^{-5}	5.8×10^{-3}	6–30	210.0	2.81
	79°N 58°E	Water	1.8×10^{-6}	2.4×10^{-3}	6–20	100.1	3.12
		Sediment	3.2×10^{-7}	3.7×10^{-4}	6–30	94.0	3.06
	76°N 20°E	Water	1.2×10^{-4}	2.5×10^{-3}	6–20	91.8	1.32
		Sediment	7.8×10^{-6}	3.7×10^{-4}	6–35	80.7	1.67
Beaufort Sea	70.5°N 143°W	Water	3.3×10^{-6}	2.2×10^{-4}	15–50	87.2	1.82
		Sediment	4.5×10^{-9}	9×10^{-5}	50–70	172.5	4.30
Central Arctic Ocean	86°N 80°E	Water	1.1×10^{-4}	7.2×10^{-4}	10–20	79.5	0.81
		Sediment	2.5×10^{-10}	4.4×10^{-4}	40–70	197.6	6.24
Davis Strait	60°N 55°W	Water	1.1×10^{-5}	4.7×10^{-5}	20–50	55.1	0.63
		Sediment	2×10^{-7}	1.2×10^{-5}	30–80	146.9	1.78
Iceland Sea	67°N 20°W	Water	2.2×10^{-6}	3.2×10^{-4}	10–30	77.1	2.16
		Sediment	1.7×10^{-9}	2.5×10^{-4}	20–50	219.1	5.16
Chukchi Sea	70°N 175°W	Water	5.2×10^{-7}	1.5×10^{-2}	10–40	220.0	4.46
		Sediment	7×10^{-10}	6×10^{-3}	20–60	223.3	6.93

Note: Water (Bq/m^3)
        Sediment (Bq/kg dw)

TABLE XXXIII. SUMMARY OF MODEL INTER-COMPARISONS FOR ^{239}Pu, INSTANTANEOUS RELEASE (1 TBq) IN ABROSIMOV FJORD

Location	Position	Medium	Minimum	Maximum	Time to max. (a)	CV (%)	Level of agreement
Kara Sea	72°N 65°E	Water	2.6×10^{-3}	2.5×10^{-1}	1–4	195.0	1.98
		Sediment	5.4×10^{-4}	2.3×10^{-2}	1–1,000	115.9	1.62
	78°N 92°E	Water	1.9×10^{-7}	1.8×10^{-3}	1–6	115.9	3.97
		Sediment	4.6×10^{-8}	5.2×10^{-3}	2–1,000	119.6	5.05
	76°N 76°E	Water	5.5×10^{-6}	1.8×10^{-3}	1–6	158.6	3.10
		Sediment	1.7×10^{-6}	5.2×10^{-3}	1–1,000	117.5	3.48
Barents Sea	72°N 45°E	Water	1×10^{-5}	1.8×10^{-3}	1–7	207.5	2.25
		Sediment	5.4×10^{-6}	9×10^{-4}	1–1,000	129.4	2.22
	79°N 58°E	Water	1.1×10^{-7}	1.2×10^{-4}	1–8	83.7	3.04
		Sediment	9.3×10^{-9}	8.2×10^{-4}	1–1,000	127.9	5.11
	76°N 20°E	Water	7.7×10^{-10}	6.4×10^{-5}	3–8	112.8	4.92
		Sediment	8.1×10^{-11}	6.2×10^{-4}	1–1,000	184.9	6.88
Beaufort Sea	70.5°N 143°W	Water	8.1×10^{-16}*	6.4×10^{-5}	10–70	144.2	1.69
		Sediment	6×10^{-10}	5.7×10^{-4}	50–1,000	198.6	5.97
Central Arctic Ocean	86°N 80°E	Water	4.5×10^{-6}	1.4×10^{-4}	10–20	105.8	1.49
		Sediment	3.1×10^{-11}	8.3×10^{-4}	50–1,000	198.8	7.42
Davis Strait	60°N 55°W	Water	3.5×10^{-7}	5.5×10^{-5}	10–240	176.3	2.19
		Sediment	1.6×10^{-7}	4.4×10^{-4}	50–1,000	118.2	3.58
Iceland Sea	67°N 20°W	Water	3.1×10^{-7}	1.2×10^{-4}	10–30	151.6	2.58
		Sediment	2.1×10^{-10}	6.9×10^{-4}	40–1,000	151.0	6.51
Chukchi Sea	70°N 175°W	Water	7×10^{-8}	6.8×10^{-4}	10–30	210.1	3.98
		Sediment	9.1×10^{-11}	2.5×10^{-3}	30–1,000	196.9	7.44

TABLE XXXIV. SUMMARY OF MODEL INTER-COMPARISONS FOR ^{239}Pu, CONTINUOUS RELEASE (1 TBq/YEAR FOR 10 YEARS) IN ABROSIMOV FJORD

Location	Position	Medium	Minimum	Maximum	Time to max. (a)	CV (%)	Level of agreement
Kara Sea	72°N 65°E	Water	1.9×10^{-3}	4.9×10^{-2}	6–10	64.3	1.41
		Sediment	3.6×10^{-4}	2.1×10^{-1}	6–1,000	87.7	2.76
	78°N 92°E	Water	5.8×10^{-7}	2.3×10^{-2}	6–12	93.4	4.60
		Sediment	1.4×10^{-7}	2.9×10^{-2}	6–1,000	60.5	5.31
	76°N 76°E	Water	9.8×10^{-6}	3.6×10^{-2}	6–12	106.5	3.56
		Sediment	1.8×10^{-6}	5.7×10^{-2}	6–1,000	80.8	4.5
Barents Sea	72°N 45°E	Water	5.9×10^{-5}	1.2×10^{-2}	6–1,000	201.2	2.31
		Sediment	5.9×10^{-6}	2.1×10^{-2}	6–1,000	137.5	3.55
	79°N 58°E	Water	3.4×10^{-7}	8.6×10^{-4}	6–15	86.7	3.40
		Sediment	1.4×10^{-9}	6.2×10^{-3}	6–1,000	98.2	6.64
	76°N 20°E	Water	3.8×10^{-9}	5.6×10^{-4}	6–15	100.1	5.17
		Sediment	3.4×10^{-10}	6.2×10^{-3}	6–1,000	119.9	7.26
Beaufort Sea	70.5°N 143°W	Water	4.3×10^{-6}	3.2×10^{-4}	30–50	87.7	1.87
		Sediment	6×10^{-9}	5.7×10^{-3}	50–1,000	171.4	5.97
Central Arctic Ocean	86°N 80°E	Water	3×10^{-4}	7.7×10^{-4}	10–30	42.1	0.41
		Sediment	3.1×10^{-10}	8.3×10^{-3}	60–1,000	168.9	7.43
Davis Strait	60°N 55°W	Water	3.4×10^{-5}	2.7×10^{-4}	40–250	112.8	0.90
		Sediment	1.3×10^{-5}	4.4×10^{-3}	50–1,000	90.7	2.53

TABLE XXXIV. (cont.)

Location	Position	Medium	Minimum	Maximum	Time to max. (a)	CV (%)	Level of agreement
Iceland Sea	67°N 20°W	Water	3×10^{-6}	5.6×10^{-4}	20–40	80.4	2.27
		Sediment	2.3×10^{-9}	6.9×10^{-3}	50–1,000	151.4	6.48
Chukchi Sea	70°N 175°W	Water	6.9×10^{-7}	6.4×10^{-3}	10–40	192.9	3.96
		Sediment	9.1×10^{-10}	2.5×10^{-2}	50–1,000	187.0	7.44

Note: Water (Bq/m^3)
           Sediment (Bq/kg dw)
           *Omitted

TABLE XXXV. SUMMARY OF MODEL INTER-COMPARISONS FOR ^{239}Pu, INSTANTANEOUS RELEASE (1 TBq) IN NOVAYA ZEMLYA TROUGH

Location	Position	Medium	Minimum	Maximum	Time to max. (a)	CV (%)	Level of agreement
Kara Sea	72°N 65°E	Water	1.1×10^{-4}	1.1×10^{-2}	1–10	96.1	2.00
		Sediment	1.4×10^{-5}	3.8×10^{-2}	1–800	121.9	3.43
	78°N 92°E	Water	1.2×10^{-8}	2.9×10^{-3}	1–5	119.6	5.38
		Sediment	2.9×10^{-9}	6.8×10^{-3}	2–1,000	115.1	6.37
	76°N 76°E	Water	2.9×10^{-7}	5×10^{-3}	1–10	161.1	4.24
		Sediment	6.4×10^{-8}	6.8×10^{-3}	1–1,000	112.4	5.02
Barents Sea	72°N 45°E	Water	2.1×10^{-7}	2.4×10^{-3}	1–10	220.6	4.06
		Sediment	2.5×10^{-8}	2.2×10^{-3}	1–1,000	145.0	4.94
	79°N 58°E	Water	3.7×10^{-9}	1.7×10^{-4}	2–10	106.7	4.66
		Sediment	$3.2 \times 10^{-10}*$	6.3×10^{-4}	1–1,000	127.3	1.57
	76°N 20°E	Water	$7.1 \times 10^{-12}*$	6.9×10^{-5}	5–10	103.7	0.75
		Sediment	$6.9 \times 10^{-13}*$	6.3×10^{-4}	2–1,000	123.9	1.47
Beaufort Sea	70.5°N 143°W	Water	$1.5 \times 10^{-16}*$	7.2×10^{-5}	10–70	117.2	1.41
		Sediment	$1.6 \times 10^{-17}*$	5.8×10^{-4}	50–1,000	123.9	2.18
Central Arctic Ocean	86°N 80°E	Water	$4.4 \times 10^{-10}*$	1.7×10^{-4}	1–20	100.8	1.39
		Sediment	$5 \times 10^{-13}*$	8.3×10^{-4}	50–1,000	169.6	2.32
Davis Strait	60°N 55°W	Water	5.8×10^{-7}	6.1×10^{-5}	20–220	170.0	2.91
		Sediment	1×10^{-6}	6.7×10^{-4}	50–1,000	118.8	1.82
Iceland Sea	67°N 20°W	Water	$4.5 \times 10^{-18}*$	1.4×10^{-4}	10–30	107.7	1.63
		Sediment	$1.1 \times 10^{-18}*$	6.9×10^{-4}	50–1,000	124.6	1.53
Chukchi Sea	70°N 175°W	Water	$2.3 \times 10^{-19}*$	7.1×10^{-4}	10–30	185.8	3.64
		Sediment	$1.3 \times 10^{-20}*$	2.5×10^{-3}	30–1,000	172.0	3.75

TABLE XXXVI. SUMMARY OF MODEL INTER-COMPARISONS FOR ^{239}Pu, CONTINUOUS RELEASE (1 TBq/YEAR FOR 10 YEARS) IN NOVAYA ZEMLYA TROUGH

Location	Position	Medium	Minimum	Maximum	Time to max. (a)	CV (%)	Level of agreement
Kara Sea	72°N 65°E	Water	1.8×10^{-4}	3.9×10^{-2}	6–10	88.2	2.33
		Sediment	2.3×10^{-5}	8.7×10^{-2}	6–800	91.9	3.58
	78°N 92°E	Water	4.7×10^{-8}	2.5×10^{-2}	6–10	117.1	5.72
		Sediment	1.1×10^{-8}	3×10^{-2}	6–1,000	97.5	6.43
	76°N 76°E	Water	8.8×10^{-7}	3.3×10^{-2}	6–10	129.9	4.57
		Sediment	1.5×10^{-7}	3.6×10^{-2}	6–1,000	96.7	5.38

TABLE XXXVI. (cont.)

Barents Sea	72°N 45°E	Water	8.8×10^{-7}	1.2×10^{-2}	6–14	203.6	4.13
		Sediment	8.4×10^{-8}	2.2×10^{-2}	6–1,000	169.5	5.42
	79°N 58°E	Water	2×10^{-8}	7.9×10^{-4}	2–12	99.7	4.59
		Sediment	9.1×10^{-10}	6.3×10^{-3}	6–1,000	113.5	6.84
	76°N 20°E	Water	4.8×10^{-11}*	5.9×10^{-4}	6–14	98.1	0.69
		Sediment	4.7×10^{-12}*	6.3×10^{-3}	6–1,000	122.1	1.45
Beaufort Sea	70.5°N 143°W	Water	8×10^{-15}*	7.5×10^{-4}	30–80	73.3	0.70
		Sediment	1.7×10^{-16}*	5.8×10^{-3}	50–1,000	124.3	1.19
Central Arctic Ocean	86°N 80°E	Water	3.4×10^{-9}	1.6×10^{-3}	10–30	81.4	5.67
		Sediment	5.5×10^{-12}*	8.3×10^{-3}	50–1,000	138.5	1.98
Davis Strait	60°N 55°W	Water	2×10^{-5}	3×10^{-4}	40–230	121.7	1.17
		Sediment	8.3×10^{-6}	4.5×10^{-3}	50–1,000	87.9	2.73
Iceland Sea	67°N 20°W	Water	1.5×10^{-16}*	6.6×10^{-4}	20–30	62.4	0.67
		Sediment	3.7×10^{-19}*	6.9×10^{-3}	20–1,000	122.6	2.40
Chukchi Sea	70°N 175°W	Water	8.2×10^{-18}*	6.7×10^{-3}	10–40	166.0	3.64
		Sediment	1.1×10^{-19}*	2.5×10^{-2}	30–1,000	94.7	3.82

Note: Water (Bq/m^3)
Sediment (Bq/kg dw)
*Omitted

TABLE XXXVII. SUMMARY OF MODEL INTER-COMPARISONS FOR ^{60}Co, INSTANTANEOUS RELEASE (1 TBq) IN ABROSIMOV FJORD

Location	Position	Medium	Minimum	Maximum	Time to max. (a)	CV (%)	Level of agreement
Kara Sea	72°N 65°E	Water	1.1×10^{-5}	9.2×10^{-3}	1–3	78.9	2.92
		Sediment	2.1×10^{-4}	1.7×10^{-2}	1–7	97.6	1.91
	78°N 92°E	Water	2.9×10^{-11}*	1.9×10^{-3}	1–4	109.9	1.67
		Sediment	7.1×10^{-10}	2.6×10^{-3}	1–8	130.9	6.56
	76°N 76°E	Water	1.9×10^{-9}	5.6×10^{-3}	1–4	183.0	6.46
		Sediment	4.2×10^{-8}	2.6×10^{-3}	1–8	119.2	4.79
Barents Sea	72°N 45°E	Water	4×10^{-8}	1.2×10^{-3}	1–4	219.2	4.47
		Sediment	3.4×10^{-7}	5.1×10^{-4}	1–8	136.4	3.17
	79°N 58°E	Water	1.7×10^{-12}*	1.2×10^{-4}	2–6	78.8	0.93
		Sediment	6.1×10^{-12}*	4.7×10^{-4}	1–10	184.8	1.52
	76°N 20°E	Water	2.9×10^{-16}*	1.2×10^{-4}	1–6	142.3	1.68
		Sediment	3.7×10^{-15}*	1.7×10^{-5}	1–10	71.0	0.75
Beaufort Sea	70.5°N 143°W	Water	6×10^{-35}*	7.6×10^{-7}	10–20	67.7	0.92
		Sediment	4.2×10^{-36}*	4.9×10^{-7}	10–20	159.1	1.57
Central Arctic Ocean	86°N 80°E	Water	4.6×10^{-17}*	2×10^{-5}	0–10	128.8	1.22
		Sediment	2.1×10^{-17}*	1×10^{-5}	0–15	169.8	2.88
Davis Strait	60°N 55°W	Water	1.2×10^{-8}	1.3×10^{-7}	10–20	82.5	1.03
		Sediment	2×10^{-9}	1.1×10^{-6}	10–30	190.6	2.74
Iceland Sea	67°N 20°W	Water	9.7×10^{-42}*	4.5×10^{-6}	0–20	106.0	1.13
		Sediment	6.2×10^{-40}*	2.8×10^{-6}	10–20	120.5	1.72
Chukchi Sea	70°N 175°W	Water	9.3×10^{-41}*	1.4×10^{-4}	0–10	199.4	3.82
		Sediment	2.7×10^{-42}*	1×10^{-4}	0–20	196.3	4.27

TABLE XXXVIII. SUMMARY OF MODEL INTER-COMPARISONS FOR ^{60}Co, CONTINUOUS RELEASE (1 TBq/YEAR FOR 10 YEARS) IN ABROSIMOV FJORD

Location	Position	Medium	Minimum	Maximum	Time to max. (a)	CV (%)	Level of agreement
Kara Sea	72°N 65°E	Water	2.3×10^{-6}	6.5×10^{-2}	10	128.9	4.45
		Sediment	4.9×10^{-5}	7.7×10^{-1}	10–13	202.6	4.19
	78°N 92°E	Water	3.7×10^{-11}*	9.2×10^{-3}	10	120.9	7.36
		Sediment	9.1×10^{-10}	2.8×10^{-2}	10–17	163.4	7.48
	76°N 76°E	Water	1.2×10^{-9}	1.4×10^{-2}	10	137.7	7.06
		Sediment	2.5×10^{-8}	9.4×10^{-3}	10–15	149.6	5.57
Barents Sea	72°N 45°E	Water	1.9×10^{-8}	6.3×10^{-3}	10	79.8	5.52
		Sediment	1.3×10^{-7}	4.3×10^{-3}	10–15	151.7	4.52
	79°N 58°E	Water	8.3×10^{-13}*	3.3×10^{-4}	10–12	121.7	2.22
		Sediment	2.9×10^{-12}*	2.5×10^{-4}	10–16	133.9	1.24
	76°N 20°E	Water	1.7×10^{-16}*	2×10^{-4}	10–12	157.4	9.25
		Sediment	2.2×10^{-15}*	3.8×10^{-4}	10–16	90.4	1.14
Beaufort Sea	70.5°N 143°W	Water	4.9×10^{-34}	8×10^{-6}	10–20	64.8	0.73
		Sediment	3.2×10^{-25}	4.6×10^{-6}	20–30	117.7	1.51
Central Arctic Ocean	86°N 80°E	Water	1.4×10^{-17}*	1.7×10^{-4}	10–15	109.8	1.28
		Sediment	1.2×10^{-16}*	9.7×10^{-5}	10–20	149.3	2.90
Davis Strait	60°N 55°W	Water	3.7×10^{-7}	1.1×10^{-6}	10–30	50.2	0.47
		Sediment	1.1×10^{-7}	5×10^{-6}	20–30	174.1	1.65
Iceland Sea	67°N 20°W	Water	7.1×10^{-41}*	4.1×10^{-5}	10–20	92.8	1.00
		Sediment	5.5×10^{-39}*	2.6×10^{-5}	10–30	124.4	1.74
Chukchi Sea	70°N 175°W	Water	6.6×10^{-40}*	1.2×10^{-3}	10–20	199.4	3.27
		Sediment	8.4×10^{-39}*	9.7×10^{-4}	10–20	198.4	3.84

Note: Water (Bq/m^3)
Sediment (Bq/kg dw)
*Omitted

TABLE XXXIX. SUMMARY OF MODEL INTER-COMPARISONS FOR ^{60}Co, INSTANTANEOUS RELEASE (1TBq) IN NOVAYA ZEMLYA TROUGH

Location	Position	Medium	Minimum	Maximum	Time to max. (a)	CV (%)	Level of agreement
Kara Sea	72°N 65°E	Water	2.3×10^{-7}	1.1×10^{-2}	1	86.4	4.68
		Sediment	1.5×10^{-6}	3×10^{-2}	1–5	141.2	4.30
	78°N 92°E	Water	3.2×10^{-13}*	1.7×10^{-3}	1–3	100.4	9.72
		Sediment	7.9×10^{-12}	4.8×10^{-3}	1–10	169.7	8.78
	76°N 76°E	Water	2.2×10^{-11}	4×10^{-3}	1–3	152.9	8.25
		Sediment	4.4×10^{-10}	4.8×10^{-3}	1–7	146.4	7.03
Barents Sea	72°N 45°E	Water	1.1×10^{-11}	1.9×10^{-3}	1–5	219.2	8.23
		Sediment	1.1×10^{-10}	9.1×10^{-4}	1–10	215.4	6.91
	79°N 58°E	Water	1.7×10^{-14}*	1.5×10^{-4}	1–4	117.2	1.24
		Sediment	6.4×10^{-14}*	9.1×10^{-4}	1–10	200.0	1.78
	76°N 20°E	Water	5×10^{-20}*	3.7×10^{-5}	1–5	111.8	0.93
		Sediment	1×10^{-20}*	2.1×10^{-5}	1–10	58.1	0.78
Beaufort Sea	70.5°N 143°W	Water	2.1×10^{-35}*	9.6×10^{-7}	5–20	33.8	0.34
		Sediment	1.4×10^{-36}*	6×10^{-7}	10–20	126.3	1.52
Central Arctic Ocean	86°N 80°E	Water	1.6×10^{-17}*	2.5×10^{-5}	0–10	80.1	0.95
		Sediment	7×10^{-18}*	1.3×10^{-5}	0–20	153.1	2.9
Davis Strait	60°N 55°W	Water	4.8×10^{-8}	2.1×10^{-7}	10–20	66.1	0.64
		Sediment	1.7×10^{-8}	1.4×10^{-4}	10–30	196.7	3.91
Iceland Sea	67°N 20°W	Water	3.2×10^{-42}*	5.7×10^{-6}	5–10	68.2	0.87
		Sediment	2.2×10^{-40}*	3.4×10^{-6}	10–20	103.2	1.75
Chukchi Sea	70°N 175°W	Water	3.2×10^{-41}*	1.8×10^{-4}	0–10	199.3	4.14
		Sediment	9×10^{-43}*	1.3×10^{-4}	10–20	195.3	4.24

TABLE XL. SUMMARY OF MODEL INTER-COMPARISONS FOR ^{60}Co, CONTINUOUS RELEASE (1 TBq/YEAR FOR 10 YEARS) IN NOVAYA ZEMLYA TROUGH

Location	Position	Medium	Minimum	Maximum	Time to max. (a)	CV (%)	Level of agreement
Kara Sea	72°N 65°E	Water	3.8×10^{-8}	2.5×10^{-2}	10	79.8	5.82
		Sediment	3.2×10^{-7}	1.2×10^{-1}	10–12	131.1	5.57
	78°N 92°E	Water	4×10^{-13}*	1.1×10^{-2}	10	121.8	2.22
		Sediment	9.8×10^{-12}	1.1×10^{-2}	10–14	107.7	9.05
	76°N 76°E	Water	1.4×10^{-11}	1.8×10^{-2}	10	157.4	9.11
		Sediment	2.7×10^{-10}	1.1×10^{-2}	10–13	105.2	7.61
Barents Sea	72°N 45°E	Water	7.2×10^{-12}*	8×10^{-3}	10–12	225.0	8.05
		Sediment	4.4×10^{-11}	5.5×10^{-3}	10–16	167.9	8.09
	79°N 58°E	Water	7.4×10^{-15}*	3.3×10^{-4}	10–12	80.7	1.47
		Sediment	2.7×10^{-14}*	3×10^{-4}	10–15	124.3	1.07
	76°N 20°E	Water	1×10^{-20}*	2.6×10^{-4}	10–12	83.2	0.81
		Sediment	1×10^{-20}*	9.4×10^{-4}	10–16	129.1	1.48
Beaufort Sea	70.5°N 143°W	Water	2.4×10^{-6}*	7.3×10^{-5}	10–20	155.8	1.44
		Sediment	1.7×10^{-7}*	1.1×10^{-5}	20–30	95.7	1.81
Central Arctic Ocean	86°N 80°E	Water	4.8×10^{-18}*	7.3×10^{-4}	10	138.7	1.71
		Sediment	4.2×10^{-17}*	1.2×10^{-4}	10–20	86.7	2.90
Davis Strait	60°N 55°W	Water	4.6×10^{-7}	9.4×10^{-6}	10–25	154.1	1.31
		Sediment	1.3×10^{-7}	7.9×10^{-6}	20–30	147.4	1.79
Iceland Sea	67°N 20°W	Water	4.8×10^{-6}*	2.3×10^{-4}	10–20	143.6	1.68
		Sediment	5.5×10^{-7}*	3.3×10^{-5}	10–30	84.0	1.78
Chukchi Sea	70°N 175°W	Water	9×10^{-7}*	1.5×10^{-3}	10–20	199.2	3.22
		Sediment	1.7×10^{-7}*	1.2×10^{-3}	10–30	197.4	3.84

Note: Water (Bq/m^3)
Sediment (Bq/kg dw)
*Omitted

TABLE XLI. SUMMARY OF MODEL INTER-COMPARISONS FOR ^{99}Tc, INSTANTANEOUS RELEASE (1 TBq) IN ABROSIMOV FJORD

Location	Position	Medium	Minimum	Maximum	Time to max. (a)	CV (%)	Level of agreement
Kara Sea	72°N 65°E	Water	7.8×10^{-3}	5.5×10^{-2}	1–2	75.3	0.85
		Sediment	1×10^{-5}	1.5×10^{-3}	2–30	184.2	2.17
	78°N 92°E	Water	4.2×10^{-4}	5.2×10^{-3}	2–5	68.9	1.09
		Sediment	1×10^{-7}	2.8×10^{-2}	2–40	232.9	5.45
	76°N 76°E	Water	6.8×10^{-4}	8.3×10^{-3}	2–3	73.7	1.08
		Sediment	4.4×10^{-7}	2.8×10^{-2}	2–20	232.6	4.80
Barents Sea	72°N 45°E	Water	1.7×10^{-5}	3.8×10^{-3}	2–6	131.7	2.35
		Sediment	3.4×10^{-7}	6.9×10^{-4}	2–100	240.7	3.30
	79°N 58°E	Water	1.2×10^{-4}	4.6×10^{-4}	3–10	58.5	0.58
		Sediment	1.2×10^{-7}	5.7×10^{-5}	1–100	191.5	2.67
	76°N 20°E	Water	1.9×10^{-5}	5.9×10^{-4}	5–10	106.2	1.49
		Sediment	1.5×10^{-7}	5.7×10^{-5}	10–100	201.0	2.58
Beaufort Sea	70.5°N 143°W	Water	1.9×10^{-5}	1×10^{-4}	20–130	63.3	0.72
		Sediment	1×10^{-8}	4×10^{-5}	100–140	199.4	3.60
Central Arctic Ocean	86°N 80°E	Water	7.2×10^{-5}	4.2×10^{-4}	7–20	72.6	0.76
		Sediment	2.5×10^{-9}	1×10^{-4}	100–1,000	199.7	4.60
Davis Strait	60°N 55°W	Water	6×10^{-6}	7.8×10^{-5}	30–500	135.1	1.11
		Sediment	8.1×10^{-9}	2.5×10^{-5}	30–800	191.3	3.48
Iceland Sea	67°N 20°W	Water	3.6×10^{-5}	2.1×10^{-4}	10–50	97.3	0.76
		Sediment	3.5×10^{-9}	1.5×10^{-4}	20–100	222.1	4.63
Chukchi Sea	70°N 175°W	Water	2.3×10^{-5}	2.2×10^{-3}	10–200	201.7	1.98
		Sediment	8×10^{-9}	9×10^{-4}	20–200	223.4	5.05

TABLE XLII. SUMMARY OF MODEL INTER-COMPARISONS FOR ^{99}Tc, CONTINUOUS RELEASE (1 TBq/YEAR FOR 10 YEARS) IN ABROSIMOV FJORD

Location	Position	Medium	Minimum	Maximum	Time to max. (a)	CV (%)	Level of agreement
Kara Sea	72°N 65°E	Water	1.7×10^{-2}	2.7×10^{-1}	10	87.7	1.20
		Sediment	5.1×10^{-5}	1.4×10^{-2}	10–30	159.9	2.44
	78°N 92°E	Water	2.7×10^{-3}	3.9×10^{-2}	10–11	85.4	1.16
		Sediment	6.6×10^{-7}	1×10^{-2}	10–50	217.1	4.18
	76°N 76°E	Water	5.3×10^{-3}	4.3×10^{-2}	10	70.0	0.91
		Sediment	2.9×10^{-6}	1×10^{-2}	10–30	208.2	3.54
Barents Sea	72°N 45°E	Water	1.5×10^{-4}	2×10^{-2}	10–14	128.7	2.12
		Sediment	3.3×10^{-6}	6.9×10^{-3}	10–100	241.7	3.32
	79°N 58°E	Water	9.4×10^{-4}	3.3×10^{-3}	10–12	60.8	0.54
		Sediment	9.1×10^{-7}	5.7×10^{-4}	10–100	200.7	2.79
	76°N 20°E	Water	1.7×10^{-4}	4.4×10^{-3}	12–20	100.1	1.41
		Sediment	1.1×10^{-6}	5.7×10^{-4}	20–100	200.7	2.71
Beaufort Sea	70.5°N 143°W	Water	1.9×10^{-4}	1×10^{-3}	20–140	66.7	0.72
		Sediment	2.1×10^{-7}	4×10^{-4}	100–140	199.3	3.28
Central Arctic Ocean	86°N 80°E	Water	6.9×10^{-4}	4.1×10^{-3}	10–30	88.0	0.77
		Sediment	2.3×10^{-7}	1×10^{-3}	70–120	199.4	3.64
Davis Strait	60°N 55°W	Water	6×10^{-5}	3.8×10^{-4}	30–500	94.8	0.80
		Sediment	8.1×10^{-8}	2.5×10^{-4}	40–800	195.4	3.49
Iceland Sea	67°N 20°W	Water	3.1×10^{-4}	9.2×10^{-4}	20–60	45.9	0.47
		Sediment	6.1×10^{-8}	7.6×10^{-4}	30–100	221.9	4.09
Chukchi Sea	70°N 175°W	Water	2×10^{-4}	1.8×10^{-2}	10–200	201.0	1.95
		Sediment	1.6×10^{-7}	9×10^{-3}	30–100	223.5	4.75

Note: Water (Bq/m^3)
Sediment (Bq/kg dw)

TABLE XLIII. SUMMARY OF MODEL INTER-COMPARISONS FOR ^{99}Tc, INSTANTANEOUS RELEASE (1 TBq) IN NOVAYA ZEMLYA TROUGH

Location	Position	Medium	Minimum	Maximum	Time to max. (a)	CV (%)	Level of agreement
Kara Sea	72°N 65°E	Water	3.9×10^{-3}	1.9×10^{-1}	0–10	99.3	1.69
		Sediment	6.4×10^{-6}	1.5×10^{-3}	1–100	171.3	2.37
	78°N 92°E	Water	3.7×10^{-5}	5.2×10^{-3}	2–10	91.4	2.15
		Sediment	7.9×10^{-8}	1×10^{-3}	5–100	222.1	4.10
	76°N 76°E	Water	4.5×10^{-4}	5.5×10^{-3}	2–10	87.8	1.09
		Sediment	3.9×10^{-7}	1×10^{-3}	3–100	213.0	3.41
Barents Sea	72°N 45°E	Water	1.5×10^{-5}	4.1×10^{-3}	2–10	134.3	2.43
		Sediment	3.3×10^{-7}	6.9×10^{-4}	2–100	241.1	3.32
	79°N 58°E	Water	6.5×10^{-5}	4.2×10^{-4}	2–11	69.6	0.81
		Sediment	1×10^{-7}	5.7×10^{-5}	10–100	192.6	2.75
	76°N 20°E	Water	1.7×10^{-5}	4.7×10^{-4}	5–11	105.0	1.44
		Sediment	1.2×10^{-7}	5.7×10^{-5}	10–100	200.8	2.67
Beaufort Sea	70.5°N 143°W	Water	1.9×10^{-5}	9.9×10^{-5}	20–140	67.7	0.72
		Sediment	9.7×10^{-9}	4.1×10^{-5}	100–140	199.4	3.62
Central Arctic Ocean	86°N 80°E	Water	9.6×10^{-5}	4×10^{-4}	10–20	86.6	0.62
		Sediment	2.7×10^{-9}	1×10^{-4}	100–1,000	199.7	4.56
Davis Strait	60°N 55°W	Water	6×10^{-6}	7.8×10^{-5}	30–500	94.5	1.11
		Sediment	8.1×10^{-9}	2.5×10^{-5}	30–800	191.3	3.49
Iceland Sea	67°N 20°W	Water	2.9×10^{-5}	2.1×10^{-4}	10–50	46.4	0.86
		Sediment	3.2×10^{-9}	7.6×10^{-5}	60–100	220.6	4.37
Chukchi Sea	70°N 175°W	Water	8×10^{-6}	2.2×10^{-3}	10–200	202.6	2.44
		Sediment	8×10^{-9}	9×10^{-4}	20–200	223.4	5.05

TABLE XLIV. SUMMARY OF MODEL INTER-COMPARISONS FOR ^{99}Tc, CONTINUOUS RELEASE (1 TBq/YEAR FOR 10 YEARS) IN NOVAYA ZEMLYA TROUGH

Location	Position	Medium	Minimum	Maximum	Time to max. (a)	CV (%)	Level of agreement
Kara Sea	72°N 65°E	Water	1.7×10^{-2}	2×10^{-1}	10	99.3	1.07
		Sediment	4.7×10^{-5}	1.5×10^{-2}	10–100	181.6	2.50
	78°N 92°E	Water	2.3×10^{-3}	3.2×10^{-2}	10–12	91.4	1.14
		Sediment	5.7×10^{-7}	1×10^{-2}	10–100	229.1	4.24
	76°N 76°E	Water	3.8×10^{-3}	3.9×10^{-2}	10–20	87.8	1.01
		Sediment	2.7×10^{-6}	1×10^{-2}	10–30	220.1	3.56
Barents Sea	72°N 45°E	Water	1.4×10^{-4}	1.8×10^{-2}	10–20	134.3	2.11
		Sediment	3.2×10^{-6}	6.9×10^{-3}	10–100	242.1	3.33
	79°N 58°E	Water	5.7×10^{-4}	3.3×10^{-3}	10–20	69.6	0.76
		Sediment	6.9×10^{-7}	5.7×10^{-4}	10–100	203.0	2.92
	76°N 20°E	Water	1.6×10^{-4}	4.4×10^{-3}	12–20	105.0	1.44
		Sediment	1.1×10^{-6}	5.7×10^{-4}	20–100	202.0	2.71
Beaufort Sea	70.5°N 143°W	Water	1.9×10^{-4}	1×10^{-3}	20–140	67.7	0.72
		Sediment	1×10^{-7}	4.1×10^{-4}	100–150	199.4	3.61
Central Arctic Ocean	86°N 80°E	Water	7.5×10^{-4}	4.1×10^{-3}	10–30	86.5	0.74
		Sediment	2.7×10^{-8}	1×10^{-3}	70–1,000	199.7	4.56
Davis Strait	60°N 55°W	Water	6×10^{-5}	3.8×10^{-4}	30–500	94.5	0.80
		Sediment	8.1×10^{-8}	2.5×10^{-4}	40–1,000	195.4	3.49
Iceland Sea	67°N 20°W	Water	2.9×10^{-4}	9.2×10^{-4}	20–60	46.4	0.50
		Sediment	3.1×10^{-8}	7.6×10^{-3}	30–100	220.0	5.39
Chukchi Sea	70°N 175°W	Water	7.3×10^{-5}	1.8×10^{-2}	10–200	202.6	2.39
		Sediment	8.1×10^{-8}	9×10^{-3}	20–200	223.5	5.04

Note: Water (Bq/m^3)
Sediment (Bq/kg dw)
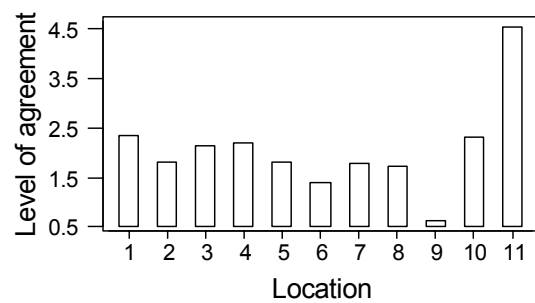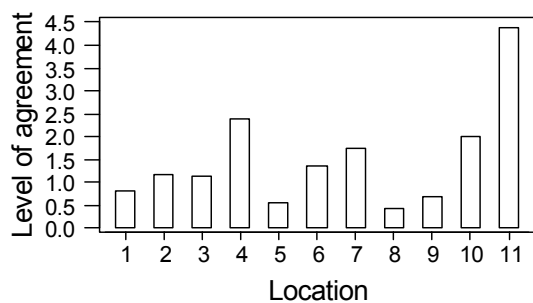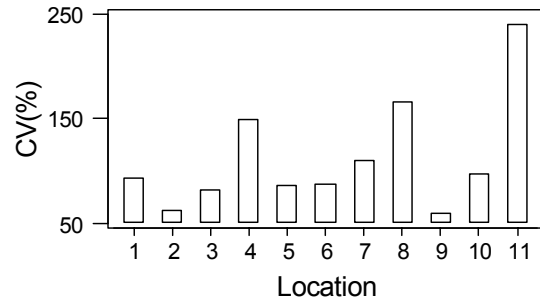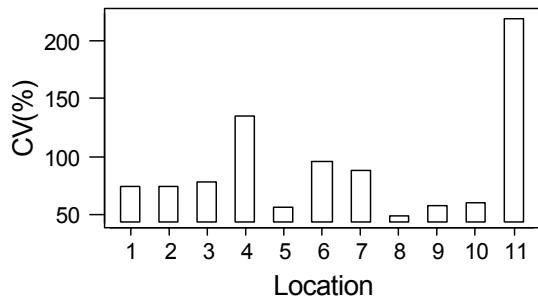
Instantaneous release at Novaya Zemlya Bay.

Continuous release at Novaya Zemlya Bay.

FIG. 16. Coefficient of variation and level of agreement for ^{137}Cs concentrations in water under benchmarking. For locations, see Table XXVIII.
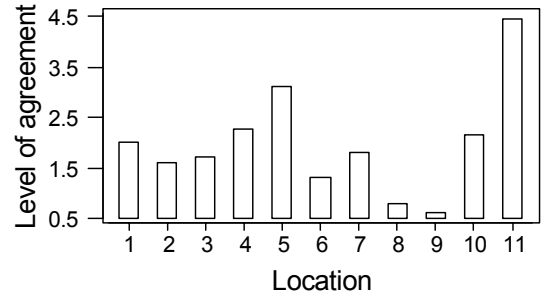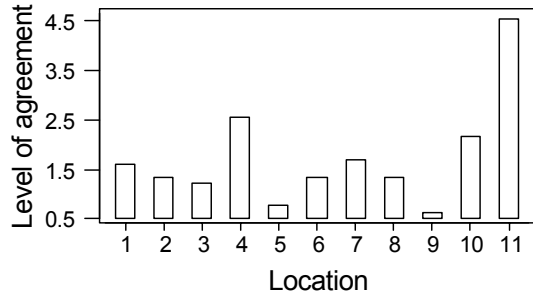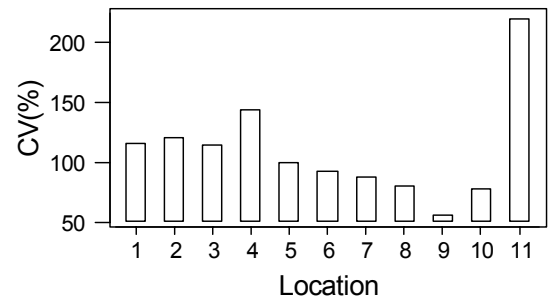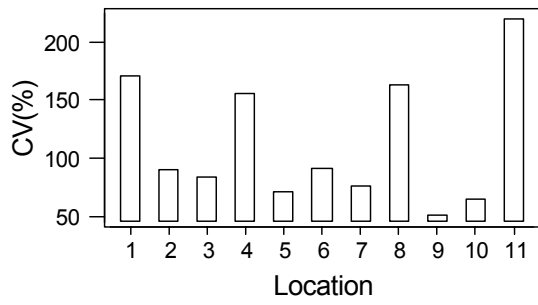
Instantaneous release at Novaya Zemlya Trough.

Continuous release at Novaya Zemlya Trough.

FIG. 17. *Coefficient of variation and level of agreement for* ^{137}Cs *concentrations in water under benchmarking. For locations, see Table XXVIII.*
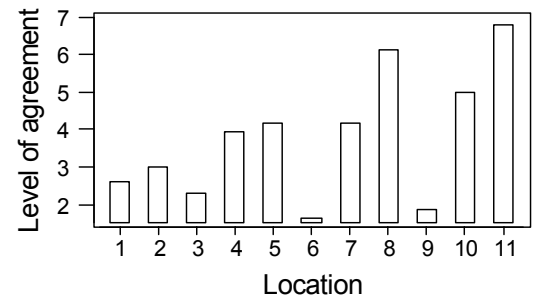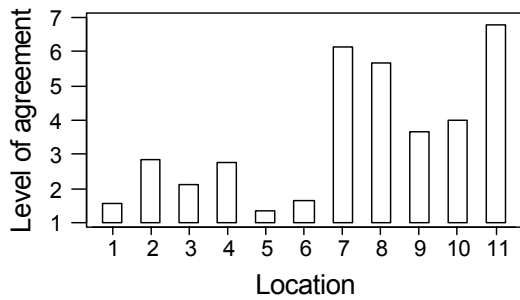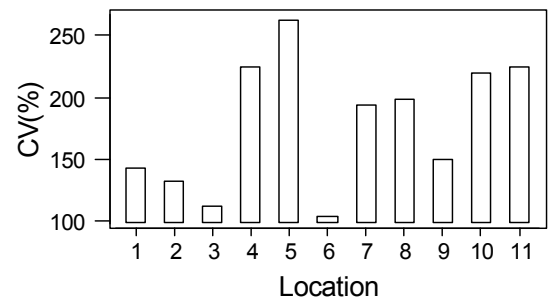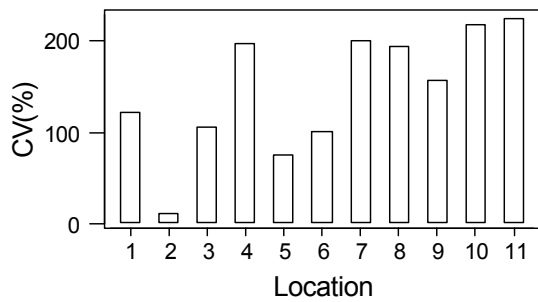
Instantaneous release at Novaya Zemlya Bay.

Continuous release at Novaya Zemlya Bay.

FIG. 18. *Coefficient of variation and level of agreement for* ^{137}Cs *concentrations in sediment under benchmarking. For locations, see Table XXVIII.*
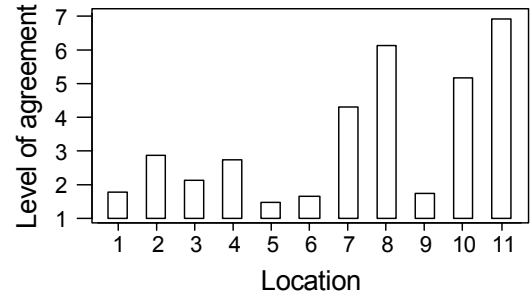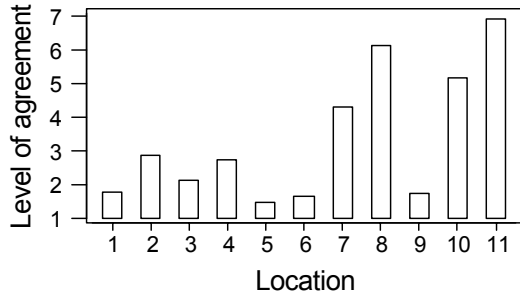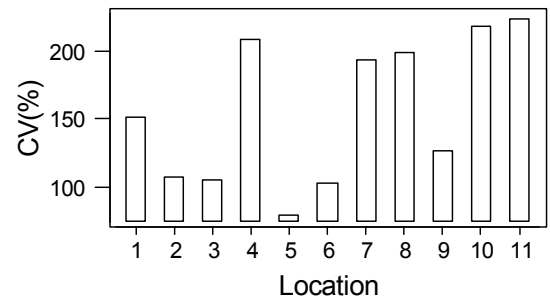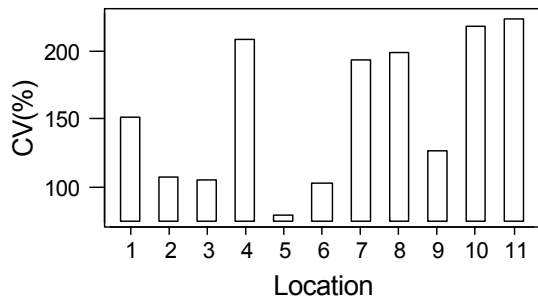
Instantaneous release at Novaya Zemlya Trough.

Continuous release at Novaya Zemlya Trough.

FIG. 19. Coefficient of variation and level of agreement for ^{137}Cs concentrations in sediment under benchmarking. For locations, see Table XXVIII.
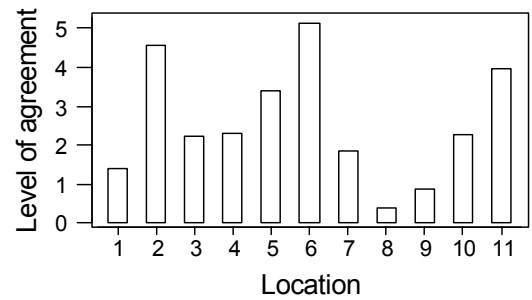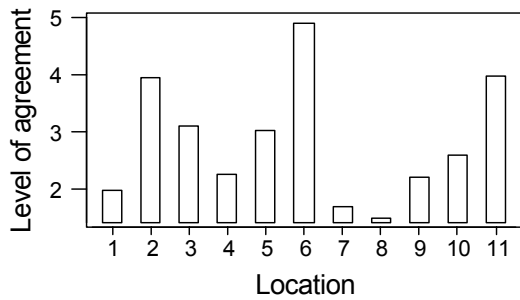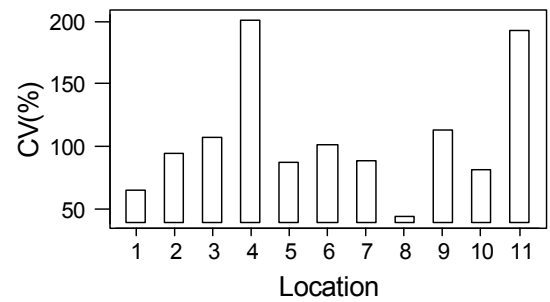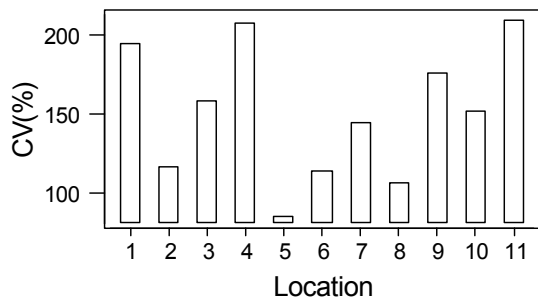
Instantaneous release at Novaya Zemlya Bay.

Continuous release at Novaya Zemlya Bay.

FIG. 20. Coefficient of variation and level of agreement for ^{239}Pu concentrations in water under benchmarking. For locations see Table XXVIII.
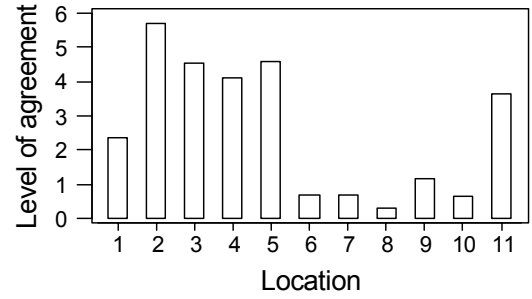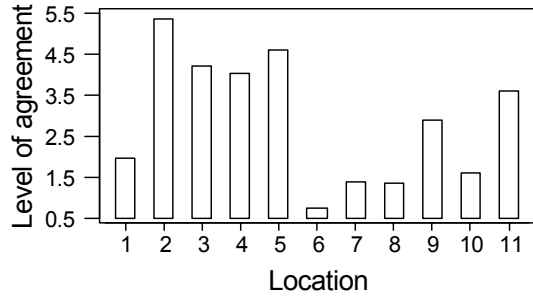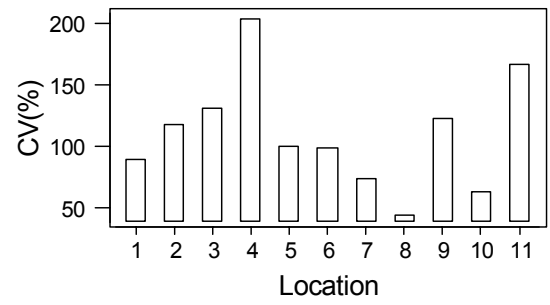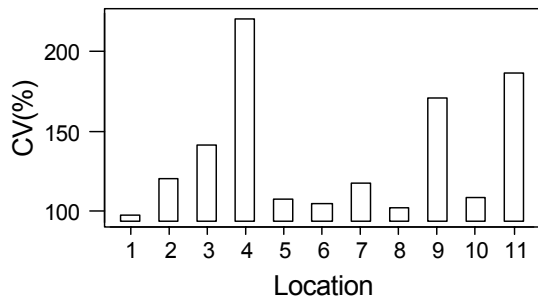
Instantaneous release at Novaya Zemlya Trough

Continuous release at Novaya Zemlya Trough.

FIG. 21. Coefficient of variation and level of agreement for ^{239}Pu concentrations in water under benchmarking. For locations see Table XXVIII.
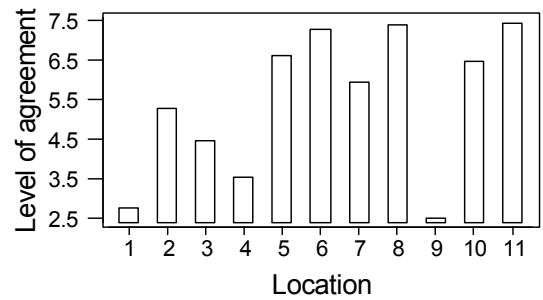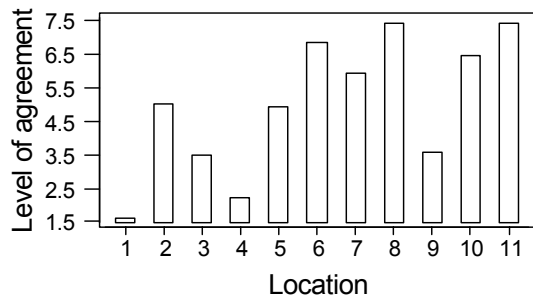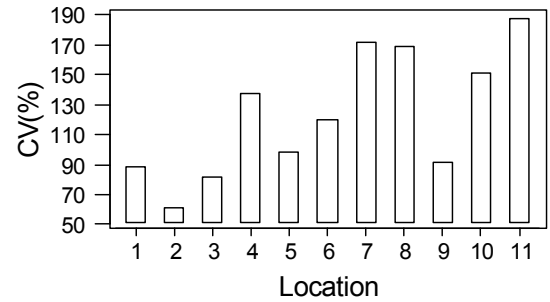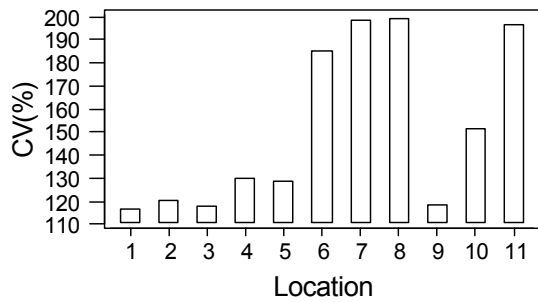
Instantaneous release at Novaya Zemlya Bay.

Continuous release at Novaya Zemlya Bay.

FIG. 22. Coefficient of variation and level of agreement for ^{239}Pu concentrations in sediment under benchmarking. For locations see Table XXVIII.
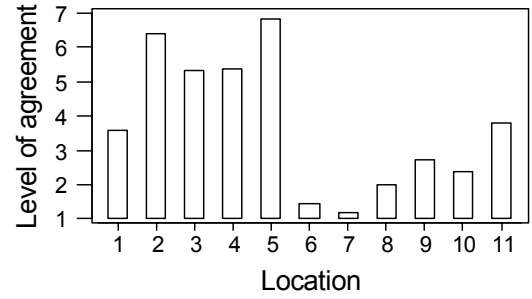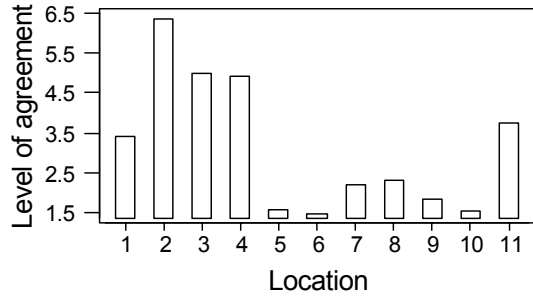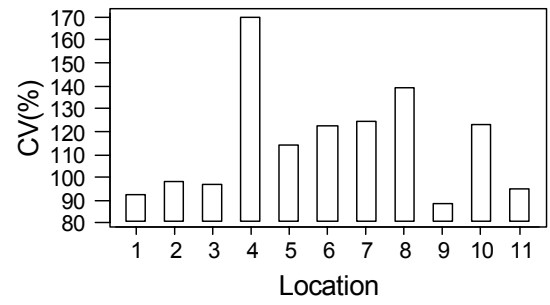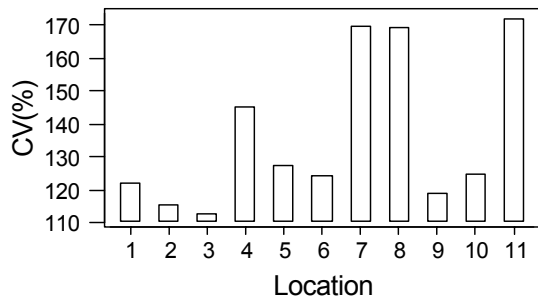
Instantaneous release at Novaya Zemlya Trough.

Continuous release at Novaya Zemlya Trough.

FIG. 23. Coefficient of variation and level of agreement for ^{239}Pu concentrations in sediment under benchmarking. For locations see Table XXVIII.
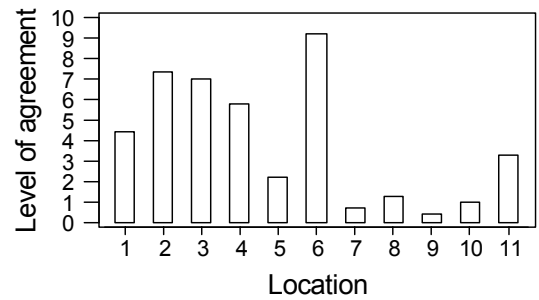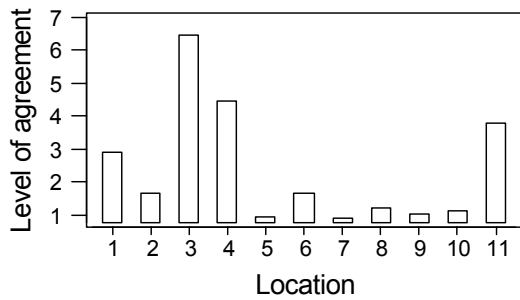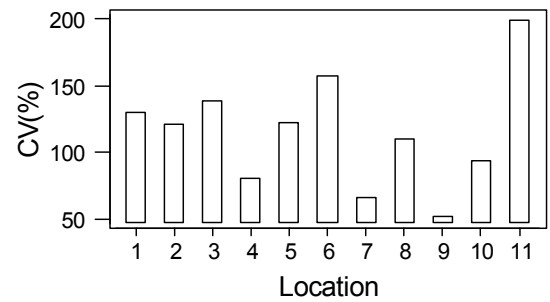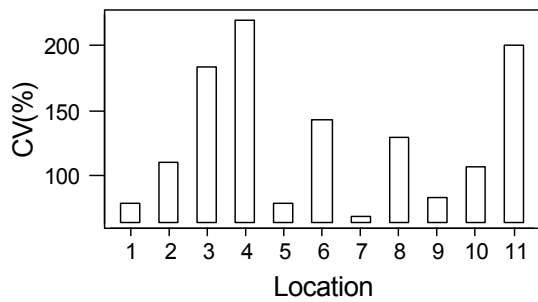
Instantaneous release at Novaya Zemlya Bay.

Continuous release at Novaya Zemlya Bay.

FIG. 24. Coefficient of variation and level of agreement for ^{60}Co concentrations in water under benchmarking. For locations see Table XXVIII.
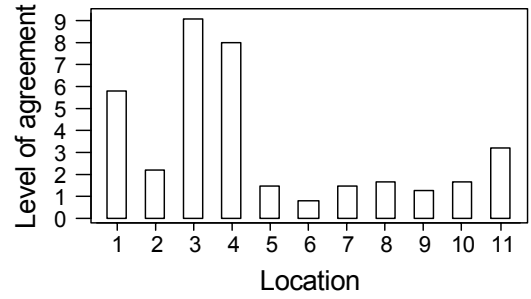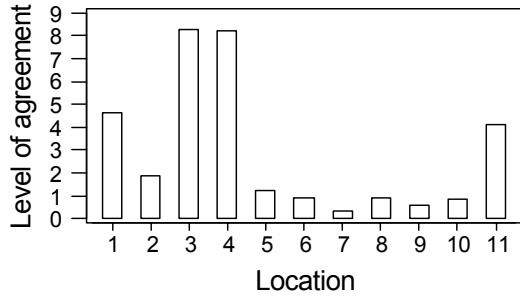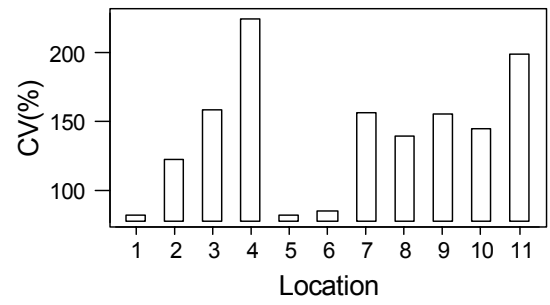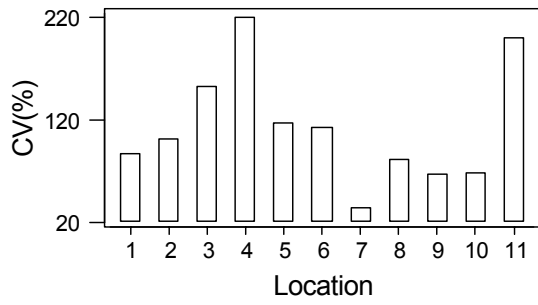
Instantaneous release at Novaya Zemlya Trough.

Continuous release at Novaya Zemlya Trough.

FIG. 25. *Coefficient of variation and level of agreement for ^{60}Co concentrations in water under benchmarking. For locations see Table XXVIII.*
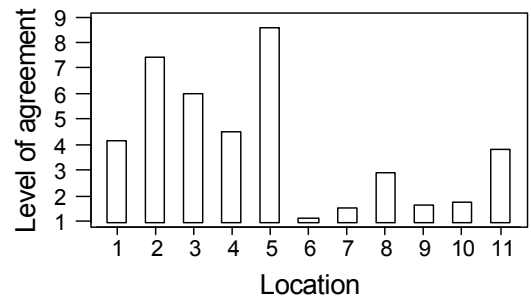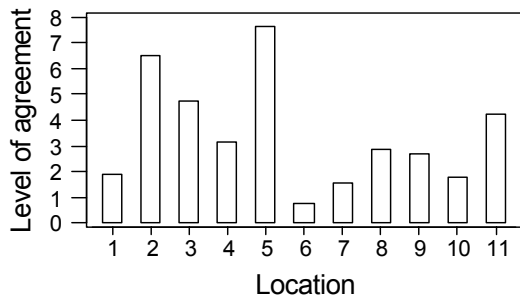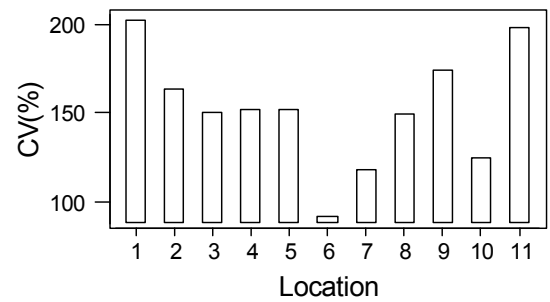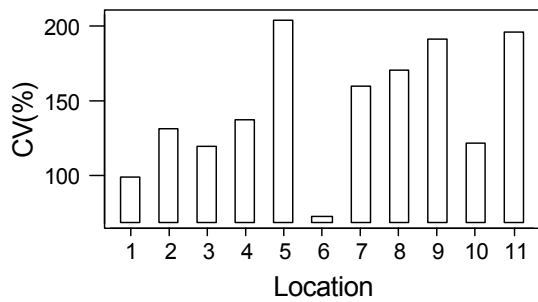
Instantaneous release at Novaya Zemlya Bay.

Continuous release at Novaya Zemlya Bay.

FIG. 26. *Coefficient of variation and level of agreement for ^{60}Co concentrations in sediment under benchmarking. For locations see Table XXVIII.*
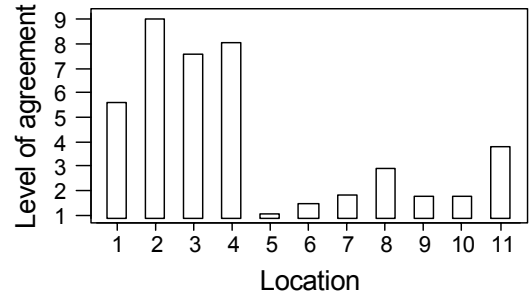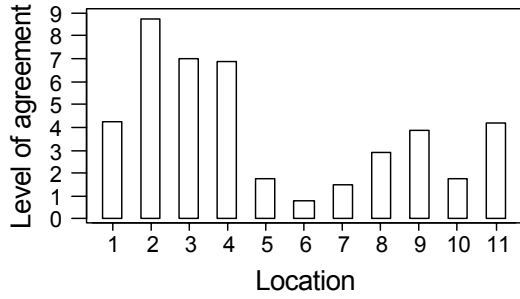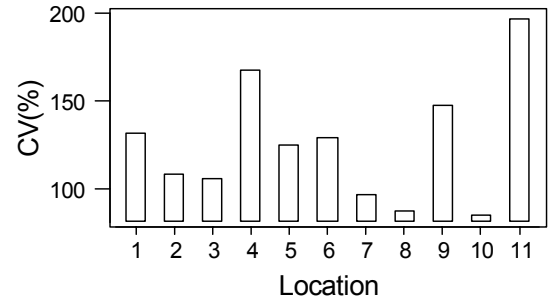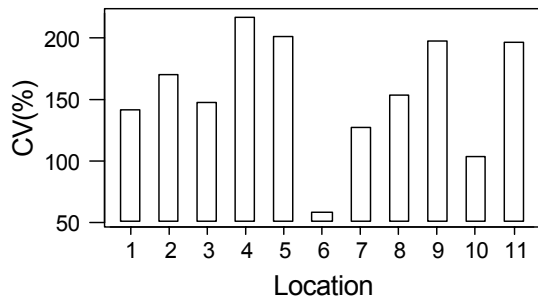
Instantaneous release at Novaya Zemlya Trough.

Continuous release at Novaya Zemlya Trough.

FIG. 27. Coefficient of variation and level of agreement for ^{60}Co concentrations in sediment under benchmarking. For locations see Table XXVIII.
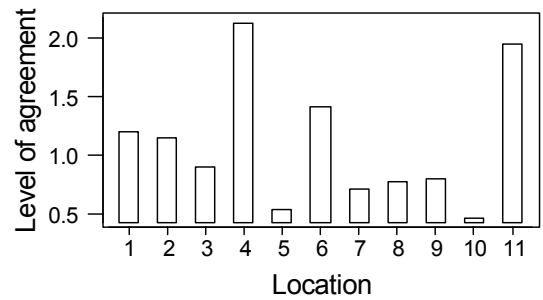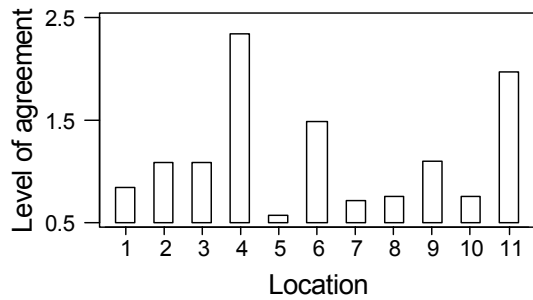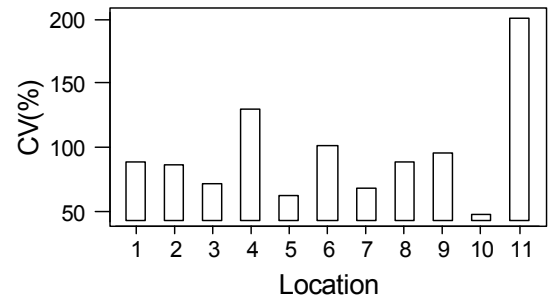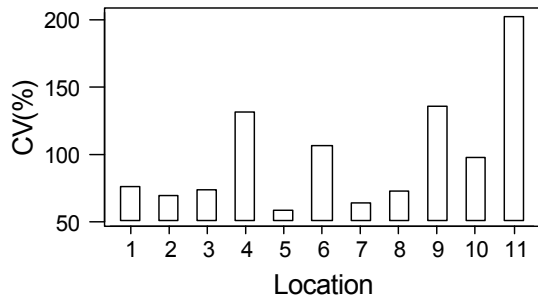
Instantaneous release at Novaya Zemlya Bay

Continuous release at Novaya Zemlya Bay.

FIG. 28. Coefficient of variation and level of agreement for ^{99}Tc concentrations in water under benchmarking. For locations see Table XXVIII.
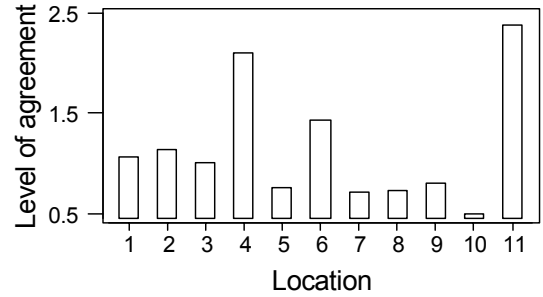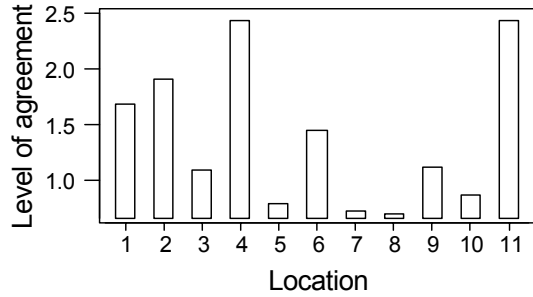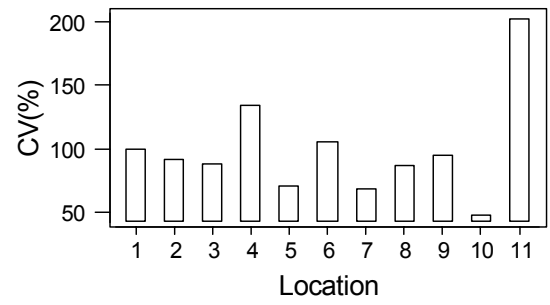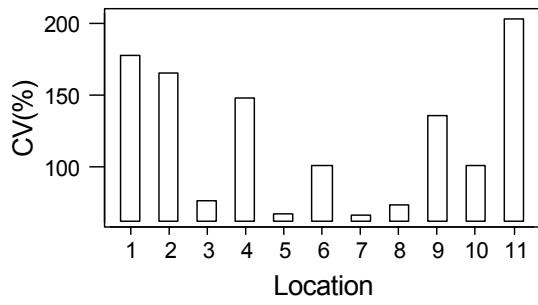
Instantaneous release at Novaya Zemlya Trough.

Continuous release at Novaya Zemlya Trough

FIG. 29. *Coefficient of variation and level of agreement for* ^{99}Tc *concentrations in water under benchmarking. For locations see Table XXVIII.*
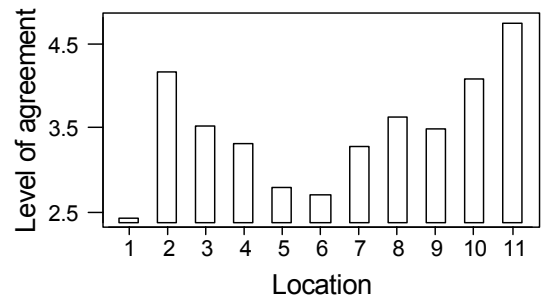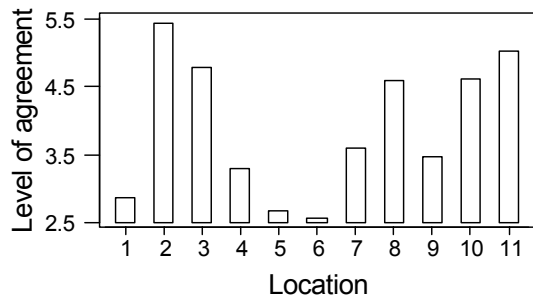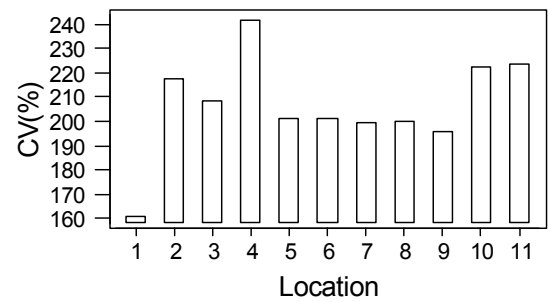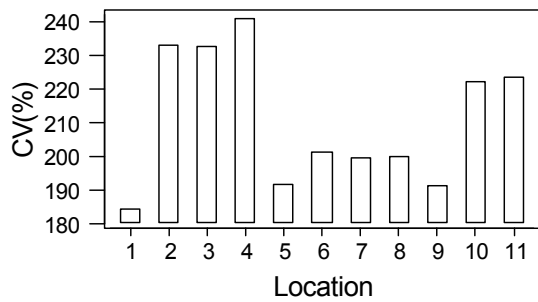
Instantaneous release at Novaya Zemlya Bay.

Continuous release at Novaya Zemlya Bay.

FIG. 30. *Coefficient of variation and level of agreement for* ^{99}Tc *concentrations in sediment under benchmarking. For locations see Table XXVIII.*
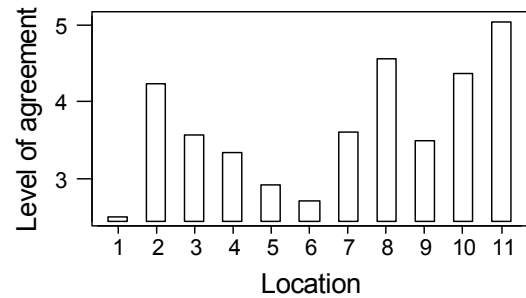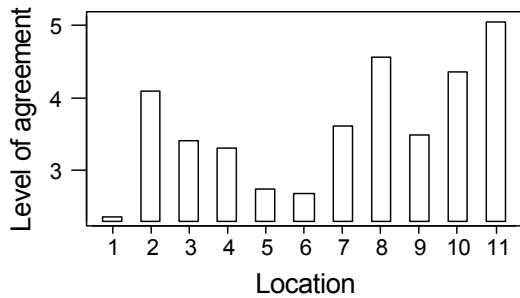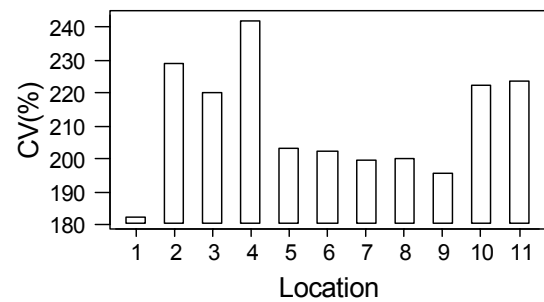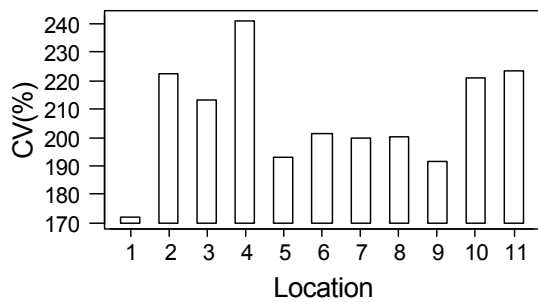
Instantaneous release at Novaya Zemlya Trough.   *Continuous release at Novaya Zemlya Trough.*

FIG. 31. Coefficient of variation and level of agreement for ^{99}Tc concentrations in sediment under benchmarking. For locations see Table XXVIII.

4.3.1. Results and analysis of model inter-comparisons

At a very general level, the CV(%) is a measure of the relative variation in the results; its main use is in aiding the comparison of variation over different locations, where the mean concentrations might vary considerably.

From Tables XXIX to XLIV, it can be seen that over all simulations the CV lies in the range of 50–250%; higher values are generally found at locations distant from the radionuclide source. There is little difference in observed CV value for each nuclide (ignoring sediment/water and other factors).

The level of agreement is another useful summary measure – it is widely accepted that agreement within 1 order of magnitude (level of agreement < 1) is very good, while agreement within two orders of magnitude (level of agreement < 2) is more common, and is acceptable.

From Tables XXIX to XLIV, it is clear that the level of agreement is generally poorer for the particle reactive radionuclides (Pu and Co) than for Tc and Cs. Again, ignoring all other factors, for Cs and Tc agreement is better than 3 orders of magnitude, while for Pu and Co, it is better than 4 orders of magnitude.

However, these summaries ignore a number of factors in the design of the simulation study, notably the site of release (Novaya Zemlya Bay or Novaya Zemlya Trough), whether it was continuous or instantaneous, the endpoint location and of course whether the prediction is made for water or sediment concentrations. Thus the remaining discussion will concentrate on these individual comparisons for each nuclide in turn, before summarising the results overall, and discussing their implications when the final radiological assessment is carried out.

4.3.1.1. Caesium-137

This radionuclide was selected for inclusion in the benchmark scenario due to its radiological significance, its 'intermediate' particle reactivity, and its potential inventory in the dumped material. The results are summarised in Tables XXIX to XXXII and Figures 16–19. The overall level of agreement is just over 2 (averaged for all results).

Generally speaking, the maximum concentrations in seawater agree within 2 orders of magnitude with exceptions at sites 4 (Barents Sea) and 11 (Chukchi Sea). The level of agreement generally falls off with distance from source (with the exception at site 9 (Davis Strait) where agreement between model predictions matches that achieved near source). Agreement in sediment results is overall only slightly poorer.

The CV values are typically around 120% for water concentrations and are higher for sediment concentrations at approximately 150%. They show little effect of whether the release point is in Novaya Zemlya Bay or Novaya Zemlya Trough. There again is a tendency for the results to be more varied at sites distant from the source compared to those close to the source.

The tables also give the time to the occurrence of the maximum concentrations. It is clear that generally there is good agreement in the results for time to maximum water concentrations near source, that the scatter in results increases at distant locations, and that overall the results for sediment show a larger range in times to maximum than for seawater.

Further analyses are reported in Table XLIII, which summarise the result in CV(%) and level of agreement for each of the factors included in the simulation design namely site (Novaya Zemlya Bay or Novaya Zemlya Trough), medium (sediment or water) release type (continuous or instantaneous) and scale (local, regional or global).

TABLE XLV. SUMMARY OF INTERCOMPARISON, RESULTS FOR CAESIUM-137

		CV(%)				Level of agreement			
		Median	Stdev	Q_1[a]	Q_3[b]	Median	Stdev	Q_1[a]	Q_3[b]
Site of source	Bay	119.9	58.89	82.1	185.5	2.20	1.78	1.59	4.12
	Trough	123.5	55.04	87.8	190.3	2.20	1.69	1.62	3.11
Medium	Sediment	144.2	52.16	96.6	195.3	2.70	1.82	1.78	4.32
	Water	101.1	59.42	75.1	160.7	1.80	1.53	1.25	2.91
Release	Continuous	136.3	57.32	91.9	196.4	2.31	1.62	1.80	4.10
	Instantaneous	113.2	55.63	75.1	170.3	1.80	1.84	1.30	3.10
Scale	Local	112.4	32.43	84.4	138.9	2.10	1.23	1.60	2.70
	Regional	101.0	57.00	85.8	153.8	2.00	1.49	1.40	3.00
	Global	163.8	64.10	81.3	212.8	2.20	2.02	1.70	4.50

[a]   Q1 is the lower quartile (i.e. the value below which 25% of the values lie).
[b]   Q3 is the upper quartile (i.e. the value above which 25% of the values lie).

Figures 32(a)–(d) show the comparison of CV for each of the design factors separately. In the figures sites have been scaled as local (sites 1–3 within the Kara Sea), regional (sites 4–6 within the Barents Sea) and global (sites 7–11). We can see possible small effects due to medium, release type and also scale. Asterisks (*) in Figures 32 and 33 indicate extreme data values.

Figures 33(a)–(d) show the comparable results for the level of agreement. These figures demonstrate the existence of very small effects due to medium and release type, but not this time due to scale.

Figure 34 shows a comparison of the CV for the eight different simulation conditions for each location, which Figure 35 shows the equivalent results for level of agreement.

These figures show clearly the existence of interactions between the simulation factors and the location, how some sites, e.g., location 6, show little difference in either CV or level of agreement over all simulation condition, while, e.g. site 5, shows a more varied profile.

Formal analysis identifies significant effects due to water/sediment and location for both CV and level of agreement.

4.3.1.2. Plutonium-239

Tables XXXIII to XXXVI summarise the results for ^{239}Pu, which was selected for its long half-life and particle reactivity. The results are also given in Figures 20–23.

Overall the average CV for Pu results is approximately 130%, and for level of agreement, approximately 3.5, increasing to 4.3 for sediment results alone.

For this nuclide, the pattern of results is different to that seen for ^{137}Cs. Generally speaking in seawater the level of agreement is better at the distant sites than close to the source (Figures 20 and 21). Generally sea water results at distant sites are within 2 orders of magnitude. Sites very near to the source also show the level of agreement better than 2 orders of magnitude. Source location also seems to have an effect, (if sited in the bay, the results are generally more varied than if the source is sited in the trough).
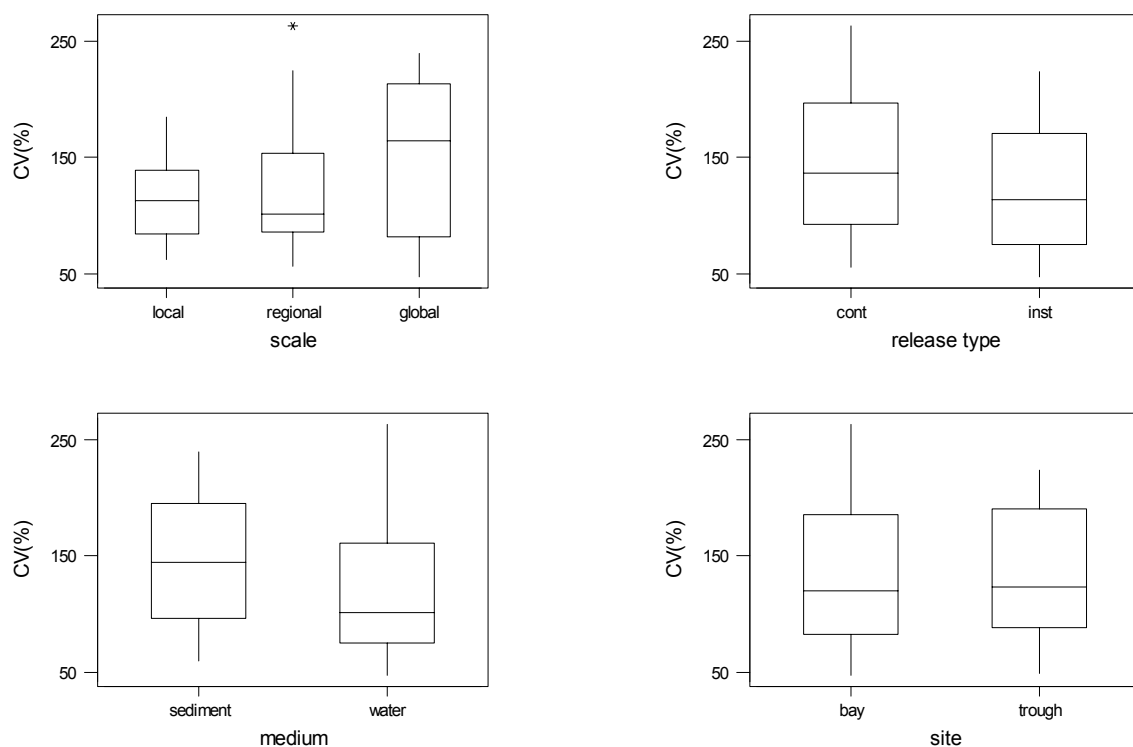
FIG. 32(a)–(d). Coefficient of variation for ^{137}Cs concentrations for the different simulation design factors.
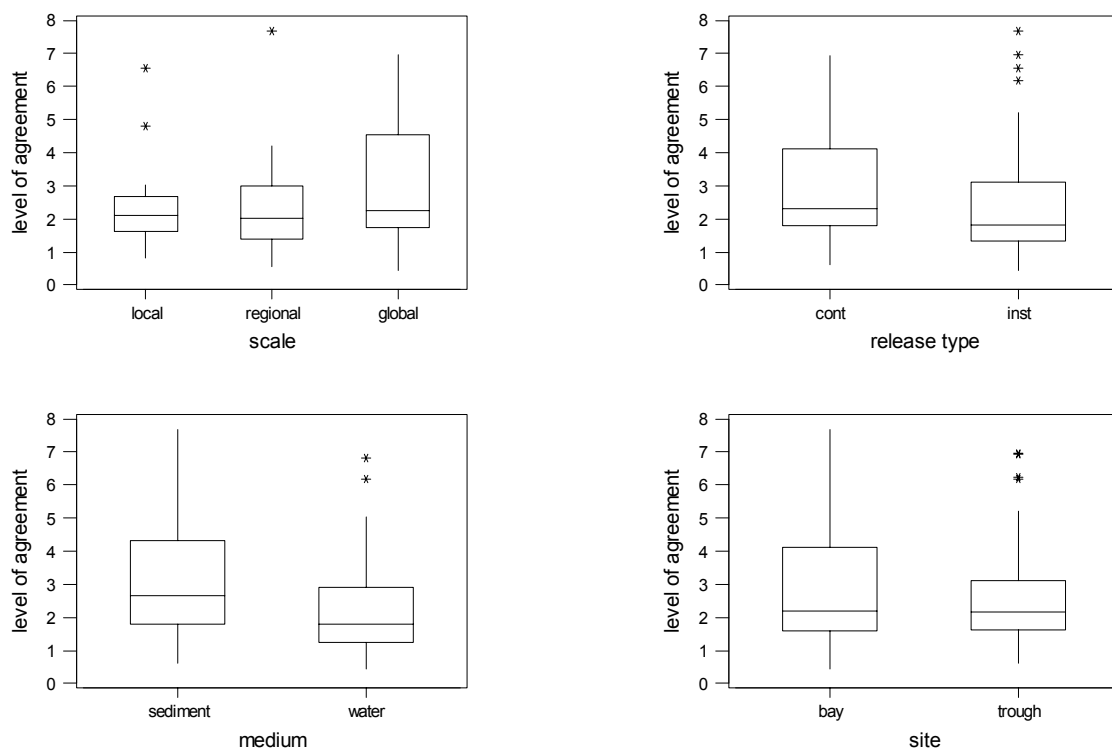
FIG. 33(a)–(d). Level of agreement for ^{137}Cs concentrations for the different simulation design factors.

Sediment results are generally more varied than seawater results (over all sites, the sediment level of agreement is approximately 4 orders of magnitude, while for seawater it is more typically 2 orders of magnitude).

The relative variation (CV) in the results shows less clear structure with distance from source, but does again indicate more variation in the sediment compared to seawater results.

For the Pu results, particularly for sediments, results for the hybrid compartmental model; particularly at the sites distant from the source have been omitted from the calculations. Thus this pre-processing has affected the interpretation of the results, particularly for level of agreement.

The time to maximum concentrations in seawater is relatively short near source (1–8 years in Kara and Barents Seas), however at distant locations, time to maximum is more typically of the order of tens of years.

The results for time to maximum in sediment show enormous variation: from tens to hundreds of years. Thus this emphasises major differences in the dynamics relating to sediment modelling. However, these differences are not considered to present a problem for radiological assessment since the concentrations and time to occurrence at near source locations will be of more significance.
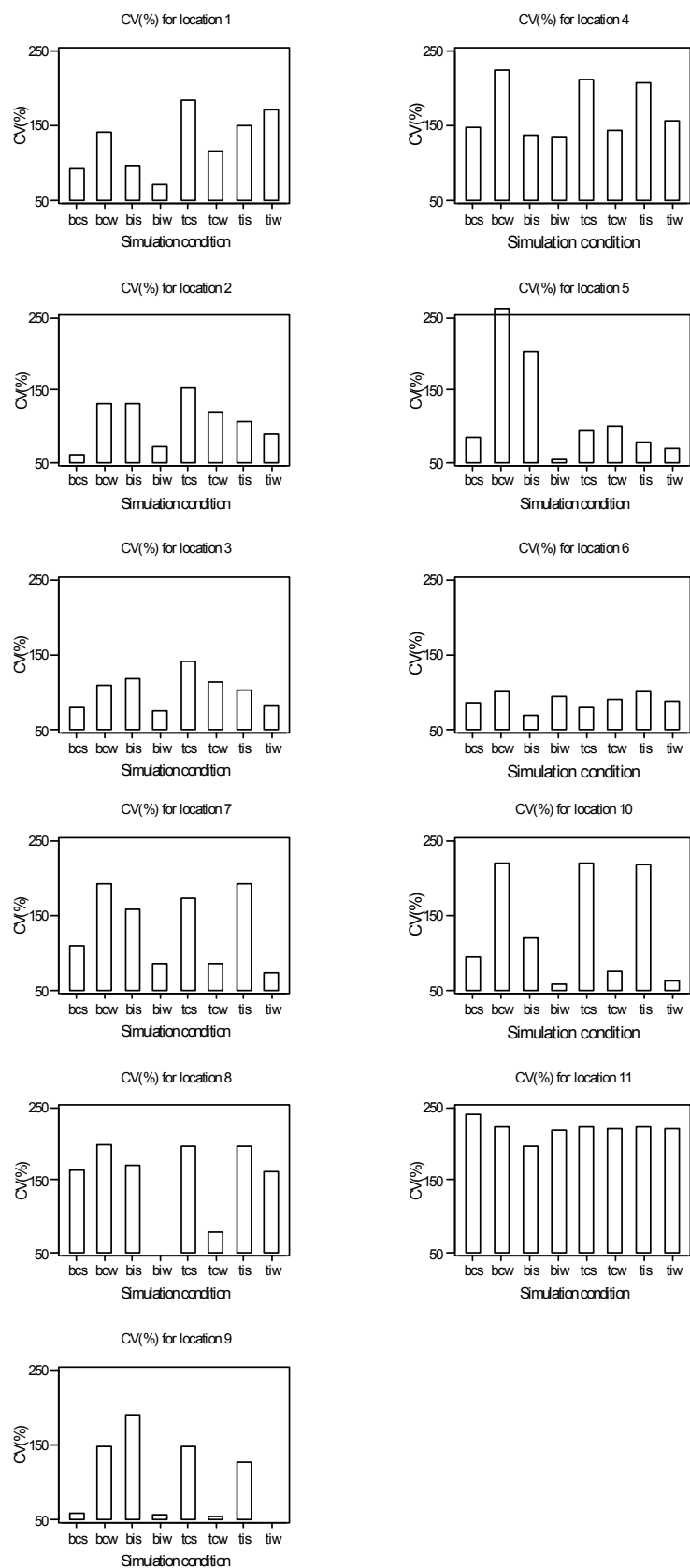
FIG. 34. Coefficient of variation for ^{137}Cs in each location under different simulation conditions.
(site: bay or trough (b or t), release type: continuous or instantaneous (c or i), medium: water or sediment (w or s).
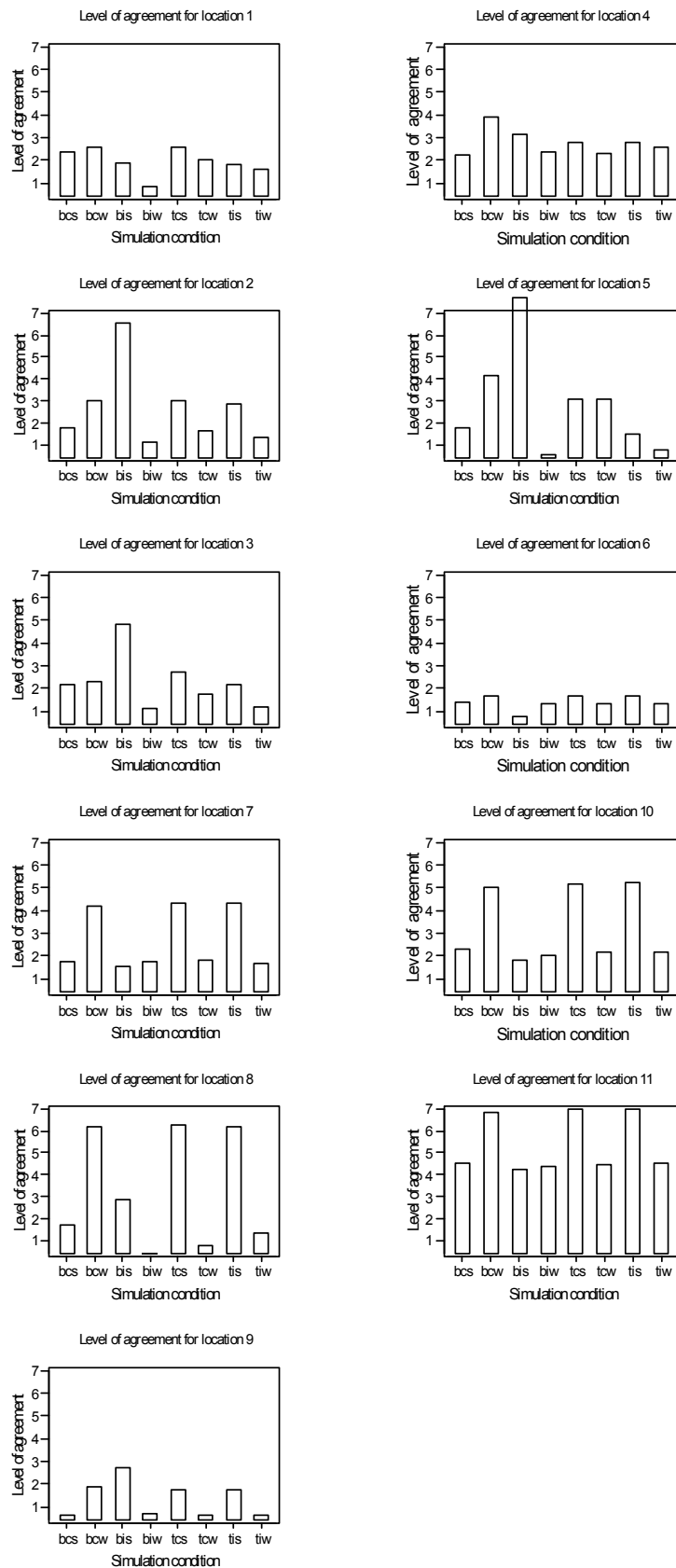
FIG. 35. Level of agreement for ^{137}Cs in each location under different simulation conditions.
(site: bay or trough (b or t), release type: continuous or instantaneous (c or i), medium: water
or sediment (w or s).

Table XLVI summarises the results for CV and level of agreement for each simulation factor separately, and the results are also shown in Figures 36(a)–(d) for CV and Figures 37(a)–(d) for level of agreement. In Figures 36(a)–(d), small effects due to medium and release type can be seen, as well as scale. In Figures 37(a)–(d), small effects due to source site (larger effect), medium and scale are clearly observed.

Figures 38 and 39 show the results for each location, under all simulation conditions. Different profiles can be observed at different locations, indicating again the existence of interactions between location and simulation condition. For CV, significant effects due to source (bay/trough) and release, as well as location, are observed, while for level of agreement significant effects due to source and medium as well as location are observed.

TABLE XLVI. SUMMARY OF INTERCOMPARISON RESULTS FOR PLUTONIUM-239

		CV(%)				Level of agreement			
		Median	Stdev	Q_1[a]	Q_3[b]	Median	Stdev	Q_1[a]	Q_3[b]
Site of source	Bay	119.7	45.76	94.6	175.1	3.6	2.06	2.2	5.8
	Trough	119.2	36.00	98.5	140.4	2.8	1.81	1.5	4.6
Medium	Sediment	123.3	34.48	112.7	164.5	4.2	2.06	2.3	6.4
	Water	112.8	47.18	94.1	164.2	2.3	1.52	1.4	4.0
Release	Continuous	99.9	40.73	87.8	135.6	3.5	2.14	1.9	5.4
	Instantaneous	127.6	36.41	115.9	171.5	3.3	1.82	1.9	4.9
Scale	Local	113.7	28.73	92.3	119.6	4.1	1.51	2.4	5.3
	Regional	123.0	41.17	101.1	163.4	4.1	1.99	2.2	5.1
	Global	131.6	45.02	102.1	171.1	2.4	2.15	1.5	3.9

[a] Q_1 is the lower quartile (i.e. the value below which 25% of the values lie).

[b] Q_3 is the upper quartile (i.e. the value above which 25% of the values lie).
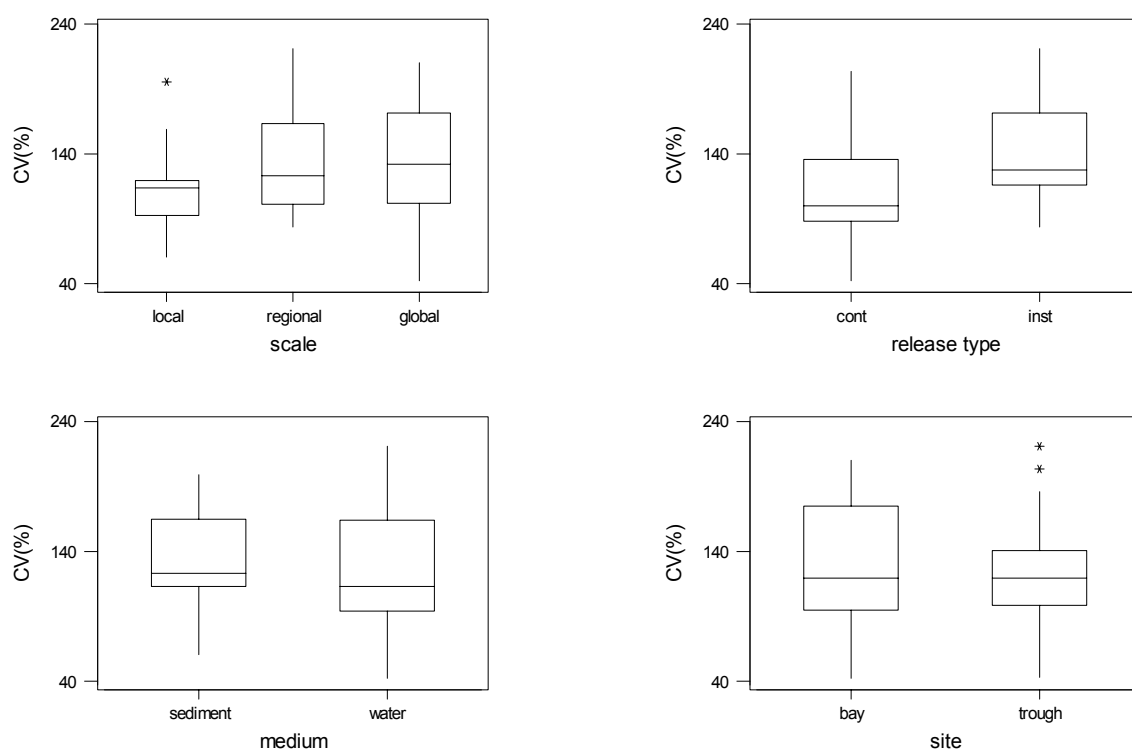
FIG. 36(a)–(d). Coefficient of variation for ^{239}Pu concentrations for the different simulation design factors.
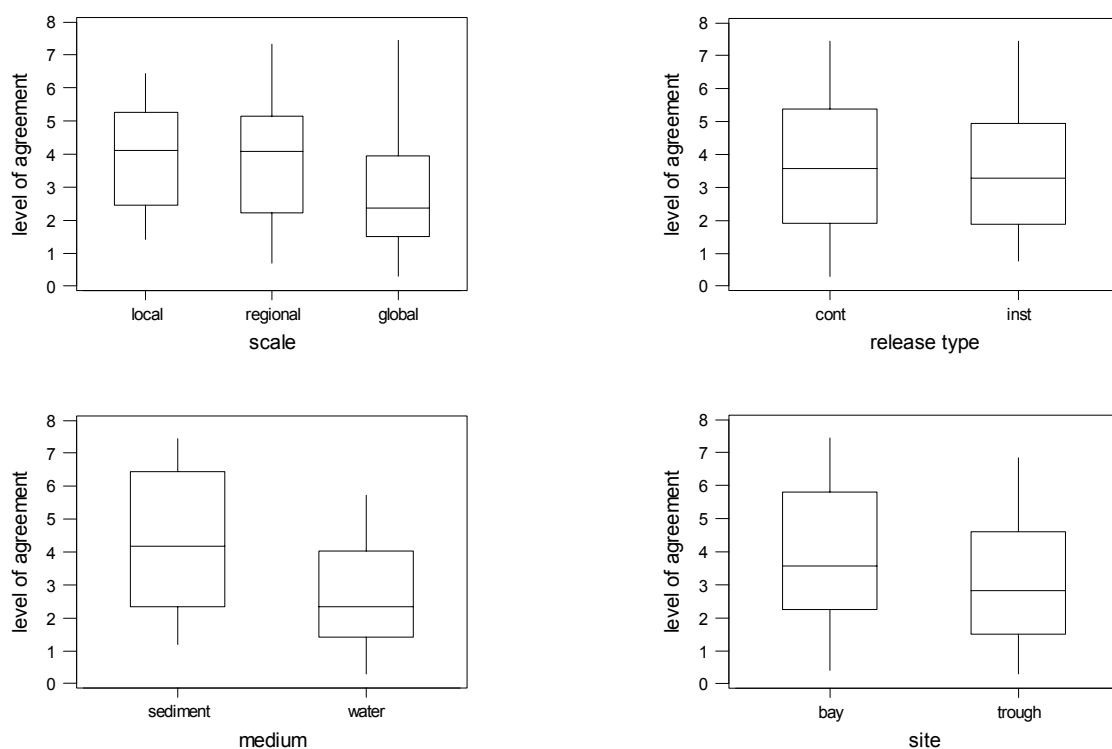
FIG. 37(a)–(d). Level of agreement for ^{239}Pu concentrations for the different simulation design factors.

4.3.1.3. Cobalt-60

This nuclide was selected due to its particle reactivity, short half-life and presumed inventory within the dumped materials. Results are summarised in Tables XXXVII to XL and in Figures 24–27.

Overall, CV values are on average 130%, with maximum 225%, while the level of agreement is approximately 3.5, but increasing to a maximum of 9. For ^{60}Co, substantive differences are found between sediment and water, and as a function of distance from the source.

As for Pu, we see a marked difference in the level of agreement near source compared to far from source (the distant sites again show better levels of agreement) in seawater. This is also true in sediment, however, it should be remarked that this effect is to some extent due to the pre-processing carried out on this data. As remarked earlier, concentrations $< 10^{-11}$ have been ignored.
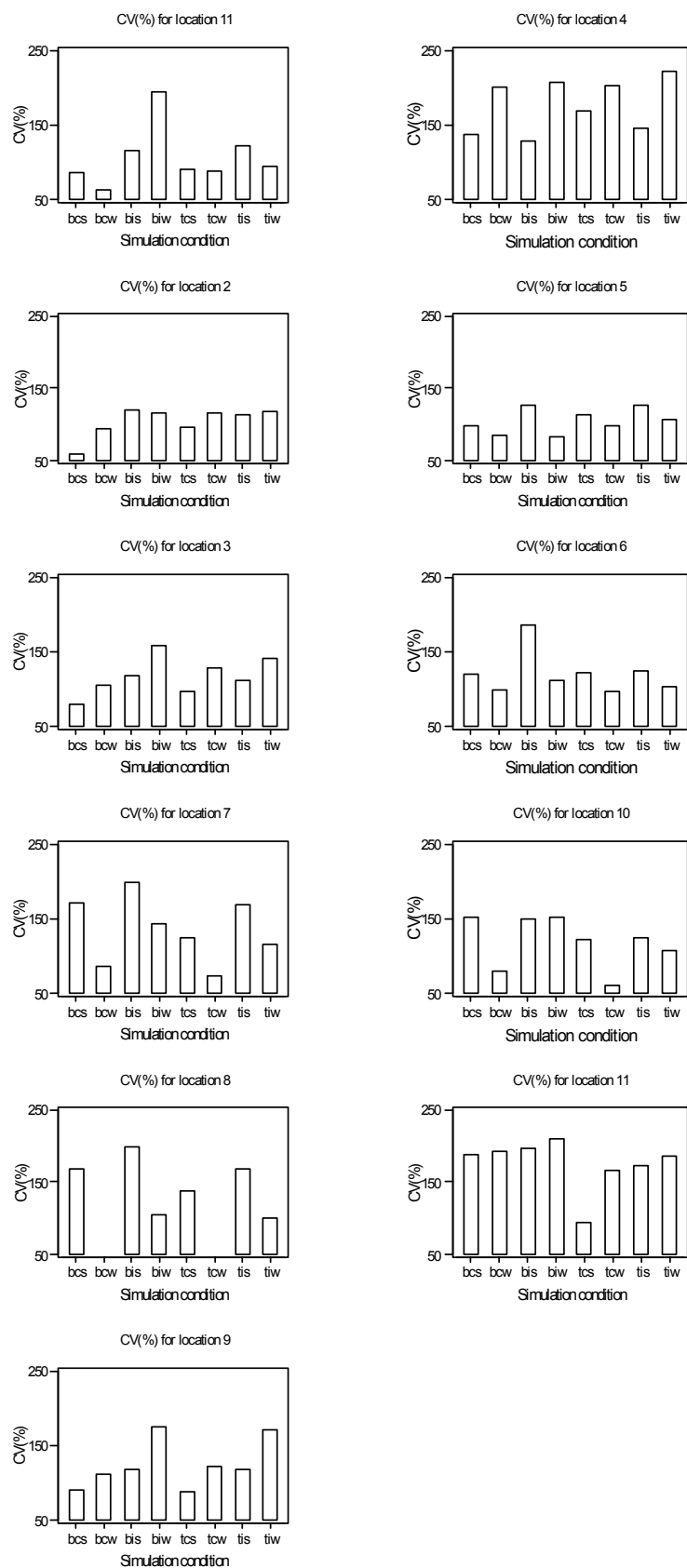
FIG. 38. Coefficient of variation for ^{239}Pu *in each location under different simulation conditions.*
(site: bay or trough (b or t), release type: continuous or instantaneous (c or i), medium: water or sediment (w or s).
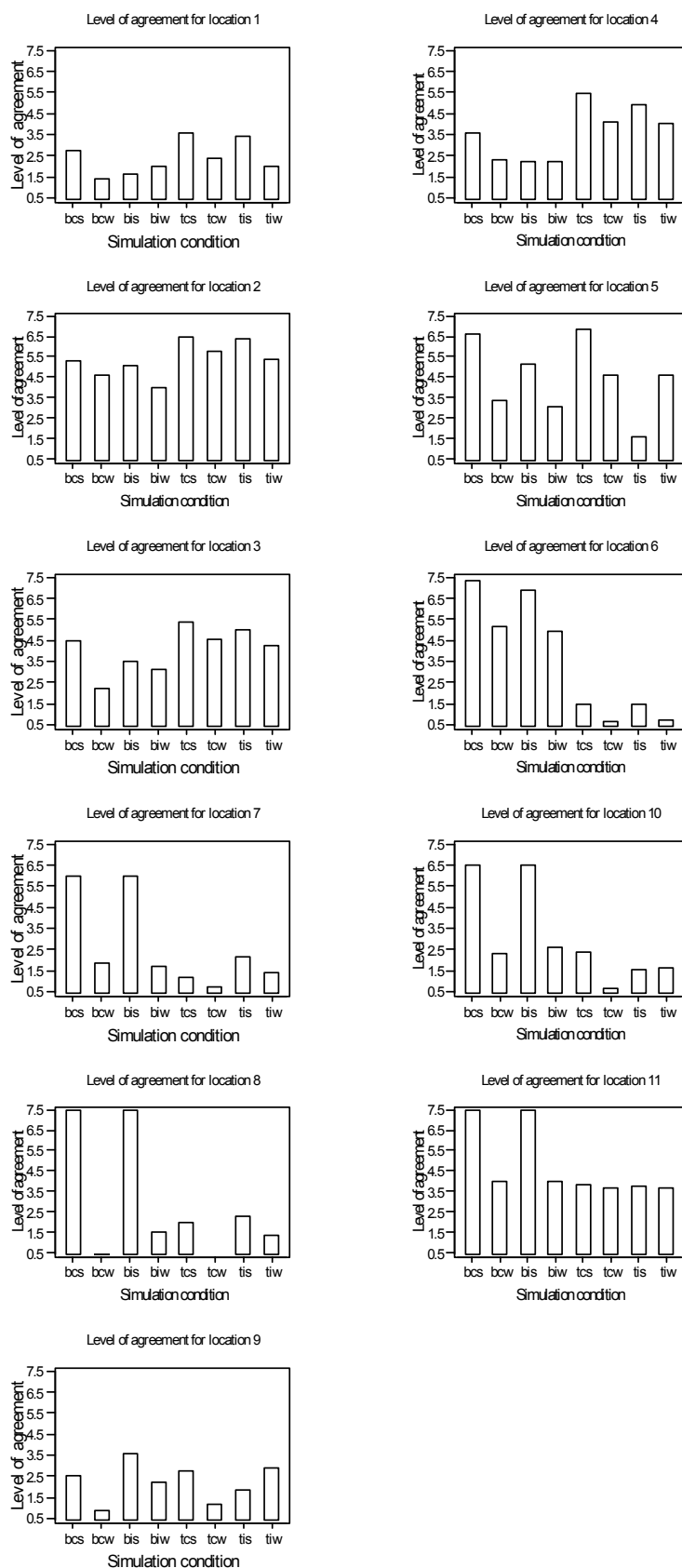
FIG. 39. Level of agreement for ^{239}Pu in each location under different simulation conditions.
(site: bay or trough (b or t), release type: continuous or instantaneous (c or i), medium: water or sediment (w or s).

The coefficient of variation is less affected than the level of agreement by this pre-processing – the result there show no effect with distance, and again confirm less variation in the seawater concentrations than in sediment. Results very near source (specifically location 1) are not markedly better than at more distant sites. Results for ^{60}Co are more extreme than those observed for [239]Pu, but again emphasise the effect of the different modelling approaches on predicted sediment concentrations.

The times to maximum concentration are short, of the order of several tens of years, with very little variation over sites.

Table XLVII and Figures 40(a)–(d) and 41(a)–(d) summarise the effects due to the simulation design factors. The relative stability of the CV can be observed, although a small effect due to medium is seen. For the level of agreement effects due to medium and scale are also observed. Figures 42 and 43 again emphasises the complexity of the benchmark, showing quite varied profiles at the different locations.

TABLE XLVII. SUMMARY OF INTERCOMPARISON RESULTS FOR COBALT-60

		CV(%)				Level of agreement			
		Median	Stdev	Q_1[a]	Q_3[b]	Median	Stdev	Q_1[a]	Q_3[b]
Site of source	Bay	129.9	44.46	99.7	168.2	2.9	2.44	1.3	4.7
	Trough	130.1	48.46	88.9	165.3	2.1	2.82	1.5	5.8
Medium	Sediment	146.9	40.37	118.1	173.0	3.0	2.51	1.7	5.9
	Water	119.1	49.75	80.3	155.4	1.7	2.72	1.0	4.6
Release	Continuous	190.1	41.10	98.1	157.0	2.9	2.80	1.5	6.0
	Instantaneous	129.8	51.34	89.2	188.8	2.3	2.43	1.1	4.4
Scale	Local	129.9	32.05	105.9	152.1	5.9	2.34	4.2	7.5
	Regional	132.8	53.00	84.9	192.0	3.8	3.13	1.1	7.5
	Global	133.7	49.83	88.2	186.5	2.1	1.17	1.1	2.9

[a] Q_1 is the lower quartile (i.e. the value below which 25% of the values lie).

[b] Q_3 is the upper quartile (i.e. the value above which 25% of the values lie).

At the distant sites, such results arise from a single model (hybrid compartmental model), thus uniformly these model results were omitted at the global scale, however near source although the concentrations are low, they do not fall below the cut-off and thus are included in the analysis. Results for seawater are in better agreement than for sediment.

Both the [239]Pu and ^{60}Co results have highlighted several problems specifically related to the modelling of the sedimentary process, which the data pre-processing has accentuated. It is clear however that there are marked differences in resulting sediment concentrations due to the different modelling approaches.

Formal analysis of the results showed significant effects in CV due to medium and location (with a significant interaction) and for level of agreement effects (and interactions) due to all factors except site of source.
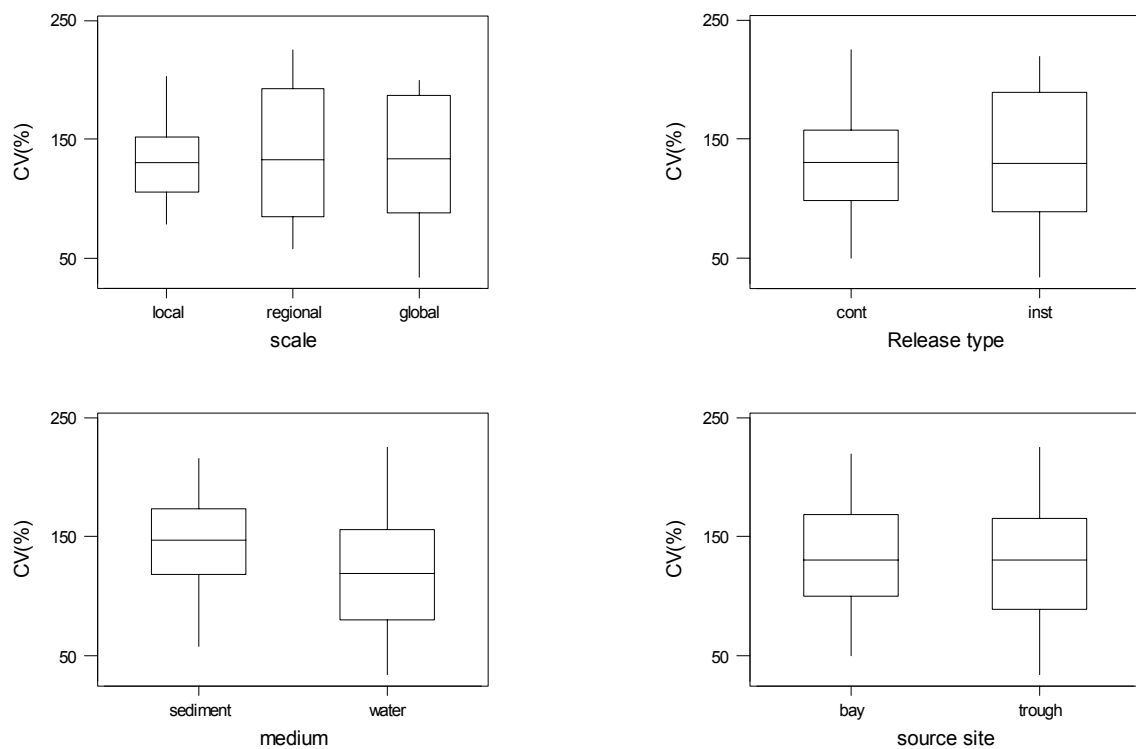
FIG. 40(a)–(d). Coefficient of variation for ^{60}Co concentrations for the different simulation design factors.
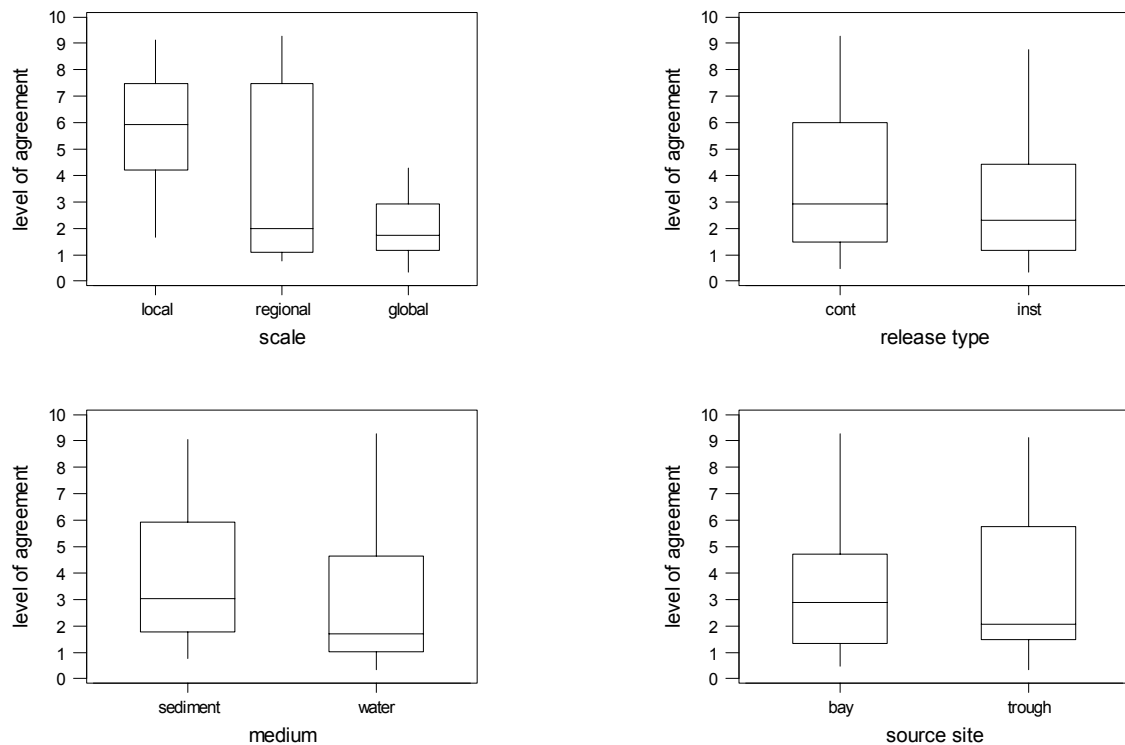
FIG. 41(a)–(d). Level of agreement for ^{60}Co concentrations for the different simulation design factors.
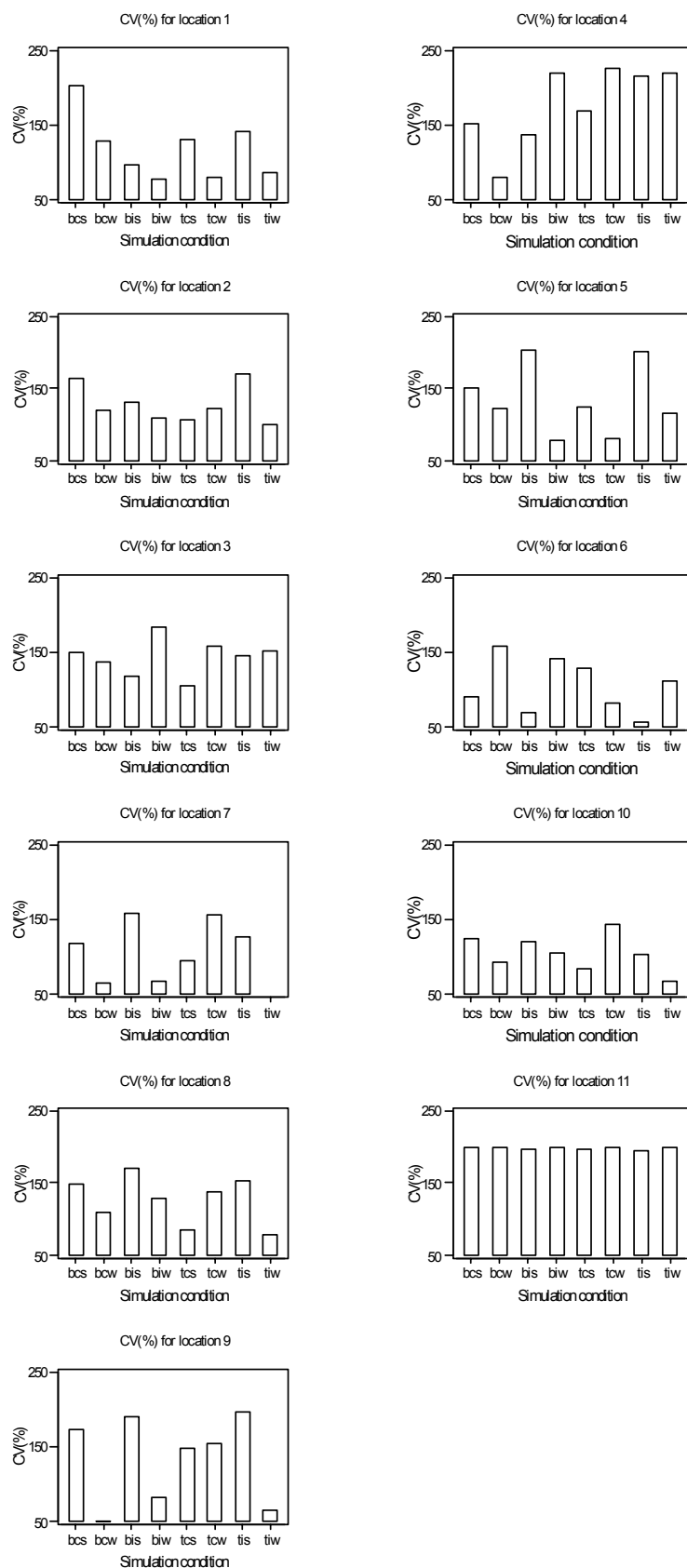
FIG. 42. Coefficient of variation for ^{60}Co in each location under different simulation conditions.
(site: bay or trough (b or t), release type: continuous or instantaneous (c or i), medium: water or sediment (w or s).
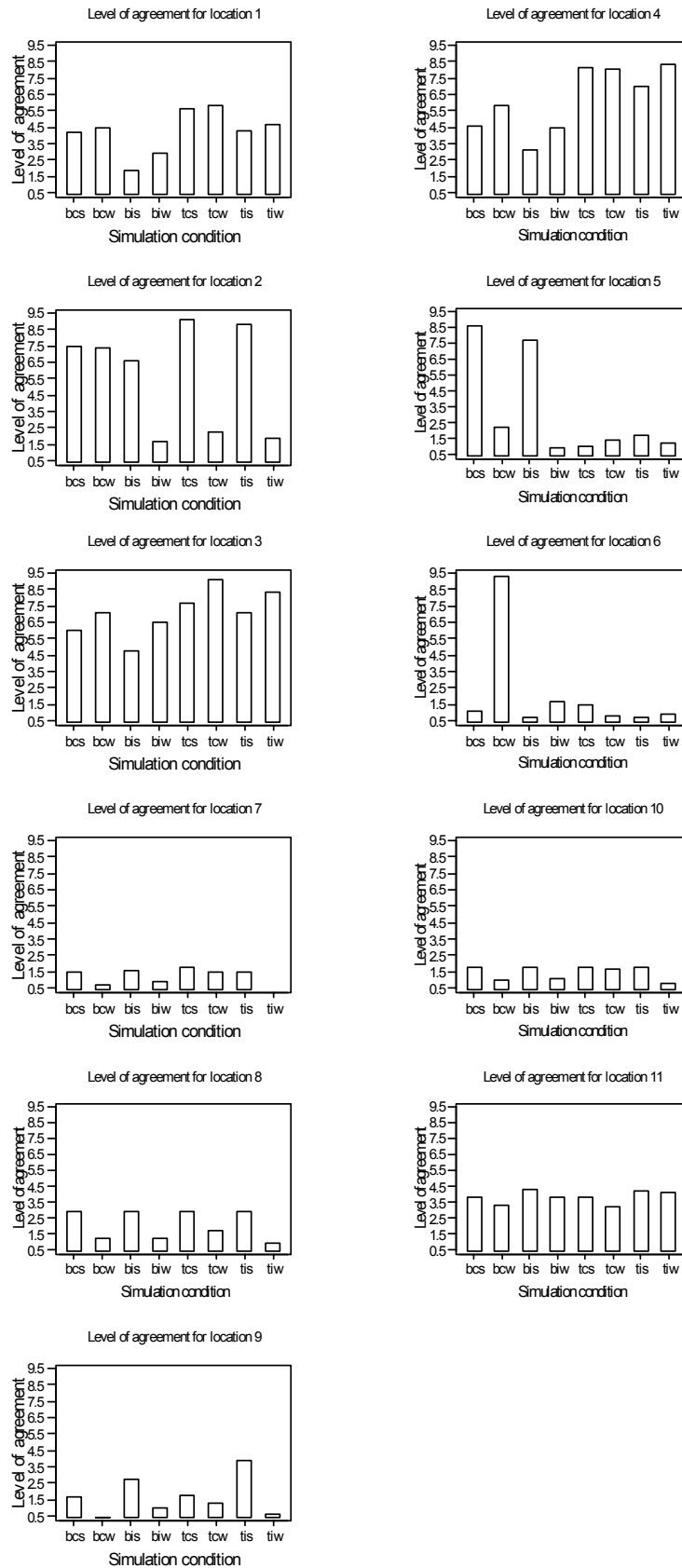
FIG. 43. Level of agreement for ^{60}Co in each location under different simulation conditions.
(site: bay or trough (b or t), release type: continuous or instantaneous (c or i), medium: water or sediment (w or s).

4.3.1.4. Technetium-99

Technetium-99 is important in the benchmark scenario, since it acts as a passive tracer of the water transport dynamics. Results for ^{99}Tc are summarised in Tables XLI to XLIV and Figures 28–31.

For water, the average CV is around 90% and level of agreement is 1 order of magnitude, while for sediment the results are much more varied at approximately 200% for CV and 3.5 for level of agreement.

In seawater, near source, levels of agreement are regularly better than two orders of magnitude, and frequently better than one. At distant locations (with the exception of location 11), the results are also in excellent agreement (better than two orders of magnitude agreement). There is no obvious deterioration in performance with distance from source.

Results for maximum sediment concentrations show poorer agreement and more relative variation. Here there is an apparent trend with distance.

The times to maximum concentration in seawater are short (of the order < 10 years in Kara and Barents Seas) increasing to several hundreds of years at most distant locations. For sediment, times to maximum are larger (< 30 years in Kara Sea, < 100 years in Barents Sea).

Further analysis is summarised in Table XLVIII, showing small effects due to medium and scale, and shown in Figures 44(a)–(d) and 45(a)–(d). Figures 46 and 47 show the results for each location over all simulation conditions. The difference between sediment and water results is clearly seen.

TABLE XLVIII. SUMMARY OF INTERCOMPARISON RESULTS FOR TECHNETIUM-99

		CV(%)				Level of agreement			
		Median	Stdev	Q_1[a]	Q_3[b]	Median	Stdev	Q_1[a]	Q_3[b]
Site of source	Bay	187.8	65.39	89.0	201.5	2.4	1.48	0.9	3.5
	Trough	186.5	63.68	91.4	202.9	2.4	1.48	1.0	3.5
Medium	Sediment	201.5	18.94	199.3	223.1	3.5	0.87	2.9	4.5
	Water	87.9	40.47	69.6	105.0	1.0	0.56	0.7	1.4
Release	Continuous	188.5	64.90	87.9	202.9	2.4	1.40	0.9	3.5
	Instantaneous	187.8	64.17	88.7	202.4	2.4	1.50	1.0	3.6
Scale	Local	129.6	64.70	87.7	216.1	1.8	1.47	1.1	3.6
	Regional	162.9	62.80	105.0	201.8	2.5	0.91	1.4	2.8
	Global	197.4	65.90	86.9	202.4	2.8	1.73	0.8	4.3

[a] Q_1 is the lower quartile (i.e. the value below which 25% of the values lie).
[b] Q_3 is the upper quartile (i.e. the value above which 25% of the values lie).

4.4. SUMMARY OF BENCHMARK FINDINGS

The benchmark scenario highlighted the level of variation in the results due to the different model structures and parameterisation processes.

Very broadly, we observed that for passive (or almost) tracers (such as ^{99}Tc and also ^{137}Cs) agreement in seawater concentrations is typically better than two orders of magnitude. Level of agreement and relative variation does in fact, vary over location, with typically agreement in remote locations being poorer than at near source sites.
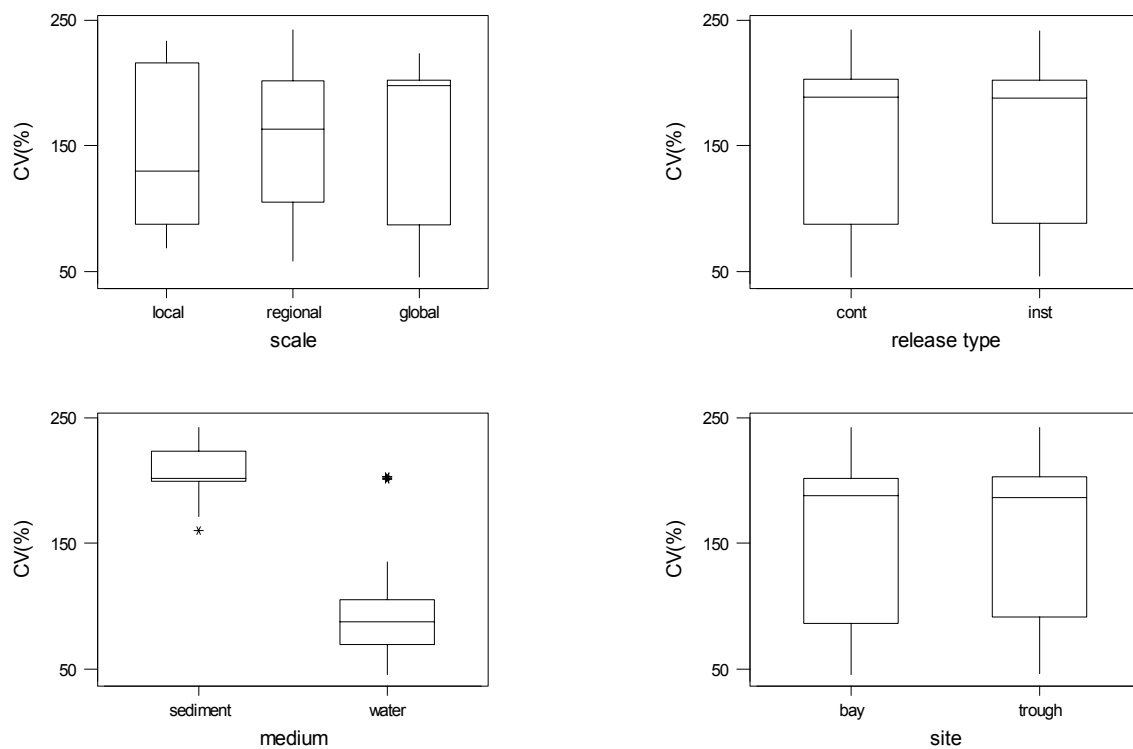
FIG. 44(a)–(d). Coefficient of variation for ^{99}Tc concentrations for the different simulation design factors.
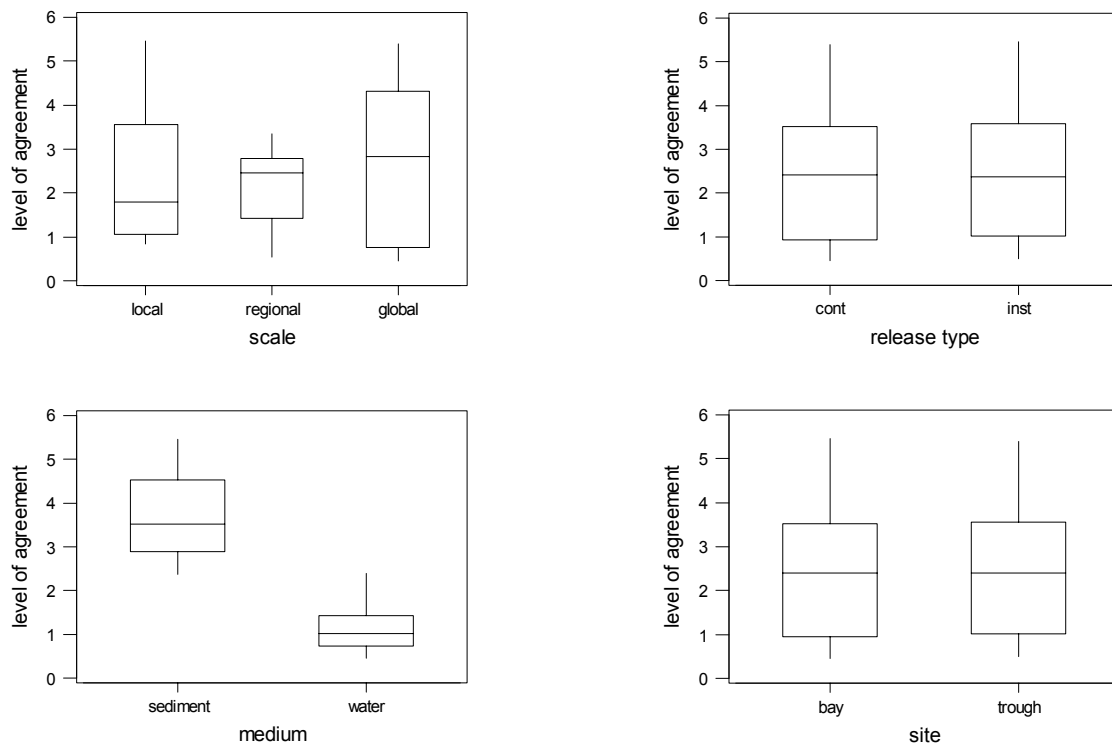
FIG. 45(a)–(d). Level of agreement for ^{99}Tc concentrations for the different simulation design factors.
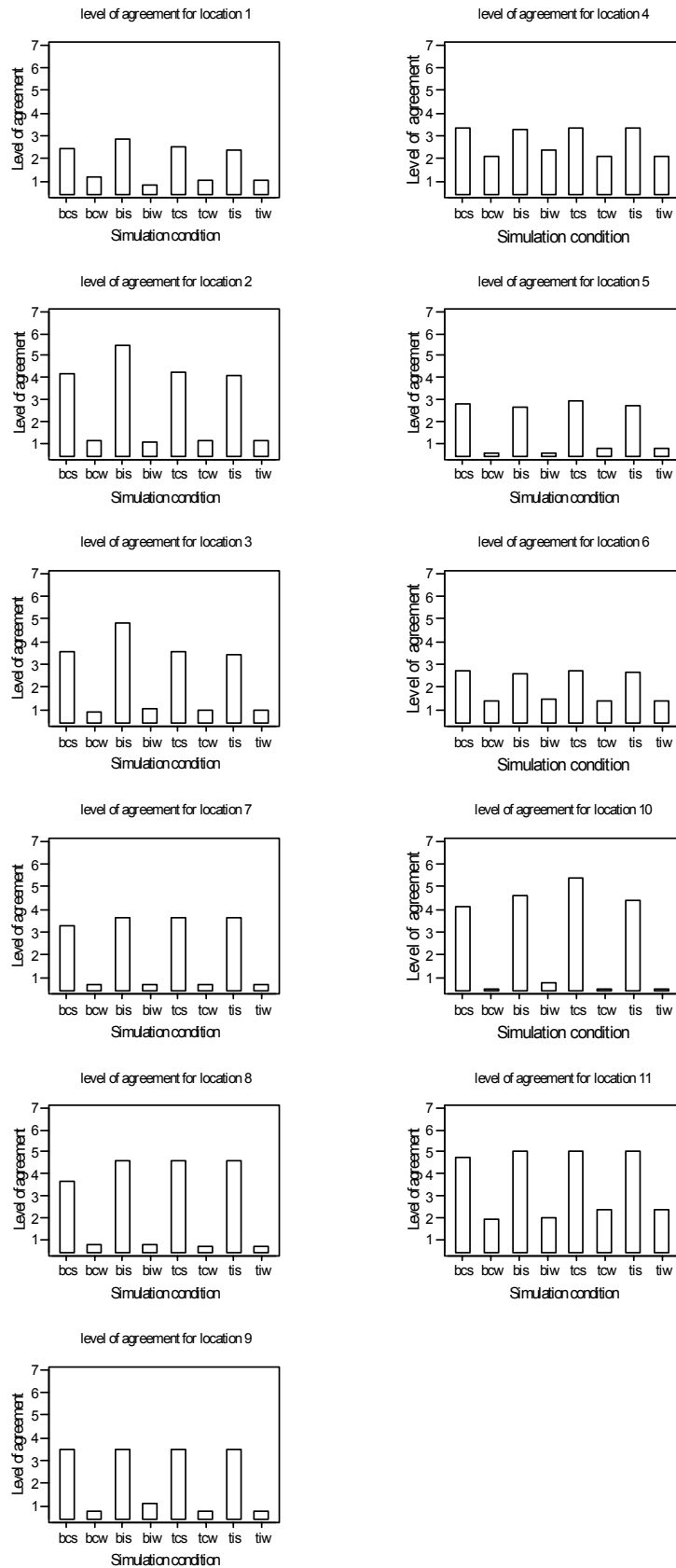
FIG. 46. *Coefficient of variation for* ^{99}Tc *in each location under different simulation conditions.*
(site: bay or trough (b or t), release type: continuous or instantaneous (c or i), medium: water or sediment (w or s).
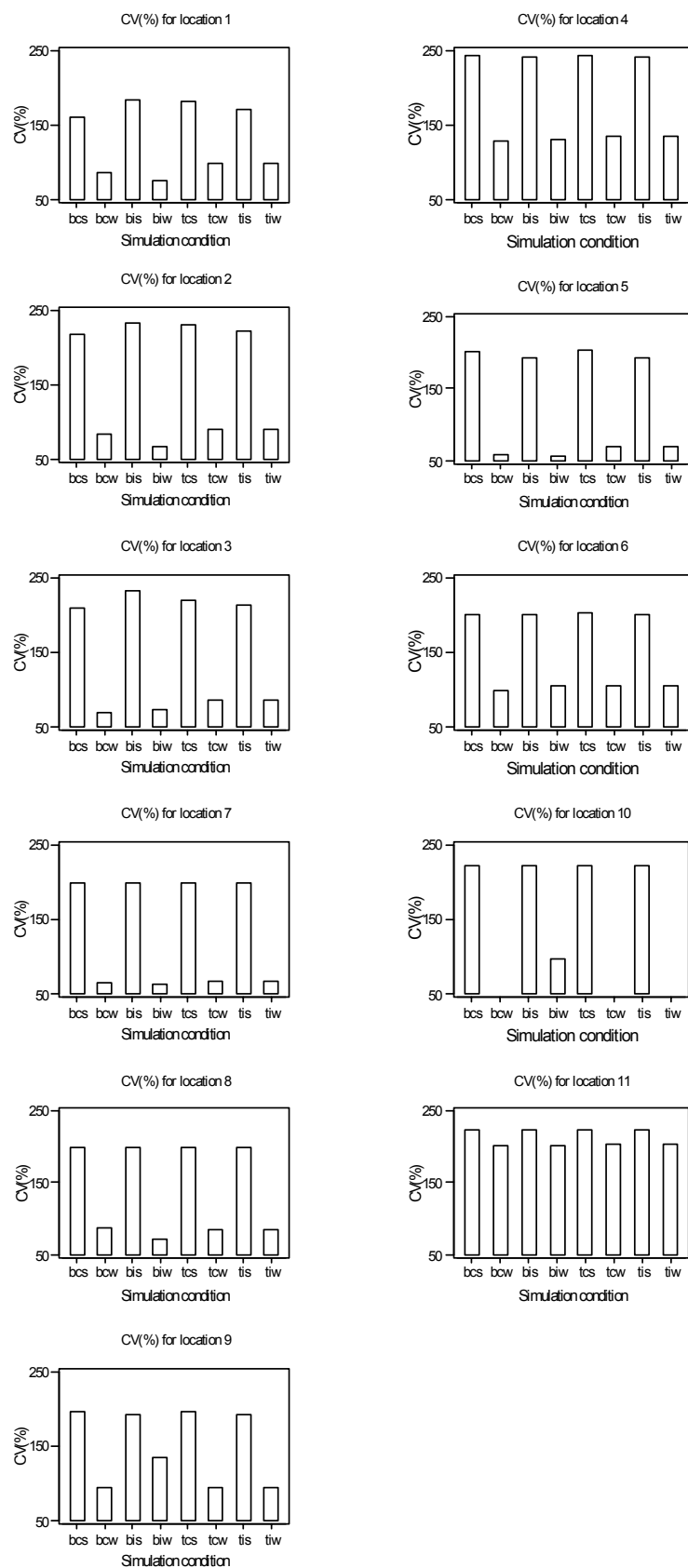
FIG. 47. Level of agreement for ^{99}Tc in each location under different simulation conditions.
(site: bay or trough (b or t), release type: continuous or instantaneous (c or i), medium: water or sediment (w or s).

There are however notable exceptions to this generalisation. At the site in the Barents Sea, close to Kara Gate; poorer agreement and more relative variation was observed which reflects the sensitivity of the results to the parameterisation of the flow from the Kara to Barents Sea (the Litke current).

The results have shown little effect due to whether the source is sited in a bay or in the Novaya Semlya Trough, nor whether the release is instantaneous or continuous.

The results for particle reactive nuclides (^{239}Pu and ^{60}Co) show larger relative variation and poorer agreement. This is in part due to the greater number of processes to be modelled and also the method of sediment modelling used.

The range in time to maximum concentrations in seawater and sediment at near field locations, are generally short, spanning a period of 10 years or so, but in far-field locations, the span increases considerably.

The differences in time to maximum are determined in part by the differences in the model structures (vertical and spatial resolution) as well as differences in the flows used.

As a result of the greater relative variation in the sediment results, a further limited sensitivity analysis was carried out by each modeller and the results are discussed briefly below.

4.5. SENSITIVITY ANALYSIS ON SEDIMENT

A limited sensitivity analysis of some of the sedimentary processes was carried out. The design of the study was as follows. Dealing only with ^{239}Pu, the parameters of concern were K_d, suspended sediment load and sedimentation rate. The source of ^{239}Pu was considered to Abrosimov Bay, with 1 TBq per year for 10 years being released. The endpoints for comparison were the maximum concentration in water (Bq/m^3) and sediment (Bq/kg dw) at two locations within the Kara Sea and one within the Barents Sea as well as the time to maximum concentration at these locations.

The parameter ranges were defined as follows:

Nuclide: ^{239}Pu
Parameters: K_d, suspended sediment load, sedimentation rate
Source: 1 TBq per year for 10 years
Location of source: Kara Sea Bay, modelled on Abrosimov Bay as in benchmark
Endpoints: maximum concentration in water (Bq/m^3) and sediment (Bq/kg dw) at:

Kara Sea:	72°N 65°E
	78°N 92°E
Barents Sea:	79°N 58°E

and time to maximum at each location for water and sediment. For water, this should not be the depth averaged maximum, but rather the maximum should be given and also the layer (and depth) at which it occurs.

It was agreed that the parameters should be varied globally (i.e. in each box of the model).

Parameters ranges: **K_d 10^4 10^5 10^6**
                                       The base case is considered to be 10^5
                                       suspended load: 1 mg/L   10 mg/L   100 mg /L
                                       The base case is 10 mg/L.
                                       sedimentation rate: 0.1 mm/a   1 mm/a   10 mm/a
                                       The base case is 1 mm/a.

Other sediment parameters were not varied and included porosity of 0.7, bulk density 2.5 and bottom thickness of 10 cm which were kept fixed.

In total, 7 cases were to be run, with case 0, all three parameters held at their base value.

The cases are described below and the results are given in Tables XLIX and L:

> **Cases to be run:** A total of 7 cases were run.
> Case 0: all three parameters at base value.
> Case 1: $K_d = 10^4$, suspended load and sedimentation rate fixed at base value.
> Case 2: $K_d = 10^6$, suspended load and sedimentation rate fixed at base value.
> Case 3: suspended load = 1 mg/L, K_d and sedimentation rate at base value.
> Case 4: suspended load = 100 mg/L, K_d and sedimentation rate at base value.
> Case 5: sedimentation rate = 0.1 mm/a, K_d and suspended load at base value.
> Case 6: sedimentation rate = 10 mm.a, K_d and suspended load at base value.

4.5.1. Discussion

Since the sensitivity study was carried out to primarily explore and help explain the sensitivity of the difference models to the sedimentary parameters, this Section concentrates only on the sediment results. The study was designed to investigate the effects of three parameters (K_d, sedimentation rate and suspended load) at three sites, two within the Kara Sea and one in the Barents Sea. Results from six different models were received, including compartmental and hydrodynamic models. Figure 48 shows the coefficient variation and level of agreement for each of the seven simulation cases (case 0, baseline values) at each site. Figure 49 shows the effect of varying K_d all other parameters remaining constant, Figure 50 shows the effect of varying suspended load, all other parameters remaining constant and Figure 51 shows the effect of varying sedimentation rate, all others remaining constant. Figure 52 shows the level of agreement and coefficient of variation for each model over all the simulation cases.

The patterns observed in the figures make clear the existence of an interation between site and parameter being studied; the size of effect for a given parameter is not the same at each site. However, some general points can still be made.

In the baseline case (case 0), Site 2 is the most varied, Site 3 the least varied and this pattern is repeated over almost all the other simulation cases. Thus, the sensitivity study has demonstrated the important of these sedimentation parameters in the very near field. Overall, the coefficient of variation lies in the range 100–250% and level of agreement in the range 1–6.

Simulation cases 5 and 6 seem generally to have a lower coefficient of variation and a level of agreement typically better than 3 with the exception of Site 2, suggesting the least sensitivity of the results to variations in the sedimentation rate.

Model 3 (a hybrid compartmental model) shows the greatest variation over all the simulation cases and so it can be concluded is the most sensitive to the sedimentation parameters.

Overall, the effects of varying the sedimentation parameters over several orders of magnitude resulted in an increased variation in the sedimentation concentration, but this is still smaller than the variation observed over models. Thus, the sedimentation parameters make a significant but non-dominating contribution to the overall variability in the results.

TABLE XLIX. SENSITIVITY STUDY, SEDIMENT RESULTS (Bq/kg dw)

Site	Case	Riso	Typhoon	Nihon U.	MEL	KEMA	MEL Regional	K_d	SSL	SR
1	0	2.4×10^{-2}	3.7×10^{-2}	1.7	1.6×10^{-1}	1.3×10^{-3}	3	1	1	1
1	1	1.8×10^{-1}	2.3×10^{-2}	5.2	1.1×10^{-1}	2.9×10^{-2}	5.3×10^{-1}	2	1	1
1	2	2.3×10^{-1}	3.7×10^{-2}	5.1×10^{-1}	1.3×10^{-1}	2.2×10^{-1}	5.4	3	1	1
1	3	1.2×10^{-1}	3.7×10^{-2}	1.5×10^{-2}	1.3×10^{-1}	1.3×10^{-1}	5.3×10^{-1}	1	2	1
1	4	3.4×10^{-1}	2.3×10^{-2}	9.4×10^{-6}	1.1×10^{-1}	4.5×10^{-2}	5.4	1	3	1
1	5	2.5×10^{-1}	1.8×10^{-2}	4.1×10^{-4}	7.1×10^{-2}	1.5×10^{-1}	–	1	1	2
1	6	2.7×10^{-2}	1.6×10^{-2}	2.2×10^{-4}	8.9×10^{-2}	5.1×10^{-2}	–	1	1	3
2	0	2.1×10^{-3}	8×10^{-3}	4.5×10^{-5}	1.1×10^{-2}	4.8×10^{-4}	9.8×10^{-1}	1	1	1
2	1	3.6×10^{-3}	1.3×10^{-2}	1×10^{-2}	2.3×10^{-2}	1.1×10^{-2}	1.7×10^{-1}	2	1	1
2	2	8.1×10^{-4}	5×10^{-3}	5.5×10^{-6}	5.7×10^{-3}	1.1×10^{-1}	1.8	3	1	1
2	3	8.9×10^{-4}	5×10^{-3}	3.7×10^{-5}	5.7×10^{-3}	4.1×10^{-2}	1.7×10^{-1}	1	2	1
2	4	5.5×10^{-3}	1.3×10^{-2}	2.1×10^{-10}	2.3×10^{-2}	2.3×10^{-2}	1.8	1	3	1
2	5	5.3×10^{-3}	1.3×10^{-2}	4.1×10^{-8}	2×10^{-2}	5.2×10^{-2}	–	1	1	2
2	6	3.2×10^{-5}	4.3×10^{-4}	1.5×10^{-8}	7.7×10^{-4}	1.5×10^{-2}	–	1	1	3
3	0	5.4×10^{-4}	2×10^{-3}	3.4×10^{-5}	8.7×10^{-4}	7.4×10^{-4}	4.5×10^{-3}	1	1	1
3	1	1.0×10^{-3}	1.5×10^{-3}	6.3×10^{-2}	1.6×10^{-3}	1.6×10^{-3}	8.1×10^{-4}	2	1	1
3	2	1.8×10^{-4}	2×10^{-3}	1.3×10^{-12}	4.7×10^{-4}	1.2×10^{-3}	8.2×10^{-3}	3	1	1
3	3	2.6×10^{-4}	2×10^{-3}	2.2×10^{-5}	4.7×10^{-4}	6.8×10^{-3}	8.1×10^{-4}	1	2	1
3	4	9.8×10^{-4}	1.5×10^{-3}	1.8×10^{-12}	1.6×10^{-3}	2.9×10^{-3}	8.2×10^{-3}	1	3	1
3	5	1.3×10^{-3}	1.2×10^{-3}	3.4×10^{-9}	1.3×10^{-3}	8×10^{-3}	–	1	1	2
3	6	5.6×10^{-6}	4.6×10^{-4}	8.2×10^{-10}	7.9×10^{-5}	2.6×10^{-3}	–	1	1	3

TABLE L. SENSITIVITY STUDY, WATER RESULTS (Bq/m^3)

Site	Case	Riso	Typhoon	Nihon U.	MEL	KEMA	MEL Regional	K_d	SSL	SR
1	0	2.1×10^{-2}	8×10^{-3}	2.6×10^{-4}	2.1×10^{-2}	1.2×10^{-2}	4.1×10^{-2}	1	1	1
1	1	1.4×10^{-1}	2.7×10^{-2}	3.6×10^{-2}	7.9×10^{-2}	3.1×10^{-2}	7.7×10^{-2}	2	1	1
1	2	2.0×10^{-3}	4.4×10^{-3}	8.3×10^{-6}	9.7×10^{-3}	1.6×10^{-2}	7.7×10^{-3}	3	1	1
1	3	1.1×10^{-2}	4.4×10^{-3}	1.5×10^{-2}	9.7×10^{-3}	1.3×10^{-2}	7.7×10^{-2}	1	2	1
1	4	2.9×10^{-2}	2.7×10^{-2}	9.4×10^{-6}	7.9×10^{-2}	3.1×10^{-2}	7.7×10^{-3}	1	3	1
1	5	1.4×10^{-1}	3.4×10^{-2}	4.1×10^{-4}	9.5×10^{-2}	2.4×10^{-2}	–	1	1	2
1	6	3.8×10^{-4}	5.1×10^{-4}	2.2×10^{-4}	1.2×10^{-3}	6.4×10^{-3}	–	1	1	3
2	0	1.8×10^{-4}	1.7×10^{-3}	2.0×10^{-8}	1.6×10^{-3}	3.2×10^{-3}	1.9×10^{-2}	1	1	1
2	1	2.5×10^{-3}	1.4×10^{-2}	1.8×10^{-4}	1.6×10^{-2}	1.2×10^{-2}	3.5×10^{-2}	2	1	1
2	2	7.1×10^{-6}	5.9×10^{-4}	1.7×10^{-10}	4.4×10^{-4}	6.7×10^{-3}	3.5×10^{-3}	3	1	1
2	3	7.7×10^{-5}	5.9×10^{-4}	3.7×10^{-5}	4.4×10^{-4}	4.1×10^{-3}	3.5×10^{-2}	1	2	1
2	4	4.3×10^{-4}	1.4×10^{-2}	2.1×10^{-10}	1.6×10^{-2}	1.1×10^{-2}	3.5×10^{-3}	1	3	1
2	5	2.5×10^{-3}	2.1×10^{-2}	4.1×10^{-8}	2.3×10^{-2}	7.4×10^{-3}	–	1	1	2
22	6	4.5×10^{-7}	1.4×10^{-5}	1.5×10^{-8}	1.1×10^{-5}	1.6×10^{-3}	–	1	1	3
3	0	7.9×10^{-5}	4.6×10^{-4}	1.3×10^{-9}	1.0×10^{-4}	5.4×10^{-4}	2.2×10^{-5}	1	1	1
3	1	1.1×10^{-3}	1.7×10^{-3}	1.2×10^{-4}	5.7×10^{-4}	1.7×10^{-3}	4.1×10^{-5}	2	1	1
3	2	2.7×10^{-6}	2.4×10^{-4}	1.3×10^{-12}	3.4×10^{-5}	7.3×10^{-4}	4.0×10^{-6}	3	1	1
3	3	3.8×10^{-5}	2.3×10^{-4}	2.2×10^{-5}	3.4×10^{-5}	6.9×10^{-4}	4.1×10^{-3}	1	2	1
3	4	1.2×10^{-4}	1.7×10^{-3}	1.8×10^{-12}	5.7×10^{-4}	1.7×10^{-3}	4.0×10^{-6}	1	3	1
3	5	9.8×10^{-4}	2.2×10^{-3}	3.4×10^{-9}	7.3×10^{-4}	1.2×10^{-3}	–	1	1	2
3	6	1.2×10^{-7}	1.5×10^{-5}	8.2×10^{-10}	1.1×10^{-6}	3.0×10^{-4}	–	1	1	3
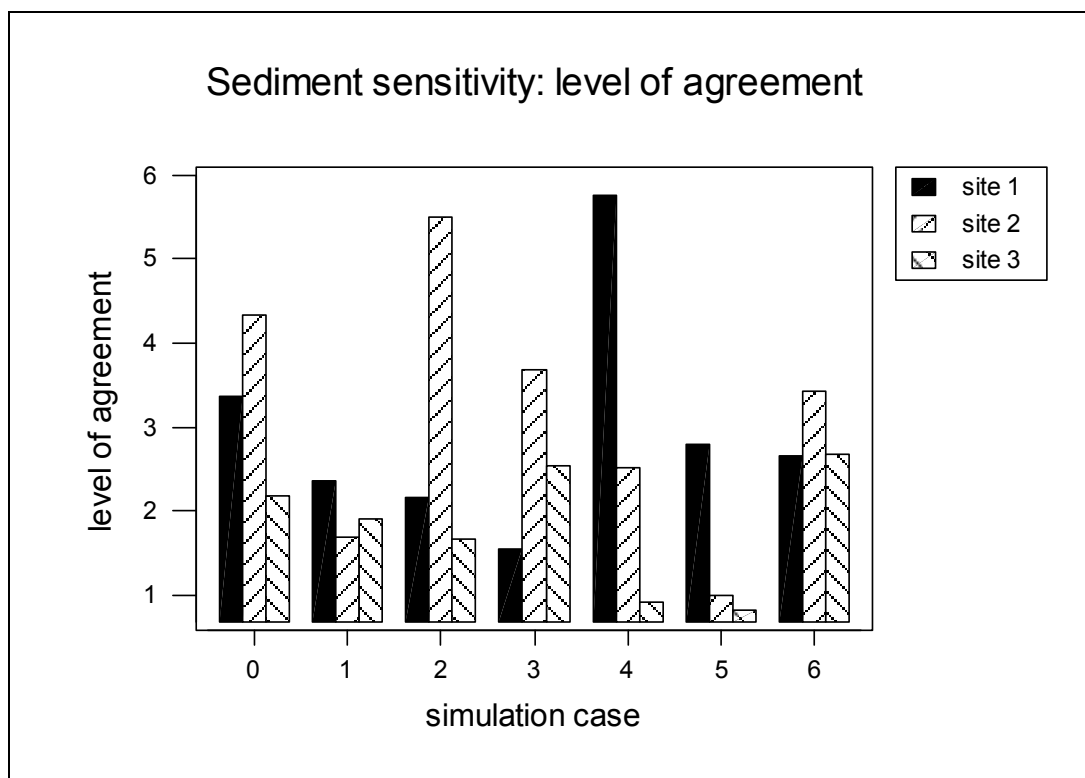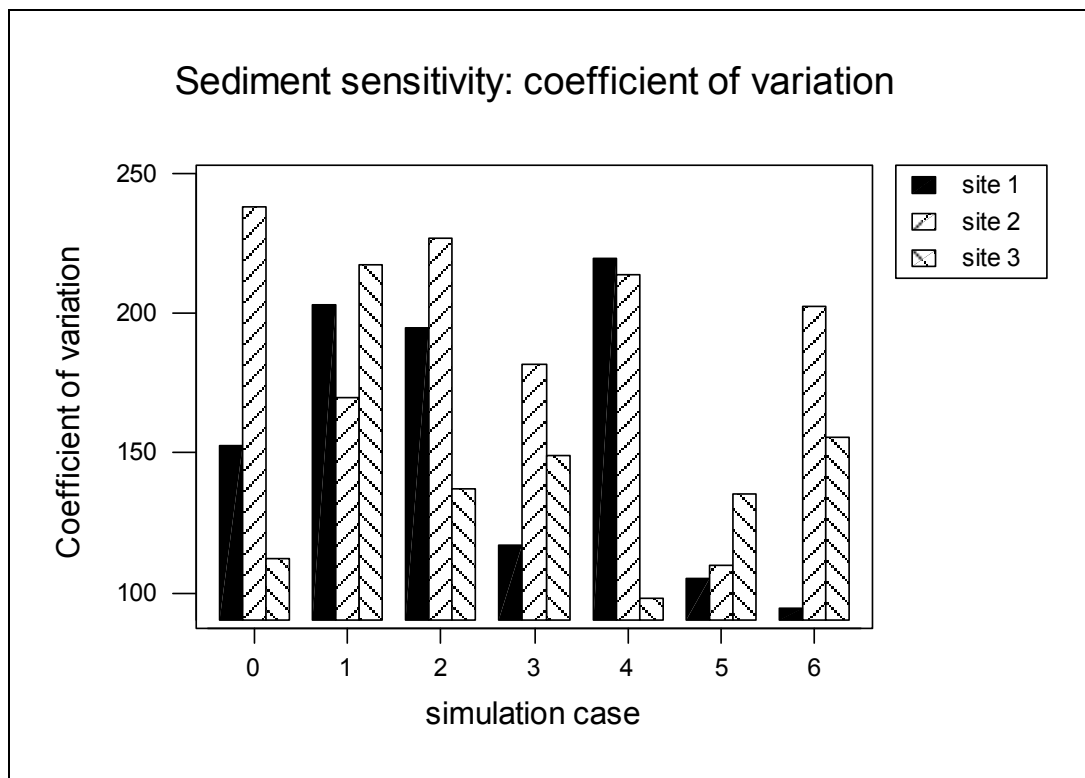
FIG. 48. The coefficient of variation and level of agreement in the sensitivity analysis of sediment concentrations in all simulation cases.
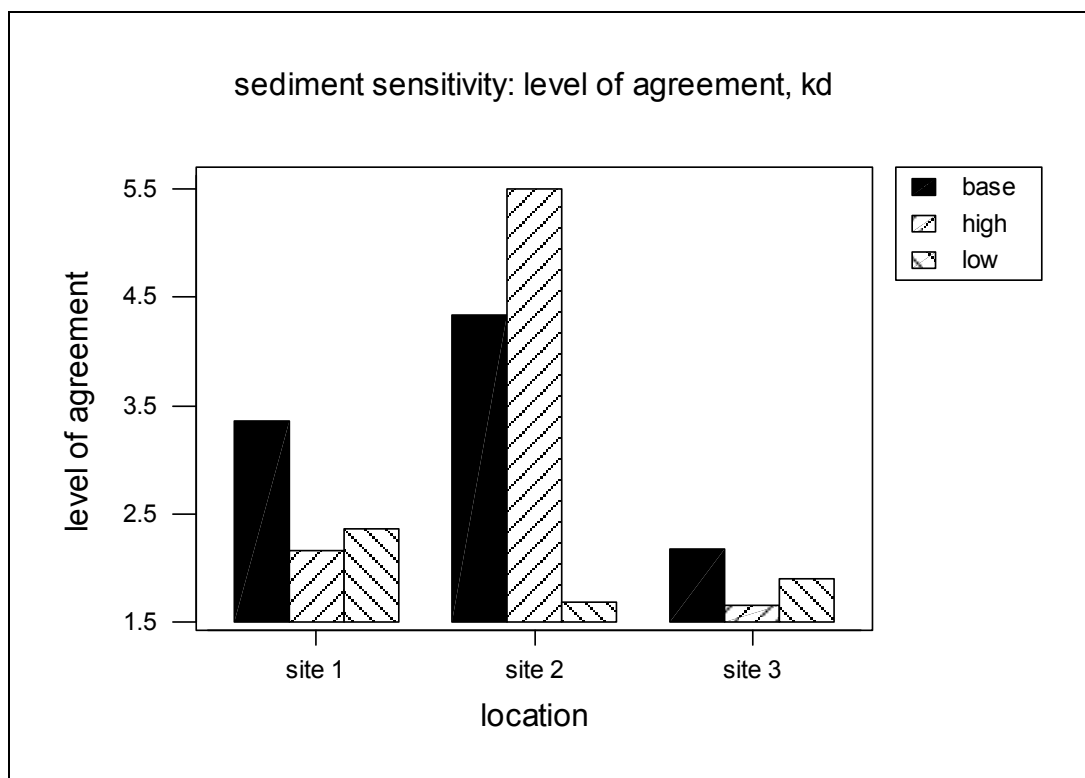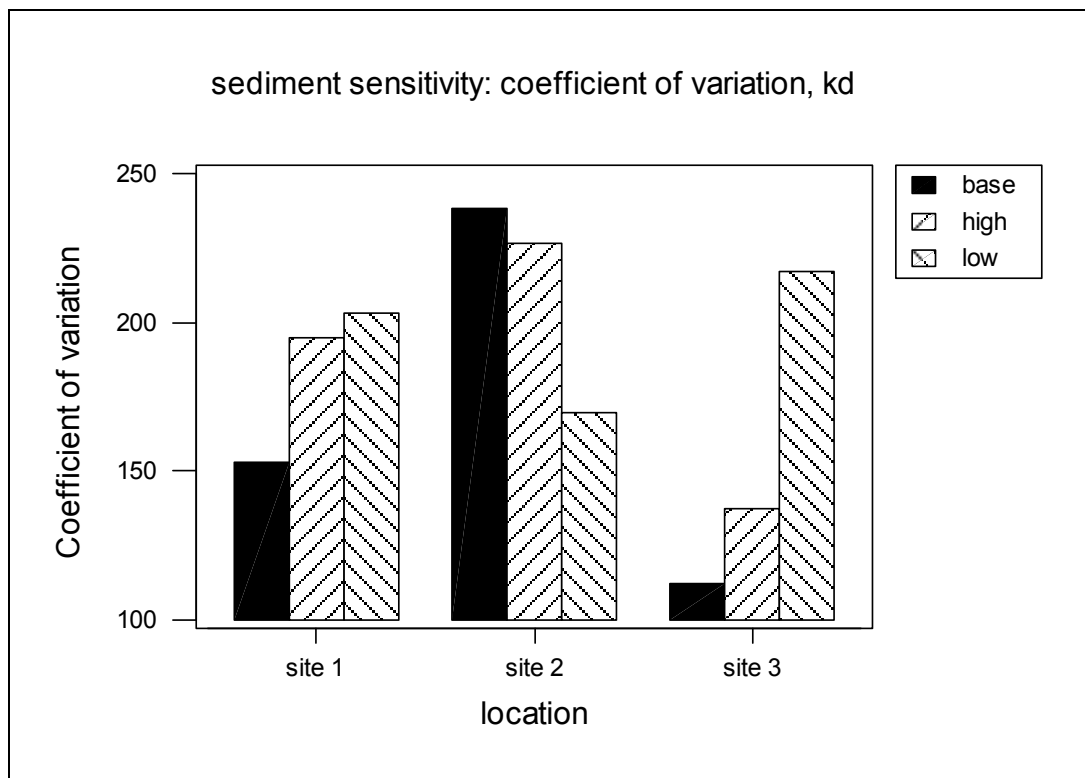
FIG. 49. The coefficient of variation and level of agreement in the sensitivity analysis of sediment in varying K_d only.
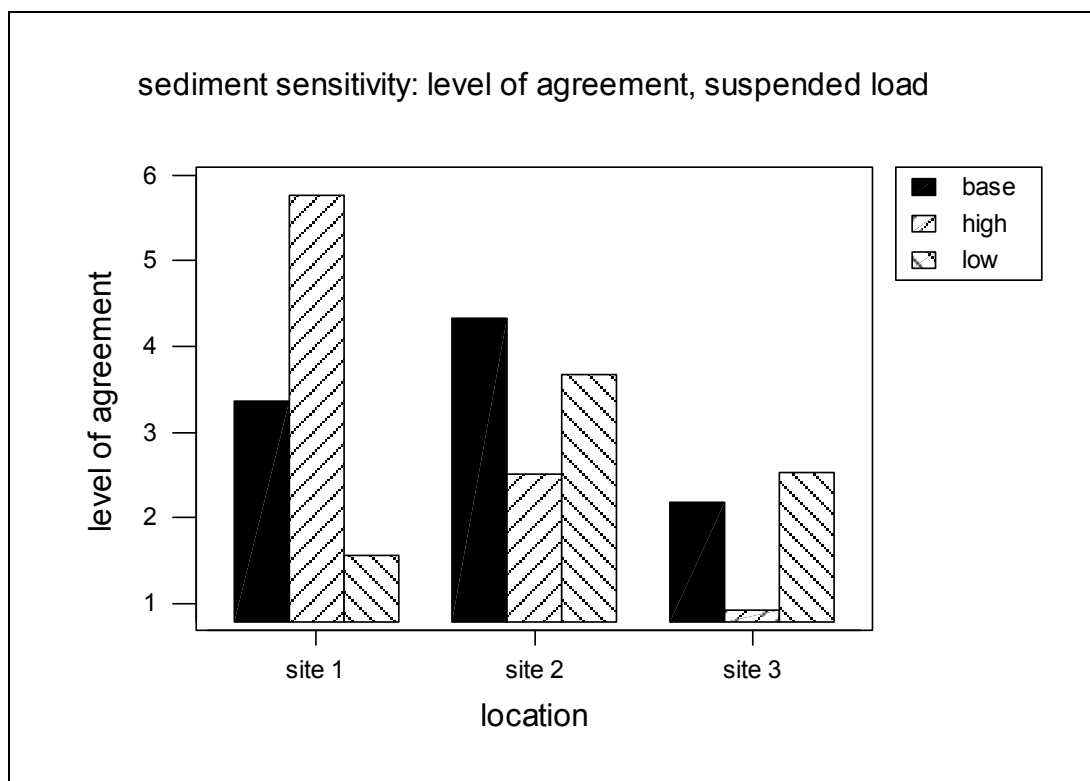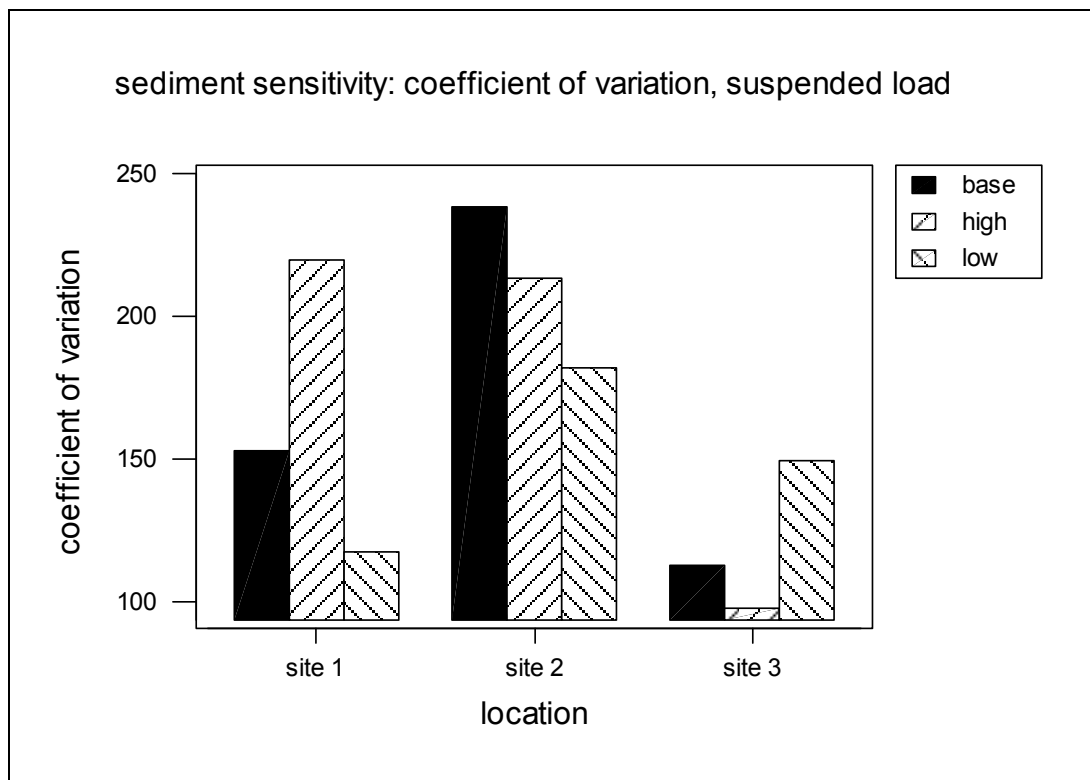
FIG. 50. The coefficient of variation and level of agreement in the sensitivity analyses of sediment in varying only the suspended load.
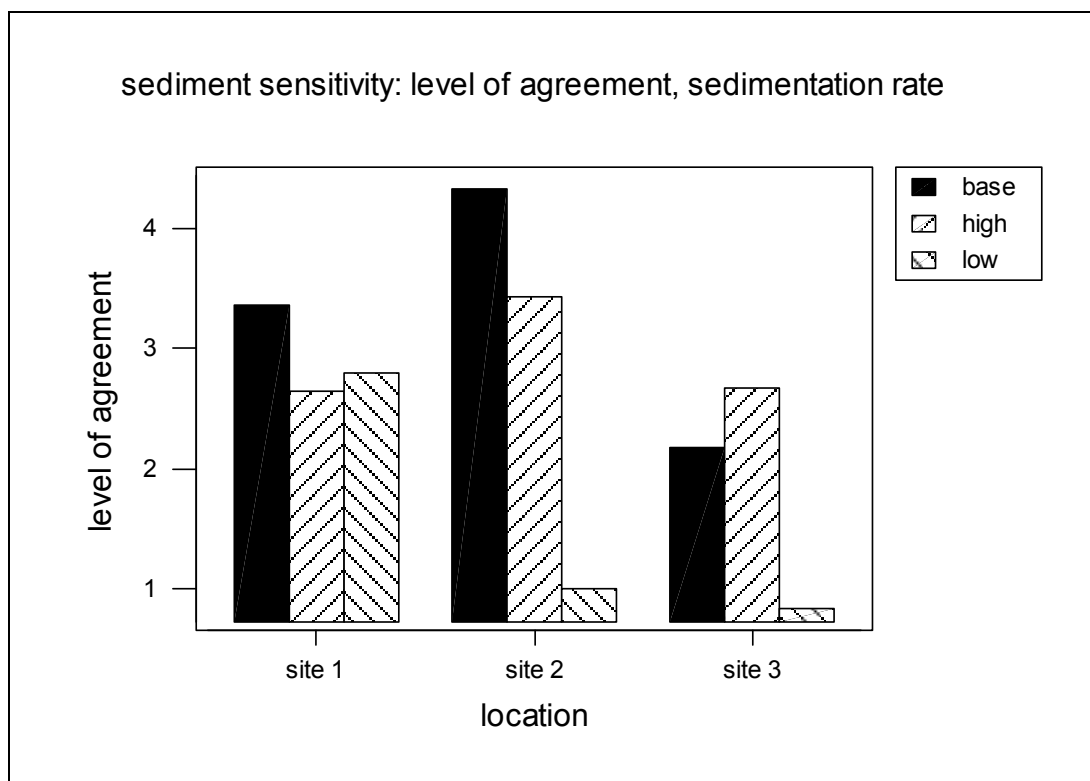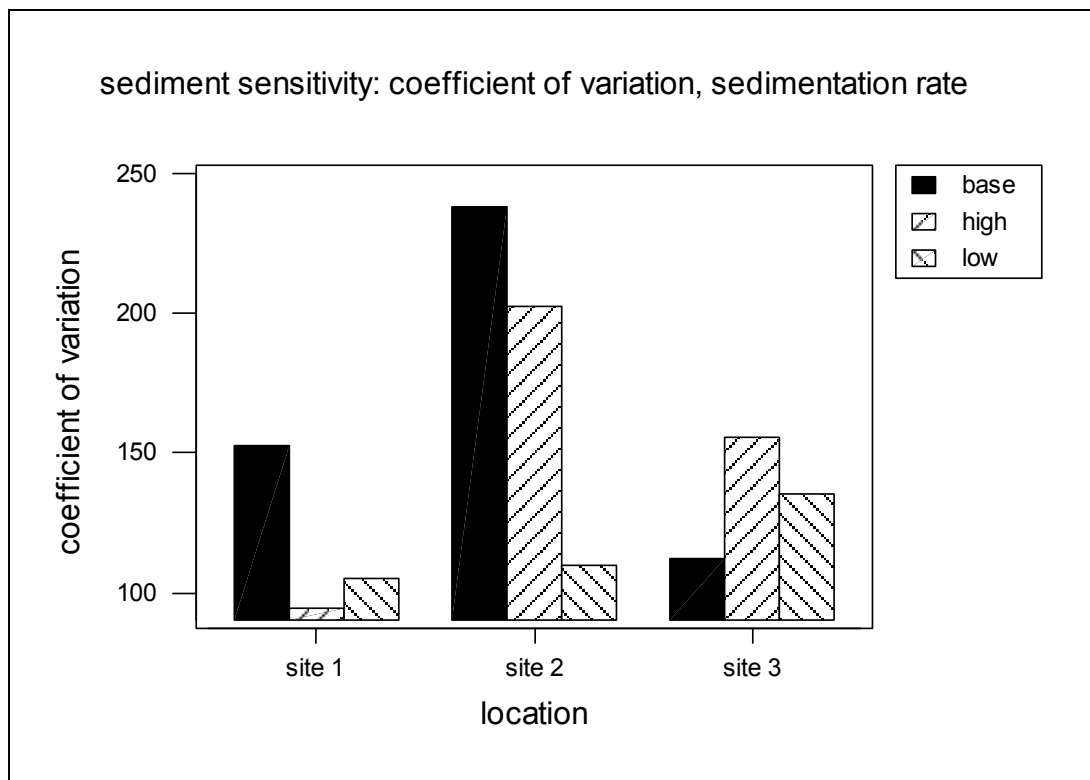
FIG. 51. The coefficient of variation and level of agreement in the sensitivity analyses in varying only the sedimentation rate.
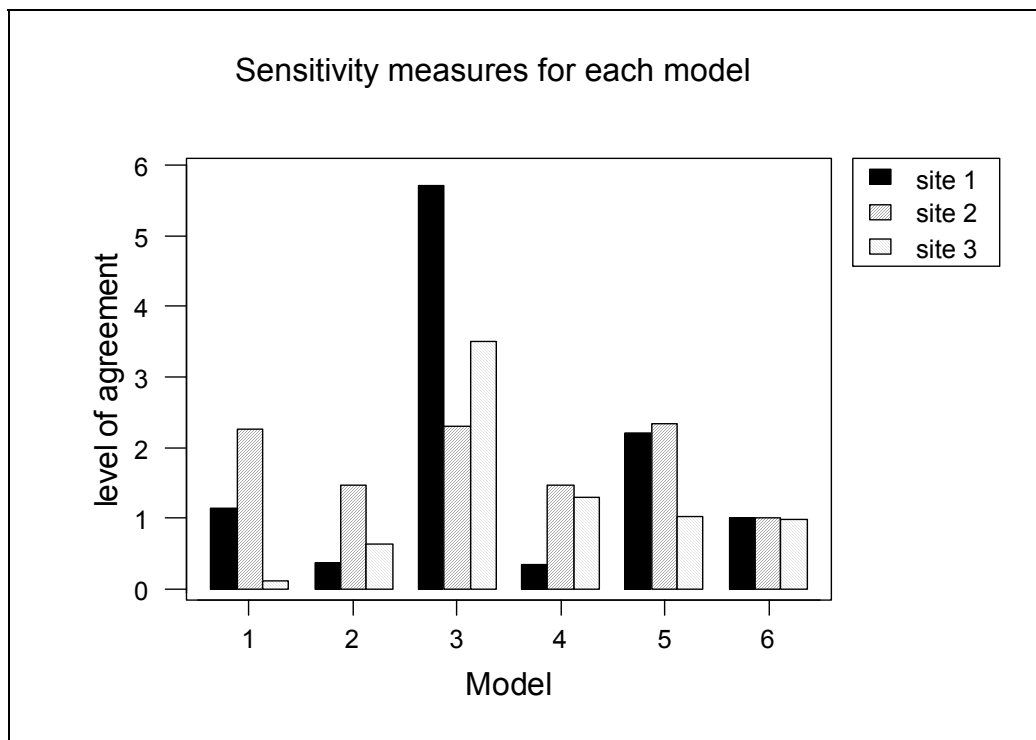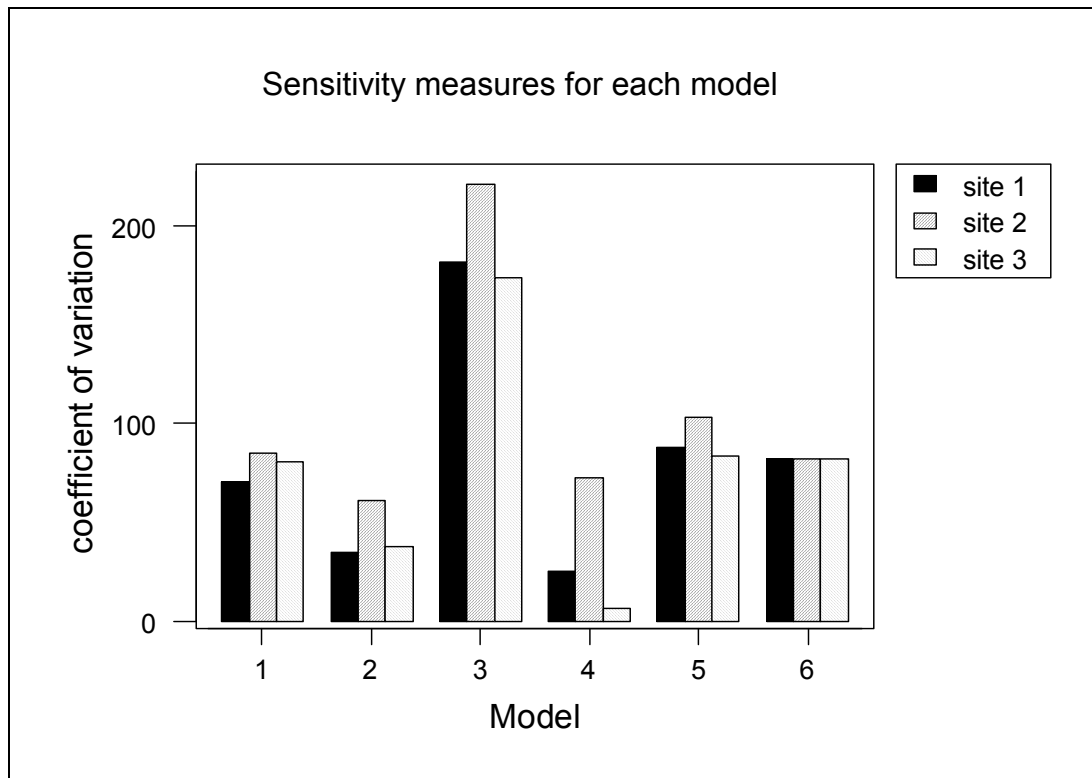
FIG. 52. The coefficient of variation and level of agreement for each model in all simulation cases.

5. RADIOLOGICAL ASSESSMENT

5.1. RADIOLOGICAL ASSESSMENT AND SOURCE SCENARIOS

As discussed briefly in Section 1, the details of the sources, their location and total activity is given in Table LI. With the exception of material dumped in Novaya Zemlya Trough, all other material was dumped in depths of water less than 60 m.

The Source Term Working Group of IASAP prepared three scenarios for consideration by the modelling group [63]. Each scenario detailed conditions under which releases could occur. At the same time, it also included source term descriptions involving both nuclide specific and time dependent release rates for each scenario.

Radionuclide release from the dumped steam generating installations was assumed to be driven by corrosion of the materials forming the reactor structure and spent nuclear fuel. Taking the best available predictions for corrosion rates in an arctic environment, models were then developed to predict the release rates of the fission product, actinide and activation product inventories in the reactors. Using the inventory and construction data, corrosion rates were applied to simple computer models of the protective barriers to produce radionuclide release rates for three scenarios labelled A, B and C. Scenario A gives the release rate produced by corrosion processes alone; scenario B, applied only to the icebreaker spent generating installation, estimates corrosion processes up to the year 2050 followed by a complete break of the containment surrounding the spent nuclear fuel due to e.g. collision or munition explosion and scenario C models corrosion up to the year 3000 followed by a sudden release caused by a glacier riding over the dumped material. In all models scenario C is identical to scenario A up to the year 3000, when a spike occurs and all remaining radionuclides are released.

It was assumed in all models that all material corroded is immediately released to the environment. This is a highly conservative assumption, as most of the corroded material will be heavy and insoluble and hence will remain inside the hull or RPV until corrosion is advanced. This assumption ensures that the IASAP models are a "worst case" realistic estimate of release rates.

5.1.1. Scenario A, "best estimate" discharge scenario

Under this scenario, the sources working group provided nuclide specific releases for each of the sources.

5.1.2. Scenario B, "plausible worst case"

Under this scenario, disruption was postulated to occur (e.g., due to collision or munitions explosion) to the icebreaker fuel dumped in Tsivolka Fjord. One further assumption was made, namely that this event took place in 2050 AD.

5.1.3. Scenario C, "worst case"

This scenario was designed to simulate a major environmental disruption where global cooling followed by glaciation scours out the fjords. Subsequent warming would then release activity directly into the Kara Sea from the disrupted reactor cores. This release was assumed to occur at 3000 AD (or 1000 years into the future).

TABLE LI. SUMMARY OF DUMPED SOURCES

Site	Year of dumping	Depth of dumping[a] (m)	Factory number	Dumped unit	Number of Reactors		Total Activity (PBq)	
					Without spent nuclear fuel	Containing spent nuclear fuel	At the time of dumping	1994
Abrosimov Fjord	1965	20 (10–15)	285	Reactor compartment	1	1	11.6	0.655
		20 (10–15)	901	Reactor compartment	–	2	2.95	0.727
		20	254	Reactor compartment	2	–	0.093	0.009
	1966	20	260	Reactor compartment	2	–	0.044	0.005
Tsivolka Fjord	1967	50 [60]	OK150	Reactor compartment & a box containing fuel	3	0.6[b]	19.5	2.2
Novaya Zemlya Trough	1972	300	421	Reactor	–	1	1.05	0.293
Stepovoy Fjord	1981	50 (30)	601	Submarine	–	2	1.72	0.838
Techeniye Fjord	1988	35–40	538	Reactors	2	–	0.006	0.005
Total					10	6.6	37	4.7

[a]   The data on depths of dumping are from reference [1]; the data in brackets are from references [6, 7], and that in square brackets from reference [63].
[b]   Core barrel containing 58% of fuel of one of the reactors.

Finally, specifically for the NS601 with liquid metal reactors dumped in Stepovoy Fjord, a further release scenario was prepared to represent early releases from these reactors. This step was taken due to the fact that in the best estimate scenario for the NS601, releases are expected some thousands of years hence which presents some difficulty in modelling.

5.2. DOSE ESTIMATION

For the scenarios outlined above, collective doses were to be calculated for scenario A and for the NS601 scenario. In all other cases, maximum individual dose rates for the full range of nuclides were to be calculated.

5.2.1. Definition of critical groups

Three distinct population groups were identified. The provision of detailed information on e.g., consumption and other living habits, was difficult and thus the groups are best defined as hypothetical, although based on as much site-specific information as was available.

5.2.1.1. Group 1

The first population group considered comprises consumers of seafood (including sea mammals). Three such groups are assumed to exist, one residing on the Ob/Yenisey estuaries (significant population centers), the second on the Yamal peninsula (significant population center) and the third on the Taymyr peninsula. This latter group was sited at this location as a result of studying the potential contaminant dispersal using the hydrodynamic model of MEL and Hamburg which showed maximum concentrations at this location. In the absence of data, these populations were assumed to have habits characteristic of subsistence fishing communities in other countries bordering the Arctic. The final habits agreed for these populations were:

> marine consumption: fish 500 g per day
> sea mammals 80 g per day
> seabirds 20 g per day
> eggs 20 g per day

In addition to the ingestion pathway, it was also decided that external exposure was a realistic pathway and so it was assumed that the population would spend 250 hours/year on the shore.

5.2.1.2. Group 2

The second group represents individuals who would be externally exposed on the foreshore of the fjords containing dumped radioactive materials. The pathways to be considered include external exposure, inhalation of sea spray and re-suspended sediment. These individuals are likely to be military personnel and from consideration of the harsh environmental conditions, an occupancy of 100 hours/year was considered appropriate if not conservative. It was noted that there was a convention that beach concentration is taken as 10% of the sediment concentration and this was adopted for the purposes of these calculations [64].

The third and final population group is considered representative of the average Russian population. This group was sited on the Kola peninsula, and fish consumption was taken as 50 kg/year (assumed caught in the Barents Sea), in addition to 0.5 kg/year molluscs and 1 kg/year crustaceans. Neither seaweed nor sea mammal consumption was considered nor was an external exposure pathway included.

5.2.2. K_d s, concentration and dose conversion factors

As part of its involvement in IASAP the IAEA Marine Environment Laboratory (IAEA-MEL) carried out laboratory and field studies to investigate the environmental parameters that affect K_ds and seafood concentration factors (CFs) in the Arctic region [65]. The result of these studies are summarised in Tables LII and LIII. The tables include K_d values and CFs for fish for some elements which could be used in the assessment of the radiological impact of the radioactive wastes dumped in the Arctic Sea. The IASAP's Modelling and Assessment Working Group agreed in general to adopt the concentration factors for fish suggested by review conducted by IAEA-MEL, with a few exceptions, but decided to use different K_ds from those provided in Table LII. For other types of seafood (crustaceans, molluscs and seaweed) and for those elements not included in the review, the groups participating in the assessment used values mainly taken from IAEA-TRS-247 [8]. Concentration factors for mammals were assumed to be the same as those for fish, the notable exception being the values for strontium and plutonium. It is worth noting that concentration factors are not used in dynamic ecological models.

Dose coefficients taken from Basic Safety Standards [66] were used. Some of the variations observed in the final dose results can be attributed to differences in the parameter values, and the importance of these parameters may also vary amongst the various models. Table LIV details the values used by the different modellers.

5.2.2.1. Pathway exposure estimation

The pathway exposure modelling was based on the definitions of the critical groups and agreed sets of parameters, however, the different modelling approaches made differing use of some of these parameters. It is clear that dynamic ecological modelling is not based on a concentration factor approach which has particular implications for specific nuclides. There are also some differences in the assumptions used within the different models.

5.2.3. Fishery statistics

Fishery statistics (based on FAO 1990 data [67] and supplemented by ICES [22] data for the Barents, Norwegian Seas and Spitsbergen areas) were provided. Sea mammal catches were also included where possible. Some modellers made use of average (over 5 years) fish catch in these areas, rather than basing results on a single year which may not be representative. For the calculations, it was assumed that 50% of the fish catch, 30% of the crustacean catch, 15% of the mollusc catch and 10% of the seaweed catch would be consumed.

These figures are widely accepted for radiological protection purposes and were recently reviewed in a major international assessment of the radiological implications of radionuclides in

northern Europe marine waters [68]. In particular, it should be noted that the figure of 50% for fish catch takes account of fish catches for industrial purposes.

For the Kara Sea, additional assumptions were necessary, since no detailed information was available. These were that 2200 tons of fish were caught annually in the southern Kara Sea, and 100% was consumed, as it is likely that fish are not caught for industrial purposes in this area. No crustaceans or mollusc catch was stated. The sea mammal catch limits for the Kara Sea were taken as actual catches, corresponding to 115 tons per year but for the Barents Sea, we assumed 63 tons per year, of which 50% was consumed [69].

A summary of the marine produce catches and % consumed as used by different modellers is given in Table LV.

TABLE LII. IASAP SELECTED K_ds [65] FOR MODELLING COMPARED WITH EXPERIMENTAL DATA AND IAEA [8] VALUES

	Fjords[a]			IAEA[c]	IASAP suggested values
	Stepovoy	Abrosimov	Kara Sea[b]		
Americium	$0.1–1 \times 10^6$	$0.1–3 \times 10^6$	$0.1–4 \times 10^5$	$1 \times 10^5 – 2 \times 10^7$	1×10^6
Plutonium	$0.5–1 \times 10^5$	$0.5–1 \times 10^5$	$0.2–5 \times 10^5$ [d]	$1 \times 10^4 – 1 \times 10^6$	1×10^5
Cobalt	$1–2 \times 10^6$	$1–2 \times 10^3$	$0.5–5 \times 10^4$	$2 \times 10^4 – 1 \times 10^6$	1×10^6
Ruthenium	$2–4 \times 10^4$	3×10^4	$1 \times 10^2 – 3 \times 10^3$	3×10^4	–
Europium	$1–2 \times 10^5$	$1–2 \times 10^5$	1×10^5	$1 \times 10^5 – 2 \times 10^6$	7×10^5
Strontium	$0.1–1 \times 10^2$	$0.1–1 \times 10^2$	$0.1–5 \times 10^1$ [d]	$1 \times 10^2 – 5 \times 10^3$	1×10^2
Caesium	$3–6 \times 10^2$	$2–3 \times 10^2$	0.15×10^2	$1 \times 10^2 – 2 \times 10^4$	5×10^3

TABLE LIII. IASAP SELECTED CFs [65] FOR MODELLING COMPARED WITH EXPERIMENTAL DATA AND IAEA [8] VALUES

	Fish (muscle)	Sea birds	Marine mammals	IAEA Fish (muscle)	IASAP suggested values for fish
Pu	$1 \times 10^3 – 4 \times 10^3$	$<2 \times 10^1 – 1.5 \times 10^2$	3×10^0	$5 \times 10^{-1} – 1 \times 10^2$	4×10^1
Cs	$3 \times 10^1 – 3 \times 10^2$	$4 \times 10^1 – 1.1 \times 10^3$	$1.3 \times 10^1 – 1.8 \times 10^2$	$1 \times 10^1 – 3 \times 10^2$	1×10^2
Sr	$2 \times 10^1 – 9 \times 10^1$	–	$4 \times 10^{-1} – 3.0 \times 10^0$	$3 \times 10^{-1} – 1 \times 10^1$	4×10^0
Ni	1×10^2	7×10^2	–	$5 \times 10^1 – 1 \times 10^3$	1×10^2
Pb	2×10^2	$2 \times 10^4 – 4 \times 10^4$	$2 \times 10^4 – 4 \times 10^4$	$1 \times 10^1 – 3 \times 10^2$	2×10^2
Sb	–	–	1×10^{-1}	$1 \times 10^2 – 1 \times 10^3$	–
I	–	–	1×10^{-1}	–	–

[a]   Laboratory experiments.
[b]   Shipboard experiments.
[c]   Coastal sediments.
[d]   Estimated K_d ranges based on measured radionuclide concentrations in water and sediment samples.

TABLE LIV. K_d, CONCENTRATION FACTORS AND DOSE COEFFICIENTS FOR INGESTION USED IN DIFFERENT MODELS

	Ni-59						
	Nihon U.	Risø	Typhoon	MAFF	KEMA	IAEA-MEL	
CF							
Fish	1×10^2	1×10^2	1×10^3	1×10^3	–	1×10^3	
Mollusc	2×10^3	2×10^3	2×10^3	2×10^3	–	2×10^3	
Crustacean	1×10^3	1×10^3	1×10^3	1×10^3	–	1×10^3	
Weed	2×10^3	2×10^3	2×10^3	–	–	2×10^3	
Mammals	1×10^2	–	1×10^3	–	–	1×10^3	
K_d	1×10^6	1×10^5	1×10^5	1×10^5	2×10^6	$1 \times 10^{5\ a}$	$1 \times 10^{6\ b}$
Dose coefficient[c]	6.3×10^{-11}	6.3×10^{-11}	6.3×10^{-11}	6.3×10^{-11}	–	6.3×10^{-11}	

	Co-60						
	Nihon U.	Risø	Typhoon	MAFF	KEMA	IAEA-MEL	
CF							
Fish	1×10^3	1×10^3	1×10^3	1×10^3	–	1×10^3	
Mollusc	5×10^3	5×10^3	5×10^3	5×10^3	–	5×10^3	
Crustacean	5×10^3	5×10^3	5×10^3	5×10^3	–	5×10^3	
Weed	1×10^4	1×10^4	1×10^4	–	–	1×10^4	
Mammals	1×10^3	–	1×10^3	–	–	1×10^3	
K_d	1×10^7	1×10^6	2×10^5	2×10^5	2×10^7	$2 \times 10^{5\ a}$	$1 \times 10^{7\ b}$
Dose coefficient[c]	3.49×10^{-9}	3.49×10^{-9}	3.49×10^{-9}	3.49×10^{-9}	–	3.4×10^{-9}	

	Ni-63						
	Nihon U.	Risø	Typhoon	MAFF	KEMA	IAEA-MEL	
CF							
Fish	1×10^2	1×10^2	1×10^3	1×10^3	–	1×10^3	
Mollusc	2×10^3	2×10^3	2×10^3	2×10^3	–	2×10^3	
Crustacean	1×10^3	1×10^3	1×10^3	1×10^3	–	1×10^3	
Weed	2×10^3	2×10^3	2×10^3	–	–	2×10^3	
Mammals	1×10^2	–	1×10^3	–	–	1×10^3	
K_d	1×10^6	1×10^5	1×10^5	1×10^5	2×10^6	$1 \times 10^{5\ a}$	$1 \times 10^{6\ b}$
Dose coefficient[c]	1.5×10^{-10}	1.5×10^{-10}	1.5×10^{-10}	1.5×10^{-10}	–	1.5×10^{-10}	

	Sr-90						
	Nihon U.	Risø	Typhoon	MAFF	KEMA	IAEA-MEL	
CF							
Fish	4	4	4	2	–	2	
Mollusc	1	1	2	1	–	1	
Crustacean	2	2	2	2	–	2	
Weed	5	5	5	–	–	5	
Mammals	1	4	2	1	–	1	
K_d	2×10^2	1×10^2	1×10^3	1×10^3	5×10^2	$1 \times 10^{3\ a}$	$2 \times 10^{2\ b}$
Dose coefficient[c]	2.8×10^{-8}	2.8×10^{-8}	2.8×10^{-8}	3.22×10^{-8}	–	2.8×10^{-8}	

[a]   coastal.
[b]   pelagic.
[c]   (Sv/Bq).

TABLE LIV. K_d, CONCENTRATION FACTORS AND DOSE COEFFICIENTS FOR INGESTION USED IN DIFFERENT MODELS (Continued)

	Nihon U.	Risø	Typhoon	MAFF	KEMA	IAEA-MEL	
Cs-137							
CF							
Fish	1×10^2	1×10^2	1×10^2	1×10^2	–	1×10^2	
Mollusc	3×10^1	3×10^1	3×10^1	3×10^1	–	3×10^1	
Crustacean	3×10^1	3×10^1	3×10^1	3×10^1	–	3×10^1	
Weed	5×10^1	5×10^1	5×10^1	–	–	5×10^1	
Mammals	1×10^2	1×10^2	1×10^3	1×10^2	–	1×10^2	
K_d	2×10^3	5×10^3	3×10^3	3×10^3	2×10^4	$3 \times 10^{3\,a}$	$2 \times 10^{3\,b}$
Dose coefficient[c]	1.3×10^{-8}	1.3×10^{-8}	1.3×10^{-8}	1.4×10^{-8}	–	1.3×10^{-8}	
Pu-239 and Pu-240							
CF							
Fish	4×10^1	4×10^1	4×10^1	4×10^1	–	4×10^1	
Mollusc	3×10^3	3×10^3	3×10^2	3×10^3	–	3×10^3	
Crustacean	3×10^2	3×10^2	3×10^2	3×10^2	–	3×10^2	
Weed	2×10^3	2×10^3	2×10^3	–	–	2×10^3	
Mammals	3	4×10^1	3	3	–	3	
K_d	1×10^5	1×10^5	1×10^5	1×10^5	1×10^6	$1 \times 10^{5\,a}$	$1 \times 10^{5\,b}$
Dose coefficient[c]	2.5×10^{-7}	2.5×10^{-7}	2.5×10^{-7}	2.5×10^{-7}	–	2.5×10^{-7}	
Pu-241							
CF							
Fish	4×10^1	4×10^1	4×10^1	4×10^1	–	4×10^1	
Mollusc	3×10^3	3×10^3	3×10^2	3×10^3	–	3×10^3	
Crustacean	3×10^2	3×10^2	3×10^2	3×10^2	–	3×10^2	
Weed	2×10^3	2×10^3	2×10^3	–	–	2×10^3	
Mammals	3	4×10^1	3	3	–	3	
K_d	1×10^5	1×10^5	1×10^5	1×10^5	1×10^6	$1 \times 10^{5\,a}$	$1 \times 10^{5\,b}$
Dose coefficient[c]	4.8×10^{-9}	4.8×10^{-9}	4.8×10^{-9}	4.8×10^{-9}	–	4.8×10^{-9}	
Am-241							
CF							
Fish	5×10^1	5×10^1	5×10^1	5×10^1	–	5×10^1	
Mollusc	2×10^4	2×10^4	2×10^4	2×10^4	–	2×10^4	
Crustacean	5×10^2	5×10^2	5×10^2	5×10^2	–	5×10^2	
Weed	8×10^3	8×10^3	8×10^3	–	–	8×10^3	
Mammals	5×10^1	5×10^1	5×10^1	–	–	5×10^1	
K_d	2×10^6	2×10^6	2×10^6	2×10^6	2×10^7	$2 \times 10^{6\,a}$	$2 \times 10^{6\,b}$
Dose coefficient[c]	2×10^{-7}	2×10^{-7}	2×10^{-7}	2.1×10^{-7}	–	2×10^{-7}	

[a] coastal.
[b] pelagic.
[c] (Sv/Bq).

TABLE LV. SUMMARY OF MARINE PRODUCE CATCHES (TONS PER YEAR) AND % CONSUMED

Location	MAFF	Risø	Fish Typhoon	IAEA-MEL	Nihon U.	KEMA
Kara Sea	2.2×10^3 100%	4.5×10^3 50%	2.2×10^3 50%	2.2×10^3 100%	2.2×10^3 100%	2.2×10^3 100%
Barents Sea	1.3×10^5 50%	7.2×10^5 50%	4.5×10^4 50%	7.9×10^5 50%	4.9×10^5 50%	2.5×10^5 100%
Rest of world	4.1×10^8 50%	6.9×10^7 50%	$-^a$	6.8×10^7 50%	$-^a$	3.4×10^6 100%
Rest of Arctic	$-^a$	$-^a$	7×10^5 50%	$-^a$	3.9×10^6 50%	$-^a$

Location	MAFF	Risø	Mollusc Typhoon	IAEA-MEL	Nihon U.	KEMA
Kara Sea	0	0	0	0	0	0
Barents Sea	3.4×10^4 15%	3.4×10^4 17%	6×10^3 15%	7.3×10^3 15%	0	2.4×10^3 100%
Rest of world	6.2×10^7 15%	4.2×10^6 17%	$-^a$	5.1×10^6 15%	$-^a$	0
Rest of Arctic	$-^a$	$-^a$	4×10^4 15%	$-^a$	0	$-^a$

Location	MAFF	Risø	Crustacean Typhoon	IAEA-MEL	Nihon U.	KEMA
Kara Sea	0	0	0	0	0	0
Barents Sea	2.7×10^3 30%	8.8×10^2 33%	3×10^4 30%	2.4×10^5 30%	3.1×10^4 30%	2.2×10^4 100%
Rest of world	9.4×10^6 30%	7.7×10^6 33%	$-^a$	4.2×10^6 30%	$-^a$	5.7×10^4 100%
Rest of Arctic	$-^a$	$-^a$	4×10^4 30%	$-^a$	1.3×10^5 30%	$-^a$

Location	MAFF	Risø	Weed Typhoon	IAEA-MEL	Nihon U.	KEMA
Kara Sea	0	0	0	0	0	0
Barents Sea	3×10^3 10%	0	0	7×10^3 10%	2.9×10^3 10%	0
Rest of world	1×10^7 10%	0	$-^a$	4.4×10^6 10%	$-^a$	0
Rest of Arctic	$-^a$	$-^a$	0	$-^a$	1.3×10^4 10%	$-^a$

Location/Model	Mammal IAEA-MEL	Nihon U.
Kara Sea	115 50%	115 50%
Barents Sea	435 50%	63 50%

Location/Model	Cephalopods[a] IAEA-MEL
Kara Sea	0
Barents Sea	4 50%
Rest of world	2.3×10^6 50%

[a]   Not applicable to the model used.
[b]   One further set of figures for cephalopods used by IAEA-MEL.

6. RESULTS

6.1. RESULTS FROM SCENARIO A

Maximum individual dose rate, time of maximum, % contribution by nuclide and pathway were provided by the modellers. Further collective doses were calculated for Scenario A and NS601.

The maximum individual dose rate is of concern in all scenarios but particularly B and C, which deal with extreme conditions. Since the populations of interest are based only in the Kara and Barents Seas, results from a 3-dimensional hydrodynamic model are also included. It should be noted that in some instances, due to the source data, there may be several peaks in the dose rate at different times; Tables LVI and LVIIa–d give the absolute maximum individual dose rate and time to maximum as well as the percentage contribution of radionuclides and pathways which are now discussed for each scenario.

6.1.1. Results from all sources combined

Table LVI shows the results of maximum individual dose rate for the identified population groups from all sources within the Kara Sea. The decision to make a series of calculations for all sources combined was made specifically for the compartmental models which had lower spatial resolution; it also gives an overall measure of the potential impact to the populations. It can be seen that for the non-military populations, maximum dose rates are very low and lie in the range of 5×10^{-12} to 6×10^{-8} Sv/year over the 4 locations which contain groups 1 and 3, with the 'average' Russian population on the Kola peninsula (group 3) receiving the lowest maximum dose rate. In all cases, the dose is mainly delivered through fish consumption with ^{137}Cs and ^{239}Pu being the dominant nuclides. The results for the military group (critical group 2) are higher although still low, with an estimated maximum dose rate of 2×10^{-5} Sv/year from external exposure and inhalation. This maximum dose rate would be delivered in the period 2100–2300.

To provide some perspective on these figures, the dose rate delivered through consumption of fish, molluscs and crustacea from ^{210}Po (a natural radionuclide) to:

(a) Group 3 on the Kola peninsula is estimated to be 1×10^{-4} Sv/a;

(b) Group 1, on the Taymyr peninsula is estimated to be 5×10^{-4} Sv/a (from fish consumption alone).

These figures are based on ^{210}Po concentrations for FAO area 27 (North East Atlantic [69]).

6.1.2. Results from individual sources

6.1.2.1. Abrosimov Fjord

Table LVIIa shows the results for discharge in Abrosimov Fjord. Maximum dose rates for the non-military populations lie in the range 4.6×10^{-11} Sv/a at Kola (which is based on marine produce caught in the Barents Sea) to 5.2×10^{-8} Sv/a at Yamal. The maximum dose rate is delivered in the period 2000–2300 and is due to ^{137}Cs with the dominant pathway being ingestion. However, one model gives the dominant pathway for all groups except Kola as external exposure.

TABLE LVI. RANGE OF MAXIMUM INDIVIDUAL DOSE RATES, ALL SOURCES COMBINED, SCENARIO A

Population group			1			2		3	
Location		Yamal		Taymyr	Ob/Yenisey		Military		Kola
Individual peak dose rates (Sv/a)		$3 \times 10^{-10} - 6 \times 10^{-8}$		$3 \times 10^{-10} - 8 \times 10^{-9}$	$3 \times 10^{-10} - 3 \times 10^{-9}$		$3 \times 10^{-8} - 2 \times 10^{-5}$		$5 \times 10^{-12} - 2 \times 10^{-9}$
In years		2100–2500		2100–2500	2100–2500		2100–2300		2000–2400
Range of estimated percentage contributions for each pathway[a]	Ingestion	77–100		77–100	78–100		28		48–100
	Inhalation	55		1	–		4–100		–
	External	17		17	17		69		–
Range of estimated percentage contributions for individual nuclides[a]		Cs-137	94	Cs-137 93–95	Cs-137	94	Cs-137	88–94	Cs-137 95
		Pu-239	30–66	Pu-239 30	Pu-239	30	Pu-239	30	Pu-239 65–67
		Pu-240	27	Sr-90 3.7	Sr-90	7	Sr-90	4–8	Pu-240 26
		Am-241	3	Ni-63 1.2			Co-60	5	Am-241 6
		Sr-90	6						

TABLE LVIIa. RANGE OF MAXIMUM INDIVIDUAL DOSE RATES, ABROSIMOV FJORD SOURCES, SCENARIO A

Population group			1			2		3	
Location		Yamal		Taymyr	Ob/Yenisey		Military		Kola
Individual peak dose rates (Sv/a)		$2 \times 10^{-10} - 5.2 \times 10^{-8}$		$2 \times 10^{-10} - 9.7 \times 10^{-9}$	$2 \times 10^{-10} - 2.4 \times 10^{-9}$		$2.3 \times 10^{-9} - 6.6 \times 10^{-5}$		$4.6 \times 10^{-11} - 1.5 \times 10^{-9}$
In years		2100		2100	2100–2300		2100–2700		2100
Range of estimated percentage contributions for each pathway[a]	Ingestion	7–98		7–98	75–77		–		90–100
	Inhalation	–		–	–		43–100		–
	External	17–93		17–93	17		5–100		–
Range of estimated percentage contributions for individual nuclides[a]		Cs-137	90–94	Cs-137 90–93	Cs-137	94	Pu-239	67	Cs-137 90–91
		Sr-90	6–11	Sr-90 7–10	Sr-90	7	Pu-240	28	Sr-90 8–11
							Am-241	5	

TABLE LVIIb. RANGE OF MAXIMUM INDIVIDUAL DOSE RATES, TSIVOLKA FJORD SOURCE, SCENARIO A

Population group			1			2		3	
Location		Yamal	Taymyr		Ob/Yenisey	Military		Kola	
Individual peak dose rates (Sv/a)		$2 \times 10^{-10} - 3 \times 10^{-8}$	$3 \times 10^{-10} - 7 \times 10^{-8}$		$3 \times 10^{-10} - 5 \times 10^{-9}$	$2 \times 10^{-8} - 6 \times 10^{-4}$		$7 \times 10^{-12} - 5.3 \times 10^{-10}$	
In years		2300–2500	2300–2500		2300–2500	2300–2310		2300–2400	
Range of estimated percentage contributions for each pathway[a]	Ingestion	7–100	7–100		95–100	–		48–100	
	Inhalation	–	–		–	61–100		–	
	External	2–93	6–93		–	100		–	
Range of estimated percentage contributions for individual nuclides[a]		Pu-239/240 88	Pu-239	65–69	Pu-239/240 87	Pu-239	32–66	Cs-137	78
		Pu-239 64–69	Pu-239/240	65	Pu-239 61–69	Am-241	54	Pu-239	67–69
		Pu-240 29–30	Pu-240	28–29	Pu-240 30	Pu-240	14	Pu-240	30
		Cs-137 10	Cs-137	4–33	Cs-137 11			Pu-239/240	17
		Am-241 1	Am-241	2				Am-241	2

[a]   A single value is reported when only one modeller gave a result for a given nuclide or a given pathway.

TABLE LVIIc. RANGE OF MAXIMUM INDIVIDUAL DOSE RATES, TECHENIYE FJORD SOURCE, SCENARIO A

Population group			1			2		3	
Location		Yamal	Taymyr		Ob/Yenisey	Military		Kola	
Individual peak dose rates (Sv/a)		$2 \times 10^{-16\,b} - 2 \times 10^{-11}$	$2 \times 10^{-16\,b} - 4 \times 10^{-13}$		$2 \times 10^{-16\,b} - 1 \times 10^{-11}$	8×10^{-12}		$5 \times 10^{-19\,b} - 7 \times 10^{-17\,b}$	
In years		2000–2200	2000–2200		2000–2200	2000		2000–2200	
Range of estimated percentage contributions for each pathway[a]	Ingestion	73	73		73	–		48–87	
	Inhalation	–	–		–	–		–	
	External	96	93		96	100		–	
Range of estimated percentage contributions for individual nuclides[a]		Co-60 100	Co-60	100	Co-60 100	Co-60	100	Co-60	97
		Ni-59 91	Ni-59	91	Ni-59 91			Ni-59	93

TABLE LVIId. RANGE OF MAXIMUM INDIVIDUAL DOSE RATES, NOVAYA ZEMLYA TROUGH SOURCE, SCENARIO A

Population group				1		2	3
Location		Yamal	Taymyr	Ob/Yenisey		Military	Kola
Individual peak dose rates (Sv/a)		$1.7 \times 10^{-11} - 1.4 \times 10^{-10}$	$5.1 \times 10^{-11} - 8.6 \times 10^{-9}$	$2.2 \times 10^{-12} - 4.1 \times 10^{-10}$		$1 \times 10^{-14} - 2 \times 10^{-6}$	$1.9 \times 10^{-12} - 2.1 \times 10^{-10}$
In years		2000–2100	2000–2100	2000–2100		2060	2000–2100
Range of estimated percentage contributions for each pathway[a]	Ingestion	75–100	75–100	75–98		–	91–99
	Inhalation	–	–	–		44	–
	External	17	17	17		–	–
Range of estimated percentage contributions for individual nuclides[a]		Cs-137 93–97	Cs-137 92–97	Cs-137 91–97		Sr-90 71	Sr-90 9–99
		Sr-90	Sr-90 7–99	Sr-90 7			Cs-137 91–92
			Pu-239 1				Pu-239 1

[a] A single value is reported when only one modeller gave a result for a given nuclide or a given pathway.

[b] It should be noted that dose rates of the order of magnitude $10^{-19} - 10^{-16}$ correspond only few radioactive decays in a human lifetime and are thus radiologically meaningless. For comprehensiveness, the calculated figures are, however, included in the report.

Again, the maximum dose rate to military personnel, as might be expected, is higher, with a maximum value of 6.6×10^{-5} Sv/a also delivered in the period 2100–2700. Inhalation and external exposure are the dominant pathways.

6.1.2.2. Tsivolka Fjord

Table LVIIb gives the results for Tsivolka Fjord, site of the icebreaker reactors and the fuel containment. Results range from a minimum of 7×10^{-12} Sv/a at the Kola peninsula to a maximum of 7×10^{-8} Sv/a at Taimyr, with maximum dose rate delivered in the period 2300–2500. The dominant pathway is ingestion (with one model exception) and with ^{239}Pu and ^{137}Cs being the major contributors to the dose. For the military group, dose rates are again higher, with a maximum value of 6×10^{-4} Sv/a, and inhalation being the dominant pathway.

6.1.2.3. Techeniye Fjord

Table LVIIc gives the results for sources in Techeniye Fjord (very low inventory) from two models (both compartmental). Maximum dose rates to the non-military populations at Kola are low, 6×10^{-19} to 7×10^{-17} Sv/a (note the footnote ^{b} in Table LVIIc). For the other locations, dose rates are in the range 2×10^{-16} to 2×10^{-11} Sv/a. The military group dose rate is at 8×10^{-12} Sv/yr. For the non-military, ingestion is the dominant pathway, with ^{60}Co and ^{59}Ni being the dominant nuclides.

6.1.2.4. Novaya Zemlya Trough

Table LVIId shows the results for the Novaya Zemlya Trough. This location is significantly deeper than any of the source other locations and there is significantly more variation in the model results close to the source (some of the reasons for this were discussed in Section 5.4). The vertical structures of the models differ and their treatment of the trough (perhaps as a separate entity within the model) accounts for these differences. Model sensitivity to vertical structure and hence migration of radionuclides was demonstrated in the initial benchmarking exercises. We also see differences in the timing of the delivery of the dose again reflecting different model structures.

The results for all non-military groups are low, in the range 2×10^{-12} to 9×10^{-9} Sv/a, fish consumption dominates, with ^{137}Cs and ^{90}Sr contributing substantially. The results for the military group are also very low (1×10^{-14} to 2×10^{-6} Sv/a).

6.1.3. Conclusions

The calculated doses from the releases to the individuals in all considered population groups bordering on the Kara and Barents Seas are summarised in Table LVIII. The range of results reflects the results of the individual models used in the assessment. Doses are presented for each source area, e.g., Stepovoy Fjord, Abrosimov Fjord, etc. the summed total for each critical group is a summation of the highest calculated dose to that group from each source. In summing doses, the fact that peak doses may occur in different years has been ignored and so the totals are conservative in this respect. However, it is interesting to note that the doses calculated by models which were run for all sources simultaneously (Table LVIII) are within an order of magnitude of the doses summed source by source.

Total annual individual doses in each population group are all less than 0.1 μSv. This dose is significantly lower than the normal variations in background radiation from placed to place that are experienced in western countries – these can be 300 μSv/a excluding variations in doses

from radon-222 which are much greater. Furthermore, annual doses from natural ^{210}Po via consumption of fish caught in the Barents Sea are of the order of 400 μSv.

No subsistence communities live on the island of Novaya Zemlya itself. The island has been used for nuclear weapons testing and it remains under military control. Thus, dose calculations have been undertaken for a hypothetical critical group of military personnel patrolling beaches on the fringes of the fjords containing radioactive wastes. These calculated doses are generally higher than those calculated for the population groups bordering the Kara and Barents Seas; the highest annual dose of about 700 μSv is calculated for military personnel patrolling Tsivolka Fjord while release are occurring from the icebreaker fuel. The annual calculated doses for the other locations are at least an order of magnitude lower. The calculations assume that military personnel patrol the beaches directly bordering each fjord for 100 hours – given the harsh environment conditions, this assumption is conservative.

6.2. RESULTS FROM SCENARIO B

Scenario B was devised to mimic a 'plausible' accident and Tsivolka Fjord, as the site of disposal of the icebreaker reactors was chosen. Disruption of the source was assumed to occur at 2050, resulting in a changed discharge pattern after this date. Up till 2050, the discharge pattern is identical to Scenario A.

6.2.1. Maximum individual dose due to Tsivolka Fjord

Table LIXa shows the results for Scenario B, Tsivolka Fjord source only. Maximum dose rates to the non-military populations are in the range 1×10^{-10} to 7×10^{-7} Sv/a. For the military personnel, there has been an increase in maximum dose rate to (at highest 4×10^{-3} Sv/a) and the year of delivery follows immediately the disruptive event. In Table LIXb only the results of Tsivolka Fjord alone, according to the accident Scenario B are compared with the results where all the other sources are included as modelled according to Scenario A, the normal case, and Tsivolka Fjord source according to the accident Scenario B.

6.2.2. Conclusions

This scenario covers the possibility of damage to the waste form due to, e.g., a munitions accident in the vicinity. The calculated annual doses to members of the public are less than 1 μSv and are still very small compared with that experienced by individuals from natural sources. Calculated doses to the critical group of military personnel patrolling the banks of Tsivolka Fjord are also higher, at up to 4 mSv/a (3300 μSv/a), than for Scenario A. However, the dose is not dissimilar to general natural background levels. Furthermore, as noted, this critical group is a hypothetical one and the assumptions concerning beach occupancy are conservative.

6.3. RESULTS FROM SCENARIO C

It should be noted that, for Scenario C, the peak release in 3000 AD may be lower than releases in earlier years as a consequence of radioactive decay.

TABLE LVIII. SUMMARY OF INDIVIDUAL DOSE RATES (Sv/a) — SCENARIO A

Population Group	1			2	3
Location	Yamal	Taymyr	Ob/Yenisey	Military	Kola
Novaya Zemlya Trough	$2 \times 10^{-11} - 2 \times 10^{-10}$	$5 \times 10^{-11} - 9 \times 10^{-9}$	$2 \times 10^{-12} - 5 \times 10^{-10}$	$1 \times 10^{-14} - 2 \times 10^{-6}$	$2 \times 10^{-12} - 3 \times 10^{-10}$
Techeniye Fjord	$2 \times 10^{-16\,a} - 2 \times 10^{-11}$	$2 \times 10^{-16\,a} - 4 \times 10^{-13}$	$2 \times 10^{-16\,a} - 1 \times 10^{-11}$	8×10^{-12}	$5 \times 10^{-19\,a} - 7 \times 10^{-17\,a}$
Tsivolka Fjord	$2 \times 10^{-10} - 3 \times 10^{-8}$	$3 \times 10^{-10} - 7 \times 10^{-8}$	$3 \times 10^{-10} - 5 \times 10^{-9}$	$2 \times 10^{-8} - 6 \times 10^{-4}$	$7 \times 10^{-12} - 6 \times 10^{-10}$
Stepovoy Fjord	$1 \times 10^{-12} - 3 \times 10^{-12}$	$5 \times 10^{-14} - 6 \times 10^{-10}$	$1 \times 10^{-13} - 4 \times 10^{-11}$	8×10^{-12}	$7 \times 10^{-14} - 3 \times 10^{-13}$
Abrosimov Fjord	$2 \times 10^{-10} - 6 \times 10^{-8}$	$2 \times 10^{-10} - 1 \times 10^{-8}$	$2 \times 10^{-10} - 3 \times 10^{-9}$	$2 \times 10^{-9} - 7 \times 10^{-5}$	$5 \times 10^{-11} - 2 \times 10^{-9}$
Totals (sum of maximum results for each source)	9×10^{-8}	9×10^{-8}	8.5×10^{-9}	6.7×10^{-4}	2.9×10^{-9}
Totals (running models with all sources)	$3 \times 10^{-10} - 6 \times 10^{-8}$	$3 \times 10^{-10} - 8 \times 10^{-9}$	$3 \times 10^{-10} - 3 \times 10^{-9}$	$3 \times 10^{-8} - 2 \times 10^{-5}$	$5 \times 10^{-12} - 2 \times 10^{-9}$

[a] It should be noted that dose rates of the order of magnitude $10^{-19} - 10^{-16}$ correspond only few radioactive decays in a human lifetime and are thus radiologically meaningless. For comprehensiveness, the calculated figures are, however, included in the report.

TABLE LIXa. RANGE OF MAXIMUM INDIVIDUAL DOSE RATES, TSIVOLKA FJORD SOURCE — SCENARIO B

Population group	1					2		3	
Location	Yamal		Taymyr		Ob/Yenisey		Military		Kola	
Individual peak dose rates (Sv/a) In years	$3.1 \times 10^{-10} - 7 \times 10^{-7}$		$3.1 \times 10^{-10} - 3 \times 10^{-7}$		3.1×10^{-10}		$1.2 \times 10^{-7} - 3.3 \times 10^{-3}$		$1.4 \times 10^{-10} - 1.1 \times 10^{-8}$	
	2100		2100		2100		2100		2100–2200	
Range of estimated percentage contributions for each pathway[a] — Ingestion	6–100		7–100		79–100		–		47–100	
Inhalation	–		–		–		50–100		–	
External	74		93		–		27		–	
Range of estimated percentage contributions for individual nuclides[a]	Cs-137	69–83	Cs-137	69–83	Cs-137	69–83	Pu-239	68	Pu-239	67
	Pu-239/240	23	Pu-239/240	23	Pu-239/240	23	Sr-90	66	Pu-239/240	89
							Pu-240	30		
							Pu-239/240	48		
							Cs-137	37		

TABLE LIXb. CATASTROPHIC RELEASE FROM ICEBREAKER LENIN IN 2050 – SCENARIO B, ALL OTHER SOURCES ACCORDING TO SCENARIO A

Population group	1			2	3
Location	Yamal	Taymyr	Ob/Yenisey	Military	Kola
Tsivolka Fjord only[b]	$3 \times 10^{-10} - 7 \times 10^{-7}$	$3 \times 10^{-10} - 3 \times 10^{-7}$	3×10^{-10} [c]	$1 \times 10^{-7} - 4 \times 10^{-3}$	$1 \times 10^{-10} - 2 \times 10^{-8}$
All sources + Tsivolka Fjord	$1 \times 10^{-7} - 3 \times 10^{-7}$	$4 \times 10^{-8} - 1 \times 10^{-7}$	1×10^{-7} [c]	$1 \times 10^{-5} - 4 \times 10^{-4}$	$4 \times 10^{-10} - 3 \times 10^{-9}$

[a]   A single value is reported when only one modeller gave a result for a given nuclide or a given pathway.

[a]   In some cases the range of results for "all sources" is lower than for "Tsivolka Fjord only" because all the models were not used in both cases.

[b]   Only one set of results.

117

6.3.1. Results from all sources combined

Table LX shows the results for all sources combined under the scenario of total release of all remaining inventory at 3000 AD. For groups 1 and 3, maximum dose rates lie in the range 6×10^{-10} to 3×10^{-7} Sv/a. These values are the same as or only slightly higher than those estimated under scenario A. The dominant pathway is ingestion. For group 2, the maximum dose rate is 2×10^{-4} Sv/a.

6.3.2. Results from individual sources

Tables LXIa to LXId show the maximum individual dose rates from each of the sources separately. Three separate models have been used for these calculations.

6.3.2.1. Abrosimov Fjord

Table LXIa shows the results for Abrosimov Fjord. Maximum dose rates for groups 1 and 3 lie in the range 2×10^{-11} to 2×10^{-8} Sv/a over the four locations. Results for the military group show a maximum value of 2×10^{-4} Sv/a, delivered around 2050.

6.3.2.2. Tsivolka Fjord

Table LXIb shows the results for Tsivolka Fjord. The maximum dose rates for groups 1 and 3 lie in the range 2×10^{-10} to 2×10^{-7} Sv/a. Maximum dose rates for the military group are in the range 2×10^{-7} to 3×10^{-3} Sv/a. ^{239}Pu is the dominant nuclide for all groups.

6.3.2.3. Techeniye Fjord

Table LXIc shows the results for Techeniye Fjord, maximum dose rates are very low in the range of 4×10^{-17} to 3×10^{-11} Sv/a for groups 1 and 3. Again for the military group, results are very low (maximum value of 3×10^{-12} Sv/a).

6.3.2.4. Novaya Zemlya Trough

Table LXId gives the results for the Novaya Zemlya Trough. Maximum dose rates for groups 1 and 3 range from 3×10^{-12} to 4×10^{-9} Sv/a. For the military on Novaya Zemlya, the maximum dose rate is of the order of 2×10^{-6} Sv/a.

6.3.3. Conclusions

Considering the subsistence communities, the highest doses from scenario C were to the critical groups of seafood consumers on the Yamal Peninsula and on the Taymyr Peninsula (Table LXII). However, the annual doses to these groups were less than 1 μSv and thus can be regarded as having no significance. The highest doses to the military personnel for scenario C were less than around 2 mSv/a.

TABLE LX. RANGE OF MAXIMUM INDIVIDUAL DOSE RATES, ALL SOURCES COMBINED, SCENARIO C

Population group		1			2	3
Location		Yamal	Taymyr	Ob/Yenisey	Military	Kola
Individual peak dose rates (Sv/yr)		$4 \times 10^{-9} - 3 \times 10^{-7}$	$4 \times 10^{-9} - 3 \times 10^{-7}$	$4 \times 10^{-9} - 3 \times 10^{-7}$	$8 \times 10^{-10} - 2 \times 10^{-4}$	$6 \times 10^{-10} - 6 \times 10^{-9}$
In years		3000–3121	3000–3121	3000–3121	2300–3000	3000–3089
Range of estimated percentage contributions for each pathway[a]	Ingestion	100	100	100	–	100
	Inhalation	–	–	–	60–100	–
	External	–	–	–	–	–
Range of estimated percentage contributions for individual nuclides[a]		Pu-240 24–30 Pu-239 70–93	Pu-240 24–30 Pu-239 70–93	Pu-240 24–30 Pu-239 70–93	Pu-240 24–30 Pu-239 60–96	Pu-240 24–30 Pu-239 69–94 Am-241 20

[a]   A single value is reported when only one modeller gave a result for a given nuclide or a given pathway.

TABLE LXIa. RANGE OF MAXIMUM INDIVIDUAL DOSE RATES, ABROSIMOV FJORD SOURCES, SCENARIO C

Population group		1			2	3
Location		Yamal	Taymyr	Ob/Yenisey	Military	Kola
Individual peak dose rates (Sv/a)		$2 \times 10^{-10} - 2 \times 10^{-8}$	$2 \times 10^{-10} - 2 \times 10^{-8}$	$2 \times 10^{-10 \ a}$	$3 \times 10^{-9} - 2 \times 10^{-4}$	$2 \times 10^{-11} - 5 \times 10^{-10}$
In years		2040–2080	2040–2080	2080	2050–2730	2040–2080
Range of estimated percentage contributions for each pathway[b]	Ingestion	8–75	7–75	75	–	90–100
	Inhalation	–	–	–	43–100	–
	External	93	93	–	–	–
Range of estimated percentage contributions for individual nuclides[b]		Cs-137 91–98 Sr-90 7	Cs-137 91–98 Sr-90 7	Cs-137 91–98	Pu-239 60–90 Pu-240 30 Am-241 10	Cs-137 90–94 Sr-90 7

TABLE LXIb. RANGE OF MAXIMUM INDIVIDUAL DOSE RATES, TSIVOLKA FJORD, SCENARIO C

Population group		1			2	3
Location		Yamal	Taymyr	Ob/Yenisey	Military	Kola
Individual peak dose rates (Sv/a)		$2 \times 10^{-9} - 2 \times 10^{-7}$	$1 \times 10^{-9} - 2 \times 10^{-7}$	2×10^{-9} [a]	$1 \times 10^{-7} - 3 \times 10^{-3}$	$2 \times 10^{-10} - 5 \times 10^{-9}$
In years		3000–3120	3000–3120	3120	2300–3000	2300–3100
Range of estimated percentage contributions for each pathway[b]	Ingestion	100[c]	100[c]	100	–	48–100
	Inhalation	–	–	–	60	–
	External	–	–	–	–	–
Range of estimated percentage contributions for individual nuclides[a]		Pu-239 69 Pu-240 28	Pu-239 69 Pu-240 28	Pu-239 69	Pu-239 64–66 Pu-240 28 Am-241 8	Pu-239 67–69 Pu-240 28 Am-241 5

[a] Only one result.
[b] A single value is reported when only one modeller gave a result for a given nuclide or a given pathway.
[c] Agreement between the different models.

TABLE LXIc. RANGE OF MAXIMUM INDIVIDUAL DOSE RATES, TECHENIYE FJORD SOURCE, SCENARIO C

Population group		1			2	3
Location		Yamal	Taymyr	Ob/Yenisey	Military	Kola
Individual peak dose rates (Sv/a)		$1 \times 10^{-16} - 3 \times 10^{-11}$	$1 \times 10^{-16} - 3 \times 10^{-11}$	1×10^{-16}	$1 \times 10^{-12} - 3 \times 10^{-12}$	$4 \times 10^{-17} - 6 \times 10^{-13}$
In years		3000–3100	3000–3100	3100	2000–2660	3000–3080
Range of estimated percentage contributions for each pathway[a]	Ingestion	73	73	73	–	48–85
	Inhalation	71	93	–	26–100	–
	External	–	–	–	–	–
Range of estimated percentage contributions for individual nuclides[a]		Ni-59 91–98 Ni-63 2–3	Ni-59 91–98 Ni-63 2–3	Ni-59 91	Co-60 100 Ni-59 57 Ni-63 10	Ni-59 93–98 Ni-63 2–3

120

TABLE LXId. RANGE OF MAXIMUM INDIVIDUAL DOSE RATES, NOVAYA ZEMLYA TROUGH SOURCE, SCENARIO C

Population group		1			2	3
Location		Yamal	Taymyr	Ob/Yenisey	Military	Kola
Individual peak dose rates (Sv/a)		$8 \times 10^{-11} - 4 \times 10^{-9}$	$2 \times 10^{-11} - 4 \times 10^{-9}$	8×10^{-11}	$1 \times 10^{-16} - 2 \times 10^{-6}$	$3 \times 10^{-12} - 8 \times 10^{-11}$
In years		2080–3000	2040–3000	2080	2040–2060	3000–3050
Range of estimated percentage contributions for each pathway[a]	Ingestion	75–100	75–100	75–100	–	38–100
	Inhalation	–	–	–	100	–
	External	–	–	–	44	–
Range of estimated percentage contributions for individual nuclides[a]		Cs-137 97	Cs-137 97	Cs-137 97	Sr-90 71	Pu-239 38–54
		Pu-239 54	Pu-239 54		Cs-137 17	Pu-240 22
		Pu-240 22	Pu-240 22			Am-241 20
		Ni-59 20	Ni-59 20			
		Sr-90 8	Sr-90 9			

[a] A single value is reported when only one modeller gave a result for a given nuclide or a given pathway.

TABLE LXII. SUMMARY OF CRITICAL GROUP DOSES (Sv/a) – SCENARIO C

Population group	1			2	3
Location	Yamal	Taymyr	Ob/Yenisey	Military	Kola
Novaya Zemlya Trough	$8 \times 10^{-11} - 4 \times 10^{-9}$	$2 \times 10^{-11} - 4 \times 10^{-9}$	8×10^{-11}	$1 \times 10^{-14} - 2 \times 10^{-6}$	$3 \times 10^{-12} - 8 \times 10^{-11}$
Techeniye Fjord	$1 \times 10^{-16} - 3 \times 10^{-11}$	$2 \times 10^{-16} - 3 \times 10^{-11}$	1×10^{-16}	$1 \times 10^{-12} - 3 \times 10^{-12}$	$4 \times 10^{-17} - 3 \times 10^{-12}$
Tsivolka Fjord	$1 \times 10^{-9} - 2 \times 10^{-7}$	$2 \times 10^{-9} - 2 \times 10^{-7}$	2×10^{-9}	$1 \times 10^{-7} - 3 \times 10^{-3}$	$2 \times 10^{-10} - 5 \times 10^{-9}$
Stepovoy Fjord	$2 \times 10^{-9} - 3 \times 10^{-8}$	$1 \times 10^{-10} - 3 \times 10^{-8}$	2×10^{-9}	$5 \times 10^{-8} - 7 \times 10^{-8}$	$3 \times 10^{-11} - 6 \times 10^{-10}$
Abrosimov Fjord	$2 \times 10^{-10} - 2 \times 10^{-8}$	$2 \times 10^{-10} - 2 \times 10^{-8}$	2×10^{-10}	$5 \times 10^{-9} - 2 \times 10^{-4}$	$2 \times 10^{-11} - 5 \times 10^{-10}$
Totals (sum of maximum results for each source)	2.5×10^{-7}	2.5×10^{-7}	5.1×10^{-9}	3.2×10^{-3}	6.2×10^{-9}
Totals (running models with all sources)	$4 \times 10^{-9} - 3 \times 10^{-7}$	$4 \times 10^{-9} - 3 \times 10^{-7}$	$4 \times 10^{-9} - 3 \times 10^{-7}$	$2 \times 10^{-7} - 2 \times 10^{-4}$	$6 \times 10^{-10} - 6 \times 10^{-9}$

6.4. SUBMARINE NO. 601

The liquid metal reactors of the submarine No. 601 in Stepovoy Fjord presented some particular difficulties to the modelling group, due to the very long release time under the most likely release scenario. Nevertheless, the results for both scenarios A and C are shown in Tables LXIIIa and LXIIIb.

6.4.1. Scenario A

Table LXIIIa shows that at Yamal, Taymyr, Kola and Ob/Yenisey the maximum dose rates are very low and lie in the range 7×10^{-14} to 6×10^{-10} Sv/a. Ingestion is the dominant pathway. The main contributing nuclides are ^{137}Cs and ^{239}Pu. For the military group, only one value is reported, 8×10^{-12} Sv/a.

6.4.2. Scenario C

Table LXIIIb shows results for scenario C. Results are low, uniformly with a maximum value of 3×10^{-8} Sv/a for groups 1 and 3 and 7×10^{-8} Sv/a for group 2. ^{239}Pu is the dominant nuclide.

6.5. COLLECTIVE DOSE CALCULATIONS

A second aspect of radiological impact that is relevant to an evaluation of the necessity for remedial actions is the collective dose. The collective dose is the sum of the doses from the source in question to all individuals in the exposed population. The collective dose to a given population from a given source represents the radiological consequences to that population from that source.

The exposure pathways to be considered include consumption of fish, crustaceans, molluscs, seaweed and mammals. The marine produce catches and % consumed as used by different modellers in collective dose calculations were discussed in Section 5.2.3.

6.5.1. Truncation times

Long-lived radionuclides may cause exposures over thousands of years, however there are increasing uncertainties in calculating doses to populations beyond a few hundred years, hence, "in decision making, less significance should be attached to collective dose estimates relating to periods beyond 500 years into the future than to those relating to shorter time periods" [70]. Therefore, after considering the postulated releases, it was decided to select truncation dates of 2050 AD (approximately 50 years; the current generation) and 3000 AD (approximately 1000 years). The latter time period covers the times of the peak release rates for normal, gradual corrosion release scenario (Scenario A). All collective dose calculations are based on compartmental models, since the hydrodynamic models are designed to deal with shorter timescales.

TABLE LXIIIa. RANGE OF MAXIMUM INDIVIDUAL DOSE RATES, STEPOVOY FJORD SOURCE, SCENARIO A

Population group				1			2		3	
Location		Yamal		Taymyr		Ob/Yenisey		Military		Kola
Individual peak dose rates (Sv/a)		$9.7 \times 10^{-13} - 2.7 \times 10^{-12}$		$4.6 \times 10^{-14} - 6 \times 10^{-10}$		$1.3 \times 10^{-13} - 4 \times 10^{-11}$		7.6×10^{-12}		$6.9 \times 10^{-14} - 3.2 \times 10^{-13}$
In years		2200–7700		2200–7700		2200–7700		2200–7700		2200–7700
Range of estimated percentage contributions for each pathway[a]	Ingestion	78–100		78–100		78–100		–		48–98
	Inhalation	16		17		17		60		–
	External	–		–		–		–		–
Range of estimated percentage contributions for individual nuclides[a]		Pu-239	45–99	Pu-239	65–99	Pu-239	64–99	Pu-239	99	Pu-239	99
		Cs-137	14–87	Cs-137	90	Cs-137	90			Cs-137	86
		Ni-63	20	Ni-63	35	Ni-63	35			Sr-90	12
		Ni-59	21	Sr-90	10	Sr-90	10				
		Sr-90	9								

TABLE LXIIIb. RANGE OF MAXIMUM INDIVIDUAL DOSE RATES, STEPOVOY FJORD SOURCE, SCENARIO C

Population group				1			2		3	
Location		Yamal		Taymyr		Ob/Yenisey		Military		Kola
Individual peak dose rates (Sv/a)		$1.3 \times 10^{-9} - 3 \times 10^{-8}$		$1 \times 10^{-10} - 3 \times 10^{-8}$		1.3×10^{-9}		$5 \times 10^{-8} - 7 \times 10^{-8}$		$3 \times 10^{-11} - 6 \times 10^{-10}$
In years		3000–3100		3000–3100		3130		3000–3020		3000–3100
Range of estimated percentage contributions for each pathway[a]	Ingestion	100		100		100		–		47.7
	Inhalation	–		–		–		60		–
	External	–		–		–		–		–
Range of estimated percentage contributions for individual nuclides[a]		Pu-239	98	Pu-239	98	Pu-239	98	Pu-239	98	Pu-239	98

[a] A single value is reported when only one modeller gave a result for a given nuclide or a given pathway.

6.5.2. Results

6.5.2.1. Collective dose to 2050 AD

Table LXIV shows the evaluated collective doses to 2050 AD. Results lie in the range 3×10^{-3} to 1×10^{-2} man·Sv which are generally very low. The dominant pathway is fish consumption, with ^{137}Cs the main contributor.

6.5.2.2. Collective dose to 3000 AD

Table LXV shows the collective dose to 3000 AD. Results lie in the range 7×10^{-2} to 1 man·Sv, which are again very low. Fish consumption is the dominating pathway with contributing nuclides ^{137}Cs, ^{239}Pu and ^{90}Sr.

For each time period, the collective doses estimated for nuclides other that ^{14}C and ^{129}I by the various models are similar and small, with all values being below 1 man·Sv.

6.5.2.3. Long-lived nuclides ^{14}C and ^{129}I

The waste inventory contains two radionuclides, ^{14}C and ^{129}I, that are long-lived and mobile. These two radionuclides circulate globally in the aquatic, atmospheric and terrestrial environments. Appropriate global circulation models have been used to calculate collective doses for these two radionuclides [71]. Assuming the entire ^{14}C inventory in the wastes is released around the year 2000 and integrating doses to the world's population 10^{10} individuals) up to the year 3000 yields a collective dose of about 8 man·Sv. The corresponding value for ^{129}I is much lover at 0.0001 man·Sv.

6.5.2.4. Special nuclides

For modelling purposes, the submarine No. 601 is dissimilar to the other sources disposed of in the Kara Sea due to the very long release period (thousands of years) and a number of more exotic radionuclides which must be considered (e.g., ^{79}Se and ^{205}Pb). Some consideration was given to such nuclides in terms of contribution to the collective dose at 3000 AD. The results are shown in Table LXVI. The contribution of these nuclides is very small.

6.5.3. Comments

The total collective dose to the world's population up to the year 3000 from the dumped radioactive waste is approximately 10 man·Sv, about 8 man·Sv arising from ^{14}C and less than 1 man·Sv from other nuclides. In comparison, the annual collective dose to the world's population from natural radionuclides in the ocean is about three orders of magnitude higher [69].

For comparative purposes, the collective dose from ^{14}C over the next 10 000 years is about 37 man·Sv and over all time is about 50 man·Sv. The corresponding values for ^{129}I are 0.002 man·Sv and 0.2 man·Sv. This leads to a total collective dose for all time of considerably less than 100 man·Sv when the contributions from other radionuclides are included. This estimate assumed current environmental conditions and population habits.

TABLE LXIV. COLLECTIVE DOSE TO 2050 AD, NUCLIDES OTHER THAN ^{14}C AND ^{129}I, SCENARIO A

Range in collective dose (man·Sv)		$2.5 \times 10^{-3} - 1 \times 10^{-2}$
Range of estimated percentage contributions for each component of the food chain	Fish	16 – 99
	Crustaceans	6.5 – 64
	Molluscs	20.1
Range of estimated percentage contributions for individual nuclides	Cs-137	71 – 95
	Sr-90	4 – 25
	Ni-59 / Ni-63	10 – 14
	Co-60	4 – 5

TABLE LXV. COLLECTIVE DOSE TO 3000 AD, NUCLIDES OTHER THAN ^{14}C AND ^{129}I, SCENARIO A

Range in collective dose (man·Sv)		$9 \times 10^{-2} - 9.1 \times 10^{-1}$
Range of estimated percentage contributions for each component of the food chain	Fish	22 – 99
	Crustaceans	1 – 7
	Molluscs	1 – 32
Range of estimated percentage contributions for individual nuclides	Cs-137	11 – 60
	Pu-239	22 – 50
	Pu-240	9 – 37
	Sr-90	7 – 46
	Ni-59 / Ni-63	7 – 17

TABLE LXVI. CONTRIBUTION OF SPECIAL NUCLIDES TO COLLECTIVE DOSE (man·Sv) TO 3000 AD, STEPOVOY FJORD, SCENARIO A

Nuclide	IAEA-MEL	KEMA
Ni-63	4.2×10^{-4}	–
Se-79	6.2×10^{-6}	–
Cs-135	2.1×10^{-7}	–
I-129	–	4.9×10^{-7}
Zr-93	1.5×10^{-9}	3.9×10^{-7}
Tc-99	–	5×10^{-8}
Bi-210m	–	1.3×10^{-8}
Sn-121m	2×10^{-9}	–
Eu-152	5.7×10^{-11}	–
Cd-113m	4.5×10^{-11}	–
Pd-107	1.5×10^{-11}	8.6×10^{-13}
Pb-205	7×10^{-13}	–
Eu-154	9×10^{-14}	–
Total	4.3×10^{-4}	9.4×10^{-7}

The majority of the collective dose arises from global circulation of ^{14}C and the dose from this radionuclide will be spread throughout the world's population leading to a vanishingly small level of individual risk. Furthermore, the calculated collective dose is very small in comparison with the annual dose from natural background to the world's population of approximately 22 million man·Sv (assuming the average 2.2 mSv/a for a world population of 10^{10} people); about 120 000 man·Sv of which arises from natural ^{14}C produced in the upper atmosphere.

It is informative to compare the collective doses estimated for the Kara Sea dumping with the collective doses estimated in other assessments of radionuclides in marine waters. EC's project MARINA [68] estimated the radiological impact of radionuclides in northern European marine waters; collective doses to 2500 AD were calculated for the European population for various practices and individual fuel reprocessing sites. Calculations gave values of 4600 man·Sv for discharges from the Sellafield reprocessing plant, and 1600 man·Sv for nuclear weapons test fallout. The radiological impact to the European population of disposals of packaged waste is estimated to give a total collective dose of 50 man·Sv, of which the majority is due to ^{14}C. A review of past dumping of radioactive waste in the north East Atlantic [72] estimated collective doses to the world population after 50 years at 1 man·Sv and after 1000 years at 3000 man·Sv. It is clear that the global contribution from the waste dumped in the Kara Sea is insignificant compared with other sources.

The estimates of collective doses by different modellers both to year 2050 and to 3000 are in good agreement and show the low collective dose delivered to the world population as a result of the dumping in the Kara Sea (Tables LXIV and LXV). The variation in the results is small, but it, as well as the differences in the contributions of the marine pathways can be explained by the differences in some of the necessary input data for the different models. In addition, the spatial domain of the models differ and this may also lead to small differences in collective dose.

6.6. CONCLUSIONS

The main findings of the modelling work are:

(1) through the use of different models with differing spatial and temporal extents, predictions of seawater, sediment and biota concentrations covering the requirements for radiological assessment at local, regional and global scales have been made;

(2) an extensive and detailed model inter-comparison has shown the levels of variations among the different models and this, at near source locations, is typically better than two orders of magnitude. This level of uncertainty on predicted concentrations has been propagated through to final dose estimates;

(3) in all cases, the results from the different models are very low;

(4) at regional and local scales, maximum individual dose rates are generally very low, and are of several orders of magnitude lower than doses due to ^{210}Po from the consumption of marine food stuffs;

(5) maximum individual dose rates for the hypothetical military critical group are higher than those for the other critical groups;

(6) at the global scale, collective dose estimates at 2050 and 3000 AD from all sources in the Kara Sea are very low, and all results are in good agreement.

6.7. OTHER FEATURES

6.7.1. Sensitivity studies — dynamic food chain models

The sensitivity of dose assessment to the method used to model fish contamination was studied for an instantaneous release of 1 TBq of ^{137}Cs in Abrosimov Bay. Three different models for the dynamics of fish contamination in the Barents Sea were used. They can be briefly summarised as:

(1)   the traditional approach based on concentration factors. The concentration in fish is found simply by multiplying the seawater concentration by an empirical concentration factor, CF;

(2)   a dynamic approach, based on a radioecological fish model. Radionuclide intake through contaminated foodstuff, loss of radioactivity due to metabolic processes and dilution due to biomass growth are all accounted for. In addition, seasonal long-distance fish migrations are also considered;

(3)   a traditional approach which accounts for fish migration, by estimating a weighted average of water concentrations, the weights corresponding to the length of time spent by fish in any given area.

The results show that using the traditional approaches, the dynamics of fish contamination follow the water concentrations exactly with no lags. Using the dynamic model however, there is a time delay in the fish concentration. A comparison of the accumulated doses over a 10 year period based on fish consumption shows that the dynamic approach somehow gives higher doses (up to 15% higher) than the traditional approach.

6.7.2. Transport of sediment in sea-ice

One further exceptional transport pathway was also considered, but not explicitly modelled; the transport of sediment-bound radionuclides by sea-ice. The best available information identifies this mechanism as a potential route for re-distribution of the radionuclides, but there is a significant lack of quantitative information necessary for actual calculation. Therefore an evaluation of the magnitude of this particular pathway is addressed by a scoping calculation in order to establish only its potential significance. The results of the scoping calculation are based on a number of assumptions which are further identified below.

A considerable amount of sediment or particulate material is transported from shallow Siberian shelves by the transpolar ice drift towards Fram Strait. Through the melting of ice, the material is released to the marine environment of the Greenland/Iceland Seas. Estimates of the total annual sediment export by sea ice through Fram Strait range from 7 million tons up to 150 million tons [73]. The Laptev Sea is one of the most important source regions and contributes approximately 28% of deep sea sediment accumulation in the European Nordic Seas. The transpolar drift is by far the shortest pathway for contaminant dispersal from the Arctic. The sediment usually accumulates at the surface as patches or as surface layers on the ice. The highest concentrations of sediment can usually be found on the surface of multiyear 'old' ice, with observed values in the central Arctic ranging from 10 mg/L to 56 000 mg/L [74].

6.7.2.1. Estimating the transport from the Kara Sea

The ice export from the Kara Sea to the Arctic Ocean has been estimated from three different locations within the Kara Sea based on the US Naval Research Laboratory's 3-dimensional

model of the Arctic [75]. The three areas considered were two along the Taymyr coastline, and the third on the eastern coastline of Novaya Zemlya and estimated ice transport figures for these areas were $167 \, km^3/a$, $209 \, km^3/a$ and $128 \, km^3/a$. Assumptions were made concerning the sediment load of the ice and the proportion of so loaded ice passing through the Fram Strait. It was then possible to estimate the magnitude of this pathway for the transport of radionuclides from the areas of the dumped wastes firstly to the Arctic Ocean and then via the transpolar drift to Fram Strait.

6.7.2.2. Simple scoping calculation

Assuming a concentration of 60 Bq/kg in sediments (corresponding to a maximum concentration of ^{137}Cs from sources in Abrosimov Fjord, as predicted by the 3-dimensional model 3DMEL); a sediment load in ice of $3 \, kg/m^3$ and an ice flux of $128 \, km^3/a$; ignoring the statement that only 20% of ice is dirty [76]; 4×10^{11} kg of sediment are exported to the Arctic per year, resulting in a transport of 24 TBq/a. Measurements of radionuclide concentrations in sea ice sediment of up to 70 Bq/kg have been reported [77] which would result in a transport of 30 TBq/a.

Extending this calculation, $3 \times 10^3 \, km^3/a$ of ice is transported from the Arctic through Fram Strait, compared to $2 \times 10^5 \, km^3/a$ of seawater. Assuming (unrealistically) that all of such ice had been formed in the Kara Sea, under the conditions described above and that the sediment load was $3 \, kg/m^3$; the radionuclide concentration in sediment was 60 Bq/kg; that all ice so formed drifts to Fram Strait (it is estimated that there is a 70% probability drift to Fram Strait) [78], then 7×10^{12} kg of sediment are transported per year to the Nordic Seas, corresponding to approximately 0.4 PBq/a of ^{137}Cs. Considering the dissolved transport of radionuclides (the corresponding model maximum concentration in sea water is $2100 \, Bq/m^3$), then approximately 410 PBq of ^{137}Cs per year would be transported.

Thus, the transport of radionuclides in sea ice sediment is three orders of magnitude lower than the corresponding dissolved transport of radionuclides. These figures scope the magnitude of this rather unusual transport pathway and show that in this context, it is dominated by the dissolved transport of radionuclides.

6.8. IMPACT ON SPECIES OTHER THAN MAN

Estimates of the incremental radiation exposure arising from radionuclides released from the packaged waste materials dumped into the Kara Sea provide the necessary basis for an assessment of the potential impact of the practice on populations of wild organisms. Dosimetry models that allow the estimation of radiation dose rates to a variety of aquatic organisms, from both internal and external sources, have been developed [79–83] and these have been utilized and, where necessary, extended for the present assessment. It is clearly not possible to make an assessment for every organism native to the Arctic Seas, but it is necessary to include a sufficient number of types both to give a realistic indication of the range of possible incremental exposures and to give explicit recognition to particular species, e.g., seals and whales, typical of this environment. The organisms considered and the geometrical models adopted to represent them are summarized in Table LXVI. Most of the dosimetry models have been used in previous assessments and the relevant references are also given. The model for the whale is new to this assessment and it is sufficiently large in relation to the ranges of α- and β-particles that the corresponding dose rates are $D_\alpha(\infty)$ and $D_\beta(\infty)$ [80]. For γ-radiation, the absorbed fraction has been extrapolated from the data given by Brownell et al [84].

TABLE LXVI. GEOMETRICAL MODELS ADOPTED TO REPRESENT MARINE ORGANISMS

Organism	Mass (kg)	Length of major axes of the representative ellipsoid (cm)	References
Pelagic zooplankton, benthic crustaceans	1.0×10^{-6}	$0.62 \times 0.31 \times 0.16$	[72, 79]
Benthic molluscs	1.0×10^{-3}	$2.5 \times 1.2 \times 0.62$	[72, 79]
Pelagic fish	1.0	$45 \times 8.7 \times 4.9$	[72, 79]
Birds	6.0×10^{-1}	$21 \times 16 \times 11^{a}$	[81, 82]
Seals	58	$180 \times 35 \times 19$	[83]
Whales	1000	$450 \times 87 \times 48$	This study

a   A bird was assumed to be an ellipsoid of solid tissue covered with a layer of feathers. [81, 82]

Because, other factors being equal, the highest concentrations and, therefore, the highest doses are likely to occur in the immediate vicinity of the dumped wastes, the peak concentrations estimated for the release from the wastes dumped in Abrosimov Fjord have been used as the basis for dose rate estimates. The radionuclide concentrations in water (averaged across the Abrosimov Fjord) and sediment (averaged over the area within 100 m of the dumped wastes) are given in Table LXVII for the Case A release scenario. Radionuclide concentrations in the organisms have been estimated using either the new data for concentration factors given in Table LIII or, in default, the data given in IAEA-TRS-247 [8]. The dose rate estimates are summarized in Table LXVIII and the contributions from α-radiation (high LET, linear energy transfer) and β- and γ-radiation (low LET) are given separately. The highest dose rate is predicted for the molluscs from internal α-emitting sources. Because the radionuclide concentrations have been estimated on the basis of whole, soft tissue concentration factors, the α-particle dose rate to particular tissues or organs will have been under-estimated if these show preferential accumulation of plutonium or americium. The highest dose rates from internal β- and γ-emitters are likely to be experienced by fish, birds, seals and whales, and arise from the accumulation of ^{137}Cs. As the greater part of the dose derives from γ-radiation, the problem of non-uniform ^{137}Cs distribution in tissues and organs is of lesser significance. The dose rate from external sources is expected to be greatest for the benthic crustaceans and molluscs and reflects the significance of the ^{60}Co contamination of the underlying sediment. Previous assessments of exposures in contaminated areas have assumed a quality factor of 20 for α-radiation and presented total doses from all radiations in terms of the Sv unit although it was recognized that this approach was open to question [79]. If comparisons, where possible, are made on this basis, the maximum total dose rates estimated for the releases to Abrosimov Fjord are within the range of expected natural background and of the same order as the dose rates predicted for the waste dumped in the deep northeast Atlantic Ocean [79].

It is also relevant to consider the dose rate to marine organisms that might colonize the exposed surfaces of the dumped packages. The maximum dose rate at the surface of the caisson containing the fuel from the icebreaker has been estimated to be 0.56 μGy/h [85]. From extensive previous experience with disposal to the northeast Atlantic dump site, the dose rates at the surface of packages of low level waste, limited on the basis of handling and transport requirements, can range up to more than 2 mGy/h (although 5% exceeded this value) [72]. It is reasonable to assume, in the absence of specific information, that considerations of worker exposure would also have limited surface dose rates for the packages dumped in the Kara Sea to similar values.

TABLE LXVII. PREDICTED PEAK RADIONUCLIDE CONCENTRATIONS IN WATER, SEDIMENT AND ORGANISMS USED TO ESTIMATE DOSE RATES

Nuclide	Water[a] (Bq/L)	Sediment[a] (Bq/kg)	Zooplankton (Bq/kg)	Molluscs (Bq/kg)	Fish (Bq/kg)	Birds (Bq/kg)	Seals (Bq/kg)	Whales (Bq/kg)
Ni-59	5.8×10^{-3}	18	5.8	12	0.58	4.1	–	–
Ni-63	8.7×10^{-3}	27	8.7	17	0.87	6.1	–	–
Co-60	9.3×10^{-3}	29	19	2.9	9.3	–	–	–
Sr-90	1.9	5.3	1.9	1.9	7.6	–	1.9	1.9
Cs-137	2.1	59	64	2.1	210	210	210	210
Pu-239	8.2×10^{-3}	24	8.2	25	0.33	0.82	2.5×10^{-2}	$2.5 \ 10^{-2}$
Pu-240	4.1×10^{-3}	11	4.1	12	0.16	0.41	1.2×10^{-2}	1.2×10^{-2}
Pu-241	8.3×10^{-4}	2.3	0.83	2.5	3.3×10^{-2}	8.3×10^{-2}	2.5×10^{-3}	2.5×10^{-3}
Am-241	5.4×10^{-4}	4.1	1.1	0.22	2.7×10^{-2}	–	–	–

[a] The concentrations of radionuclides have been obtained from 3-D hydrodynamic modelling. The concentrations in water are averages across the whole of Abrosimov Fjord and the concentrations in sediment are averages within 100 m of the waste packages.

TABLE LXVIII. ESTIMATED MAXIMUM DOSE RATES TO MARINE ORGANISMS FROM RADIONUCLIDES RELEASED FROM WASTES DUMPED IN ABROSIMOV FJORD

Organism	Alpha radiation, internal (μGy/h)	Beta and gamma radiation	
		Internal (μGy/h)	External (μGy/h)
Pelagic zooplankton	4.1×10^{-2}	8.0×10^{-3}	1.5×10^{-3}
Benthic crustaceans	4.1×10^{-2}	8.0×10^{-3}	1.7×10^{-2}
Benthic molluscs	1.1×10^{-1}	1.6×10^{-3}	1.6×10^{-2}
Pelagic fish	1.6×10^{-3}	3.8×10^{-2}	6.2×10^{-4}
Birds	3.7×10^{-3}	2.9×10^{-2}	7.1×10^{-3}
Seals	1.1×10^{-4}	4.7×10^{-2}	5.5×10^{-3}
Whales	1.1×10^{-4}	8.6×10^{-2}	7.0×10^{-5}

Note: The times to peak environmental concentrations are different for different radionuclides; simple summing of the estimated peak dose rates from each radionuclide will, therefore, result in an over estimate of the maximum radiation exposure.

There has been a number of reviews of the available information concerning the effects of ionizing radiation on aquatic organisms [79, 81, 86] and these have concluded that dose rates less than 0.4 mGy/h to the maximally exposed members of populations of aquatic organisms are very unlikely to have any detrimental effects on the attributes such as morbidity, mortality, fertility, fecundity and mutation rate that may influence the maintenance of healthy populations. The dose rates predicted in this assessment are very much smaller than 0.4 mGy/h (by at least two orders of magnitude, even allowing for the likely increased biological effectiveness of high LET radiation), and can affect only a very small proportion of the populations. It may be reasonably concluded, therefore, that the dumping practice can have no detrimental impact on populations of aquatic organisms.

7. FINAL CONCLUSIONS

The reliability of the final results for use in the assessment and decision-making process was of prime concern to the modelling group and as a result, considerable effort was made to assess the uncertainties in the results and to explore some of the sensitivities to model structure and parameter values used. As a result, the final dose estimates are presented in the form of ranges, indicating the variability in predictions arising from the different models.

Models should be fit for the purpose for which they were designed, and in this case the modelling group were faced with a single purpose: the assessment of the dominating transfer mechanisms to the contaminant dispersal and ultimately the risks to human health and the environment. However, this assessment was required to be carried out at quite different time and spatial scales. As a result different models were required; compartmental models for long time, far field predictions and hydrodynamic models for near-field and short time scale predictions (including some of the bays).

Model development and testing were made difficult by the lack of detailed information concerning the Arctic region, particularly the Kara Sea. Thus modellers used judgement and knowledge to develop new and extend existing models. This lack of knowledge contributes to the uncertainty concerning the final results.

In the first instance, the models were compared in an extensive model inter-comparison, including a small scale sensitivity study on some aspects of the sedimentary sub-models.

The results from the model inter-comparison demonstrated the levels of variation among the different models and how this varied depending on the radionuclide characteristics and the distance from source. Near source, the level of variation was typically less than two orders of magnitude. One significant source of variation was the sedimentary parameters which were subsequently studied separately. This analysis showed that although important, the sediment modelling was not the dominant source of variability.

Following the model inter-comparison which had modelled concentrations in seawater and sediment, further development work was carried out in preparing the description of the assessment situations, specifically the definition of the populations at risk and also quantifying their habits. Again lack of site-specific information meant that the groups identified should only be considered hypothetical although realistic, in the quantification of population habits, the conservative principle was obeyed thus ensuring that any dose estimates should provide limits. Three critical population groups were identified, including a hypothetical military critical group based on Novaya Zemlya itself.

The actual assessment calculations were made for three separate release scenarios with the information provided on nuclide composition, quantities and rate of release by the Source Term working group. In all cases, the maximum individual dose rates were calculated taking into account ingestion, inhalation and external exposure. In all cases, the estimated dose rates resulting from the different models are very low and are several orders of magnitude lower than doses to ^{210}Po from the consumption of marine foodstuffs. The maximum individual dose rates for the hypothetical military critical group are higher than those for the other critical groups.

For one scenario, the 'best estimate discharge' scenario, collective doses were also calculated, but truncated at 2050 AD and 3000 AD. Separate calculations were made of the collective

dose due to ^{129}I and ^{14}C. At the global scale, the collective dose estimates at 2050 and 3000 AD from all sources in the Kara Sea are very low, and all results are in good agreement.

Doses to marine organisms were also considered and a geometrical model was for the first time applied to whales. The estimated maxiumum total dose rates to wild organisms from predicted releases in Abrosimov Fjord were within the range of expected doses from natural background. Therefore, dumping is not considered to have radiological impact on populations of aquatic organisms.

Finally, a scoping calculation of the possible impact of contaminated sediment in sea ice was also made under a number of simplifying assumptions. The transport of contaminated sediment in ice from the solid waste dumped in the Kara Sea is of low global significance when compared with the transport in water.

APPENDIX I

COMPLETE RESULTS FROM BENCHMARK CALCULATIONS

TABLE I-Ia. ^{137}Cs CONCENTRATIONS IN WATER AT KARA SEA ENDPOINTS, SOURCE LOCATION: ABRASIMOV FJORD, INSTANTANEOUS RELEASE 1 TBq

Kara Sea		Risø	MAFF	Typhoon	KEMA	Nihon U.	MEL box
72°N 65°E	water (Bq/m^3)	4.8×10^{-2}	8.2×10^{-3}	1.1×10^{-2}	7.3×10^{-3}	3.7×10^{-2}	2.9×10^{-2}
	time to max (a)	0.9	2	1	1.1	1	2
78°N 92°E	water (Bq/m^3)	5.2×10^{-4}	4.6×10^{-3}	$<4 \times 10^{-3}$	2.6×10^{-3}	3.0×10^{-4}	3.9×10^{-3}
	time to max (a)	2.5	3	3.5	1.7	5	4
76°N 76°E	water (Bq/m^3)	5.2×10^{-4}	4.6×10^{-3}	7.5×10^{-3}	2.6×10^{-3}	1×10^{-3}	3.9×10^{-3}
	time to max (a)	2.5	3	2.5	1.7	2	4

TABLE I-Ib. ^{137}Cs CONCENTRATIONS IN WATER AT KARA SEA ENDPOINTS, CONTINUOUS RELEASE 1 TBq PER YEAR FOR 10 YEARS, SOURCE LOCATION: ABRASIMOV FJORD

Kara Sea		Risø	MAFF	Typhoon	KEMA	Nihon U.	MEL regional	MEL box	USN
72°N 65°E	water (Bq/m^3)	2×10^{-1}	3.5×10^{-2}	4.4×10^{-2}	1.5×10^{-3}	1.8×10^{-1}	8.2×10^{-2}	1×10^{-1}	3.5×10^{-1}
	time to max (a)		10	10	10	10	6	10	
78°N 92°E	water (Bq/m^3)	3.6×10^{-2}	2.3×10^{-2}	$<3 \times 10^{-2}$	5.9×10^{-4}	2×10^{-3}	3.8×10^{-2}	2.6×10^{-2}	3.3×10^{-2}
	time to max (a)		10	11	10	10	6	11	
76°N 76°E	water (Bq/m^3)	3.6×10^{-2}	2.3×10^{-2}	3.5×10^{-2}	5.9×10^{-4}	7.5×10^{-3}	6.1×10^{-2}	2.6×10^{-2}	8.6×10^{-2}
	time to max (a)		10	10.5	10	10	6	11	

TABLE I-Ic. ^{137}Cs CONCENTRATIONS IN SEDIMENT AT KARA SEA ENDPOINTS, SOURCE LOCATION: ABRASIMOV FJORD, INSTANTANEOUS RELEASE 1 TBq

Kara Sea		Risø	MAFF	Typhoon	KEMA	Nihon U.	MEL box
72°N 65°E	sediment (Bq/kg dw)	6.3×10^{-3}	1.2×10^{-3}	1.7×10^{-4}	6.2×10^{-4}	1.8×10^{-4}	3.7×10^{-3}
	(Bq/m^2)	4.7×10^{-1}	1.8×10^{-1}	6.3×10^{-3}	3.1×10^{-2}	7.3×10^{-2}	2.6×10^{-1}
	time to max (a)	12	8.5	8	2.2	1	8
78°N 62°E	sediment (Bq/kg dw)	1.3×10^{-4}	8.3×10^{-4}	$<1.2 \times 10^{-4}$	2.3×10^{-4}	1.4×10^{-6}	9.8×10^{-4}
	(Bq/m^2)	9.7×10^{-3}	1.2×10^{-1}	$<4.4 \times 10^{-3}$	1.7×10^{-2}	6×10^{-4}	6.9×10^{-2}
	time to max (a)	16	9.75	13	2.6	5	14
76°N 76°E	sediment (Bq/kg dw)	1.3×10^{-4}	8.3×10^{-4}	1.5×10^{-4}	2.3×10^{-4}	7.1×10^{-6}	9.8×10^{-4}
	(Bq/m^2)	9.7×10^{-3}	1.2×10^{-1}	5.6×10^{-3}	1.7×10^{-2}	2.9×10^{-3}	6.9×10^{-2}
	time to max (a)	16	9.75	11	2.6	2	14

TABLE I-Id. ^{137}Cs CONCENTRATIONS IN SEDIMENT AT KARA SEA ENDPOINTS, CONTINUOUS RELEASE 1 TBq PER YEAR FOR 10 YEARS, SOURCE LOCATION: ABRASIMOV FJORD

Kara Sea		Risø	MAFF	Typhoon	KEMA	Nihon U.	MEL regional	MEL box
72°N 65°E	sediment (Bq/kg dw)	6.2×10^{-2}	1.2×10^{-2}	$<1.2 \times 10^{-3}$	1.5×10^{-4}	8.3×10^{-4}	4.9×10^{-3}	3.5×10^{-2}
	(Bq/m^2)	4.6	1.8	$<4.4 \times 10^{-2}$	7.5×10^{-3}	3.4×10^{-1}	1.8×10^{-1}	2.5
	time to max (a)		15	14	10	10	6	14
78°N 62°E	sediment (Bq/kg dw)	1.3×10^{-3}	8.3×10^{-3}	$<1.2 \times 10^{-3}$	5.9×10^{-5}	9.6×10^{-6}	1.2×10^{-3}	9.7×10^{-3}
	(Bq/m^2)	9.7×10^{-2}	1.2	6.4×10^{-2}	2.9×10^{-3}	3.9×10^{-3}	2.9×10^{-2}	6.8×10^{-1}
	time to max (a)		16	20	10	10	6	19
76°N 76°E	sediment (Bq/kg dw)	1.3×10^{-3}	8.3×10^{-3}	1.4×10^{-3}	5.9×10^{-4}	4.4×10^{-5}	2.9×10^{-3}	9.7×10^{-3}
	(Bq/m^2)	9.7×10^{-2}	1.2	5.2×10^{-2}	2.9×10^{-2}	1.8×10^{-2}	1.9×10^{-1}	6.8×10^{-1}
	time to max (a)		16	17	10	10	6	19

TABLE I-IIa. ^{137}Cs CONCENTRATIONS IN WATER AT KARA SEA ENDPOINTS, SOURCE LOCATION: NOVAYA ZEMLYA TROUGH INSTANTANEOUS RELEASE 1 TBq

Kara Sea		Risø	MAFF	Typhoon	KEMA	Nihon U.	MEL box
72°N 65°E	water (Bq/m^3)	1.5×10^{-1}	9.1×10^{-3}	7.1×10^{-3}	1.1×10^{-2}	2.1×10^{-2}	3.5×10^{-3}
	time to max (a)	10	1.3	1.2	initial	5	3
78°N 92°E	water (Bq/m^3)	3×10^{-4}	4.9×10^{-3}	$<3.2 \times 10^{-3}$	3.1×10^{-3}	2.2×10^{-4}	1×10^{-3}
	time to max (a)	10	2.25	>5	0.9	5	5
76°N 76°E	water (Bq/m^3)	3×10^{-4}	4.9×10^{-3}	5×10^{-3}	3.1×10^{-3}	9.1×10^{-4}	1×10^{-3}
	time to max (a)	10	2.25	3	0.9	5	5

TABLE I-IIb. ^{137}Cs CONCENTRATIONS IN WATER AT KARA SEA ENDPOINTS, CONTINUOUS RELEASE 1 TBq PER YEAR FOR 10 YEARS, SOURCE LOCATION: NOVAYA ZEMLYA TROUGH

Kara Sea		Risø	MAFF	Typhoon	KEMA	Nihon U.	MEL regional	MEL box
72°N 65°E	water (Bq/m^3)	1.5×10^{-1}	3.6×10^{-2}	4×10^{-2}	1.5×10^{-3}	1.6×10^{-1}	2.4×10^{-3}	2×10^{-2}
	time to max (a)	10	10	10	10	10	6	10
78°N 92°E	water (Bq/m^3)	2.5×10^{-3}	2.4×10^{-2}	$<2.5 \times 10^{-2}$	6×10^{-4}	1.6×10^{-3}	1.5×10^{-3}	7.7×10^{-3}
	time to max (a)	10	10	11	10	10	6	11
76°N 76°E	water (Bq/m^3)	2.5×10^{-3}	2.4×10^{-2}	3.3×10^{-2}	6×10^{-4}	6.5×10^{-3}	2.4×10^{-3}	7.7×10^{-3}
	time to max (a)	10	10	10.5	10	10	6	11

TABLE I-IIc. ^{137}Cs CONCENTRATIONS IN SEDIMENT AT KARA SEA ENDPOINTS, SOURCE LOCATIONS: NOVAYA ZEMLYA TROUGH, INSTANTANEOUS RELEASE 1TBq

Kara Sea		Risø	MAFF	Typhoon	KEMA	Nihon U.	MEL box
72°N 65°E	sediment (Bq/kg dw)	6.1×10^{-3}	1.3×10^{-3}	1.6×10^{-4}	6.9×10^{-4}	9.6×10^{-5}	7.5×10^{-4}
	(Bq/m^2)	4.6×10^{-1}	1.9×10^{-1}	5.9×10^{-3}	3.5×10^{-3}	3.9×10^{-2}	5.3×10^{-2}
	time to max (a)	20	8	11	1.4	5	11
78°N 92°E	sediment (Bq/kg dw)	1.3×10^{-4}	8.3×10^{-4}	$<1.2 \times 10^{-4}$	2.5×10^{-4}	1.1×10^{-6}	3.1×10^{-4}
	(Bq/m^2)	9.7×10^{-3}	1.2×10^{-1}	$<4.4 \times 10^{-3}$	1.3×10^{-3}	4.5×10^{-4}	2.2×10^{-2}
	time to max (a)	20	9.25	17	2.2	5	12
76°N 76°E	sediment (Bq/kg dw)	1.3×10^{-4}	8.3×10^{-4}	1.4×10^{-4}	2.5×10^{-4}	5.6×10^{-6}	3.1×10^{-4}
	(Bq/m^2)	9.7×10^{-3}	1.2×10^{-1}	5.2×10^{-3}	1.3×10^{-3}	2.3×10^{-3}	2.2×10^{-2}
	time to max (a)	20	9.25	15	0.9	5	12

TABLE I-IId. ^{137}Cs CONCENTRATIONS IN SEDIMENT AT KARA SEA ENDPOINTS, CONTINUOUS RELEASE 1 TBq PER YEAR FOR 10 YEARS, SOURCE LOCATION: NOVAYA ZEMLYA TROUGH

Kara Sea		Risø	MAFF	Typhoon	KEMA	Nihon U.	MEL regional	MEL box
72°N 65°E	sediment (Bq/kg dw)	5.8×10^{-2}	1.2×10^{-2}	1.6×10^{-3}	1.6×10^{-4}	7.3×10^{-4}	1.4×10^{-4}	7.3×10^{-3}
	(Bq/m^2)	4.4	1.8	5.9×10^{-2}	8×10^{-3}	3×10^{-1}	6.1×10^{-3}	5.1×10^{-1}
	time to max (a)	20	15	17	10	10	6	17
78°N 92°E	sediment (Bq/kg dw)	1.2×10^{-3}	8.3×10^{-3}	$<1 \times 10^{-3}$	6×10^{-5}	7.8×10^{-6}	4.9×10^{-5}	3×10^{-3}
	(Bq/m^2)	9×10^{-2}	1.2	$<3.7 \times 10^{-2}$	3×10^{-3}	3.2×10^{-3}	1.1×10^{-3}	2.1×10^{-1}
	time to max (a)	30	16	>22	10	14	6	21
76°N 76°E	sediment (Bq/kg dw)	1.2×10^{-3}	8.3×10^{-3}	1.4×10^{-3}	6.0×10^{-5}	1.6×10^{-5}	1.1×10^{-4}	3×10^{-3}
	(Bq/m^2)	9×10^{-2}	1.2	5.2×10^{-2}	3×10^{-3}	6.7×10^{-3}	7.5×10^{-3}	2.1×10^{-1}
	time to max (a)	30	16	20	10	5	6	21

TABLE I-IIIa. ^{137}Cs CONCENTRATIONS IN WATER AT BARENTS SEA ENDPOINTS, SOURCE LOCATION: ABRASIMOV FJORD, INSTANTANEOUS RELEASE 1TBq

Barents Sea		Risø	MAFF	Typhoon	KEMA	Nihon U.	MEL box
72°N 45°E	water (Bq/m³)	2.8×10^{-4}	3.6×10^{-3}	1.4×10^{-5}	3×10^{-4}	2.2×10^{-3}	1.6×10^{-4}
	time to max (a)	2.6	2	6	2.6	2	3
79°N 58°E	water (Bq/m³)	2.1×10^{-4}	1.1×10^{-4}	1×10^{-4}	3×10^{-4}	3.6×10^{-4}	1.1×10^{-4}
	time to max (a)	4.5	5	4	2.6	10	8
76°N 20°E	water (Bq/m³)	2.1×10^{-4}	1.1×10^{-4}	1.6×10^{-5}		3.7×10^{-4}	4.9×10^{-5}
	time to max (a)	4.5	5	5.5		10	8

TABLE I-IIIb. ^{137}Cs CONCENTRATIONS IN WATER AT BARENTS SEA ENDPOINTS, CONTINUOUS RELEASE 1 TBq PER YEAR FOR 10 YEARS, SOURCE LOCATION: ABRASIMOV FJORD

Barents Sea		Risø	MAFF	Typhoon	KEMA	Nihon U.	MEL regional	MEL box	USN
72°N 45°E	water (Bq/m³)	1.8×10^{-3}	1.6×10^{-2}	1.1×10^{-4}	3.9×10^{-4}	1.8×10^{-2}	7.2×10^{-4}	9.9×10^{-4}	2.1×10^{-3}
	time to max (a)	10	10	13	10	10	6	10	10
79°N 58°E	water (Bq/m³)	1.5×10^{-3}	8.6×10^{-4}	8.3×10^{-4}	8.7×10^{-5}	2.7×10^{-3}	4.2×10^{-5}	7.2×10^{-4}	2.2×10^{-3}
	time to max (a)		12	12	10	10	6	10	
76°N 20°E	water (Bq/m³)	1.5×10^{-3}	8.6×10^{-4}	1.3×10^{-4}		2.6×10^{-3}	7.2×10^{-4}	4.5×10^{-4}	3.4×10^{-3}
	time to max (a)		12	12		20	6	14	

TABLE I-IIIc. ^{137}Cs CONCENTRATIONS IN SEDIMENT AT BARENTS SEA ENDPOINTS, SOURCE LOCATION: ABRASIMOV FJORD, INSTANTANEOUS RELEASE 1 TBq

Barents Sea		Risø	MAFF	Typhoon	KEMA	Nihon U.	MEL box
72°N 45°E	sediment (Bq/kg dw)	6.4×10^{-5}	5.9×10^{-4}	1×10^{-6}	2×10^{-5}	1.6×10^{-5}	1.8×10^{-5}
	(Bq/m²)	4.8×10^{-3}	8.5×10^{-2}	3.7×10^{-5}	1×10^{-3}	6.5×10^{-3}	1.3×10^{-3}
	time to max (a)	16	9	17	3.5	2	13
79°N 58°E	sediment (Bq/kg dw)	3.2×10^{-5}	3.6×10^{-5}	5.7×10^{-6}	2×10^{-5}	1.6×10^{-6}	1.5×10^{-5}
	(Bq/m²)	2.4×10^{-3}	5.2×10^{-3}	2.1×10^{-4}	1×10^{-3}	6.6×10^{-4}	1.1×10^{-3}
	time to max (a)	21	18	17	3.6	5	28
76°N 20°E	sediment (Bq/kg dw)	3.2×10^{-5}	3.6×10^{-5}	8×10^{-7}		1.6×10^{-6}	1.2×10^{-5}
	(Bq/m²)	2.4×10^{-3}	5.2×10^{-3}	2.9×10^{-5}		6.8×10^{-4}	8.7×10^{-4}
	time to max (a)	21	18	18		10	28

TABLE I-IIId. ^{137}Cs CONCENTRATIONS IN SEDIMENT AT BARENTS SEA ENDPOINTS, CONTINUOUS RELEASE 1 TBq PER YEAR FOR 10 YEARS, SOURCE LOCATION: ABRASIMOV FJORD

Barents Sea		Risø	MAFF	Typhoon	KEMA	Nihon U.	MEL regional	MEL box
72°N 45°E	sediment (Bq/kg dw)	6.2×10^{-4}	5.7×10^{-3}	1×10^{-5}	8.7×10^{-2}	9.8×10^{-5}		1.8×10^{-4}
	(Bq/m²)	4.6×10^{-2}	8.2×10^{-1}	3.7×10^{-4}	4.3	4×10^{-2}		1.3×10^{-2}
	time to max (a)	20	16	24	10	10		19
79°N 58°E	sediment (Bq/kg dw)	3.1×10^{-4}	3.6×10^{-4}	5.6×10^{-5}	8.7×10^{-2}	1.2×10^{-5}	7.4×10^{-6}	1.5×10^{-4}
	(Bq/m²)	2.3×10^{-2}	5.2×10^{-2}	2.1×10^{-3}	4.3	4.8×10^{-3}	3.7×10^{-4}	1.1×10^{-2}
	time to max (a)	30	24	23	10	10	6	19
76°N 20°E	sediment (Bq/kg dw)	3.1×10^{-4}	3.6×10^{-4}	7.9×10^{-6}		1.1×10^{-5}		1.2×10^{-4}
	(Bq/m²)	2.3×10^{-2}	5.2×10^{-2}	2.9×10^{-4}		4.7×10^{-3}		8.7×10^{-3}
	time to max (a)	30	24	24		20		33

TABLE I-IVa. ^{137}Cs CONCENTRATIONS IN WATER AT BARENTS SEA ENDPOINTS, SOURCE LOCATION: NOVAYA ZEMLYA TROUGH, INSTANTANEOUS RELEASE 1 TBq

Barents Sea		Risø	MAFF	Typhoon	KEMA	Nihon U.	MEL box
72°N 45°E	water (Bq/m^3)	1.4×10^{-4}	4×10^{-3}	1.1×10^{-5}	3.3×10^{-4}	1.5×10^{-3}	6.7×10^{-5}
	time to max (a)	10	1.4	7	2	5	4
79°N 58°E	water (Bq/m^3)	1.4×10^{-4}	1.1×10^{-4}	8.3×10^{-5}	3.3×10^{-4}	3.2×10^{-4}	5.6×10^{-5}
	time to max (a)	10	4.5	5.5	2	10	9
76°N 20°E	water (Bq/m^3)	1.4×10^{-4}	1.1×10^{-4}	1.3×10^{-5}		2.9×10^{-4}	4.6×10^{-5}
	time to max (a)	10	4.5	7		10	9

TABLE I-IVb. ^{137}Cs CONCENTRATIONS IN WATER AT BARENTS SEA ENDPOINTS, CONTINUOUS RELEASE 1 TBq PER YEAR FOR 10 YEARS, SOURCE LOCATION: NOVAYA ZEMLYA TROUGH

Barents Sea		Risø	MAFF	Typhoon	KEMA	Nihon U.	MEL box	MEL region
72°N 45°E	water (Bq/m^3)	1.3×10^{-3}	1.7×10^{-2}	1×10^{-4}	8.8×10^{-5}	1.2×10^{-2}	4.6×10^{-4}	
	time to max (a)	10	10	14	10	10	11	
79°N 58°E	water (Bq/m^3)	1.1×10^{-3}	8.7×10^{-4}	7.6×10^{-4}	8.9×10^{-5}	2.4×10^{-3}	4.4×10^{4}	1.8×10^{-6}
	time to max (a)	20	11	13	10	10	15	6
76°N 20°E	water (Bq/m^3)	1.1×10^{-3}	8.7×10^{-4}	1.2×10^{-4}		2.5×10^{-3}	4.2×10^{-4}	
	time to max (a)	20	11	13		20	15	

TABLE I-IVc. ^{137}Cs CONCENTRATIONS IN SEDIMENT AT BARENTS SEA ENDPOINTS, SOURCE LOCATION: NOVAYA ZEMLYA TROUGH INSTANTANEOUS RELEASE 1 TBq

Barents Sea		Risø	MAFF	Typhoon	KEMA	Nihon U.	MEL box	MEL region
72°N 45°E	sediment (Bq/kg dw)	6×10^{-4}	5.8×10^{-3}	1×10^{-5}	3×10^{-5}	6.6×10^{-5}	8.8×10^{-5}	
	(Bq/m^2)	4.5×10^{-2}	8.4×10^{-1}	3.7×10^{-4}	1.5×10^{-3}	2.7×10^{-2}	6.2×10^{-3}	
	time to max (a)	30	15	26	10	10	21	
79°N 58°E	sediment (Bq/kg dw)	3.1×10^{-4}	3.7×10^{-4}	5.6×10^{-5}	8.9×10^{-5}	8.1×10^{-6}	1.0×10^{-4}	3.2×10^{-7}
	(Bq/m^2)	2.3×10^{-2}	5.3×10^{-2}	2.1×10^{-3}	4.5×10^{-3}	3.3×10^{-3}	7.2×10^{-3}	1.6×10^{-5}
	time to max (a)	30	12	25	10	10	21	6
76°N 20°E	sediment (Bq/kg dw)	3.1×10^{-4}	3.7×10^{-4}	7.8×10^{-6}		1.1×10^{-5}	1.2×10^{-4}	
	(Bq/m^2)	2.3×10^{-2}	5.3×10^{-2}	2.9×10^{-4}		4.6×10^{-3}	8.5×10^{-3}	
	time to max (a)	30	23	27		20	35	

TABLE I-IVd. ^{137}Cs CONCENTRATIONS IN SEDIMENT AT BARENTS SEA ENDPOINTS, CONTINUOUS RELEASE 1 TBq PER YEAR FOR 10 YEARS, SOURCE LOCATION: NOVAYA ZEMLYA TROUGH

Barents Sea		Risø	MAFF	Typhoon	KEMA	Nihon U.	MEL box
72°N 45°E	sediment (Bq/kg dw)	6.1×10^{-5}	6×10^{-4}	1×10^{-6}	8.9×10^{-6}	9.3×10^{-6}	9×10^{-6}
	(Bq/m^2)	4.6×10^{-3}	8.7×10^{-2}	3.7×10^{-5}	4.5×10^{-4}	3.8×10^{-3}	6.3×10^{-4}
	time to max (a)	20	8.5	21	2	5	15
79°N 58°E	sediment (Bq/kg dw)	3×10^{-5}	3.7×10^{-5}	5.5×10^{-6}	3×10^{-5}	1.2×10^{-6}	1.1×10^{-5}
	(Bq/m^2)	2.3×10^{-3}	5.4×10^{-3}	2×10^{-4}	1.5×10^{-3}	5×10^{-4}	7.2×10^{-4}
	time to max (a)	30	18	20	2	10	30
76°N 20°E	sediment (Bq/kg dw)	3×10^{-5}	3.7×10^{-5}	7.7×10^{-7}		1.3×10^{-6}	1.2×10^{-5}
	(Bq/m^2)	2.3×10^{-3}	5.4×10^{-3}	2.8×10^{-5}		5.3×10^{-4}	8.6×10^{-4}
	time to max (a)	30	18	21		10	30

TABLE I-Va. ^{239}Pu CONCENTRATIONS IN WATER AT KARA SEA ENDPOINTS, SOURCE LOCATION: ABRASIMOV FJORD, INSTANTANEOUS RELEASE 1 TBq

Kara Sea		Risø	MAFF	Typhoon	KEMA	Nihon U.	MEL box
72°N 65°E	water (Bq/m^3)	2×10^{-2}	4×10^{-3}	1.1×10^{-2}	2.6×10^{-3}	2.5×10^{-1}	1.4×10^{-2}
	time to max (a)	0.4	3.5	1	2.5	0.2	1
78°N 92°E	water (Bq/m^3)	8.8×10^{-5}	1.8×10^{-3}	$<3 \times 10^{-4}$	7.1×10^{-4}	1.9×10^{-7}	5.1×10^{-4}
	time to max (a)	0.9	5.2	>3	6.5	2	1
76°N 76°E	water (Bq/m^3)	8.8×10^{-5}	1.8×10^{-3}	7×10^{-3}	7.1×10^{-4}	5.5×10^{-6}	5.1×10^{-4}
	time to max (a)	0.9	5.2	2.5	6.5	0.5	1

TABLE I-Vb. ^{239}Pu CONCENTRATIONS IN WATER AT KARA SEA ENDPOINTS, CONTINUOUS RELEASE 1 TBq PER YEAR FOR 10 YEARS SOURCE LOCATION: ABRASIMOV FJORD

Kara Sea		Risø	MAFF	Typhoon	KEMA	Nihon U.	MEL box	MEL regional
72°N 65°E	water (Bq/m^3)	2.5×10^{-2}	2.6×10^{-2}	3×10^{-2}	1.2×10^{-2}	1.9×10^{-3}	1.8×10^{-2}	4.9×10^{-2}
	time to max (a)		11	10	10	10	10	6
78°N 92°E	water (Bq/m^3)	$>2.1 \times 10^{-4}$	1.3×10^{-2}	$<1.9 \times 10^{-2}$	3.2×10^{-3}	5.8×10^{-7}	1×10^{-2}	2.3×10^{-2}
	time to max (a)	>10	12	>10.5	12.1	10	10	6
76°N 76°E	water (Bq/m^3)	$>2.1 \times 10^{-4}$	1.3×10^{-2}	2.5×10^{-2}	3.2×10^{-3}	9.8×10^{-6}	1×10^{-2}	3.6×10^{-2}
	time to max (a)	10	12	10.5	12.5	10	1	6

TABLE I-Vc. ^{239}Pu CONCENTRATIONS IN SEDIMENT AT KARA SEA ENDPOINTS, SOURCE LOCATION: ABRASIMOV FJORD, INSTANTANEOUS RELEASE 1 TBq

Kara Sea		Risø	MAFF	Typhoon	KEMA	Nihon U.	MEL box
72°N 65°E	sediment (Bq/kg dw)	2.3×10^{-2}	4×10^{-3}	2.8×10^{-3}	1.6×10^{-2}	5.4×10^{-4}	1.6×10^{-3}
	(Bq/m^2)	1.7	5.8×10^{-1}	1×10^{-1}	8×10^{-1}	2.2×10^{-1}	1.1×10^{-1}
	time to max (a)	6	900	18	4	0.2	9
78°N 92°E	sediment (Bq/kg dw)	2×10^{-4}	2.9×10^{-3}	$<2 \times 10^{-3}$	5.2×10^{-3}	4.6×10^{-8}	9.7×10^{-5}
	(Bq/m^2)	1.5×10^{-2}	4.2×10^{-1}	$<7.4 \times 10^{-2}$	2.6×10^{-1}	1.9×10^{-5}	6.8×10^{-3}
	time to max (a)	9	1000	>24	7.6	2	17
76°N 76°E	sediment (Bq/kg dw)	2×10^{-4}	2.9×10^{-3}	2.2×10^{-3}	5.2×10^{-3}	1.7×10^{-6}	9.7×10^{-5}
	(Bq/m^2)	1.5×10^{-2}	4.2×10^{-1}	8.1×10^{-2}	2.6×10^{-1}	6.9×10^{-4}	6.8×10^{-3}
	time to max (a)	9	1000	21	7.6	0.5	17

TABLE I-Vd. ^{239}Pu CONCENTRATIONS IN SEDIMENT AT KARA SEA ENDPOINTS, CONTINUOUS RELEASE 1 TBq PER YEAR FOR 10 YEARS, SOURCE LOCATION: ABRASIMOV FJORD

Kara Sea		Risø	MAFF	Typhoon	KEMA	Nihon U.	MEL box	MEL regional
72°N 65°E	sediment (Bq/kg dw)	$>2.1 \times 10^{-1}$	4×10^{-2}	2.8×10^{-2}	6.7×10^{-2}	3.6×10^{-4}	1.6×10^{-1}	9.6×10^{-2}
	(Bq/m^2)	$>1.6 \times 10^{-1}$	5.8	1	3.3	1.5×10^{-1}	11.4	4.8
	time to max (a)	>10	910	>23	11	10	17	6
78°N 92°E	sediment (Bq/kg dw)		2.9×10^{-2}	$<2 \times 10^{-2}$	2.4×10^{-2}	1.4×10^{-7}	1×10^{-2}	2.5×10^{-2}
	(Bq/m^2)		4.2	$<7.4 \times 10^{-1}$	1.2	5.8×10^{-5}	0.7	1.2
	time to max (a)		100	>28	13.6	10	20	6
76°N 76°E	sediment (Bq/kg dw)		2.9×10^{-2}	2.4×10^{-2}	2.4×10^{-2}	1.8×10^{-6}	1×10^{-2}	5.7×10^{-2}
	(Bq/m^2)		4.2	2.1	1.2	7.3×10^{-4}	0.7	2.8
	time to max (a)		1000	25	13.6	10	20	6

TABLE I-VIa. ^{239}Pu CONCENTRATIONS IN WATER AT KARA SEA ENDPOINTS, SOURCE LOCATION: NOVAYA ZEMLYA TROUGH, INSTANTANEOUS RELEASE 1 TBq

Kara Sea		Risø	MAFF	Typhoon	KEMA	Nihon U.	MEL box
72°N 65°E	water (Bq/m³)	1.2×10^{-3}	5.4×10^{-3}	7.2×10^{-3}	1.1×10^{-2}	1.1×10^{-4}	1.5×10^{-3}
	time to max (a)	10	1.7	1.2	initial	0.2	1
78°N 92°E	water (Bq/m³)	1.5×10^{-5}	2.2×10^{-3}	$<2.9 \times 10^{-3}$	9.6×10^{-4}	1.2×10^{-8}	1.6×10^{-4}
	time to max (a)		3.5	>4.5	3.2	2	1
76°N 76°E	water (Bq/m³)	1.5×10^{-5}	2.2×10^{-3}	5×10^{-3}	9.6×10^{-4}	2.9×10^{-7}	1.6×10^{-4}
	time to max (a)	10	3.5	2.8	3.2	1	1

TABLE I-VIb. ^{239}Pu CONCENTRATIONS IN WATER AT KARA SEA ENDPOINTS, CONTINUOUS RELEASE 1 TBq PER YEAR FOR 10 YEARS, SOURCE LOCATION: NOVAYA ZEMLYA TROUGH

Kara Sea		MAFF	Typhoon	KEMA	Nihon U.	MEL box	MEL regional
72°N 65°E	water (Bq/m³)	2.7×10^{-2}	4.1×10^{-2}	1.4×10^{-2}	1.8×10^{-4}	3.9×10^{-2}	1.4×10^{-3}
	time to max (a)	10	10	10	10	10	6
78°N 92°E	water (Bq/m³)	1.4×10^{-2}	$<2.5 \times 10^{-2}$	4.2×10^{-3}	4.7×10^{-8}	5.1×10^{-3}	9.2×10^{-4}
	time to max (a)	11	11	10	10	10	6
76°N 76°E	water (Bq/m³)	1.4×10^{-2}	3.3×10^{-2}	4.2×10^{-3}	8.8×10^{-7}	5.1×10^{-3}	1.4×10^{-3}
	time to max (a)	11	10.5	10	10	10	6

TABLE I-VIc. ^{239}Pu CONCENTRATIONS IN SEDIMENT AT KARA SEA ENDPOINBTS, SOURCE LOCATION: NOVAYA ZEMLYA TROUGH, INSTANTANEOUS RELEASE 1 TBq

Kara Sea		Risø	MAFF	Typhoon	KEMA	Nihon U.	MEL box
72°N 65°E	sediment (Bq/kg dw)	3.8×10^{-2}	4.1×10^{-3}	4×10^{-3}	2.9×10^{-2}	1.4×10^{-5}	3.8×10^{-3}
	(Bq/m²)	2.8	5.9×10^{-1}	1.5×10^{-1}	1.4	5.9×10^{-3}	2.7×10^{-1}
	time to max (a)	10	820	23	1.4	0.5	>50
78°N 92°E	sediment (Bq/kg dw)	3.3×10^{-4}	2.9×10^{-3}	$<3 \times 10^{-3}$	6.8×10^{-3}	2.9×10^{-9}	4.8×10^{-4}
	(Bq/m²)	2.5×10^{-2}	4.3×10^{-1}	$<1.1 \times 10^{-1}$	3.4×10^{-1}	1.2×10^{-6}	3.4×10^{-2}
	time to max (a)	10	1000	>29	4.5	2	>50
76°N 76°E	sediment (Bq/kg dw)	3.3×10^{-4}	2.9×10^{-3}	3.5×10^{-3}	6.8×10^{-3}	6.4×10^{-8}	4.8×10^{-4}
	(Bq/m²)	2.5×10^{-2}	4.3×10^{-1}	1.3×10^{-1}	3.4×10^{-1}	2.6×10^{-5}	3.4×10^{-2}
	time to max (a)	10	1000	25	4.5	1	>50

TABLE I-VId. ^{239}Pu CONCENTRATIONS IN SEDIMENT AT KARA SEA ENDPOINTS, CONTINUOUS RELEASE 1 TBq PER YEAR FOR 10 YEARS, SOURCE LOCATION: NOVAYA ZEMLYA TROUGH

Kara Sea		MAFF	Typhoon	KEMA	Nihon U.	MEL box	MEL regional
72°N 65°E	sediment (Bq/kg dw)	4.1×10^{-2}	4.2×10^{-2}	8.7×10^{-2}	2.3×10^{-5}	3.5×10^{-2}	2.8×10^{-3}
	(Bq/m²)	5.9	1.5	4.3	9.3×10^{-3}	2.5	1.4×10^{-1}
	time to max (a)	830	29	10	10	>50	6
78°N 92°E	sediment (Bqkg dw)	2.9×10^{-2}	$<3.1 \times 10^{-2}$	3×10^{-2}	1.1×10^{-8}	4.7×10^{-3}	9.9×10^{-4}
	(Bq/m²)	4.3	<1.1	1.5	4.7×10^{-6}	3.3×10^{-1}	4.9×10^{-2}
	time to max (a)	1000	>36	13.1	10	>50	6
76°N 76°E	sediment (Bq/kg dw)	2.9×10^{-2}	3.6×10^{-2}	3×10^{-2}	1.5×10^{-7}	4.7×10^{-3}	2.2×10^{-3}
	(Bq/m²)	4.3	1.3	1.5	6.3×10^{-5}	3.3×10^{-1}	1.1×10^{-1}
	time to max (a)	1000	33	13.1	10	>50	6

TABLE I-VIIa. ^{239}Pu CONCENTRATIONS IN WATER AT BARENTS SEA ENDPOINTS, SOURCE LOCATION: ABRASIMOV FJORD, INSTANTANEOUS RELEASE 1 TBq

Barents Sea		Risø	MAFF	Typhoon	KEMA	Nihon U.	MEL box
72°N 45°E	water (Bq/m^3)	5.8×10^{-5}	1.8×10^{-3}	1×10^{-5}	1.2×10^{-4}	3.6×10^{-5}	4.1×10^{-5}
	time to max (a)	1.1	3.5	5	6.8	0.5	1
79°N 58°E	water (Bq/m^3)	2.7×10^{-5}	6.4×10^{-5}	7.8×10^{-5}	1.2×10^{-4}	1.1×10^{-7}	2.4×10^{-5}
	time to max (a)	2.1	7.8	4	5.8	1	3
76°N 20°E	water (Bq/m^3)	2.7×10^{-5}	6.4×10^{-5}	1.5×10^{-5}		7.7×10^{-10}	6.3×10^{-6}
	time to max (a)	2.1	7.8	5		2	3

TABLE I-VIIb. ^{239}Pu CONCENTRATIONS IN WATER AT BARENTS SEA ENDPOINTS, CONTINUOUS RELEASE 1 TBq PER YEAR FOR 10 YEARS, SOURCE LOCATION: ABRASIMOV FJORD

Barents Sea		Risø	MAFF	Typhoon	KEMA	Nihon U.	MEL box	MEL regional
72°N 45°E	water (Bq/m^3)	1.7×10^{-4}	1.2×10^{-2}	8.3×10^{-5}	5.4×10^{-4}	5.9×10^{-5}	1.3×10^{-3}	
	time to max (a)		1000	36	13	10	10	
79°N 58°E	water (Bq/m^3)	$>1.2 \times 10^{-4}$	5.6×10^{-4}	6×10^{-4}	5.4×10^{-4}	3.4×10^{-7}	8.6×10^{-4}	2.5×10^{-5}
	time to max (a)	>10	14	11	12	10	10	6
76°N 20°E	water (Bq/m^3)	$>1.2 \times 10^{-4}$	5.6×10^{-4}	9.3×10^{-5}		3.8×10^{-9}	4.2×10^{-4}	
	time to max (a)	>10	14	12		10	10	

TABLE I-VIIc. ^{239}Pu CONCENTRATIONS IN SEDIMENT AT BARENTS SEA ENDPOINTS, SOURCE LOCATION: ABRASIMOV FJORD, INSTANTANEOUS RELEASE 1 TBq

Barents Sea		Risø	MAFF	Typhoon	KEMA	Nihon U.	MEL box
72°N 45°E	sediment (Bq/kg dw)	1.3×10^{-4}	9×10^{-4}	1.8×10^{-5}	8.2×10^{-4}	5.4×10^{-6}	6.8×10^{-5}
	(Bq/m^2)	9.7×10^{-3}	3.1×10^{-1}	6.7×10^{-4}	4.1×10^{-2}	2.2×10^{-3}	4.8×10^{-3}
	time to max (a)	9	1000	29	7	0.5	>50
79°N 58°E	sediment (Bq/kg dw)	4.8×10^{-5}	6.2×10^{-4}	1.1×10^{-4}	8.2×10^{-4}	9.3×10^{-9}	5.3×10^{-5}
	(Bq/m^2)	3.6×10^{-3}	9×10^{-2}	4.1×10^{-3}	4.1×10^{-2}	3.8×10^{-6}	3.8×10^{-3}
	time to max (a)	14	1000	29	7	1	>50
76°N 20°E	sediment (Bq/kg dw)	4.8×10^{-5}	6.2×10^{-4}	1.5×10^{-5}		8.1×10^{-11}	3.8×10^{-5}
	(Bq/m^2)	3.6×10^{-3}	9×10^{-2}	5.5×10^{-4}		3.3×10^{-8}	2.7×10^{-3}
	time to max (a)	14	1000	30		1	>50

TABLE I-VIId. ^{239}Pu CONCENTRATIONS IN SEDIMENT AT BARENTS SEA ENDPOINTS, CONTINUOUS RELEASE 1 TBq PER YEAR FOR 10 YEARS, SOURCE LOCATION: ABRASIMOV FJORD

Barents Sea		MAFF	Typhoon	KEMA	Nihon U.	MEL box	MEL regional
72°N 45°E	sediment (Bq/kg dw)	2.1×10^{-2}	1.8×10^{-4}	3.7×10^{-3}	5.9×10^{-6}	6.6×10^{-3}	
	(Bq/m^2)	3.1	6.7×10^{-3}	1.8×10^{-2}	2.4×10^{-3}	4.6×10^{-1}	
	time to max (a)	1000	36	13	10	>50	
79°N 58°E	sediment (Bq/kg dw)	6.2×10^{-3}	1.1×10^{-3}	3.7×10^{-3}	1.4×10^{-9}	5.1×10^{-3}	1.5×10^{-4}
	(Bq/m^2)	9×10^{-1}	4.1×10^{-2}	1.8×10^{-2}	5.9×10^{-6}	3.7×10^{-1}	7.5×10^{-3}
	time to max (a)	1000	36	13	10	>50	6
76°N 20°E	sediment (Bq/kg dw)	6.2×10^{-3}	1.5×10^{-4}		3.4×10^{-10}	3.6×10^{3}	
	(Bq/m^2)	9×10^{-1}	5.6×10^{-3}		1.4×10^{-7}	2.5×10^{-1}	
	time to max (a)	1000	14		10	>50	

TABLE I-VIIIa. ^{239}Pu CONCENTRATIONS IN WATER AT BARENTS SEA ENDPOINTS, SOURCE LOCATION: NOVAYA ZEMLYA TROUGH, INSTANTANEOUS RELEASE 1 TBq

Barents Sea		Risø	MAFF	Typhoon	KEMA	Nihon U.	MEL box
72°N 45°E	water (Bq/m³)	1.2×10^{-5}	2.4×10^{-3}	1.1×10^{-5}	1.7×10^{-4}	2.1×10^{-7}	2.8×10^{-5}
	time to max (a)	10	1.7	7	2.3	1	2
79°N 58°E	water (Bq/m³)	1.2×10^{-5}	6.9×10^{-5}	8.6×10^{-5}	1.7×10^{-4}	3.7×10^{-9}	2.1×10^{-5}
	time to max (a)	10	5.7	6.2	2.3	2	6
76°N 20°E	water (Bq/m³)	1.2×10^{-5}	6.9×10^{-5}	1.3×10^{-5}		7.1×10^{-12}	1.4×10^{-5}
	time to max (a)	10	5.7	7		5	6

TABLE I-VIIIb. ^{239}Pu CONCENTRATIONS IN WATER AT BARENTS SEA ENDPOINTS, CONTINUOUS RELEASE 1 TBq PER YEAR FOR 10 YEARS, SOURCE LOCATION NOVAYA ZEMLYA TROUGH

Barents Sea		MAFF	Typhoon	KEMA	Nihon U.	MEL box	MEL regional
72°N 45°E	water (Bq/m³)	1.2×10^{-2}	1.1×10^{-4}	7.1×10^{-4}	8.8×10^{-7}	1.2×10^{-4}	
	time to max (a)	10	14	10.2	10	10	
79°N 58°E	water (Bq/m³)	5.9×10^{-4}	7.9×10^{-4}	7.1×10^{-4}	2×10^{-8}	1.2×10^{-4}	1.1×10^{-6}
	time to max (a)	12	13	10.3	10	12	6
76°N 20°E	water (Bq/m³)	5.9×10^{-4}	1.2×10^{-4}		4.8×10^{-11}	1.2×10^{-4}	
	time to max (a)	12	14		10	12	

TABLE I-VIIIc. ^{239}Pu CONCENTRATIONS IN SEDIMENT AT BARENTS SEA ENDPOINTS, SOURCE LOCATION: NOVAYA ZEMLYA TROUGH, INSTANTANEOUS RELEASE 1 TBq

Barents Sea		Risø	MAFF	Typhoon	KEMA	Nihon U.	MEL box
72°N 45°E	sediment (Bq/kg dw)	2.1×10^{-4}	2.2×10^{-3}	2.7×10^{-5}	1.2×10^{-3}	2.5×10^{-8}	7.8×10^{-5}
	(Bq/m²)	1.6×10^{-2}	3.2×10^{-1}	1×10^{-2}	6×10^{-2}	1×10^{-5}	5.5×10^{-3}
	time to max (a)	20	1000	34	4	1	>50
79°N 58°E	sediment (Bq/kg dw)	8.3×10^{-5}	6.3×10^{-4}	1.6×10^{-4}	1.2×10^{-3}	3.2×10^{-10}	1.2×10^{-4}
	(Bq/m²)	6.2×10^{-3}	9.1×10^{-2}	5.9×10^{-3}	6×10^{-2}	1.3×10^{-7}	8.7×10^{-3}
	time to max (a)	20	1000	33	4	1	>50
76°N 20°E	sediment (Bq/kg dw)	8.3×10^{-5}	6.3×10^{-4}	2.1×10^{-5}		6.9×10^{-13}	1.6×10^{-4}
	(Bq/m²)	6.2×10^{-3}	9.1×10^{-2}	7.8×10^{-4}		2.8×10^{-10}	1.1×10^{-2}
	time to max (a)	20	1000	37		2	>50

TABLE I-VIIId. ^{239}Pu CONCENTRATIONS IN SEDIMENT AT BARENTS SEA ENDPOINTS, CONTINUOUS RELEASE 1 TBq PER YEAR FOR 10 YEARS, SOURCE LOCATION: NOVAYA ZEMLYA TROUGH

Barents Sea		MAFF	Typhoon	KEMA	Nihon U.	MEL box	MEL regional
72°N 45°E	sediment (Bq/kg dw)	2.2×10^{-2}	2.8×10^{-4}	4.7×10^{-3}	8.4×10^{-8}	7.3×10^{-4}	
	(Bq/m²)	3.2	1×10^{-2}	2.3×10^{-1}	3.4×10^{-5}	5.1×10^{-2}	
	time to max (a)	1000	39	13	10	>50	
79°N 58°E	sediment (Bq/kg dw)	6.3×10^{-3}	1.7×10^{-3}	4.7×10^{-3}	9.1×10^{-10}	1.1×10^{-3}	6.5×10^{-6}
	(Bq/m²)	9.1×10^{-1}	6.3×10^{-2}	2.3×10^{-1}	3.7×10^{-7}	7.9×10^{-2}	3.2×10^{-4}
	time to max (a)	1000	42	10.3	10	>50	6
76°N 20°E	sediment (Bq/kg dw)	6.3×10^{-3}	2.2×10^{-4}		4.7×10^{-12}	1.4×10^{-3}	
	(Bq/m²)	9.1×10^{-1}	8.1×10^{-3}		1.9×10^{-9}	9.6×10^{-2}	
	time to max (a)	1000	42		10	>50	

TABLE I-IXa. ^{60}Co CONCENTRATIONS IN WATER AT KARA SEA ENDPOINTS, SOURCE LOCATION: ABRASIMOV FJORD, INSTANTANEOUS RELEASE 1 TBq

Kara Sea		Risø	MAFF	Typhoon	KEMA	MEL box	Nihon U.
72°N 65°E	water (Bq/m^3)	4.9×10^{-3}	2.7×10^{-3}	9.2×10^{-3}	2×10^{-3}	6.4×10^{-3}	1.1×10^{-5}
	time to max (a)	1	2.7	0.6	0.5	1	0.1
78°N 92°E	water (Bq/m^3)	4×10^{-5}	9.9×10^{-4}	$<1.9 \times 10^{-3}$	2.6×10^{-4}	2.8×10^{-4}	2.9×10^{-11}
	time to max (a)	1	4.2	>2	4	1	1
76°N 76°E	water (Bq/m^3)	4×10^{-5}	9.9×10^{-4}	5.6×10^{-3}	2.6×10^{-4}	2.8×10^{-4}	1.9×10^{-9}
	time to max (a)	1	4.2	1.3	4	1	0.5

TABLE I-IXb. ^{60}Co CONCENTRATIONS IN WATER AT KARA SEA ENDPOINTS, CONTINUOUS RELEASE 1 TBq PER YEAR FOR 10 YEARS, SOURCE LOCATION: ABRASIMOV FJORD

Kara Sea		Risø	MAFF	Typhoon	KEMA	MEL box	Nihon U.
72°N 65°E	water (Bq/m^3)	1.3×10^{-2}	1.4×10^{-2}	2×10^{-2}	1.9×10^{-4}	6.5×10^{-2}	2.3×10^{-6}
	time to max (a)		10	9.5	10	10	10
78°N 92°E	water (Bq/m^3)	7.4×10^{-5}	6.1×10^{-3}	$<9.2 \times 10^{-3}$	4.1×10^{-5}	3.8×10^{-3}	3.7×10^{-11}
	time to max (a)	10	11	>10	10	10	10
76°N 76°E	water (Bq/m^3)	7.4×10^{-5}	6.1×10^{-3}	1.4×10^{-2}	4.1×10^{-5}	3.8×10^{-3}	1.2×10^{-9}
	time to max (a)	10	11	10	10	10	10

TABLE I-IXc. ^{60}Co CONCENTRACTIONS IN SEDIMENT AT KARA SEA ENDPOINTS, SOURCE LOCATION: ABRASIMOV FJORD, INSTANTANEOUS RELEASE 1 TBq

Kara Sea		Risø	MAFF	Typhoon	KEMA	MEL box	Nihon U.
72°N 65°E	sediment (Bq/kg dw)	1.7×10^{-2}	1.1×10^{-3}	1.7×10^{-3}	1.2×10^{-2}	1.4×10^{-2}	2.1×10^{-4}
	(Bq/m^2)	1.3	1.6×10^{-1}	6.3×10^{-2}	6×10^{-1}	1	8.7×10^{-2}
	time to max (a)	2	6.7	3.3	2.5	2	0.1
78°N 92°E	sediment (Bq/kg dw)	8.6×10^{-5}	5.8×10^{-4}	$<6.8 \times 10^{-4}$	2.6×10^{-3}	4.3×10^{-4}	7.1×10^{-10}
	(Bq/m^2)	6.5×10^{-3}	8.4×10^{-2}	$<2.5 \times 10^{-2}$	1.3×10^{-1}	3×10^{-2}	2.9×10^{-7}
	time to max (a)	2	8.2	>6	5	2	1
76°N 76°E	sediment (Bq/kg dw)	8.6×10^{-5}	5.8×10^{-4}	1.2×10^{-3}	2.6×10^{-3}	4.3×10^{-4}	4.2×10^{-8}
	(Bq/m^2)	6.5×10^{-3}	8.4×10^{-2}	4.4×10^{-2}	1.3×10^{-1}	3×10^{-2}	1.7×10^{-5}
	time to max (a)	2	8.2	4.7	5	2	0.2

TABLE I-IXd. ^{60}Co CONCENTRATIONS IN SEDIMENT AT KARA SEA ENDPOINTS, CONTINUOUS RELEASE 1 TBq PER YEAR FOR 10 YEARS, SOURCE LOCATION: ABRASIMOV FJORD

Kara Sea		Risø	MAFF	Typhoon	KEMA	MEL box	Nihon U.
72°N 65°E	sediment (Bq/kg dw)	1.1×10^{-1}	9×10^{-3}	1.3×10^{-2}	1.6×10^{-3}	7.7×10^{-1}	4.9×10^{-5}
	(Bq/m^2)	8.2	1.3	4.8×10^{-1}	8×10^{-2}	54	2×10^{-2}
	time to max (a)	10	13	11	10	10	10
78°N 92°E	sediment (Bq/kg dw)	6.2×10^{-4}	4.9×10^{-3}	$<5.7 \times 10^{-3}$	4.1×10^{-4}	2.8×10^{-2}	9.1×10^{-10}
	(Bq/m^2)	4.6×10^{-2}	7.1×10^{-1}	$<2.1 \times 10^{-1}$	2.1×10^{-2}	2	3.7×10^{-7}
	time to max (a)	12	15	17	10.1	10	10
76°N 76°E	sediment (Bq/kg dw)	6.2×10^{-4}	4.9×10^{-3}	9.4×10^{-3}	4.1×10^{-4}	2.8×10^{-2}	2.5×10^{-8}
	(Bq/m^2)	4.6×10^{-2}	7.2×10^{-1}	3.5×10^{-1}	2.1×10^{-2}	2	1×10^{-5}
	time to max (a)	12	15	12	10.1	10	10

TABLE I-Xa. ^{60}Co CONCENTRATIONS IN WATER AT KARA SEA ENDPOINTS, SOURCE LOCATION: NOVAYA ZEMLYA TROUGH, INSTANTANEOUS RELEASE 1 TBq

Kara Sea		Risø	MAFF	Typhoon	KEMA	MEL box	Nihon U.
72°N 65°E	water (Bq/m^3)	4.8×10^{-3}	4.3×10^{-3}	6.3×10^{-3}	1.1×10^{-2}	1×10^{-3}	2.3×10^{-7}
	time to max (a)	1	1.4	0.9	initial	1	0.1
78°N 92°E	water (Bq/m^3)	2.2×10^{-5}	1.4×10^{-3}	$<1.7 \times 10^{-3}$	6.1×10^{-4}	7.2×10^{-5}	3.2×10^{-13}
	time to max (a)	1.5	2.7	>3	0.2	1	1
76°N 76°E	water (Bq/m^3)	2.2×10^{-5}	1.4×10^{-3}	4×10^{-3}	6.1×10^{-4}	7.2×10^{-5}	2.2×10^{-11}
	time to max (a)	1.5	2.7	2	0.2	1	0.5

TABLE I-Xb. ^{60}Co CONCENTRATIONS IN WATER AT KARA SEA ENDPOINTS, CONTINUOUS RELEASE 1 TBq PER YEAR FOR 10 YEARS, SOURCE LOCATION: NOVAYA ZEMLYA TROUGH

Kara Sea		Risø	MAFF	Typhoon	KEMA	MEL box	Nihon U.
72°N 65°E	water (Bq/m^3)	1.7×10^{-2}	1.8×10^{-2}	2.5×10^{-2}	2.9×10^{-4}	1.7×10^{-2}	3.8×10^{-8}
	time to max (a)	10	10	10	10	10	10
78°N 92°E	water (Bq/m^3)	9.1×10^{-5}	7.7×10^{-3}	$<1.1 \times 10^{-2}$	6.6×10^{-5}	1.6×10^{-3}	4×10^{-13}
	time to max (a)	10	10	>10	10	10	10
76°N 76°E	water (Bq/m^3)	9.1×10^{-5}	7.7×10^{-3}	1.8×10^{-2}	6.6×10^{-5}	1.6×10^{-3}	1.4×10^{-11}
	time to max (a)	10	10	10	10	10	10

TABLE I-Xc. ^{60}Co CONCENTRATIONS IN SEDIMENT AT KARA SEA ENDPOINTS, SOURCE LOCATION: NOVAYA ZEMLYA TROUGH, INSTANTANEOUS RELEASE 1 TBq

Kara Sea		Risø	MAFF	Typhoon	KEMA	MEL box	Nihon U.
72°N 65°E	sediment (Bq/kg dw)	1.6×10^{-2}	1.4×10^{-3}	1.8×10^{-3}	3×10^{-2}	1.8×10^{-3}	1.5×10^{-6}
	(Bq/m^2)	1.2	2.1×10^{-1}	6.7×10^{-2}	1.5	1.3×10^{-1}	6.1×10^{-4}
	time to max (a)	4	5	5	1.1	2	0.1
78°N 92°E	sediment (Bq/kg dw)	8.4×10^{-5}	7.7×10^{-4}	$<7.6 \times 10^{-4}$	4.8×10^{-3}	1.5×10^{-4}	7.9×10^{-12}
	(Bq/m^2)	6.3×10^{-3}	1.1×10^{-1}	$<2.8 \times 10^{-2}$	2.4×10^{-1}	1.1×10^{-2}	3.2×10^{-9}
	time to max (a)	5	6.7	>8	3	3	1
76°N 76°E	sediment (Bq/kg dw)	8.4×10^{-5}	7.7×10^{-4}	1.3×10^{-3}	4.8×10^{-3}	1.5×10^{-4}	4.4×10^{-10}
	(Bq/m^2)	6.3×10^{-3}	1.1×10^{-1}	4.8×10^{-2}	2.4×10^{-1}	1.1×10^{-2}	1.8×10^{-7}
	time to max (a)	5	6.7	6.5	3	3	0.2

TABLE I-Xd. ^{60}Co CONCENTRATIONS IN SEDIMENT AT KARA SEA ENDPOINTS, CONTINUOUS RELEASE 1 TBq PER YEAR FOR 10 YEARS, SOURCE LOCATION: NOVAYA ZEMLYA TROUGH

Kara Sea		Risø	MAFF	Typhoon	KEMA	MEL box	Nihon U.
72°N 65°E	sediment (Bq/kg dw)	1.3×10^{-1}	1.2×10^{-2}	1.5×10^{-2}	2.4×10^{-3}	1.2×10^{-1}	3.2×10^{-7}
	(Bq/m^2)	9.7	1.7	5.6×10^{-1}	1.2×10^{-1}	8.5	1.3×10^{-4}
	time to max (a)	11	12	12	10	10	10
78°N 92°E	sediment (Bq/kg dw)	7×10^{-4}	6.4×10^{-3}	$<6.7 \times 10^{-3}$	6.7×10^{-4}	1.1×10^{-2}	9.8×10^{-12}
	(Bq/m^2)	5.2×10^{-2}	9.2×10^{-1}	$<2.5 \times 10^{-1}$	3.3×10^{-2}	8×10^{-1}	4×10^{-9}
	time to max (a)	12	13	>14	10	10	10
76°N 76°E	sediment (Bq/kg dw)	7×10^{-4}	6.4×10^{-3}	1.1×10^{-2}	6.7×10^{-4}	1.1×10^{-2}	2.7×10^{-10}
	(Bq/m^2)	5.2×10^{-2}	9.2×10^{-1}	4.1×10^{-1}	3.3×10^{-2}	8×10^{-1}	1.1×10^{-7}
	time to max (a)	12	13	13	10	10	10

TABLE I-XIa. ^{60}Co CONCENTRATIONS IN WATER AT BARENTS SEA ENDPOINTS, SOURCE LOCATION: ABRASIMOV FJORD, INSTANTANEOUS RELEASE 1 TBq

Barents Sea		Risø	MAFF	Typhoon	KEMA	MEL box	Nihon U.
72°N 45°E	water (Bq/m³)	3.4×10^{-5}	1.2×10^{-3}	5×10^{-6}	5.3×10^{-5}	2.4×10^{-5}	4×10^{-8}
	time to max (a)	1	2.7	3.8	3.6	1	0.2
79°N 58°E	water (Bq/m³)	1.2×10^{-4}	2.7×10^{-5}	4.6×10^{-5}	5.3×10^{-5}	1.4×10^{-5}	1.7×10^{-12}
	time to max (a)	2	5.5	2.8	3.6	2	0.5
76°N 20°E	water (Bq/m³)	1.2×10^{-4}	2.7×10^{-5}	5.7×10^{-6}		2.5×10^{-6}	2.9×10^{-16}
	time to max (a)	2	5.5	4		2	0.5

TABLE I-XIb. ^{60}Co CONCENTRATIONS IN WATER AT BARENTS SEA ENDPOINTS, CONTINUOUS RELEASE 1 TBq PER YEAR FOR 10 YEARS, SOURCE LOCATION: ABRASIMOV FJORD

Barents Sea		Risø	MAFF	Typhoon	KEMA	MEL box	Nihon U.
72°N 45°E	water (Bq/m³)	6.8×10^{-5}	6.3×10^{-3}	3.1×10^{-5}	7.7×10^{-6}	5.6×10^{-4}	1.9×10^{-8}
	time to max (a)	10	10	11	10	10	10
79°N 58°E	water (Bq/m³)	3.7×10^{-5}	2×10^{-4}	2.7×10^{-4}	7.7×10^{-6}	3.4×10^{-4}	8.5×10^{-13}
	time to max (a)	10	12	11	10	10	10
76°N 20°E	water (Bq/m³)	3.7×10^{-5}	2×10^{-4}	3.6×10^{-5}		1.1×10^{-4}	1.7×10^{-16}
	time to max (a)	10	12	11		11	10

TABLE I-XIc. ^{60}Co CONCENTRATIONS IN SEDIMENT AT BARENTS SEA ENDPOINTS, SOURCE LOCATION: ABRASIMOV FJORD, INSTANTANEOUS RELEASE 1 TBq

Barents Sea		Risø	MAFF	Typhoon	KEMA	MEL box	Nihon U.
72°N 45°E	sediment (Bq/kg dw)	5.7×10^{-5}	5.1×10^{-4}	3.8×10^{-6}	4.7×10^{-4}	2.7×10^{-5}	3.4×10^{-7}
	(Bq/m²)	4.3×10^{-2}	7.4×10^{-2}	1.4×10^{-4}	2.3×10^{-2}	1.9×10^{-3}	1.4×10^{-4}
	time to max (a)	3	6.7	8.3	4.5	3	0.2
79°N 58°E	sediment (Bq/kg dw)	1.4×10^{-5}	1.7×10^{-5}	2.9×10^{-5}	4.7×10^{-4}	1.6×10^{-5}	6.1×10^{-12}
	(Bq/m²)	1×10^{-3}	2.5×10^{-3}	1.1×10^{-3}	2.3×10^{-2}	1.2×10^{-3}	2.5×10^{-9}
	time to max (a)	4	10	7	4.5	6	0.5
76°N 20°E	sediment (Bq/kg dw)	1.4×10^{-5}	1.7×10^{-5}	3×10^{-6}		4.7×10^{-6}	3.7×10^{-15}
	(Bq/m²)	1×10^{-3}	2.5×10^{-3}	1.1×10^{-4}		3.3×10^{-4}	1.5×10^{-12}
	time to max (a)	4	10	8		6	0.5

TABLE I-XId. ^{60}Co CONCENTRATIONS IN SEDIMENT AT BARENTS SEA ENDPOINTS, CONTINUOUS RELEASE 1 TBq PER YEAR FOR 10 YEARS, SOURCE LOCATION: ABRASIMOV FJORD

Barents Sea		Risø	MAFF	Typhoon	KEMA	MEL box	Nihon U.
72°N 45°E	sediment (Bq/kg dw)	4.1×10^{-4}	4.3×10^{-3}	3.1×10^{-5}	6.9×10^{-5}	2×10^{-3}	1.3×10^{-7}
	(Bq/m²)	3.1×10^{-2}	6.2×10^{-1}	1.1×10^{-3}	3.4×10^{-3}	1.4×10^{-1}	5.5×10^{-5}
	time to max (a)	12	13	15	10	10	10
79°N 58°E	sediment (Bq/kg dw)	1.1×10^{-4}	1.5×10^{-4}	2.5×10^{-4}	6.9×10^{-5}	1.2×10^{-3}	2.9×10^{-12}
	(Bq/m²)	8.2×10^{-3}	2.2×10^{-2}	9.2×10^{-3}	3.4×10^{-3}	8.7×10^{-2}	1.2×10^{-9}
	time to max (a)	12	16	14	10	12	10
76°N 20°E	sediment (Bq/kg dw)	1.1×10^{-4}	1.5×10^{-4}	2.7×10^{-5}		3.8×10^{-4}	2.2×10^{-15}
	(Bq/m²)	8.2×10^{-3}	2.2×10^{-2}	1×10^{-3}		2.7×10^{-2}	8.9×10^{-13}
	time to max (a)	12	16	15		12	10

TABLE I-XIIa. ^{60}Co CONCENTRATIONS IN WATER AT BARENTS SEA ENDPOINTS, SOURCE LOCATION: NOVAYA ZEMLYA TROUGH, INSTANTANEOUS RELEASE 1 TBq

Barents Sea		Risø	MAFF	Typhoon	KEMA	MEL box	Nihon U.
72°N 45°E	water (Bq/m^3)	1.8×10^{-5}	1.9×10^{-3}	5×10^{-6}	1.5×10^{-4}	1.4×10^{-5}	1.1×10^{-11}
	time to max (a)	2	1.4	5	1	1	0.2
79°N 58°E	water (Bq/m^3)	8.5×10^{-6}	3.7×10^{-5}	4.4×10^{-5}	1.5×10^{-4}	9.1×10^{-6}	1.7×10^{-14}
	time to max (a)	3	4	3.5	1	1	0.5
76°N 20°E	water (Bq/m^3)	8.5×10^{-6}	3.7×10^{-5}	5.7×10^{-6}		4.3×10^{-6}	5×10^{-20}
	time to max (a)	3	4	5		3	0.5

TABLE I-XIIb. ^{60}Co CONCENTRATIONS IN WATER AT BARENTS SEA ENDPOINTS, CONTINUOUS RELEASE 1 TBq PER YEAR FOR 10 YEARS, SOURCE LOCATION: NOVAYA ZEMLYA TROUGH

Barents Sea		Risø	MAFF	Typhoon	KEMA	MEL box	Nihon U.
72°N 45°E	water (Bq/m^3)	8.2×10^{-5}	8×10^{-3}	3.7×10^{-5}	1.2×10^{-5}	4.4×10^{-4}	7.2×10^{-12}
	time to max (a)	10	10	12	10	10	10
79°N 58°E	water (Bq/m^3)	4.5×10^{-5}	2.6×10^{-4}	3.1×10^{-4}	1.2×10^{-5}	3.6×10^{-4}	7.4×10^{-15}
	time to max (a)	10	11	11	10	10	10
76°N 20°E	water (Bq/m^3)	4.5×10^{-5}	2.6×10^{-4}	4.2×10^{-5}		2.7×10^{-4}	$<1 \times 10^{-20}$
	time to max (a)	10	11	12		10	

TABLE I-XIIc. ^{60}Co CONCENTRATIONS IN SEDIMENT AT BARENTS SEA ENDPOINTS, SOURCE LOCATION: NOVAYA ZEMLYA TROUGH, INSTANTANEOUS RELEASE 1 TBq

Barents Sea		Risø	MAFF	Typhoon	KEMA	MEL box	Nihon U.
72°N 45°E	sediment (Bq/kg dw)	5.6×10^{-5}	2.2×10^{-5}	4.3×10^{-6}	9.1×10^{-4}	2.1×10^{-5}	1.1×10^{-10}
	(Bq/m^2)	4.2×10^{-3}	9.6×10^{-2}	1.6×10^{-4}	4.5×10^{-2}	1.5×10^{-3}	4.3×10^{-8}
	time to max (a)	6	5	10	2.6	4	0.2
79°N 58°E	sediment (Bq/kg dw)	1.5×10^{-5}	2.1×10^{-5}	3.3×10^{-5}	9.1×10^{-4}	1.6×10^{-5}	6.4×10^{-14}
	(Bq/m^2)	1.1×10^{-3}	3.1×10^{-3}	1.2×10^{-3}	4.5×10^{-2}	1.2×10^{-3}	2.6×10^{-11}
	time to max (a)	7	9	9	2.6	8	0.5
76°N 20°E	sediment (Bq/kg dw)	1.5×10^{-5}	2.1×10^{-5}	3.5×10^{-6}		1.1×10^{-5}	$<1 \times 10^{-20}$
	(Bq/m^2)	1.1×10^{-3}	3.1×10^{-3}	1.3×10^{-5}		7.5×10^{-4}	$<1 \times 10^{-20}$
	time to max (a)	7	9	10		8	

TABLE I-XIId. ^{60}Co CONCENTRATIONS IN SEDIMENT AT BARENTS SEA ENDPOINTS, CONTINUOUS RELEASE 1 TBq PER YEAR FOR 10 YEARS, SOURCE LOCATION: NOVAYA ZEMLYA TROUGH

Barents Sea		Risø	MAFF	Typhoon	KEMA	MEL box	Nihon U.
72°N 45°E	sediment (Bq/kg dw)	4.6×10^{-4}	5.5×10^{-3}	3.9×10^{-5}	1.1×10^{-4}	1.6×10^{-3}	4.4×10^{-11}
	(Bq/m^2)	3.5×10^{-2}	7.9×10^{-1}	1.4×10^{-3}	5.5×10^{-3}	1.1×10^{-1}	1.8×10^{-8}
	time to max (a)	12	12	16	10	11	10
79°N 58°E	sediment (Bq/kg dw)	1.3×10^{-4}	1.9×10^{-4}	3×10^{-4}	1.1×10^{-4}	1.3×10^{-3}	2.7×10^{-14}
	(Bq/m^2)	9.7×10^{-3}	2.8×10^{-2}	1.1×10^{-2}	5.5×10^{-3}	9.4×10^{-2}	1.1×10^{-11}
	time to max (a)	13	15	15	10	14	10
76°N 20°E	sediment (Bq/kg dw)	1.3×10^{-4}	1.9×10^{-4}	3.1×10^{-5}		9.4×10^{-4}	$<1 \times 10^{-20}$
	(Bq/m^2)	9.7×10^{-3}	2.8×10^{-2}	1.1×10^{-3}		6.6×10^{-2}	$<1 \times 10^{-20}$
	time to max (a)	13	15	16		14	

TABLE I-XIIIa. ^{99}Tc CONCENTRATIONS IN WATER AT KARA SEA ENDPOINTS, SOURCE LOCATION: ABRASIMOV FJORD, INSTANTANEOUS RELEASE 1 TBq

Kara Sea		Risø	MAFF	Typhoon	KEMA	MEL box	Nihon U.
72°N 65°E	water (Bq/m^3)	5.5×10^{-2}	8.6×10^{-3}	1.2×10^{-2}	7.8×10^{-3}	3.2×10^{-2}	4×10^{-2}
	time to max (a)	1	2	0.9	1.2	2	1
78°N 92°E	water (Bq/m^3)	6.8×10^{-4}	5×10^{-3}	$<4.5 \times 10^{-3}$	2.9×10^{-3}	5.2×10^{-3}	4.2×10^{-4}
	time to max (a)	3	3	>4	1.6	4	5
76°N 76°E	water (Bq/m^3)	6.8×10^{-4}	5×10^{-3}	8.3×10^{-3}	2.9×10^{-3}	5.2×10^{-3}	1.2×10^{-3}
	time to max (a)	3	3	2.5	1.6	4	2

TABLE I-XIIIb. ^{99}Tc CONCENTRATIONS IN WATER AT KARA SEA ENDPOINTS, CONTINUOUS RELEASE 1 TBq PER YEAR FOR 10 YEARS, SOURCE LOCATION: ABRASIMOV FJORD

Kara Sea		Risø	MAFF	Typhoon	KEMA	MEL box	Nihon U.
72°N 65°E	water (Bq/m^3)	2.7×10^{-1}	3.8×10^{-2}	4.9×10^{-2}	1.7×10^{-2}	1.2×10^{-1}	2.1×10^{-1}
	time to max (a)		10	10	10	10	10
78°N 92°E	water (Bq/m^3)	5.3×10^{-3}	2.6×10^{-2}	$<3.6 \times 10^{-2}$	6.4×10^{-3}	3.9×10^{-2}	2.7×10^{-3}
	time to max (a)		10	>11	10.1	11	10
76°N 76°E	water (Bq/m^3)	5.3×10^{-3}	2.6×10^{-2}	4.3×10^{-2}	6.4×10^{-3}	3.9×10^{-2}	9.1×10^{-3}
	time to max (a)		10	10.5	10.1	11	10

TABLE I-XIIIc. ^{99}Tc CONCENTRATIONS IN SEDIMENT AT KARA SEA ENDPOINTS, SOURCE LOCATION: ABRASIMOV FJORD, INSTANTANEOUS RELEASE 1 TBq

Kara Sea		Risø	MAFF	Typhoon	KEMA	MEL box	Nihon U.
72°N 65°E	sediment (Bq/kg dw)	3×10^{-4}	1.5×10^{-3}	1.2×10^{-4}	7.6×10^{-3}	1.8×10^{-4}	1.0×10^{-5}
	(Bq/m^2)	2.2×10^{-2}	2.2×10^{-1}	4.4×10^{-3}	3.8×10^{-1}	1.3×10^{-2}	4.1×10^{-3}
	time to max (a)	16	11	4	1.5	28	1
78°N 92°E	sediment (Bq/kg dw)	7.1×10^{-6}	1.0×10^{-3}	$<2.4 \times 10^{-5}$	2.8×10^{-2}	7.1×10^{-5}	1.0×10^{-7}
	(Bq/m^2)	5.3×10^{-4}	1.5×10^{-1}	$<8.9 \times 10^{-4}$	1.4	5×10^{-3}	4.2×10^{-5}
	time to max (a)	20	13	>9	2	40	5
76°N 76°E	sediment (Bq/kg dw)	7.1×10^{-6}	1.0×10^{-3}	7.2×10^{-5}	2.8×10^{-2}	7.1×10^{-5}	4.4×10^{-7}
	(Bq/m^2)	5.3×10^{-4}	1.5×10^{-1}	2.7×10^{-3}	1.4	5×10^{-3}	1.8×10^{-4}
	time to max (a)	20	13	6.6	2	40	2

TABLE I-XIIId. ^{99}Tc CONCENTRATIONS IN SEDIMENT AT KARA SEA ENDPOINTS, CONTINUOUS RELEASE 1 TBq PER YEAR FOR 10 YEARS, SOURCE LOCATION: ABRASIMOV FJORD

Kara Sea		Risø	MAFF	Typhoon	KEMA	MEL box	Nihon U.
72°N 65°E	sediment (Bq/kg dw)	3×10^{-3}	1.4×10^{-2}	1×10^{-3}	1.7×10^{-4}	1.8×10^{-3}	5.1×10^{-5}
	(Bq/m^2)	2.2×10^{-1}	2.1	3.7×10^{-2}	8.5×10^{-3}	1.3×10^{-1}	2.1×10^{-2}
	time to max (a)		18	12	10.1	33	10
78°N 92°E	sediment (Bq/kg dw)	6.9×10^{-5}	1.0×10^{-2}	$<2.2 \times 10^{-4}$	6.5×10^{-5}	7.1×10^{-4}	6.6×10^{-7}
	(Bq/m^2)	5.2×10^{-3}	1.5	$<8.1 \times 10^{-3}$	3.2×10^{-3}	5×10^{-2}	2.7×10^{-4}
	time to max (a)	30	19	15	10.2	46	10
76°N 76°E	sediment (Bq/kg dw)	6.9×10^{-5}	1.0×10^{-2}	6.1×10^{-4}	6.5×10^{-5}	7.1×10^{-4}	2.9×10^{-6}
	(Bq/m^2)	5.2×10^{-3}	1.5	2.2×10^{-2}	3.2×10^{-3}	5×10^{-2}	1.2×10^{-3}
	time to max (a)	30	19	13.5	10.2	46	10

TABLE I-XIVa. ^{99}Tc CONCENTRATIONS IN WATER AT KARA SEA ENDPOINTS, SOURCE LOCATION NOVAYA ZEMLYA TROUGH, INSTANTANEOUS RELEASE 1 TBq

Kara Sea		Risø	MAFF	Typhoon	KEMA	MEL box	Nihon U.
72°N 65°E	water (Bq/m³)	1.9×10^{-1}	9.4×10^{-3}	7.4×10^{-3}	1.1×10^{-2}	3.9×10^{-3}	2.6×10^{-2}
	time to max (a)	10	1.4	1.2	initial	3	5
78°N 92°E	water (Bq/m³)	4.5×10^{-4}	5.2×10^{-3}	$<3.7 \times 10^{-3}$	3.3×10^{-3}	1.4×10^{-3}	3.7×10^{-5}
	time to max (a)	10	2.5	>5.5	9.1	6	2
76°N 76°E	water (Bq/m³)	4.5×10^{-4}	5.2×10^{-3}	5.5×10^{-3}	3.3×10^{-3}	1.4×10^{-3}	1.2×10^{-3}
	time to max (a)	10	2.5	3.4	9.1	6	5

TABLE I-XIVb. ^{99}Tc CONCENTRATIONS IN WATER AT KARA SEA ENDPOINTS, CONTINUOUS RELEASE 1 TBq PER YEAR FOR 10 YEARS, SOURCE LOCATION: NOVAYA ZEMLYA TROUGH

Kara Sea		Risø	MAFF	Typhoon	KEMA	MEL box	Nihon U.
72°N 65°E	water (Bq/m³)	1.9×10^{-1}	3.9×10^{-2}	4.5×10^{-2}	1.7×10^{-2}	2.4×10^{-2}	2×10^{-1}
	time to max (a)	10	10	10	10	10	10
78°N 92°E	water (Bq/m³)	3.8×10^{-3}	2.6×10^{-2}	$<3.2 \times 10^{-2}$	6.5×10^{-3}	1.1×10^{-2}	2.3×10^{-3}
	time to max (a)	10	10	>12	10	12	10
76°N 76°E	water (Bq/m³)	3.8×10^{-3}	2.6×10^{-2}	3.9×10^{-2}	6.5×10^{-3}	1.1×10^{-2}	8.1×10^{-3}
	time to max (a)	20	10	11	10	12	10

TABLE I-XIVc. ^{99}Tc CONCENTRATIONS IN SEDIMENT AT KARA SEA ENDPOINTS, SOURCE LOCATION: NOVAYA ZEMLYA TROUGH, INSTANTANEOUS RELEASE 1 TBq

Kara Sea		Risø	MAFF	Typhoon	KEMA	MEL box	Nihon U.
72°N 65°E	sediment (Bq/kg dw)	2.9×10^{-4}	1.5×10^{-3}	1×10^{-4}	8.8×10^{-5}	4×10^{-5}	6.4×10^{-6}
	(Bq/m²)	2.2×10^{-2}	2.2×10^{-1}	3.7×10^{-3}	4.4×10^{-3}	2.8×10^{-3}	2.6×10^{-3}
	time to max (a)	20	11	6	0.7	>100	5
78°N 92°E	sediment (Bq/kg dw)	8.6×10^{-6}	1.0×10^{-3}	$<2.2 \times 10^{-5}$	3.1×10^{-5}	2.3×10^{-5}	7.9×10^{-8}
	(Bq/m²)	6.4×10^{-4}	1.5×10^{-1}	$<8.1 \times 10^{-4}$	1.5×10^{-3}	1.6×10^{-3}	3.2×10^{-5}
	time to max (a)	30	12	>12	13.2	>100	5
76°N 76°E	sediment (Bq/kg dw)	8.6×10^{-6}	1.0×10^{-3}	6×10^{-5}	3.1×10^{-5}	2.3×10^{-5}	3.9×10^{-7}
	(Bq/m²)	6.4×10^{-4}	1.5×10^{-1}	2.2×10^{-3}	1.5×10^{-3}	1.6×10^{-3}	1.6×10^{-4}
	time to max (a)	30	12	9	13.2	>100	5

TABLE I-XIVd. ^{99}Tc CONCENTRATIONS IN SEDIMENT AT KARA SEA ENDPOINTS: CONTINUOUS RELEASE 1 TBq PER YEAR FOR 10 YEARS, SOURCE LOCATION: NOVAYA ZEMLYA TROUGH

Kara Sea		Risø	MAFF	Typhoon	KEMA	MEL box	Nihon U.
72°N 65°E	sediment (Bq/kg dw)	2.8×10^{-3}	1.5×10^{-2}	9.3×10^{-4}	1.7×10^{-4}	4×10^{-4}	4.7×10^{-5}
	(Bq/m²)	2.1×10^{-1}	2.2	3.4×10^{-2}	8.5×10^{-3}	2.8×10^{-2}	1.9×10^{-2}
	time to max (a)	30	17	13	10	>100	10
78°N 92°E	sediment (Bq/kg dw)	6.8×10^{-5}	1×10^{-2}	$<2.1 \times 10^{-4}$	6.5×10^{-5}	2.3×10^{-4}	5.7×10^{-7}
	(Bq/m²)	5.1×10^{-3}	1.5	$<7.8 \times 10^{-3}$	3.2×10^{-3}	1.6×10^{-2}	2.3×10^{-4}
	time to max (a)	30	19	>17	10	>100	10
76°N 76°E	sediment (Bq/kg dw)	6.8×10^{-5}	1×10^{-2}	5.7×10^{-4}	6.5×10^{-5}	2.3×10^{-4}	2.7×10^{-6}
	(Bq/m²)	5.1×10^{-3}	1.5	2.1×10^{-2}	3.2×10^{-3}	1.6×10^{-2}	1.1×10^{-3}
	time to max (a)	30	19	15	10	>100	10

TABLE I-XVa. ^{99}Tc CONCENTRATIONS IN WATER AT BARENTS SEA ENDPOINTS, SOURCE LOCATION: ABRASIMOV FJORD, INSTANTANEOUS RELEASE 1 TBq

Barents Sea		Risø	MAFF	Typhoon	KEMA	MEL box	Nihon U.
72°N 45°E	water (Bq/m^3)	3.5×10^{-4}	3.8×10^{-3}	1.7×10^{-5}	3.3×10^{-4}	1.9×10^{-4}	2.4×10^{-3}
	time to max (a)	3	2	6.5	2.6	4	2
79°N 58°E	water (Bq/m^3)	2.9×10^{-4}	1.2×10^{-4}	1.2×10^{-4}	3.3×10^{-4}	1.3×10^{-4}	4.6×10^{-4}
	time to max (a)	5	5.5	5.2	2.6	9	10
76°N 20°E	water (Bq/m^3)	2.9×10^{-4}	1.2×10^{-4}	1.9×10^{-5}		7.1×10^{-5}	5.9×10^{-4}
	time to max (a)	5	5.5	6.5		9	10

TABLE I-XVb. ^{99}Tc CONCENTRATIONS IN WATER AT BARENTS SEA ENDPOINTS, CONTINUOUS RELEASE 1 TBq PER YEAR FOR 10 YEARS, SOURCE LOCATION: ABRASIMOV FJORD

Barents Sea		Risø	MAFF	Typhoon	KEMA	MEL box	Nihon U.
72°N 45°E	water (Bq/m^3)	2.6×10^{-3}	1.8×10^{-2}	1.5×10^{-4}	9.4×10^{-4}	1.3×10^{-3}	2×10^{-2}
	time to max (a)	10	10	14	10.4	11	10
79°N 58°E	water (Bq/m^3)	2.2×10^{-3}	1×10^{-3}	1.1×10^{-3}	9.4×10^{-4}	9.9×10^{-4}	3.3×10^{-3}
	time to max (a)	10	12	12	10.4	15	10
76°N 20°E	water (Bq/m^3)	2.2×10^{-3}	1×10^{-3}	1.7×10^{-4}		6.7×10^{-4}	4.4×10^{-3}
	time to max (a)	10	12	13		15	20

TABLE I-XVc. ^{99}Tc CONCENTRATIONS IN SEDIMENT AT BARENTS SEA ENDPOINTS, SOURCE LOCATION: ABRASIMOV FJORD, INSTANTANEOUS RELEASE 1 TBq

Barents Sea		Risø	MAFF	Typhoon	KEMA	MEL box	Nihon U.
72°N 45°E	sediment (Bq/kg dw)	3.3×10^{-6}	6.9×10^{-4}	3.4×10^{-7}	3.3×10^{-6}	2.3×10^{-6}	9.8×10^{-7}
	(Bq/m^2)	2.5×10^{-4}	1×10^{-1}	1.2×10^{-5}	1.6×10^{-4}	1.6×10^{-4}	4×10^{-4}
	time to max (a)	20	12	13	3	>100	2
79°N 58°E	sediment (Bq/kg dw)	1.7×10^{-6}	5.7×10^{-5}	5.1×10^{-6}	3.3×10^{-6}	2.6×10^{-6}	1.2×10^{-7}
	(Bq/m^2)	1.3×10^{-4}	8.2×10^{-3}	1.9×10^{-4}	1.6×10^{-4}	1.9×10^{-4}	5×10^{-5}
	time to max (a)	20	40	12	3	>100	5
76°N 20°E	sediment (Bq/kg dw)	1.7×10^{-6}	5.7×10^{-5}	2.3×10^{-7}		3×10^{-6}	1.5×10^{-7}
	(Bq/m^2)	1.3×10^{-4}	8.2×10^{-3}	8.5×10^{-6}		2.1×10^{-4}	6×10^{-5}
	time to max (a)	20	40	13		>100	10

TABLE I-XVd. ^{99}Tc CONCENTRATIONS IN SEDIMENT AT BARENTS SEA ENDPOINTS, CONTINUOUS RELEASE 1 TBq PER YEAR FOR 10 YEARS, SOURCE LOCATION: ABRASIMOV FJORD

Barents Sea		Risø	MAFF	Typhoon	KEMA	MEL box	Nihon U.
72°N 45°E	sediment (Bq/kg dw)	3.3×10^{-5}	6.9×10^{-3}	3.3×10^{-6}	9.4×10^{-6}	2.3×10^{-5}	6.6×10^{-6}
	(Bq/m^2)	2.5×10^{-3}	1	1.2×10^{-4}	4.7×10^{-4}	1.6×10^{-3}	2.7×10^{-3}
	time to max (a)	30	19	19	10.6	>100	10
79°N 58°E	sediment (Bq/kg dw)	1.8×10^{-5}	5.7×10^{-4}	4.8×10^{-5}	9.4×10^{-6}	2.6×10^{-5}	9.1×10^{-7}
	(Bq/m^2)	1.3×10^{-3}	8.2×10^{-2}	1.7×10^{-3}	4.7×10^{-4}	1.9×10^{-3}	3.7×10^{-4}
	time to max (a)	30	45	18	10.5	>100	10
76°N 20°E	sediment (Bq/kg dw)	1.8×10^{-5}	5.7×10^{-4}	2.2×10^{-6}		3×10^{-5}	1.1×10^{-6}
	(Bq/m^2)	1.3×10^{-3}	8.2×10^{-2}	8.1×10^{-5}		2.1×10^{-3}	4.4×10^{-4}
	time to max (a)	30	45	19		>100	20

TABLE I-XVIa. ^{99}Tc CONCENTRATIONS IN WATER AT BARENTS SEA ENDPOINTS, SOURCE LOCATION: NOVAYA ZEMLYA TROUGH, INSTANTANEOUS RELEASE 1 TBq

Barents Sea		Risø	MAFF	Typhoon	KEMA	MEL box	Nihon U.
72°N 45°E	water (Bq/m^3)	2.1×10^{-4}	4.1×10^{-3}	1.5×10^{-5}	3.5×10^{-4}	7.7×10^{-5}	1.8×10^{-3}
	time to max (a)	10	1.4	8.5	2.1	5	5
79°N 58°E	water (Bq/m^3)	2.1×10^{-4}	1.3×10^{-4}	1×10^{-4}	3.5×10^{-4}	6.9×10^{-5}	4.2×10^{-4}
	time to max (a)	10	4.7	7.5	2.1	11	10
76°N 20°E	water (Bq/m^3)	2.1×10^{-4}	1.3×10^{-4}	1.7×10^{-5}		6.2×10^{-5}	4.7×10^{-4}
	time to max (a)	10	4.7	8.5		11	10

TABLE I-XVIb. ^{99}Tc CONCENTRATIONS IN WATER AT BARENTS SEA ENDPOINTS, CONTINUOUS RELEASE 1 TBq PER YEAR FOR 10 YEARS, SOURCE LOCATION: NOVAYA ZEMLYA TROUGH

Barents Sea		Risø	MAFF	Typhoon	KEMA	MEL box	Nihon U.
72°N 45°E	water (Bq/m^3)	1.8×10^{-3}	1.8×10^{-2}	1.4×10^{-4}	9.5×10^{-4}	5.6×10^{-4}	1.4×10^{-2}
	time to max (a)	20	10	15	10	11	10
79°N 58°E	water (Bq/m^3)	1.9×10^{-3}	1×10^{-3}	9.7×10^{-4}	9.5×10^{-4}	5.7×10^{-4}	3.3×10^{-3}
	time to max (a)	20	12	14	10	16	20
76°N 20°E	water (Bq/m^3)	1.9×10^{-3}	1×10^{-3}	1.6×10^{-4}		5.8×10^{-4}	4.4×10^{-3}
	time to max (a)	20	12	15		16	20

TABLE I-XVIc. ^{99}Tc CONCENTRATIONS IN SEDIMENT AT BARENTS SEA ENDPOINTS, SOURCE LOCATION: NOVAYA ZEMLYA TROUGH, INSTANTANEOUS RELEASE 1 TBq

Barents Sea		Risø	MAFF	Typhoon	KEMA	MEL box	Nihon U.
72°N 45°E	sediment (Bq/kg dw)	3.2×10^{-6}	6.9×10^{-4}	3.3×10^{-7}	3.4×10^{-6}	1.6×10^{-6}	6.6×10^{-7}
	(Bq/m^2)	2.4×10^{-4}	1×10^{-1}	1.2×10^{-5}	1.7×10^{-4}	1.1×10^{-4}	2.7×10^{-4}
	time to max (a)	30	12	16	2.6	>100	5
79°N 58°E	sediment (Bq/kg dw)	1.8×10^{-6}	5.7×10^{-5}	4.9×10^{-6}	3.4×10^{-6}	2.3×10^{-6}	1×10^{-7}
	(Bq/m^2)	1.3×10^{-4}	8.3×10^{-3}	1.8×10^{-4}	1.7×10^{-4}	1.7×10^{-4}	4.1×10^{-5}
	time to max (a)	30	39	14	2.6	>100	10
76°N 20°E	sediment (Bq/kg dw)	1.8×10^{-6}	5.7×10^{-5}	2.2×10^{-7}		3×10^{-6}	1.2×10^{-7}
	(Bq/m^2)	1.3×10^{-4}	8.3×10^{-3}	8.1×10^{-6}		2.1×10^{-4}	4.8×10^{-5}
	time to max (a)	30	39	16		>100	10

TABLE I-XVId. ^{99}Tc CONCENTRATIONS IN SEDIMENT AT BARENTS SEA ENDPOINTS, CONTINUOUS RELEASE 1 TBq PER YEAR FOR 10 YEARS, SOURCE LOCATION: NOVAYA ZEMLYA TROUGH

Barents Sea		Risø	MAFF	Typhoon	KEMA	MEL box	Nihon U.
72°N 45°E	sediment (Bq/kg dw)	3.2×10^{-5}	6.9×10^{-3}	3.2×10^{-6}	9.5×10^{-6}	1.7×10^{-5}	4.6×10^{-6}
	(Bq/m^2)	2.4×10^{-3}	1	1.2×10^{-4}	4.7×10^{-4}	1.2×10^{-3}	1.9×10^{-3}
	time to max (a)	30	18	21	10.3	>100	10
79°N 58°E	sediment (Bq/kg dw)	1.7×10^{-5}	5.7×10^{-4}	4.7×10^{-5}	9.5×10^{-6}	2.2×10^{-5}	6.9×10^{-7}
	(Bq/m^2)	1.3×10^{-3}	8.3×10^{-2}	1.7×10^{-3}	4.7×10^{-4}	1.6×10^{-3}	2.8×10^{-4}
	time to max (a)	40	44	20	10.3	>100	20
76°N 20°E	sediment (Bq/kg dw)	1.7×10^{-5}	5.7×10^{-4}	2.1×10^{-6}		2.8×10^{-5}	1.1×10^{-6}
	(Bq/m^2)	1.3×10^{-3}	8.3×10^{-2}	7.8×10^{-5}		2×10^{-3}	4.4×10^{-4}
	time to max (a)	40	44	21		>100	20

TABLE I-XVIIa. ^{137}Cs CONCENTRATIONS IN WATER AT DISTANT ENPOINTS, SOURCE LOCATION: ABRASIMOV FJORD, INSTANTANEOUS RELEASE 1 TBq

Area		Risø	MAFF	KEMA	Nihon U.	MEL box
70.5°N 143°W	water (Bq/m^3)	2.6×10^{-5}	1.1×10^{-5}	6.1×10^{-6}	4.4×10^{-7}	1.1×10^{-5}
(Beaufort Sea)	time to max (a)	11	19	9.6	39	23
86°N 80°E	water (Bq/m^3)	9.7×10^{-5}	7.5×10^{-5}	3.5×10^{-5}	3.5×10^{-5}	4.6×10^{-5}
(Central Arctic)	time to max (a)	5.6	9.5	1.7	7	16
60°N 55°W	water (Bq/m^3)	5×10^{-6}	1×10^{-6}	4.4×10^{-6}		2.4×10^{-6}
(Davis Strait)	time to max (a)	18	44	17		31
67°N 20°W	water (Bq/m^3)	2.3×10^{-5}	3.2×10^{-5}	1.9×10^{-5}	3.1×10^{-7}	2.3×10^{-5}
(Iceland Sea)	time to max (a)	6.7	19	4.6	26	16
70°N 175°W	water (Bq/m^3)	1.5×10^{-5}	1.8×10^{-3}	3.3×10^{-6}	7×10^{-8}	1.2×10^{-5}
(Chukchi Sea)	time to max (a)	15	7.7	10	33	9

TABLE I-XVIIb. ^{137}Cs CONCENTRATIONS IN WATER AT DISTANT ENDPOINTS, CONTINUOUS RELEASE 1 TBq PER YEAR FOR 10 YEARS, SOURCE LOCATION: ABRASIMOV FJORD

Area		Risø	MAFF	KEMA	Nihon U.	MEL box	USN
70.5°N 143°W	water (Bq/m^3)	2.4×10^{-4}	1.1×10^{-4}	2.9×10^{-5}	4.3×10^{-6}	1.1×10^{-4}	4×10^{-6}
(Beaufort Sea)	time to max (a)	20	25	15.6	44	28	
86°N 80°E	water (Bq/m^3)	7.2×10^{-4}	7.1×10^{-4}	1.1×10^{-4}	3×10^{-4}	4.3×10^{-4}	$6. \times 10^{-3}$
(Central Arctic)	time to max (a)	10	16	10.3	14	22	
60°N 55°W	water (Bq/m^3)	4.7×10^{-5}	1×10^{-5}	2.1×10^{-5}		2.4×10^{-5}	1.5×10^{-5}
(Davis Strait)	time to max (a)	20	50	22.5		36	
67°N 20°W	water (Bq/m^3)	1.6×10^{-4}	3.1×10^{-4}	7.8×10^{-5}	3×10^{-6}	2.2×10^{-4}	1.5×10^{-6}
(Iceland Sea)	time to max (a)	15	25	11.6	31	21	
70°N 175°W	water (Bq/m^3)	1.5×10^{-4}	1.4×10^{-2}	1.6×10^{-5}	6.9×10^{-7}	1×10^{-4}	4×10^{-7}
(Chukchi Sea)	time to max(yr)	20	14	16.1	39	15	

TABLE I-XVIIc. ^{137}Cs CONCENTRATIONS IN SEDIMENT AT DISTANT ENDPOINTS, SOURCE LOCATION: ABRASIMOV FJORD, INSTANTANEOUS RELEASE 1 TBq

Area		Risø	MAFF	KEMA	Nihon U.	MEL box
70.5°N 143°W	sediment (Bq/kg dw)	1.8×10^{-7}	9×10^{-6}		5.9×10^{-10}	7.1×10^{-8}
(Beaufort Sea)	(Bq/m^2)	1.3×10^{-5}	1.3×10^{-2}		2.4×10^{-7}	5×10^{-6}
	time to max (a)	56	48		42	54
86°N 80°E	sediment (Bq/kg dw)	1.6×10^{-7}	1.5×10^{-5}		3.2×10^{-11}	1.7×10^{-7}
(Central Arctic)	(Bq/m^2)	1.2×10^{-5}	6.3×10^{-3}		1.3×10^{-8}	1.2×10^{-5}
	time to max (a)	60	33		52	43
60°N 55°W	sediment (Bq/kg dw)	7.9×10^{-8}	1.2×10^{-6}	4.1×10^{-7}		1.6×10^{-8}
(Davis Strait)	(Bq/m^2)	5.9×10^{-6}	1.7×10^{-4}	2×10^{-5}		1.1×10^{-6}
	time to max (a)	48	79	24		63
67°N 20°W	sediment (Bq/kg dw)	1.6×10^{-7}	2.4×10^{-5}	2.4×10^{-7}	2.3×10^{-10}	1×10^{-7}
(Iceland Sea)	(Bq/m^2)	1.2×10^{-5}	3.5×10^{-3}	1.2×10^{-5}	9.3×10^{-8}	7.4×10^{-6}
	time to max (a)	38	44	16.3	34	39
70°N 175°W	sediment (Bq/kg dw)	1.9×10^{-7}	6×10^{-4}	3.3×10^{-7}	9.2×10^{-11}	2.3×10^{-7}
(Chukchi Sea)	(Bq/m^2)	1.4×10^{-5}	8.7×10^{-2}	1.6×10^{-5}	3.7×10^{-8}	1.6×10^{-5}
	time to max (a)	53	18	10.9	37	22

TABLE I-XVIId. ^{137}Cs CONCENTRATIONS IN SEDIMENT AT DISTANT ENDPOINTS, CONTINUOUS RELEASE 1 TBq PER YEAR FOR 10 YEARS, SOURCE LOCATION: ABRASIMOV FJORD

Area		Risø	MAFF	KEMA	Nihon U.	MEL box
70.5°N 143°W	sediment (Bq/kg dw)	1.8×10^{-6}	9×10^{-5}		5.9×10^{-9}	7.1×10^{-7}
(Beaufort Sea)	(Bq/m^2)	1.3×10^{-4}	1.3×10^{-2}		2.4×10^{-6}	5×10^{-5}
	time to max (a)	60	53		48	55
86°N 80°E	sediment (Bq/kg dw)	1.6×10^{-6}	4.4×10^{-4}		3.2×10^{-10}	1.7×10^{-6}
(Central Arctic)	(Bq/m^2)	1.2×10^{-4}	6.3×10^{-2}		1.3×10^{-7}	1.2×10^{-4}
	time to max (a)	70	38		57	47
60°N 55°W	sediment (Bq/kg dw)	7.9×10^{-7}	1.2×10^{-5}	2×10^{-6}		1.6×10^{-7}
(Davis Strait)	(Bq/m^2)	5.9×10^{-5}	1.7×10^{-3}	1×10^{-4}		1.1×10^{-5}
	time to max (a)	50	84	29.5		67
67°N 20°W	sediment (Bq/kg dw)	1.6×10^{-6}	2.4×10^{-4}	1.2×10^{-6}	2.3×10^{-9}	1×10^{-6}
(Iceland Sea)	(Bq/m^2)	1.2×10^{-4}	3.5×10^{-2}	6×10^{-5}	9.2×10^{-7}	7.4×10^{-5}
	time to max (a)	40	49	22.1	39	44
70°N 175°W	sediment (Bq/kg dw)	1.8×10^{-6}	5.9×10^{-3}	1.6×10^{-6}	9.2×10^{-10}	2.3×10^{-6}
(Chukchi Sea)	(Bq/m^2)	1.3×10^{-4}	8.5×10^{-1}	8×10^{-5}	3.7×10^{-7}	1.6×10^{-4}
	time to max (a)	60	24	17	43	27

TABLE I-XVIIIa. ^{137}Cs CONCENTRATIONS IN WATER AT DISTANT ENDPOINTS, SOURCE LOCATION: NOVAYA ZEMLYA TROUGH, INSTANTANEOUS RELEASE 1 TBq

Area		Risø	MAFF	KEMA	Nihon U.	MEL box
70.5° N 143° W	water (Bq/m^3)	2.2×10^{-5}	1.2×10^{-5}	6.2×10^{-6}	4.4×10^{-7}	1.4×10^{-5}
(Beaufort Sea)	time to max (a)	20	18	9	39	22
86° N 80° E	water (Bq/m^3)	7.7×10^{-4}	7.7×10^{-5}	4.1×10^{-5}	3.5×10^{-5}	6.4×10^{-5}
(Central Arctic)	time to max (a)	10	9	0.9	7	7
60° N 55° W	water (Bq/m^3)	4.7×10^{-6}	1.1×10^{-6}	4.5×10^{-6}		3.1×10^{-6}
(Davis Strait)	time to max (a)	20	44	16.3		29
67° N 20° W	water (Bq/m^3)	1.8×10^{-5}	3.3×10^{-5}	2×10^{-5}	2.1×10^{-7}	3×10^{-5}
(Iceland Sea)	time to max (a)	10	18	4	27	14
70° N 175° W	water (Bq/m^3)	1.4×10^{-5}	1.8×10^{-3}	3.4×10^{-6}	5.1×10^{-8}	4.3×10^{-6}
(Chukchi Sea)	time to max (a)	20	7.2	9.4	35	11

TABLE I-XVIIIb. ^{137}Cs CONCENTRATIONS IN WATER AT DISTANT ENDPOINTS, CONTINUOUS RELEASE 1 TBq PER YEAR FOR 10 YEARS, SOURCE LOCATION: NOVAYA ZEMLYA TROUGH

Area		Risø	MAFF	KEMA	Nihon U.	MEL box
70.5°N 143°W	water (Bq/m^3)	2.2×10^{-4}	1.1×10^{-4}	3×10^{-5}	3.3×10^{-6}	1.3×10^{-4}
(Beaufort Sea)	time to max (a)	20	24	15	46	27
86°N 80°E	water (Bq/m^3)	6.4×10^{-4}	7.2×10^{-4}	1.1×10^{-4}	2.2×10^{-4}	1.4×10^{-4}
(Central Arctic)	time to max (a)	20	15	10	14	20
60°N 55°W	water (Bq/m^3)	4.7×10^{-5}	1.1×10^{-5}	2.2×10^{-5}		3×10^{-5}
(Davis Strait)	time to max (a)	30	49	22		34
67°N 20°W	water (Bq/m^3)	1.7×10^{-4}	3.2×10^{-4}	8×10^{-5}	2.2×10^{-6}	2.9×10^{-4}
(Iceland Sea)	time to max (a)	20	24	11.1	33	19
70°N 175°W	water (Bq/m^3)	1.4×10^{-4}	1.5×10^{-2}	1.6×10^{-5}	5.2×10^{-7}	3.8×10^{-5}
(Chukchi Sea)	time to max (a)	30	13	15.8	41	17

TABLE I-XVIIIc. ^{137}Cs CONCENTRATIONS IN SEDIMENT AT DISTANT ENDPOINTS, SOURCE LOCATION: NOVAYA ZEMLYA TROUGH, INSTANTANEOUS RELEASE 1 TBq

Area		Risø	MAFF	KEMA	Nihon U.	MEL box
70.5°N 143°W	sediment (Bq/kg dw)	1.8×10^{-7}	9×10^{-6}		4.2×10^{-10}	8.9×10^{-8}
(Beaufort Sea)	(Bq/m^2)	1.4×10^{-5}	1.3×10^{-3}		1.7×10^{-7}	6.2×10^{-6}
	time to max (a)	60	48			53
86°N 80°E	sediment (Bq/kg dw)	1.6×10^{-7}	4.4×10^{-5}		2.5×10^{-11}	2.3×10^{-7}
(Central Arctic)	(Bq/m^2)	1.2×10^{-5}	6.4×10^{-3}		9.8×10^{-9}	1.6×10^{-5}
	time to max (a)	65	32		55	41
60°N 55°W	sediment (Bq/kg dw)	7.9×10^{-8}	1.2×10^{-6}	4.2×10^{-7}		2×10^{-8}
(Davis Strait)	(Bq/m^2)	5.9×10^{-6}	1.7×10^{-4}	2.1×10^{-5}		1.4×10^{-6}
	time to max (a)	50	78	23.5		60
67°N 20°W	sediment (Bq/kg dw)	1.6×10^{-7}	2.5×10^{-5}	2.5×10^{-7}	1.6×10^{-10}	1.3×10^{-7}
(Iceland Sea)	(Bq/m^2)	1.2×10^{-5}	3.6×10^{-3}	1.2×10^{-5}	6.6×10^{-8}	9.5×10^{-6}
	time to max (a)	40	43	15.6	35	37
70°N 175°W	sediment (Bq/kg dw)	1.9×10^{-7}	6.2×10^{-4}	3.4×10^{-7}	6.7×10^{-11}	1×10^{-7}
(Chukchi Sea)	(Bq/m^2)	1.4×10^{-5}	8.9×10^{-2}	1.7×10^{-5}	2.7×10^{-8}	7.3×10^{-6}
	time to max (a)	60	18	10.2	39	31

TABLE I-XVIIId. ^{137}Cs CONCENTRATIONS IN SEDIMENT AT DISTANT ENDPOINTS, CONTINUOUS RELEASE 1 TBq PER YEAR FOR 10 YEARS, SOURCE LOCATION: NOVAYA ZEMLYA TROUGH

Area		Risø	MAFF	KEMA	Nihon U.	MEL box
70.5°N 143°W	sediment (Bq/kg dw)	1.8×10^{-6}	9×10^{-5}		4.5×10^{-9}	8.8×10^{-6}
(Beaufort Sea)	(Bq/m^2)	1.3×10^{-4}	1.3×10^{-2}		1.8×10^{-6}	6.2×10^{-4}
	time to max (a)	70	52		49	57
86°N 80°E	sediment (Bq/kg dw)	1.6×10^{-6}	4.4×10^{-4}		2.5×10^{-10}	2.3×10^{-6}
(Central Arctic)	(Bq/m^2)	1.2×10^{-4}	6.4×10^{-2}		1×10^{-7}	1.6×10^{-4}
	time to max(yr)	70	38		60	46
60°N 55°W	sediment (Bq/kg dw)	7.9×10^{-7}	1.2×10^{-5}	2.1×10^{-6}		2×10^{-7}
(Davis Strait)	(Bq/m^2)	5.9×10^{-5}	1.7×10^{-3}	1×10^{-4}		1.4×10^{-5}
	time to max(yr)	60	83	28.8		65
67°N 20°W	sediment (Bq/kg dw)	1.6×10^{-6}	2.5×10^{-4}	1.2×10^{-6}	1.7×10^{-9}	1.3×10^{-6}
(Iceland Sea)	(Bq/m^2)	1.2×10^{-4}	3.6×10^{-2}	6×10^{-5}	6.7×10^{-7}	9.4×10^{-5}
	time to max (a)	50	48	21.5	41	41
70°N 175°W	sediment (Bq/kg dw)	1.9×10^{-6}	6×10^{-3}	1.6×10^{-6}	7×10^{-10}	1×10^{-6}
(Chukchi Sea)	(Bq/m^2)	1.4×10^{-4}	8.7×10^{-1}	8×10^{-5}	2.8×10^{-7}	7.3×10^{-5}
	time to max (a)	60	24	16.3	45	36

TABLE I-XIXa. ^{239}Pu CONCENTRATIONS IN WATER AT DISTANT ENDPOINTS, SOURCE LOCATION: ABRASIMOV FJORD, INSTANTANEOUS RELEASE 1 TBq

Area		Risø	MAFF	KEMA	MEL box	Nihon U.
70.5°N 143°W	water (Bq/m³)	1.9×10^{-6}	1.5×10^{-5}	6.4×10^{-5}	1.3×10^{-6}	8.1×10^{-16}
(Beaufort Sea)	time to max (a)	7	41	24.3	30	67
86°N 80°E	water (Bq/m³)	9.2×10^{-6}	7.9×10^{-5}	1.4×10^{-4}	4.5×10^{-6}	3.5×10^{-5}
(Central Arctic)	time to max (a)	2.1	15	10.1	17	7
60°N 55°W	water (Bq/m³)	3.6×10^{-7}	4.8×10^{-6}	5.5×10^{-5}	3.5×10^{-7}	
(Davis Strait)	time to max (a)	11	230	33.3	41	
67°N 20°W	water (Bq/m³)	2.5×10^{-6}	4.5×10^{-5}	1.2×10^{-4}	2.3×10^{-6}	3.1×10^{-7}
(Iceland Sea)	time to max (a)	4	28	13.3	13	26
70°N 175°W	water (Bq/m³)	1.1×10^{-6}	6.8×10^{-4}	3.4×10^{-5}	1.1×10^{-7}	7×10^{-8}
(Chukchi Sea)	time to max (a)	9	15	26.4	3	33

TABLE I-XIXb. ^{239}Pu CONCENTRATIONS IN WATER AT DISTANT ENDPOINTS, CONTINUOUS RELEASE 1 TBq PER YEAR FOR 10 YEARS, SOURCE LOCATION: ABRASIMOV FJORD

Area		MAFF	KEMA	MEL box	Nihon U.
70.5°N 143°W	water (Bq/m³)	1.5×10^{-4}	3.2×10^{-4}	1.2×10^{-4}	4.3×10^{-6}
(Beaufort Sea)	time to max (a)	47	29.6	35	44
86°N 80°E	water (Bq/m³)	7.7×10^{-4}	6.8×10^{-4}	3.9×10^{-4}	3×10^{-4}
(Central Arctic)	time to max (a)	21	16.3	24	14
60°N 55°W	water (Bq/m³)	4.8×10^{-5}	2.7×10^{-4}	3.4×10^{-5}	
(Davis Strait)	time to max (a)	230	38.6	46	
67°N 20°W	water (Bq/m³)	4.5×10^{-4}	5.6×10^{-4}	2.2×10^{-4}	3×10^{-6}
(Iceland Sea)	time to max (a)	34	19	18	31
70°N 175°W	water (Bq/m³)	6.4×10^{-3}	1.7×10^{-4}	5.1×10^{-6}	6.9×10^{-7}
(Chukchi Sea)	time to max (a)	21	32	10	39

TABLE I-XIXc. ^{239}Pu CONCENTRATIONS IN SEDIMENT AT DISTANT ENDPOINTS, SOURCE LOCATION: ABRASIMOV FJORD, INSTANTANEOUS RELEASE 1 TBq

Area		Risø	MAFF	KEMA	MEL box	Nihon U.
70.5°N 143°W	sediment (Bq/kg dw)	2.2×10^{-6}	5.7×10^{-4}		6.8×10^{-7}	6×10^{-10}
(Beaufort Sea)	(Bq/m²)	1.6×10^{-4}	8.2×10^{-2}		4.8×10^{-5}	2.4×10^{-7}
	time to max (a)	500	1000		>50	42
86°N 80°E	sediment (Bq/kg dw)	2.2×10^{-6}	8.3×10^{-4}		1.6×10^{-6}	3.1×10^{-11}
(Central Arctic)	(Bq/m²)	1.6×10^{-4}	1.2×10^{-1}		1.1×10^{-4}	1.3×10^{-8}
	time to max (a)	500	1000		>50	52
60°N 55°W	sediment (Bq/kg dw)	8.4×10^{-7}	4.4×10^{-4}	6.1×10^{-4}	1.6×10^{-7}	
(Davis Strait)	(Bq/m²)	6.3×10^{-5}	6.4×10^{-2}	3×10^{-2}	1.1×10^{-5}	
	time to max (a)	500	1000	44	>50	
67°N 20°W	sediment (Bq/kg dw)	1.1×10^{-6}	6.9×10^{-4}	3.2×10^{-4}	1×10^{-6}	2.1×10^{-10}
(Iceland Sea)	(Bq/m²)	8.2×10^{-5}	1×10^{-1}	1.6×10^{-2}	7.1×10^{-5}	9.3×10^{-8}
	time to max (a)	460	1000	45.4	>50	34
70°N 175°W	sediment (Bq/kg dw)	1.9×10^{-6}	2.5×10^{-3}	2.7×10^{-4}	9.8×10^{-8}	9.1×10^{-11}
(Chukchi Sea)	(Bq/m²)	1.4×10^{-4}	3.6×10^{-1}	1.3×10^{-2}	6.9×10^{-6}	3.7×10^{-8}
	time to max (a)	430	1000	27.5	>50	37

TABLE I-XIXd. ^{239}Pu CONCENTRATIONS IN SEDIMENT AT DISTANT ENDPOINTS, CONTINUOUS RELEASE 1 TBq PER YEAR FOR 10 YEARS, SOURCE LOCATION: ABRASIMOV FJORD

Area		MAFF	KEMA	MEL box	Nihon U.
70.5°N 143°W	sediment (Bq/kg dw)	5.7×10^{-3}		5.8×10^{-5}	6×10^{-9}
(Beaufort Sea)	(Bq/m²)	8.2×10^{-1}		4.1×10^{-3}	2.4×10^{-6}
	time to max (a)	1000		>50	48
86°N 80°E	sediment (Bq/kg dw)	8.3×10^{-3}		1.4×10^{-4}	3.1×10^{-10}
(Central Arctic)	(Bq/m²)	1.2		9.6×10^{-3}	1.3×10^{-7}
	time to max (a)	1000		>50	57
60°N 55°W	sediment (Bq/kg dw)	4.4×10^{-3}	3×10^{-3}	1.3×10^{-5}	
(Davis Strait)	(Bq/m²)	6.4×10^{-1}	1.5×10^{-1}	9.4×10^{-4}	
	time to max (a)	1000	50	>50	
67°N 20°W	sediment (Bq/kg dw)	6.9×10^{-3}	1.6×10^{-3}	9.1×10^{-5}	2.3×10^{-9}
(Iceland Sea)	(Bq/m²)	1	8×10^{-2}	6.4×10^{-3}	9.2×10^{-7}
	time to max (a)	1000	50.6	>50	39
70°N 175°W	sediment (Bq/kg dw)	2.5×10^{-2}	1.3×10^{-3}	8.7×10^{-6}	9.1×10^{-10}
(Chukchi Sea)	(Bq/m²)	3.6	6.5×10^{-2}	6.1×10^{-4}	3.7×10^{-7}
	time to max (a)	1000	33	>50	43

TABLE I-XXa. ^{239}Pu CONCENTRATIONS IN WATER AT DISTANT ENDPOINTS, SOURCE LOCATION: NOVAYA ZEMLYA TROUGH, INSTANTANEOUS RELEASE 1 TBq

Area		Risø	MAFF	MEL box	Nihon U.	KEMA
70.5°N 143°W	water (Bq/m³)	2.8×10^{-6}	1.5×10^{-5}	7.8×10^{-6}	1.5×10^{-16}	7.2×10^{-5}
(Beaufort Sea)	time to max (a)	10	40	29	69	21
86°N 80°E	water (Bq/m³)	6.9×10^{-6}	8.1×10^{-5}	2.9×10^{-5}	4.4×10^{-10}	1.7×10^{-4}
(Central Arctic)	time to max (a)	10	13	17	1	6.8
60°N 55°W	water (Bq/m³)	5.8×10^{-7}	4.8×10^{-6}	2.1×10^{-6}		6.1×10^{-5}
(Davis Strait)	time to max (a)	20	220	40		30.3
67°N 20°W	water (Bq/m³)	2.3×10^{-6}	4.6×10^{-5}	1.4×10^{-5}	4.5×10^{-18}	1.4×10^{-4}
(Iceland Sea)	time to max (a)	10	27	12	9	10.1
70°N 175°W	water (Bq/m³)	1.5×10^{-6}	7.1×10^{-4}	1.6×10^{-7}	2.3×10^{-19}	3.9×10^{-5}
(Chukchi Sea)	time to max (a)	10	13	34	7	23.2

TABLE I-XXb. ^{239}Pu CONCENTRATIONS IN WATER AT DISTANT ENDPOINTS, CONTINUOUS RELEASE 1 TBq PER YEAR FOR 10 YEARS, SOURCE LOCATION: NOVAYA ZEMLYA TROUGH

Area		MAFF	MEL box	Nihon U.	KEMA
70.5°N 143°W	water (Bq/m³)	1.5×10^{-4}	7.5×10^{-4}	8×10^{-15}	3.5×10^{-4}
(Beaufort Sea)	time to max (a)	46	34	73	26.5
86°N 80°E	water (Bq/m³)	7.9×10^{-4}	1.6×10^{-3}	3.4×10^{-9}	8.2×10^{-4}
(Central Arctic)	time to max (a)	19	23	10	13
60°N 55°W	water (Bq/m³)	4.8×10^{-5}	2.0×10^{-5}		3×10^{-4}
(Davis Strait)	time to max (a)	230	45		35.6
67°N 20°W	water (Bq/m³)	4.6×10^{-4}	1.4×10^{-4}	1.5×10^{-16}	6.6×10^{-4}
(Iceland Sea)	time to max (a)	32	18	15	16
70°N 175°W	water (Bq/m³)	6.7×10^{-3}	1.5×10^{-6}	8.2×10^{-18}	1.9×10^{-4}
(Chukchi Sea)	time to max (a)	19	39	14	28.6

TABLE I-XXc. ^{239}Pu CONCENTRATIONS IN SEDIMENT AT DISTANT ENDPOINTS, SOURCE LOCATION: NOVAYA ZEMLYA TROUGH, INSTANTANEOUS RELEASE 1 TBq

Area		Risø	MAFF	MEL box	Nihon U.	KEMA
70.5°N 143°W	sediment (Bq/kg dw)	3.8×10^{-6}	5.8×10^{-4}	4.3×10^{-6}	1.6×10^{-17}	
(Beaufort Sea)	(Bq/m²)	2.8×10^{-4}	8.3×10^{-2}	3×10^{-4}	6.4×10^{-15}	
	time to max (a)	500	1000	>50	1000	
86°N 80°E	sediment (Bq/kg dw)	3.9×10^{-6}	8.3×10^{-4}	9.3×10^{-6}	5×10^{-13}	
(Central Arctic)	(Bq/m²)	2.9×10^{-4}	1.2×10^{-1}	6.5×10^{-4}	2×10^{-10}	
	time to max (a)	500	1000	>50	1000	
60°N 55°W	sediment (Bq/kg dw)	1.5×10^{-6}	4.6×10^{-4}	1×10^{-6}		6.7×10^{-4}
(Davis Strait)	(Bq/m²)	1.1×10^{-4}	6.6×10^{-2}	7×10^{-5}		3.3×10^{-2}
	time to max (a)	500	1000	>50		41.1
67°N 20°W	sediment (Bq/kg dw)	2×10^{-6}	6.9×10^{-4}	6.1×10^{-6}	1.1×10^{-18}	3.6×10^{-4}
(Iceland Sea)	(Bq/m²)	1.5×10^{-4}	1×10^{-1}	4.3×10^{-4}	4.5×10^{-16}	1.8×10^{-2}
	time to max (a)	600	1000	>50	1000	42.2
70°N 175°W	sediment (Bq/kg dw)	3.5×10^{-6}	2.5×10^{-3}	4.4×10^{-7}	1.3×10^{-20}	3.1×10^{-4}
(Chukchi Sea)	(Bq/m²)	2.6×10^{-4}	3.6×10^{-1}	3.1×10^{-5}	5.3×10^{-18}	1.5×10^{-2}
	time to max (a)	500	1000	>50	1000	24.3

TABLE I-XXd. ^{239}Pu CONCENTRATIONS IN SEDIMENT AT DISTANT ENDPOINTS, CONTINUOUS RELEASE 1 TBq PER YEAR FOR 10 YEARS, SOURCE LOCATION: NOVAYA ZEMLYA TROUGH

Area		MAFF	MEL box	Nihon U.	KEMA
70.5°N 143°W	sediment (Bq/kg dw)	5.8×10^{-3}	3.7×10^{-4}	1.7×10^{-16}	
(Beaufort Sea)	(Bq/m²)	8.3×10^{-1}	2.6×10^{-2}	6.8×10^{-14}	
	time to max (a)	1000	>50	1000	
86°N 80°E	sediment (Bq/kg dw)	8.3×10^{-3}	8.5×10^{-5}	5.5×10^{-12}	
(Central Arctic)	(Bq/m²)	1.2	6×10^{-3}	2.2×10^{-9}	
	time to max (a)	1000	>50	1000	
60°N 55°W	sediment (Bq/kg dw)	4.5×10^{-3}	8.3×10^{-6}		3.6×10^{-3}
(Davis Strait)	(Bq/m²)	6.5×10^{-1}	5.8×10^{-4}		1.8×10^{-1}
	time to max (a)	1000	>50		46.1
67°N 20°W	sediment (Bq/kg dw)	6.9×10^{-3}	2.7×10^{-5}	3.7×10^{-19}	1.8×10^{-3}
(Iceland Sea)	(Bq/m²)	1	3.9×10^{-3}	1.5×10^{-16}	9×10^{-2}
	time to max (a)	1000	>50	15	47.5
70°N 175°W	sediment (Bq/kg dw)	2.5×10^{-2}	3.7×10^{-6}	1.1×10^{-19}	1.5×10^{-2}
(Chukchi Sea)	(Bq/m²)	3.6	2.6×10^{-4}	5.5×10^{-17}	7.5×10^{-1}
	time to max (a)	1000	>50	1000	30

TABLE I-XXIa. ^{60}Co CONCENTRATIONS IN WATER AT DISTANT ENDPOINTS, SOURCE LOCATION: ABRASIMOV FJORD, INSTANTANEOUS RELEASE 1 TBq

Area		Risø	MAFF	KEMA	MEL box	Nihon U.
70.5°N 143°W (Beaufort Sea)	water (Bq/m^3)	4.4×10^{-7}	7.6×10^{-7}	3.4×10^{-7}	9.2×10^{-8}	6×10^{-35}
	time to max (a)	5	16	6.5	8	16
86°N 80°E (Central Arctic)	water (Bq/m^3)	3.6×10^{-6}	2×10^{-5}	2.6×10^{-6}	1.2×10^{-6}	4.6×10^{-17}
	time to max (a)	2	8.2	2	5	0
60°N 55°W (Davis Strait)	water (Bq/m^3)	6.4×10^{-8}	3.9×10^{-8}	1.3×10^{-7}	1.2×10^{-8}	
	time to max (a)	6	19	10	11	
67°N 20°W (Iceland Sea)	water (Bq/m^3)	9.2×10^{-7}	4.5×10^{-6}	1.3×10^{-6}	3.3×10^{-7}	9.7×10^{-42}
	time to max (a)	3	12	4.2	6	7
70°N 175°W (Chukchi Sea)	water (Bq/m^3)	1.9×10^{-7}	1.4×10^{-4}	1.2×10^{-7}	2.1×10^{-8}	9.3×10^{-41}
	time to max (a)	6	9.7	8.4	3	10

TABLE I-XXIb. ^{60}Co CONCENTRATIONS IN WATER AT DISTANT ENDPOINTS, CONTINUOUS RELEASE 1 TBq PER YEAR FOR 10 YEARS, SOURCE LOCATION: ABRASIMOV FJORD

Area		Risø	MAFF	KEMA	MEL box	Nihon U.
70.5°N 143°W (Beaufort Sea)	water (Bq/m^3)	2.9×10^{-6}	7.1×10^{-6}	1.5×10^{-6}	8×10^{-6}	4.9×10^{-34}
	time to max (a)	12	21	12.6	13	22
86°N 80°E (Central Arctic)	water (Bq/m^3)	1.5×10^{-5}	1.7×10^{-4}	8.8×10^{-6}	7.9×10^{-5}	1.4×10^{-17}
	time to max (a)	10	14	10	10	10
60°N 55°W (Davis Strait)	water (Bq/m^3)	5×10^{-7}	3.7×10^{-7}	5.8×10^{-7}	1.1×10^{-6}	
	time to max (a)	13	24	16	17	
67°N 20°W (Iceland Sea)	water (Bq/m^3)	4.1×10^{-6}	4.1×10^{-5}	5.1×10^{-6}	2.7×10^{-5}	7.1×10^{-41}
	time to max (a)	12	18	12.1	12	15
70°N 175°W (Chukchi Sea)	water (Bq/m^3)	1.4×10^{-6}	1.2×10^{-3}	5.6×10^{-7}	6.4×10^{-7}	6.6×10^{-40}
	time to max (a)	13	16	14.5	12	16

TABLE I-XXIc. ^{60}Co CONCENTRATIONS IN SEDIMENT AT DISTANT ENDPOINTS, SOURCE LOCATION: ABRASIMOV FJORD, INSTANTANEOUS RELEASE 1 TBq

Area		Risø	MAFF	KEMA	MEL box	Nihon U.
70.5°N 143°W (Beaufort Sea)	sediment (Bq/kg dw)	1.5×10^{-8}	4.9×10^{-7}		1.3×10^{-8}	4.2×10^{-36}
	(Bq/m^2)	1.1×10^{-6}	7×10^{-5}		9.3×10^{-7}	1.7×10^{-33}
	time to max (a)	14	22		14	18
86°N 80°E (Central Arctic)	sediment (Bq/kg dw)	1.3×10^{-8}	1×10^{-5}		1.2×10^{-7}	2.1×10^{-17}
	(Bq/m^2)	9.7×10^{-7}	1.5×10^{-3}		8.4×10^{-6}	8.3×10^{-15}
	time to max (a)	12	14		11	4
60°N 55°W (Davis Strait)	sediment (Bq/kg dw)	1.2×10^{-8}	2.6×10^{-8}	1.1×10^{-6}	2×10^{-9}	
	(Bq/m^2)	9×10^{-7}	3.8×10^{-6}	5.5×10^{-5}	1.4×10^{-7}	
	time to max (a)	12	26	14.2	18	
67°N 20°W (Iceland Sea)	sediment (Bq/kg dw)	5.3×10^{-8}	2.8×10^{-6}	1.5×10^{-6}	4.3×10^{-8}	6.2×10^{-40}
	(Bq/m^2)	4×10^{-6}	4×10^{-4}	7.5×10^{-5}	3×10^{-6}	2.7×10^{-37}
	time to max (a)	8	19	9.1	12	10
70°N 175°W (Chukchi Sea)	sediment (Bq/kg dw)	1.5×10^{-8}	1×10^{-4}	1.4×10^{-6}	5.4×10^{-9}	2.7×10^{-42}
	(Bq/m^2)	1.1×10^{-6}	1.5×10^{-2}	7×10^{-5}	3.8×10^{-7}	1.1×10^{-39}
	time to max (a)	15	15	9.4	4	12

TABLE I-XXId. ^{60}Co CONCENTRATIONS IN SEDIMENT AT DISTANT ENDPOINTS, CONTINUOUS RELEASE 1 TBq PER YEAR FOR 10 YEARS, SOURCE LOCATION: ABRASIMOV FJORD

Area		Risø	MAFF	KEMA	MEL box	Nihon U.
70.5°N 143°W (Beaufort Sea)	sediment (Bq/kg dw)	1.4×10^{-7}	4.6×10^{-6}		1.2×10^{-6}	3.2×10^{-35}
	(Bq/m^2)	1×10^{-5}	6.7×10^{-4}		8.5×10^{-5}	1.4×10^{-32}
	time to max (a)	20	27		20	24
86°N 80°E (Central Arctic)	sediment (Bq/kg dw)	1.2×10^{-7}	9.7×10^{-5}		1×10^{-5}	1.2×10^{-16}
	(Bq/m^2)	9×10^{-6}	1.4×10^{-2}		7.4×10^{-4}	5×10^{-14}
	time to max (a)	18	20		14	11
60°N 55°W (Davis Strait)	sediment (Bq/kg dw)	1.1×10^{-7}	2.6×10^{-7}	5×10^{-6}	1.7×10^{-7}	
	(Bq/m^2)	8.2×10^{-6}	3.7×10^{-5}	2.5×10^{-4}	1.2×10^{-5}	
	time to max (a)	18	31	20	23	
67°N 20°W (Iceland Sea)	sediment (Bq/kg dw)	4.7×10^{-7}	2.6×10^{-5}	6.6×10^{-6}	3.8×10^{-6}	5.5×10^{-39}
	(Bq/m^2)	3.5×10^{-5}	3.8×10^{-3}	3.3×10^{-4}	2.7×10^{-4}	2.2×10^{-36}
	time to max (a)	13	24	15.4	17	17
70°N 175°W (Chukchi Sea)	sediment (Bq/kg dw)	1.4×10^{-7}	9.7×10^{-4}	6.3×10^{-6}	4.1×10^{-7}	2.1×10^{-41}
	(Bq/m^2)	1×10^{-5}	1.4×10^{-1}	3.1×10^{-4}	2.9×10^{-5}	8.4×10^{-39}
	time to max (a)	22	21	15.3	13	18

TABLE I-XXIIa. ^{60}Co CONCENTRATIONS IN WATER AT DISTANT ENDPOINTS, SOURCE LOCATION: NOVAYA ZEMLYA TROUGH, INSTANTANEOUS RELEASE 1 TBq

Area		Risø	MAFF	MEL box	Nihon U.	KEMA
70.5°N 143°W	water (Bq/m^3)	4.4×10^{-7}	9.6×10^{-7}	8.5×10^{-7}	2.1×10^{-35}	5.8×10^{-7}
(Beaufort Sea)	time to max (a)	7	14	7	16	4.4
86°N 80°E	water (Bq/m^3)	2.8×10^{-6}	2.5×10^{-5}	1.2×10^{-5}	1.6×10^{-17}	7.7×10^{-6}
(Central Arctic)	time to max (a)	3	6.7	4	0	0.2
60°N 55°W	water (Bq/m^3)	6.8×10^{-8}	4.8×10^{-8}	1.1×10^{-7}		2.1×10^{-7}
(Davis Strait)	time to max (a)	8	18	11		8
67°N 20°W	water (Bq/m^3)	7.6×10^{-7}	5.7×10^{-6}	2.9×10^{-6}	3.2×10^{-42}	2.6×10^{-6}
(Iceland Sea)	time to max (a)	4.5	11	5	7	2.5
70°N 175°W	water (Bq/m^3)	2×10^{-7}	1.8×10^{-4}	1.3×10^{-8}	3.2×10^{-41}	2.1×10^{-7}
(Chukchi Sea)	time to max (a)	8	8.5	3	10	6.4

TABLE I-XXIIb. ^{60}Co CONCENTRATIONS IN WATER AT DISTANT ENDPOINTS, CONTINUOUS RELEASE 1 TBq PER YEAR FOR 10 YEARS, SOURCE LOCATION: NOVAYA ZEMLYA TROUGH

Area		Risø	MAFF	MEL box	Nihon U.	KEMA
70.5°N 143°W	water (Bq/m^3)	3.4×10^{-6}	8.9×10^{-6}	7.3×10^{-5}	1.7×10^{-34}	2.4×10^{-6}
(Beaufort Sea)	time to max (a)	13	20	13	22	11.1
86°N 80°E	water (Bq/m^3)	1.8×10^{-5}	2.1×10^{-4}	7.3×10^{-4}	4.8×10^{-18}	1.4×10^{-5}
(Central Arctic)	time to max (a)	12	13	12	10	10
60°N 55°W	water (Bq/m^3)	5.7×10^{-7}	4.6×10^{-7}	9.4×10^{-6}		9.3×10^{-7}
(Davis Strait)	time to max (a)	14	23	16		14
67°N 20°W	water (Bq/m^3)	4.8×10^{-6}	5.2×10^{-5}	2.3×10^{-4}	2.4×10^{-41}	8.5×10^{-6}
(Iceland Sea)	time to max (a)	12	17	12	15	10.3
70°N 175°W	water (Bq/m^3)	1.6×10^{-6}	1.5×10^{-3}	1×10^{-6}	2.2×10^{-40}	9×10^{-7}
(Chukchi Sea)	time to max (a)	14	15	11	16	12.6

TABLE I-XXIIc. ^{60}Co CONCENTRATIONS IN SEDIMENT AT DISTANT ENDPOINTS, SOURCE LOCATION: NOVAYA ZEMLYA TROUGH, INSTANTANEOUS RELEASE 1 TBq

Area		Risø	MAFF	MEL box	Nihon U.	KEMA
70.5°N 143°W	sediment (Bq/kg dw)	1.8×10^{-8}	6×10^{-7}	1.2×10^{-7}	1.4×10^{-36}	
(Beaufort Sea)	(Bq/m^2)	1.3×10^{-6}	8.7×10^{-5}	8.5×10^{-6}	5.7×10^{-34}	
	time to max (a)	17	21	14	18	
86°N 80°E	sediment (Bq/kg dw)	1.6×10^{-8}	1.3×10^{-5}	1.1×10^{-6}	7×10^{-18}	
(Central Arctic)	(Bq/m^2)	1.2×10^{-6}	1.9×10^{-3}	7.8×10^{-5}	2.8×10^{-15}	
	time to max (a)	15	13	11	4	
60°N 55°W	sediment (Bq/kg dw)	1.4×10^{-4}	3.3×10^{-8}	1.7×10^{-8}		1.7×10^{-6}
(Davis Strait)	(Bq/m^2)	1×10^{-2}	4.7×10^{-6}	1.2×10^{-6}		8.5×10^{-5}
	time to max (a)	14	25	17		12.3
67°N 20°W	sediment (Bq/kg dw)	6×10^{-8}	3.4×10^{-6}	3.7×10^{-7}	2.2×10^{-40}	2.4×10^{-6}
(Iceland Sea)	(Bq/m^2)	4.5×10^{-6}	4.9×10^{-4}	2.6×10^{-5}	8.7×10^{-38}	1.2×10^{-4}
	time to max (a)	10	17	11	10	7.4
70°N 175°W	sediment (Bq/kg dw)	1.8×10^{-8}	1.3×10^{-4}	7.4×10^{-9}	9×10^{-43}	2.3×10^{-6}
(Chukchi Sea)	(Bq/m^2)	1.3×10^{-6}	1.9×10^{-2}	5.2×10^{-7}	3.6×10^{-40}	1.1×10^{-4}
	time to max (a)	18	14	12	12	7.4

TABLE I-XXIId. ^{60}Co CONCENTRATIONS IN SEDIMENT AT DISTANT ENDPOINTS, CONTINUOUS RELEASE 1 TBq PER YEAR FOR 10 YEARS, SOURCE LOCATION: NOVAYA ZEMLYA TROUGH

Area		Risø	MAFF	MEL box	Nihon U.	KEMA
70.5°N 143°W	sediment (Bq/kg dw)	1.7×10^{-7}	5.8×10^{-6}	1.1×10^{-5}	1.2×10^{-35}	
(Beaufort Sea)	(Bq/m^2)	1.3×10^{-5}	8.4×10^{-4}	7.8×10^{-4}	4.9×10^{-33}	
	time to max (a)	22	26	19	24	
86°N 80°E	sediment (Bq/kg dw)	1.5×10^{-7}	1.2×10^{-4}	1.1×10^{-4}	4.2×10^{-17}	
(Central Arctic)	(Bq/m^2)	1.1×10^{-5}	1.8×10^{-2}	7.8×10^{-3}	1.7×10^{-14}	
	time to max (a)	20	18	16	11	
60°N 55°W	sediment (Bq/kg dw)	1.3×10^{-7}	3.2×10^{-7}	1.6×10^{-6}		7.9×10^{-6}
(Davis Strait)	(Bq/m^2)	9.7×10^{-6}	4.6×10^{-5}	1.1×10^{-4}		3.9×10^{-4}
	time to max (a)	20	30	23		18
67°N 20°W	sediment (Bq/kg dw)	5.5×10^{-7}	3.3×10^{-5}	3.3×10^{-5}	1.8×10^{-39}	1.1×10^{-5}
(Iceland Sea)	(Bq/m^2)	4.1×10^{-5}	4.7×10^{-3}	2.3×10^{-3}	7.4×10^{-37}	5.5×10^{-4}
	time to max (a)	17	23	17	17	13.6
70°N 175°W	sediment (Bq/kg dw)	1.7×10^{-7}	1.2×10^{-3}	6.7×10^{-7}	7×10^{-42}	1×10^{-5}
(Chukchi Sea)	(Bq/m^2)	1.3×10^{-5}	1.7×10^{-1}	4.7×10^{-5}	2.8×10^{-39}	5×10^{-4}
	time to max (a)	23	21	18	18	13.5

TABLE I-XXIIIa. ^{99}Tc CONCENTRATIONS IN WATER AT DISTANT ENDPOINTS, SOURCE LOCATION: ABRASIMOV FJORD, INSTANTANEOUS RELEASE 1 TBq

Area		Risø	MAFF	KEMA	MEL box	Nihon U.
70.5°N 143°W	water (Bq/m^3)	4.7×10^{-5}	1.9×10^{-5}	8.8×10^{-5}	2.9×10^{-5}	1×10^{-4}
(Beaufort Sea)	time to max (a)	15	26	16.5	37	131
86°N 80°E	water (Bq/m^3)	1.4×10^{-4}	9.6×10^{-5}	2.7×10^{-4}	7.2×10^{-5}	4.2×10^{-4}
(Central Arctic)	time to max (a)	7	11	5.2	24	15
60°N 55°W	water (Bq/m^3)	1.2×10^{-5}	6×10^{-6}	7.8×10^{-5}	7.3×10^{-6}	
(Davis Strait)	time to max (a)	33	510	25	50	
67°N 20°W	water (Bq/m^3)	3.6×10^{-5}	5.3×10^{-5}	2.1×10^{-4}	4.3×10^{-5}	4.2×10^{-5}
(Iceland Sea)	time to max (a)	8	25	8.3	20	50
70°N 175°W	water (Bq/m^3)	3.2×10^{-5}	2.2×10^{-3}	4.9×10^{-5}	2.3×10^{-5}	8.4×10^{-5}
(Chukchi Sea)	time to max (a)	25	8	17	11	184

TABLE I-XXIIIb. ^{99}Tc CONCENTRATIONS IN WATER AT DISTANT ENDPOINTS, CONTINUOUS RELEASE 1 TBq PER YEAR FOR 10 YEARS, SOURCE LOCATION: ABRASIMOV FJORD

Area		Risø	MAFF	KEMA	MEL box	Nihon U.
70.5°N 143°W	water (Bq/m^3)	4.6×10^{-4}	1.9×10^{-4}	4.3×10^{-4}	2.8×10^{-4}	1×10^{-3}
(Beaufort Sea)	time to max (a)	20	32	22.1	42	136
86°N 80°E	water (Bq/m^3)	1.1×10^{-3}	9.2×10^{-4}	1.2×10^{-3}	6.9×10^{-4}	4.1×10^{-3}
(Central Arctic)	time to max (a)	20	18	12	30	21
60°N 55°W	water (Bq/m^3)	1.2×10^{-4}	6×10^{-5}	3.8×10^{-4}	7.3×10^{-5}	
(Davis Strait)	time to max (a)	40	520	30.5	55	
67°N 20°W	water (Bq/m^3)	3.1×10^{-4}	5.3×10^{-4}	9.2×10^{-4}	4.2×10^{-4}	4.1×10^{-4}
(Iceland Sea)	time to max (a)	20	31	14.5	25	55
70°N 175°W	water (Bq/m^3)	3.2×10^{-4}	1.8×10^{-2}	2.3×10^{-4}	2×10^{-4}	8.4×10^{-4}
(Chukchi Sea)	time to max (a)	30	14	22.8	16	181

TABLE I-XXIIIc. ^{99}Tc CONCENTRATIONS IN SEDIMENT AT DISTANT ENDPOINTS, SOURCE LOCATION: ABRASIMOV FJORD, INSTANTANEOUS RELEASE 1 TBq

Area		Risø	MAFF	KEMA	MEL box	Nihon U.
70.5°N 143°W	sediment (Bq/kg dw)	$>2.4 \times 10^{-8}$	4×10^{-5}		6.1×10^{-8}	1×10^{-8}
(Beaufort Sea)	(Bq/m^2)	$>1.8 \times 10^{-6}$	5.8×10^{-3}		4.3×10^{-6}	4×10^{-6}
	time to max (a)	>100	140		>100	140
86°N 80°E	sediment (Bq/kg dw)	$>2.3 \times 10^{-8}$	1×10^{-4}		6.7×10^{-8}	2.5×10^{-9}
(Central Arctic)	(Bq/m^2)	$>1.7 \times 10^{-6}$	1.5×10^{-2}		4.7×10^{-6}	1.1×10^{-6}
	time to max (a)	>100	66		>100	976
60°N 55°W	sediment (Bq/kg dw)	8.1×10^{-9}	2.5×10^{-5}	8.2×10^{-7}	2.1×10^{-8}	
(Davis Strait)	(Bq/m^2)	6.1×10^{-7}	3.6×10^{-3}	4.1×10^{-5}	1.5×10^{-6}	
	time to max (a)	76	790	28.3	>100	
67°N 20°W	sediment (Bq/kg dw)	1.3×10^{-8}	1.5×10^{-4}	7.5×10^{-7}	5.4×10^{-8}	3.5×10^{-9}
(Iceland Sea)	(Bq/m^2)	9.7×10^{-7}	1.1×10^{-2}	3.7×10^{-5}	3.8×10^{-6}	1.4×10^{-6}
	time to max (a)	57	81	22.3	>100	60
70°N 175°W	sediment (Bq/kg dw)	2.2×10^{-8}	9×10^{-4}	4.9×10^{-7}	6.4×10^{-8}	8×10^{-9}
(Chukchi Sea)	(Bq/m^2)	1.6×10^{-6}	1.3×10^{-1}	2.4×10^{-5}	4.5×10^{-6}	3.3×10^{-6}
	time to max (a)	88	23	17.3	>100	184

TABLE I-XXIIId. ^{99}Tc CONCENTRATIONS IN SEDIMENT AT DISTANT ENDPOINTS, CONTINUOUS RELEASE 1 TBq PER YEAR FOR 10 YEARS, SOURCE LOCATION: ABRASIMOV FJORD

Area		Risø	MAFF	KEMA	MEL box	Nihon U.
70.5°N 143°W	sediment (Bq/kg dw)	2.4×10^{-7}	4×10^{-4}		6.1×10^{-7}	2.1×10^{-7}
(Beaufort Sea)	(Bq/m^2)	1.8×10^{-5}	5.8×10^{-2}		4.3×10^{-5}	8.5×10^{-5}
	time to max (a)	100	140		>100	100
86°N 80°E	sediment (Bq/kg dw)	2.3×10^{-7}	1×10^{-3}		6.7×10^{-7}	1.2×10^{-6}
(Central Arctic)	(Bq/m^2)	1.7×10^{-5}	1.5×10^{-1}		4.7×10^{-5}	4.9×10^{-4}
	time to max (a)	120	70		>100	20
60°N 55°W	sediment (Bq/kg dw)	8.1×10^{-8}	2.5×10^{-4}	4.1×10^{-6}	2.1×10^{-7}	
(Davis Strait)	(Bq/m^2)	6.1×10^{-6}	3.6×10^{-2}	2×10^{-4}	1.5×10^{-5}	
	time to max (a)	80	800	34	>100	
67°N 20°W	sediment (Bq/kg dw)	1.3×10^{-7}	7.6×10^{-4}	3.7×10^{-6}	5.4×10^{-7}	6.1×10^{-8}
(Iceland Sea)	(Bq/m^2)	9.7×10^{-6}	1.1×10^{-1}	1.8×10^{-4}	3.8×10^{-5}	2.5×10^{-5}
	time to max (a)	60	86	28	>100	50
70°N 175°W	sediment (Bq/kg dw)	2.2×10^{-7}	9×10^{-3}	2.4×10^{-6}	6.3×10^{-7}	1.6×10^{-7}
(Chukchi Sea)	(Bq/m^2)	1.6×10^{-5}	1.3	1.2×10^{-4}	4.4×10^{-5}	6.6×10^{-5}
	time to max (a)	100	29	23	>100	100

TABLE I-XXIVa. ^{99}Tc CONCENTRATIONS IN WATER AT DISTANT ENDPOINTS, SOURCE LOCATION: NOVAYA ZEMLYA TROUGH, INSTANTANEOUS RELEASE 1 TBq

Area		Risø	MAFF	MEL box	Nihon U.	KEMA
70.5°N 143°W	water (Bq/m^3)	4.3×10^{-5}	1.9×10^{-5}	2.8×10^{-5}	9.9×10^{-5}	8.8×10^{-5}
(Beaufort Sea)	time to max (a)	20	26	35	134	16
86°N 80°E	water (Bq/m^3)	1.1×10^{-4}	9.6×10^{-5}	8×10^{-5}	4×10^{-4}	2.8×10^{-4}
(Central Arctic)	time to max (a)	10	11	20	15	4.6
60°N 55°W	water (Bq/m^3)	1.2×10^{-5}	6×10^{-6}	7.4×10^{-6}		7.8×10^{-5}
(Davis Strait)	time to max (a)	40	460	47		24.6
67°N 20°W	water (Bq/m^3)	2.9×10^{-5}	5.3×10^{-5}	4.5×10^{-5}	3.9×10^{-5}	2.1×10^{-4}
(Iceland Sea)	time to max (a)	20	25	17	50	7.7
70°N 175°W	water (Bq/m^3)	3.2×10^{-5}	2.2×10^{-3}	8×10^{-6}	8.1×10^{-5}	4.9×10^{-5}
(Chukchi Sea)	time to max (a)	30	7.5	13	178	16.3

TABLE I-XXIVb. ^{99}Tc CONCENTRATIONS IN WATER AT DISTANT ENDPOINTS, CONTINUOUS RELEASE 1 TBq PER YEAR FOR 10 YEARS, SOURCE LOCATION: NOVAYA ZEMLYA TROUGH

Area		Risø	MAFF	MEL box	Nihon U.	KEMA
70.5°N 143°W	water (Bq/m^3)	4.3×10^{-4}	1.9×10^{-4}	2.8×10^{-4}	1×10^{-3}	4.3×10^{-4}
(Beaufort Sea)	time to max (a)	30	32	40	136	21.5
86°N 80°E	water (Bq/m^3)	1.1×10^{-3}	9.3×10^{-4}	7.5×10^{-4}	4.1×10^{-3}	1.2×10^{-3}
(Central Arctic)	time to max (a)	20	17	27	21	11.3
60°N 55°W	water (Bq/m^3)	1.2×10^{-4}	6×10^{-5}	7.4×10^{-5}		3.8×10^{-4}
(Davis Strait)	time to max (a)	40	470	52		30
67°N 20°W	water (Bq/m^3)	2.9×10^{-4}	5.3×10^{-4}	4.4×10^{-4}	4.1×10^{-4}	9.2×10^{-4}
(Iceland Sea)	time to max (a)	20	30	22	55	14
70°N 175°W	water (Bq/m^3)	3.2×10^{-4}	1.8×10^{-2}	7.3×10^{-5}	8.4×10^{-4}	2.4×10^{-4}
(Chukchi Sea)	time to max (a)	40	14	19	181	22

TABLE I-XXIVc. ^{99}Tc CONCENTRATIONS IN SEDIMENT AT DISTANT ENDPOINTS, SOURCE LOCATION: NOVAYA ZEMLYA TROUGH, INSTANTANEOUS RELEASE 1 TBq

Area		Risø	MAFF	MEL box	Nihon U.	KEMA
70.5°N 143°W	sediment (Bq/kg dw)	2.4×10^{-8}	4.1×10^{-5}	6.1×10^{-8}	9.7×10^{-9}	
(Beaufort Sea)	(Bq/m^2)	1.8×10^{-6}	5.9×10^{-3}	4.3×10^{-6}	3.9×10^{-6}	
	time to max (a)	100	140	>100	142	
86°N 80°E	sediment (Bq/kg dw)	2.3×10^{-8}	1×10^{-4}	6.8×10^{-8}	2.7×10^{-9}	
(Central Arctic)	(Bq/m^2)	1.7×10^{-6}	1.5×10^{-2}	4.8×10^{-6}	1.1×10^{-6}	
	time to max (a)	100	65	>100	978	
60°N 55°W	sediment (Bq/kg dw)	8.1×10^{-9}	2.5×10^{-5}	2.1×10^{-8}		8.2×10^{-7}
(Davis Strait)	(Bq/m^2)	6.1×10^{-7}	3.6×10^{-3}	1.5×10^{-6}		4.1×10^{-5}
	time to max (a)	80	780	>100		28
67°N 20°W	sediment (Bq/kg dw)	1.3×10^{-8}	7.6×10^{-5}	5.4×10^{-8}	3.2×10^{-9}	7.5×10^{-7}
(Iceland Sea)	(Bq/m^2)	9.7×10^{-7}	1.1×10^{-2}	3.8×10^{-6}	1.3×10^{-6}	3.7×10^{-5}
	time to max (a)	60	80	>100	61	21.6
70°N 175°W	sediment (Bq/kg dw)	2.2×10^{-8}	9×10^{-4}	4.8×10^{-8}	8×10^{-9}	4.9×10^{-7}
(Chukchi Sea)	(Bq/m^2)	1.6×10^{-6}	1.3×10^{-1}	3.4×10^{-6}	3.2×10^{-6}	2.4×10^{-5}
	time to max (a)	90	22	>100	187	16.5

TABLE I-XXIVd. ^{99}Tc CONCENTRATIONS IN SEDIMENT AT DISTANT ENDPOINTS, CONTINUOUS RELEASE 1 TBq PER YEAR FOR 10 YEARS, SOURCE LOCATION: NOVAYA ZEMLYA TROUGH

Area		Risø	MAFF	MEL box	Nihon U.	KEMA
70.5°N 143°W	sediment (Bq/kg dw)	2.4×10^{-7}	4.1×10^{-4}	6.1×10^{-7}	1×10^{-7}	
(Beaufort Sea)	(Bq/m^2)	1.8×10^{-5}	5.9×10^{-2}	4.3×10^{-5}	4×10^{-5}	
	time to max (a)	110	140	>100	147	
86°N 80°E	sediment (Bq/kg dw)	2.3×10^{-7}	1×10^{-3}	6.8×10^{-7}	2.7×10^{-8}	
(Central Arctic)	(Bq/m^2)	1.7×10^{-5}	1.5×10^{-1}	4.8×10^{-5}	1.1×10^{-5}	
	time to max (a)	120	71	>100	983	
60°N 55°W	sediment (Bq/kg dw)	8.1×10^{-8}	2.5×10^{-4}	2.1×10^{-7}		4.1×10^{-6}
(Davis Strait)	(Bq/m^2)	6.1×10^{-6}	3.6×10^{-2}	1.5×10^{-5}		2×10^{-4}
	time to max (a)	90	790	>100		33.3
67°N 20°W	sediment (Bq/kg dw)	1.3×10^{-7}	7.6×10^{-3}	5.4×10^{-7}	3.1×10^{-8}	3.7×10^{-6}
(Iceland Sea)	(Bq/m^2)	9.7×10^{-6}	1.1	3.8×10^{-5}	1.3×10^{-5}	1.8×10^{-4}
	time to max (a)	70	85	>100	66	27.3
70°N 175°W	sediment (Bq/kg dw)	2.2×10^{-7}	9×10^{-3}	4.8×10^{-7}	8.1×10^{-8}	2.4×10^{-6}
(Chukchi Sea)	(Bq/m^2)	1.6×10^{-5}	1.3	3.4×10^{-5}	3.3×10^{-5}	1.2×10^{-4}
	time to max (a)	100	28	>100	192	22.3

REFERENCES

[1] Facts and Problems Related to Radioactive Waste Disposal in the Seas Adjacent to the Territory of the Russian Federation, Materials for a Report by the Governmental Commission on Matters Related to Radioactive Waste Disposal at Sea, Established by Decree No. 613 of the Russian Federation President, Moscow, 24 October 1992 (1993) (Original in Russian, English Translation by International Maritime Organization, LC16/INF.2 (1993)).

[2] A Survey of Artificial Radionuclides in the Kara Sea, Results from the Russian–Norwegian 1992 Expedition to the Barents and Kara Seas, Joint Russian–Norwegian Expert Group for Investigation of Radioactive Contamination in the Northern Seas, Norwegian Radiation Protection Authority, Oslo (1993).

[3] PAVLOV, V.K., "Peculiarities of the formation of structure and modification hydrometeorological processes in the Kara Sea water area", (Proc. Conf. of Radioactivity and Environmental Security in the Oceans, Woods Hole (1993)).

[4] PAVLOV, V.K., Oceanographical description of the Kara and Barents Seas, IAEA-IASAP Working Material No. 2, Arctic and Antarctic Research Institute, St. Petersburg (1994).

[5] IVANOV, V., Sedimentological description of the Barents and Kara Seas, IAEA-IASAP Working Material No. 3, All-Russian Research Institute for Geology and Mineral Resources of the World Oceans, St. Petersburg (1994).

[6] FOYN, L., NIKITIN, A., The Joint Norwegian/Russian Expedition to the Dump Sites for Radioactive Waste in the open Kara Sea, the Tsivolki Fjord and the Stepovogo Fjord. September–October 1993 (cruise report) Bergen (1993).

[7] FOYN, L., NIKITIN, A., Joint Norwegian/Russian Expedition to the Dump Sites for Radioactive Waste in the Abrosimov Fjord and Stepovogo Fjord. August–September 1994 (cruise report) Bergen (1994).

[8] INTERNATIONAL ATOMIC ENERGY AGENCY, Sediment K_ds and Concentration Factors for Radionuclides in the Marine Environment, Technical Reports Series No. 247, IAEA, Vienna (1985).

[9] LOENG, H., Features of the physical oceanographic conditions in the Barents Sea, Polar Research **10** 1 (1991) 5–18.

[10] BLINDHEIM, J., Cascading of Barents Sea bottom water into the Norwegian Sea, Rapp. P-v Reun. Cons. Int. Explor. Mer, **188** (1989) 49–58.

[11] SCHLOSSER, P., SWIFT, J.H., LEWIS, D., "Large-scale circulation of the Arctic Ocean: implications for pollutant transport", Proc. Conf. on Radioactivity and Environmental Security in the Oceans, Woods Hole (1993).

[12] DIETRICH, G., KALLE, W., KRAUSS, W., SIEDLER, G., General Oceanography, J. Wiley & Sons (1975).

[13] INTERNATIONAL ATOMIC ENERGY AGENCY, CRP on Modelling of the Radiological Impact of Radioactive Waste Dumping in the Arctic Seas, Benchmarking Scenario, IAEA-IASAP Working Material No. 7, IAEA, Vienna (1994).

[14] SAZYKINA, T.G., KRYSHEV, I.I., Provision of site specific input data for an assessment of radiological impact of waste dumping into the Barents and Kara Seas, IAEA-IASAP Working Material No. 3, Scientific Production Association "Typhoon", Obninsk (1994).

[15] TIMOFEEV, S.F., Macroplankton of the Kara Sea. A Study on Biology, Morphology and Physiology of Hydrobionts, Apatity, USSR Acad. Sci. Kola Sci. Center Publ. House, Murmansk (1983) (in Russian) 17–22.

[16] MATISOV, G.G. (Ed), Ecology and Bioresources of the Kara Sea, Apatity, USSR Acad. Sci. Kola Sci. Center Publ. House, Murmansk (1989) (in Russian) 1–183.

[17] BORKIN, I.V., OZHIGIN, V.K., SHLEINIK, V.N., "Effect of oceanographical factors on the abundance of the Barents Sea polar cod year classes. The effect of oceanographic conditions on distribution and population dynamics of commercial fish stocks in the Barents Sea", Proc. of the 3rd Soviet-Norwegian Symposium, Murmansk, 26–28 May 1986 (LONG, H., Ed.) Institute of Marine Research, Bergen (1987) 169–180.

[18] KRINITSYN, V.S., Peculiarities of biology and distribution of commercial fish in the Yenisei Gulf. GOSNIORH: Collected Scientific Papers, 296, Moscow (1989) (in Russian) 130–141.

[19] USSR catch limits of sea mammals in the Barents and Kara Seas, 1991–1993. Regulative documents of USSR Ministry of Fisheries, No. 457 (1990), No. 314 (1991); Regulative documents of Fisheries Committee of the Russian Federation, No. 37 (1992) (in Russian).

[20] DOBROVOLSKY, A.D., ZALOGIN, B.S., The USSR Seas, Moscow Univ. Publ. House, Moscow (1982) (in Russian).

[21] Ecology and Biological Resources of the Barents Sea, Nauka, Moscow (1990) (in Russian).

[22] INTERNATIONAL COUNCIL FOR EXPLORATION OF THE SEA, Bull. Stat. Peches Mar. Vol. 70–73, ICES, Copenhagen (1988–1992).

[23] BERENHOIM, B.I., Stocks of invertebrates and prospects of their fishery in the Barents Sea. In: PINRO complex fisheries research in the North Basin: results and outlooks. Selected Papers, PINRO Publ. House, Murmansk (1991) (in Russian) 166–171.

[24] MASLOV, N.A. The bottom-fishes of the Barents Sea and their fisheries. Trudy PINRO, M.-L., VIII, Murmansk (1944) (in Russian).

[25] OZHIGIN, V.K., LUKA, G.I., Some peculiarities of capelin migrations depending on thermal conditions in the Barents Sea. In: Proc. Soviet-Norwegian Symposium on the Barents Sea Capelin, Bergen, Norway, Institute of Marine Research (1985) 135–147.

[26] USSR national economy in 1990: a statistical year-book, Finances and Statistical Publ. House, Moscow (1991) (in Russian).

[27] The Population of the World, Demographic handbook, Moscow (1989) (in Russian).

[28] PEROVA, A.A., "The influence of nutrition on some population groups of the Extreme North", Problems of Hygiene and Physiology of Nutrition (KADYKOV, B.I., Ed.) Publishing House of the Ministry of Public Health of the RSFSR, Leningrad (1960) 76–79 (in Russian).

[29] GUSEV, D.I., Doctoral Dissertation (1967) (unpublished in Russian).

[30] TROITSKAYA, et al., ^{137}Cs and ^{90}Sr in the biosphere of the Extreme North of the USSR, The USSR State Committee of the Utilization of Atomic Energy, Moscow N 80–20 (1980) (in Russian).

[31] Consumption of main food products by the population of Russian Federation, Moscow, State Statistical Committee of Russia (1994).

[32] I think: The visual thinking tool for the 90's. High Performance Systems Inc., 45 Lyme Road, Hanover NH 03755 (1992).

[33] HELING, R., VAN DER STEEN, J., Risks of Unit Discharges of Naturally Occurring Radioactive Matter by Oil and Gas Production Platforms on the Dutch Part of the Continental Shelf, Report KEMA 40287-NUC 94-5752 (1994).

[34] KIRCHNER, T.B., TIME ZERO, The integrated modeling environment, Ecol. Modell., **47** (1989) 33–52.

[35] ROUND, G.D., et al., MIRMAID, The MAFF Irish Sea Model, CEFAS Environmental Tech. Note RL7/98, CEFAS, Lowestoft, UK (1998).

[36] MOBBS, S.F., HILL, M.D., GURBUTT, P.A., SHEPHERD, J.G., KILLWORTH, P.D., "Development of a compartmental model of the ocean" Oceanic processes in marine pollution, Volume 2. Physicochemical processes and wastes in the ocean (O'CONNOR, T.P., BURT, W.V. and DUEDALL, I.W., Eds.) Robert E. Kreiger Publishing Company, Malabar, Florida (1987) 81–89.

[37] AAGARD, K., Synthesis of the Arctic Ocean circulation, Rapp. P-V. Reunion. Cons. Int. Explor. Mer., 188, 11–22 (1989).

[38] SAWYER HOPKINS, T., The GIN Sea – a synthesis of its physical oceanography and literature review 1972–1985, Earth Science Review **30** (1991) 175–138.

[39] COMMISSION OF THE EUROPEAN COMMUNITIES, The radiological exposure of the population of the European Community from radioactivity in the North European marine waters, Project "MARINA", Radiation Protection 47, CEC, Luxembourg (1990).

[40] NUCLEAR ENERGY AGENCY – Organization for Economic Co-operation and Development, Interim oceanographic description of the North-East Atlantic site for the disposal of low-level radioactive waste, NEA-OECD, Paris (1989).

[41] INTERNATIONAL ATOMIC ENERGY AGENCY, International basic safety standards for protection against ionising radiation and for the safety of radiation sources, Safety Series No. 115-I, IAEA, Vienna (1994).

[42] HALLSTADIUS, L., A computer program for the determination of transfer coefficients in a compartment model, Radiation Physics Dept., University of Lund, LUNDFD6/INFRA 3059, Lund (1985).

[43] SCHLOSSER, P., SWIFT, J.H., LEWIS, D., PFIRMAN, S., The role of the large-scale Arctic Ocean circulation in the transport of contaminants, Deep Sea Res. **42** 6 (1995) 1341–1367.

[44] COX, M., A Primitive Equation, 3-Dimensional Model of the Ocean, GFDL Ocean Group Tech. Rep. 1, Geophys. Fluid Dyn. Lab., Princeton, NJ (1984).

[45] SARMIENTO, J.L., BRYAN, K., An ocean transport model for the North Atlantic, J. Geophys. Res., **87** (1982) 395–408.

[46] CHANG, A., PRELLER, R., An ice-ocean coupled model for the Northern Hemisphere, Geophys. Res. Let., **19** (1992) 901–904.

[47] HIBLER, W.D. III, A dynamic thermodynamic sea ice model, J. Phys. Oceanogr. **9** (1979) 815–864.

[48] HIBLER, W.D. III, Modeling a variable thickness sea ice cover, Monthly Weather Review **198** (1980) 1942–1973.

[49] LEVITUS, S., Climatological Atlas of the World Ocean, National Oceanic and Atmospheric Administration Professional Paper 13, US Department of Commerce: NOAA, Washington DC (1982) 173.

[50] AAGAARD, K., CARMACK, E.C., The role of sea ice and other fresh water in the arctic circulation, J. Geophys. Res. **94** (1989) 14485–14498.

[51] SHIKLOMANOV, I., SKAKALSKY, B., "Studying Water, Sediment and Contaminant Runoff of Siberian Rivers: Modern Stats and Prospects", in Proc. Interagency Arctic Research Policy Committee, Workshop on Arctic Contamination, Anchorage, AK, May 2–7 (1993).

[52] BACKHAUS, J.O., A three-dimensional model for the simulation of shelf sea dynamics, Deutsche Hydrographische Zeitschrift, Z. **38** 4 (1985).

[53] HAINBUCKER, D., POHLMAN, T., BACKHAUS, J.O., Transport of conservative passive tracers in the North Sea: First results of a circulation and transport model, Continental Shelf Research, **7** 10 (1987).

[54] POHLMAN, T., BACKHAUS, J.O., HAINBUCHER, D., Validation of a three-dimensional dispersion model for Cs-137 in the North European Sea Shelf, ICES – paper C.M. 1987, Copenhagen (1987).

[55] HARMS, I.H., Watermass transformation in the Barents Sea, Application of the HAMburg Shelf Ocean Model (HAMSOM), ICES – Journal of Marine Science **54** (1997) 351–365.

[56] HARMS, I.H., A numerical study of the barotopic circulation in the Barents and Kara Seas, Continental Sheld Research, **12** 9 (1992).

[57] HARMS, I.H., BACKHAUS, J.O., "Numerical dispersion studies of passive tracers in the Barents and Kara Seas", Proc. of the Second Int. Offshore and Polar Engineering Conf., Golden, Colorado, USA (1992).

[58] STRONACH, J.A., BACKHAUS, J.O., MURTY, T.S., An update on the numerical simulation of oceanographic processes in the waters between Vancouver Island and the mainland: the GF8 model, Oceanogr. Mar. Biol. Ann. Rev. **13**, UCL Press, pp. 1–86 (1993).

[59] HELLERMAN, S., ROSENSTEIN, M., Normal monthly windstress over the world ocean with error estimates, Journal of Physical Oceanography **13** (1983).

[60] GJEVIK, B., STRAUME, T., Model simulations of the M2 and the K1 tides in the Nordic Seas and the Arctic Ocean, Tellus **41 A** 73 (1989).

[61] MILLIGAN, D., Oceanographic survey results: Kara Sea, summer and fall 1965, Technical report, US Naval Oceanographic Officer, Washington DC, TR-217 (1969).

[62] LOENG, H., OZHIGIN, V., AADLANDSVIK, B., SAGAN, H., Current Measurements in the Northeastern Barents Sea, ICES – paper, C.M. **C:41**, Copenhagen (1993).

[63] INTERNATIONAL ATOMIC ENERGY AGENCY, Predicted Radionuclide Release from Marine Reactors Dumped in the Kara Sea, Report of the Source Term Working Group of the International Arctic Seas Assessment Project (IASAP), IAEA-TECDOC-938, IAEA, Vienna (1997).

[64] CIGNA, A., DELFANTI, R., SERRO, E., (Eds), The radiological exposure of the population of the European Community to radioactivity in the Mediterranean Sea, Marina Med. Project, (Proc. Seminar, Roma), EUR 15564, EC, Luxembourg (1994).

[65] INTERNATIONAL ATOMIC ENERGY AGENCY, Radioactivity in the Arctic Seas, Report for the International Arctic Seas Assessment Project (IASAP), IAEA-TECDOC-1075, IAEA, Monaco (1999).

[66] FOOD AND AGRICULTURE ORGANIZATION OF THE UNITED NATIONS, INTERNATIONAL ATOMIC ENERGY AGENCY, INTERNATIONAL LABOUR ORGANISATION, OECD NUCLEAR ENERGY AGENCY, PAN AMERICAN HEALTH ORGANIZATION AND WORLD HEALTH ORGANIZATION, International Basic Safety Standards for Protection against Ionizing Radiation and for the Safety of Radiation Sources, IAEA Safety Series No.115, IAEA, Vienna (1996).

[67] FOOD AND AGRICULTURE ORGANIZATION OF THE UNITED NATIONS, Fishery Statistics, Vols. 70–77, FAO, Rome (1992).

[68] COMMISSION OF THE EUROPEAN COMMUNITIES, The Radiological Exposure of the Population of the European Community from Radioactivity in North European Marine Waters, Project "Marina", Report EUR 12483 EN, EC Luxembourg (1990).

[69] INTERNATIONAL ATOMIC ENERGY AGENCY, Sources of Radioactivity in the Marine Environment and their Relative Contributions to Overall Dose Assessment from Marine Radioactivity, (MARDOS), IAEA-TECDOC-838, IAEA, Vienna (1995).

[70] BARRACLOUGH, I.N., ROBB, J.D., ROBINSON, C.A., SMITH, V.R., COOPER, J.R., The use of estimates of collective dose to the public, J. Radiol. Prot. **16** 2 (1996) 73–80.

[71] TITLEY, J.G., CABIANCA, T., LAWSON, G., MOBBS, S.F., SIMMONDS, J.R., Improved global dispersion models for Iodine-129 and Carbon-14, EUR 15880 EN, EC, Luxembourg (1995).

[72] NUCLEAR ENERGY AGENCY – Organization for Economic Co-operation and Development, Review of the Continued Suitability of the Dumping Site for Radioactive Waste in the North-East Atlantic, NEA-OECD, Paris (1985).

[73] WOLLENBURG, I., Sediment Transport by Arctic Sea Ice: The Recent Load of Lithogenic and Biogenic Material. Berichte zur Polarforschung **127** Alfred Wegener Institut, Hamburg (1993).

[74] NURNBERG, D., et al., Sediments in Arctic Sea ice: Implications for entrainment, transport and release. Marine Geology **119** (1994).

[75] CHANG, A., PRELLER, R.H., The Development of an Ice-Ocean Coupled Model for the Northern Hemisphere, NRL Formal Report, NRL/FR/7322-95-9627, Washington DC (1996).

[76] PFIRMAN, S., LANGE, M.A., WOLLENBURG, I., SCHLOSSER, P., Sea Ice Characteristics and the Role of Sediment Inclusions in Deep-Sea Depositions: Arctic – Antarctic, Comparisons in Geological History of the Polar Oceans: Arctic Versus Antarctic (BLEIL, U., THIEDE, J., Eds), Kluwer Academic (1990).

[77] MEESE, D., et al., "Caesium-137 Contamination in Sea Ice" Procs. of workshop on Monitoring Nuclear Contamination in the Arctic Seas, Naval Research Laboratory, Washington DC (1995).

[78] COLONY, R., THORNDIKE, A.S., Sea ice motion as drunkard's walk. JGR, J. Geogr. Res. **90** (1985).

[78] INTERNATIONAL ATOMIC ENERGY AGENCY, Assessing the Impact of Deep Sea Disposal of Low Level Radioactive Waste on Living Marine Resources, Technical Report Series 288, IAEA, Vienna (1988).

[80] INTERNATIONAL ATOMIC ENERGY AGENCY, Methodology for Assessing Impacts of Radioactivity on Aquatic Ecosystems, Technical Report Series 190, IAEA, Vienna (1979).

[81] NATIONAL COUNCIL ON RADIATION PROTECTION AND MEASUREMENTS, Effects of Ionizing Radiation on Aquatic Organisms, NCRP Report 109, Bethesda MD (1991).

[82] WOODHEAD, D.S., The radiation exposure of black-headed gulls *(Larus ridibundus)* in the Ravenglass Estuary, Cumbria, UK: A Preliminary Assessment, Sci. Tot. Environ. **58** (1986) 273–281.

[83] CALMET, D., WOODHEAD, D., ANDRÉ, J.M., ^{210}Pb, ^{137}Cs and ^{40}K in three species of porpoises caught in eastern tropical Pacific Ocean, J. Environ. Radioactivity **15** (1992) 153–169.

[84] BROWNELL, G.L., ELLETT, W.H., REDDY, A.R., Absorbed fractions for photon dosimetry, J. Nuclear Medicine, Suppl. 1 (1968) 27–39.

[85] INTERNATIONAL ATOMIC ENERGY AGENCY, Radiological Conditions of the Western Kara Sea, Assessment of the Radiological Impact of the Dumping of Radioactive Waste in the Arctic Seas – Report of the International Arcitic Seas Assessment Project (IASAP), Radiological Assessment Reports Series, IAEA, Vienna (1998).

[86] INTERNATIONAL ATOMIC ENERGY AGENCY, Effects of Ionizing Radiation on Plants and Animals at Levels Implied by Current Radiation Protection Standards, Technical Report Series 332, IAEA, Vienna (1992).

CONTRIBUTORS TO DRAFTING AND REVIEW

Cabianca, T.	International Atomic Energy Agency
Gurbutt, P.	CEFAS, United Kingdom
Harms, I.	University of Hamburg, Germany
Heling, R.	KEMA Nederland B.V., Netherlands
Kinehara, Y.	Research Center for Safety Engineering, Japan
Nielsen, S.P.	Risø National Laboratory, Denmark
Osvath, I.	International Atomic Energy Agency, Monaco
Preller, R.	Naval Research Laboratory, United States of America
Sazykina, T.	SPA "Typhoon", Russian Federation
Scott, M.	University of Glasgow, United Kingdom
Sjoeblom, K.-L.	International Atomic Energy Agency
Wada, A.	Nihon University, Japan
Woodhead, D.	CEFAS, United Kingdom
Zuur, E.	Limocéane, Université de Neuchâtel, Switzerland

Research Co-ordination Meetings

Vienna, Austria: 21–25 February 1994
Vienna, Austria: 13–17 March 1995
Vienna, Austria: 6–10 May 1996

Consultants Meetings

Vienna, Austria: 26–30 September 1994
Glasgow, United Kingdom: 6–10 November 1995
Vienna, Austria: 11–15 November 1996
Vienna, Austria: 23–27 February 1998
Vienna, Austria: 28 June–2 July 1999
Vienna, Austria: 27–29 June 2001